NATIONAL BUREAU OF STANDARDS
MICROCOPY RESOLUTION TEST CHART

(2) (14) FR79-11-1127

FINAL REPORT ON PHASE 2

OF THE

(6) ADAPTIVE TRACKING SYSTEM STUDY

(11) October 1979

AD-A 392   (12) 221

Prepared Under

Contract Number (15) N00024-77-C-6251

For The

Naval Sea Systems Command Code 63R

(9) Final rept. Oct 78 - Oct 79 on Phase 2

By

(10) Paul **P.**L. Feintuch,
Frances **F.**A. Reed,
N.J. Bershad
curtis **C.**M. Flynn

Hughes Aircraft Company
Ground Systems Group
Fullerton, California

79 12 13 043

172 370   JOB

FOREWORD

This report documents the second phase of the effort performed for the Naval Sea Systems Command Code 63R under contract N00024-77-C-6251, under Project Serial Number 806H150572, and covers the period from October 1978 to October 1979. It includes all material found in the three Quarterly Reports, work performed in the fourth quarter, connective material, the conclusions of the second phase and the approach for the third phase of the study. This study has as its goal the examination of the application of adaptive filters to passive sonar bearing tracking. Major steps toward this goal have been realized via a combination of statistical modeling and analysis, with verification by computer simulation.

ACKNOWLEDGEMENTS

This work was initiated under the direction of Mr. John Neely of NAVSEA Code 16H1. With the transfer of Mr. Neely to Code 63D and the code change from 06H1 to 63R, Mr. Daniel E. Porter became the director of the remaining effort and of the follow-on effort in Phase 3.

The studies were performed at Hughes by the principal investigator, Dr. Paul L. Feintuch, with the major analytic support of Mr. Francis A. Reed. Consulting services were provided by Dr. N.J. Bershad, and the computer simulations were performed by Mr. Curtis M. Flynn.

TABLE OF CONTENTS

SECTION 1.0
INTRODUCTION

1.0 INTRODUCTION

This is the final report on phase 2 of a study contract to determine the usefulness of the LMS adaptive filter in a bearing tracker structure for passive sonar. Three potential advantages of such a structure over conventional trackers motivated the study, as follows

a. While conventional trackers require a priori knowledge of the input power specta to optimize performance, the adaptive tracker is estimating the input spectra. This suggests that the adaptive tracker may be insensitive to incorrect a priori assumptions and variations of the input spectra,

b. Since all the correlation information between the split array outputs is contained in the adaptive filter weights, the potential exists to perform broadband and narrowband tracking simultaneously, and

c. Conventional trackers are essentially designed for stationary targets, modified for use with dynamic targets with the addition of a tracking loop. However, the adaptive filter weights are adjusted iteratively (dynamically) to satisfy a minimum mean square error criteria, which may provide advantages against moving targets.

The first phase of this study [1] addressed the feasibility of such a tracker using the Least Mean Square (LMS) adaptive filter algorithm, and developed the tracker structure of Figure 1-1. In this structure, the two beamformed split array outputs are provided as the two inputs to an LMS adaptive filter configured as a canceller. The output of one half array processed by a non-recursive adaptive filter, is subtracted from the other half array to yield an error signal. The error signal is then used to recursively update the adaptive filter weights, or impulse response such that the mean square error is minimized. If $x(nT_s)$ and $d(nT_s)$ are the two inputs, with T_s the sample rate and the time index, the adaptive filter stores the data vector

$$\underline{X}(n) = [x[nT_s] \, x[(n-1)T_s] \ldots x[(n-M+1)T_s]]^T \tag{1}$$

where $\underline{X}^T$ denotes $\underline{X}$ transpose. The output of the adaptive filter is

$$y(n) = \underline{W}^T(n)\underline{X}(n) \tag{2}$$

where $\underline{W}(n)$ is a vector of M weights at time nT_s. The error output is therefore

$$\epsilon(n) = d(n) - \underline{W}^T(n)\underline{X}(n). \tag{3}$$

The LMS algorithm updates the weight vector on each iteration as

$$\underline{W}(n+1) = \underline{W}(n) + \mu \epsilon(n)\underline{X}(n) \tag{4}$$

where μ is a weight update coefficient. This parameter controls the rate of convergence, algorithm noise, and, ultimately, the stability of the algorithm.
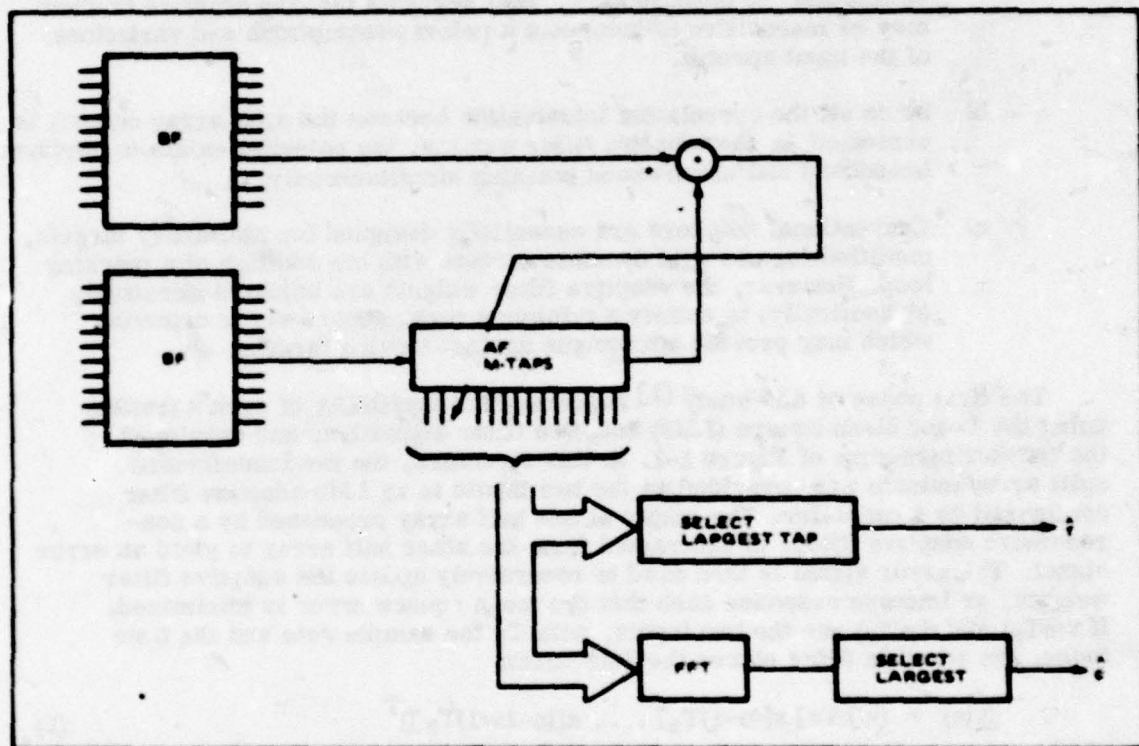
1

Figure 1-1. Adaptive Tracker Structure

In converging to minimize the mean square error between half array outputs, the adaptive filter must incorporate any time delay (or for narrowband sources, phase shift) between its inputs in the weight vector. For broadband inputs, the weights have the same shape as the signal autocorrelation function with the peak located at the delay between the phase centers. Hence, the tracker must determine the location of the peak of the weights, using interpolation between discrete taps if necessary. For sinusoidal inputs, the weights converge to a sinusoid with phase equal to the phase shift between array halves. The tracker then determines the phase shift by means of spectrum analysis of the weight vector. Either the time delay or phase shift is easily converted to a bearing estimate.

The first phase of the study also provided many of the analytical techniques required for analysis of the adaptive tracker. In particular, if provided the frequency domain model for the adaptive tracker shown in Figure 1-2. In the frequency domain version, the two inputs are Fast Fourier Transformed (FFT'd) and a single tap, complex LMS adaptive filter performed independently in each FFT bin. It was shown that this configuration performs equivalently to the time domain filter, both in transient and steady state operation, under certain conditions on the filter design parameters. The primary advantage of the frequency domain model is that both the mean and variance of the weights can be predicted. By careful selection of filter parameters, this model can then be used to predict the variance of the time domain weights, which cannot be obtained by analysis in the time domain.

Given the statistics of the time and frequency domain weights, it was possible to obtain predictions of the bearing estimate statistics for broadband inputs. A continuous adaptive tracker was shown to perform within 0.5 dB of the Cramer-Rao Lower Bound on the variance of all unbiased estimators. Performance results were also derived for a practical realization of the tracker, operating at a reasonable sampling rate with interpolation between samples providing fine delay (hence bearing) resolution. These results were shown to be comparable to a conventional tracker. The first phase of the study also developed the mean weight of the adaptive filter with dynamic broadband and narrowband inputs. The results are applied here in the analysis of tracker performance for dynamic targets. Finally, the first phase developed extensive simulation programs for the tracker structure, which were used to validate the analyses, and provide an initial look at dynamic tracking performance.

The first final report established the feasibility of the adaptive tracker structure, particularly for broadband targets. This report addresses in greater detail the potential advantages given in items a through c, above. The material given consists of the results reported in the first three quarterly reports, plus work done during the fourth quarter. Section 2.0 summarizes the results of the study without detailed description of mathematical models or derivations, which are included as appendices. Some expressions and figures from the appendices are repeated in the summary for convenience. Section 3.0 draws general conclusions and relates the result given in this report to efforts planned for phase 3.
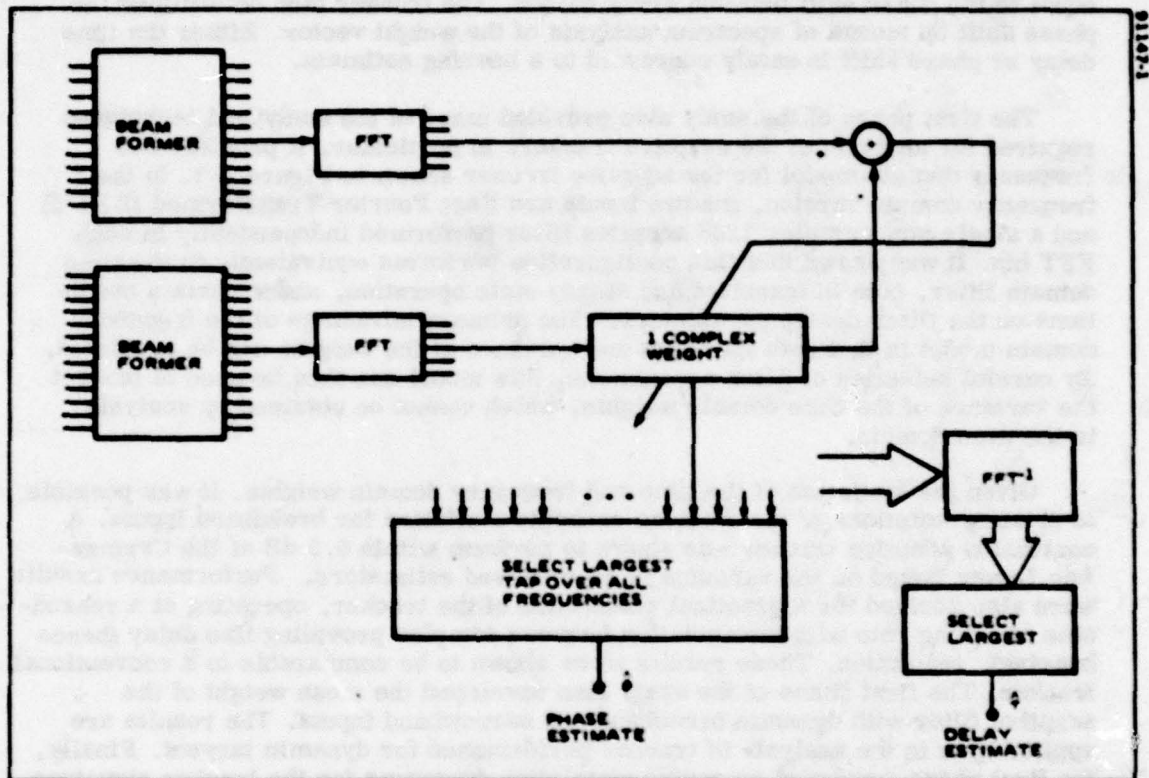
Figure 1-2. Frequency Domain Model For The Adaptive Tracker

4

SECTION 2.0
SUMMARY OF RESULTS

2.0 SUMMARY OF RESULTS

This section presents the results of the second phase of the Adaptive Tracking System Study in summary form, without detailed derivations and analyses, which are given in the appendices. The results fall into six categories, discussed separately below.

Section 2.1 considers the bearing estimation performance of the narrowband (NB) adaptive tracker with a narrowband target in uncorrelated background noise. The statistics of the bearing estimate are derived, and the variance compared with the Cramer-Rao Lower Bound. In section 2.2, the effects on the NB adaptive tracker of broadband noise emanating from the same target are studied. Using essentially the same analysis, Section 2.3 considers the NB adaptive tracker with a NB target in the presence of a broadband interference from another direction. In particular, the bias due to the interference and the effects on the bearing estimate variance are given.

One motivation for studying the adaptive tracker has been its possible insensitivity to incorrect assumptions on input spectra relation to conventional trackers. Section 2.4 discusses the relative performance of the adaptive tracker and a conventional split beam tracker (SBT) when either the noise or signal spectra differ from those assumed.

Section 2.5 deals with the performance of the broadband adaptive tracker with a broadband target and a broadband interference. Both a continuous realization and a discrete version of the adaptive filter are considered. Finally, section 2.6 considers the performance of the broadband adaptive tracker with a broadband target whose bearing is changing linearly with time. This is analytically compared with a Bearing Deviation Indicator (BDI) with the same dynamic input.

2.1 Narrowband Adaptive Tracker Performance With Stationary Narrowband Target. The adaptive tracker structure for estimating bearing from broadband and narrowband signals is shown in Figure 1-1. The outputs of half array beamformers steered in the vicinity of the target are provided as inputs to an LMS adaptive filter configured as a canceller. The filter, in minimizing the mean square error between the filter output and the reference inputs, would ideally insert a time delay equal to the time delay between half array phase centers. This can be interpreted as a phase shift for narrowband signals. This ideal result is corrupted by background noise, finite observation time, the discrete (in time) nature of the filter, and correlation properties of the signal and noise.

For a narrowband target, the mean adaptive filter weights converge to a sinusoid at the frequency of the target line, with a phase equal to the phase shift between array halves. To extract this phase, the weight vector is Fast Fourier Transformed (FFT'd), and the phase of the FFT bin containing the signal is used as the phase estimate. Conversion of the phase estimate to bearing requires knowledge of the line frequency, which is estimated as the center frequency of the FFT bin containing the signal, assumed to be the one with the largest magnitude.

5

During Phase 1 of this study [1], a frequency domain model for the adaptive tracker was developed which allowed determination of both the mean and variance of the adaptive tracker weights for broadband inputs. Using this model, the mean and variance of the FFT of the weight vector for the case of a narrowband target in broadband noise are derived, as given in the first section of Appendix A. Based upon the large number of iterations required for convergence of the adaptive filter, the frequency domain weights are assumed to be complex gaussian random variables. This allows determination of the density of the phase in each FFT bin by transformation to polar coordinates, then integrating out the magnitude. The bearing is related to the phase by

$$\hat{\theta} = \sin^{-1}\left(\frac{c}{d\hat{\omega}_o}\hat{\phi}\right) \tag{5}$$

where c is the speed of sound, d the distance between half array phase centers, $\hat{\phi}$ the phase estimate in the FFT bin, and $\hat{\omega}_o$ the estimated radian frequency of the line, approximated here by the FFT bin center. By numerical integration of this function and its square over the phase density, the mean and variance of the bearing estimate are obtained. The analysis assumes that the bin containing the line is selected for phase extraction. This means that either the signal-to-noise ratio in the bin must be sufficiently high or else some other means, such as additional non-coherent integration must be used to identify the bin containing the signal if the predictions are to be valid. The details of the analysis are given in Appendix A.

The analysis shows that the bearing estimate is essentially unbiased, and this is confirmed by simulations. Figure 2-1 shows the r.m.s bearing error, determined as above, for a particular adaptive tracker. The signal is a 100 Hz sinusoid emanating from a target at 0° bearing and observed by an array with 150 feet between half array phase centers. The FFT is an 128 point transform with 2 Hz frequency resolution. Also shown in the figure are the results of computer simulations of the same tracker, demonstrating excellent agreement with the analytical predictions.

An approximation for the variance of the phase in the FFT bin containing the signal is derived using a Taylor expansion of the inverse tangent, as used to obtain the phase from the FFT weights. By retaining only second order and lower terms, then integrating the result over the phase density, it is possible to obtain simple approximations to the phase variance at high signal to noise ratio. For bearing angles near the maximum response axis (MRA) of the array, this is easily mapped to a bearing variance approximation, given by

$$\text{Var}[\hat{\theta}] \approx \frac{M^2 T_s^2}{(2\pi k)^2} \frac{c^2}{d^2} \frac{2\gamma^3 + 4\gamma^2 + 4\gamma + 1}{\gamma^2 \left[2(\gamma+1) - \mu M \sigma_n^2 (\gamma^2 + 4\gamma + 2)\right](\gamma+1)\tau_I} \tag{6}$$

where M is the number of FFT points, k the index of the FFT bin containing the signal, T_s the sample rate, γ the signal to noise ratio in the FFT bin, and τ_I the adaptive filter time constant in iterations. This can be further approximated as
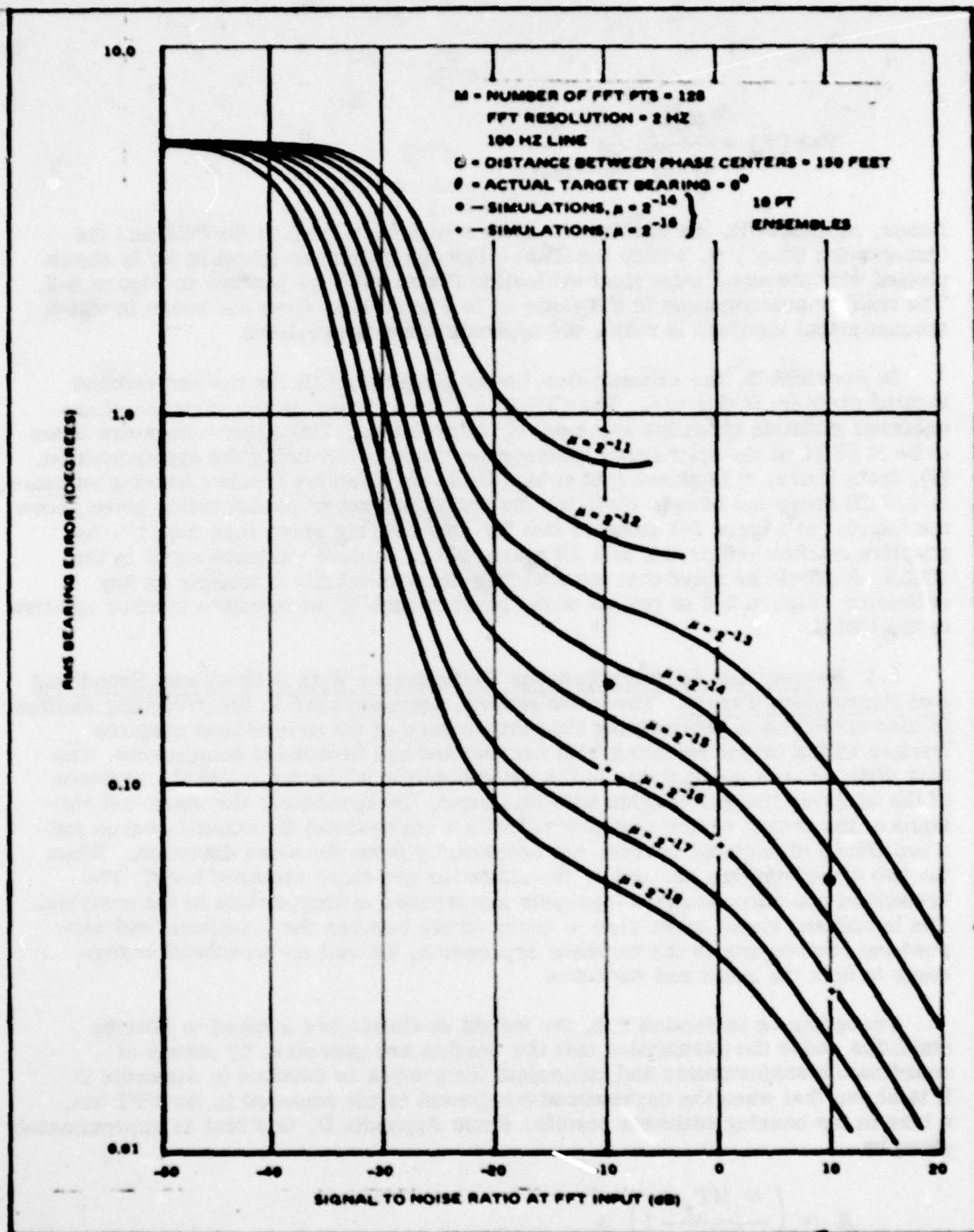
6

Figure 2-1: Adaptive Tracker RMS Bearing Error For Static Narrowband Target.

$$\text{Var}[\hat{\theta}] \approx \frac{M^2 T_s^2}{(2\pi k)^2} \frac{c^2}{d^2} \frac{1}{2\tau_I^{\gamma}}$$

Hence, at high SNR, the variance is inversely proportional to the SNR and the "integration time", τ_I, within the filter. The approximation given in (6) is shown plotted with the exact numerical evaluation for an adaptive tracker in Figure 2-2. The tracker configuration is the same as is Figure 2-1. Over the range in which the numerical analysis is valid, the approximation is excellent.

In Appendix B, the Cramer-Rao Lower Bound (CRLB) for the narrowband tacking problem is derived. The CRLB is a lower bound on the variance of any unbiased estimate given the same set of observations. The observations are taken to be N FFTs of the split array beamformer outputs. By using the approximation, (7), from above, it is shown that at high SNR, the adaptive tracker bearing variance, is 0.5 dB above the bound. Plots for the adaptive tracker configuration given above for the plot of Figure 2-1 indicate that for rms bearing error less than 1°, the adaptive tracker requires 1 to 5 dB more SNR to achieve variance equal to the CRLB. It should be noted that the CRLB is not necessarily attainable by any estimator. Figure 2-3 is typical of the performance of the adaptive tracker relative to the CRLB.

2.2 Narrowband Adaptive Tracker Performance With A Combined Broadband And Narrowband Target. The same general approach used in the preceding section is also employed in determining the performance of the narrowband adaptive tracker with a target radiating both narrowband and broadband components. The only difference in the analysis is the determination of the mean and the variance of the adaptive tracker weights with this input. In Appendix C the mean and variance of the weight vector is rederived with a narrowband directional source and a broadband directional source, not necessarily from the same direction. When the two directions are set equal, the statistics are those required here. The broadband and narrowband components are treated as independent in the analysis. The broadband signal gives rise to cross terms between the broadband and narrowband components in the variance expression, as well as broadband components in both the mean and variance.

Proceding as in Section 2.1, the weight statistics are mapped to bearing statistics under the assumption that the weights are gaussian, by means of coordinate transformation and numerical integration as detailed in Appendix D. It is shown that when the narrowband component is not centered in the FFT bin, a bias in the bearing estimate results. From Appendix D, this bias is approximately given by

$$B \approx \left(\frac{\omega_o M T_s}{2\pi k} - 1 \right) \theta_s \qquad (8)$$
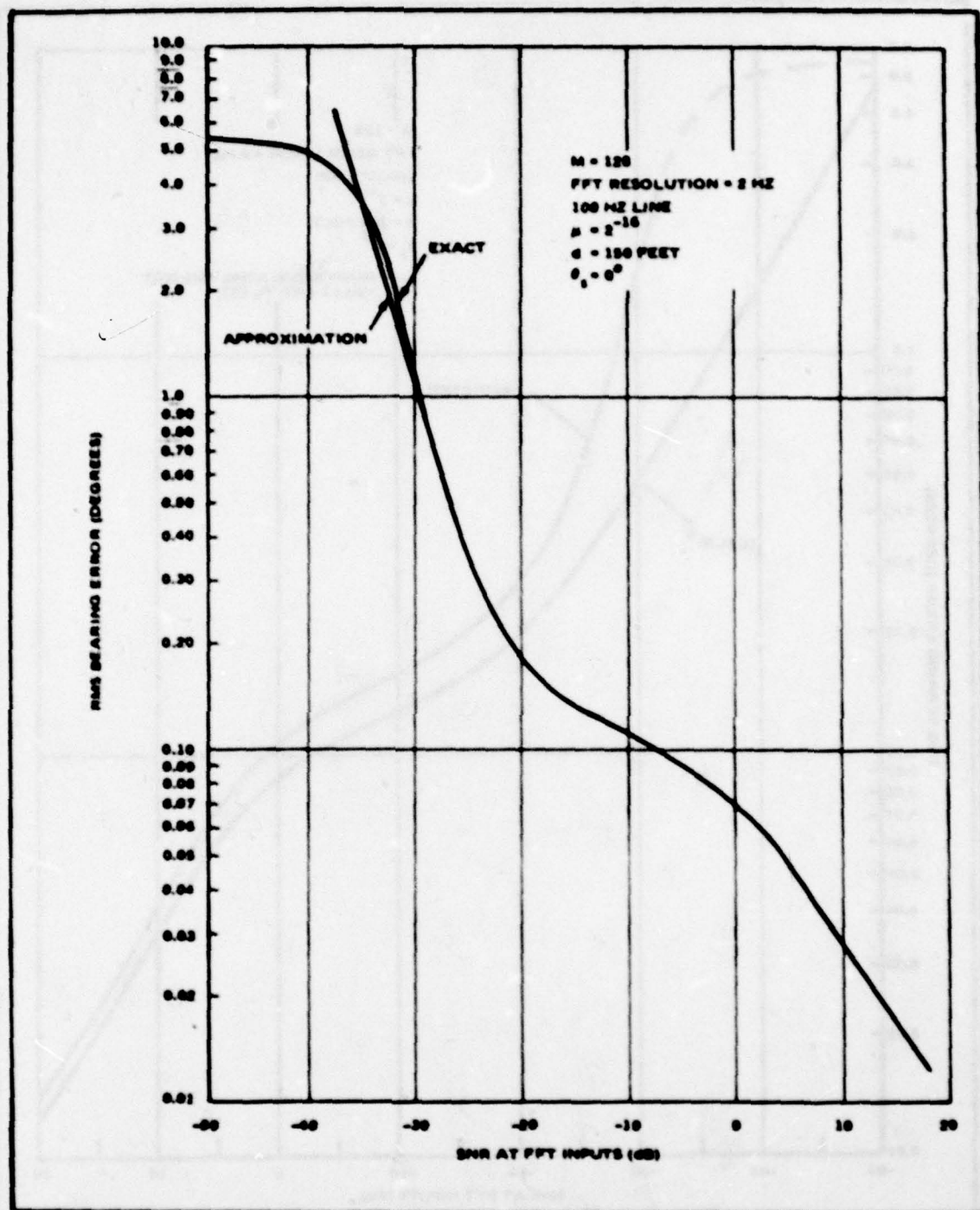
8

Figure 2-2: Comparison Of Narrowband Tracker RMS Bearing Error With Approximation
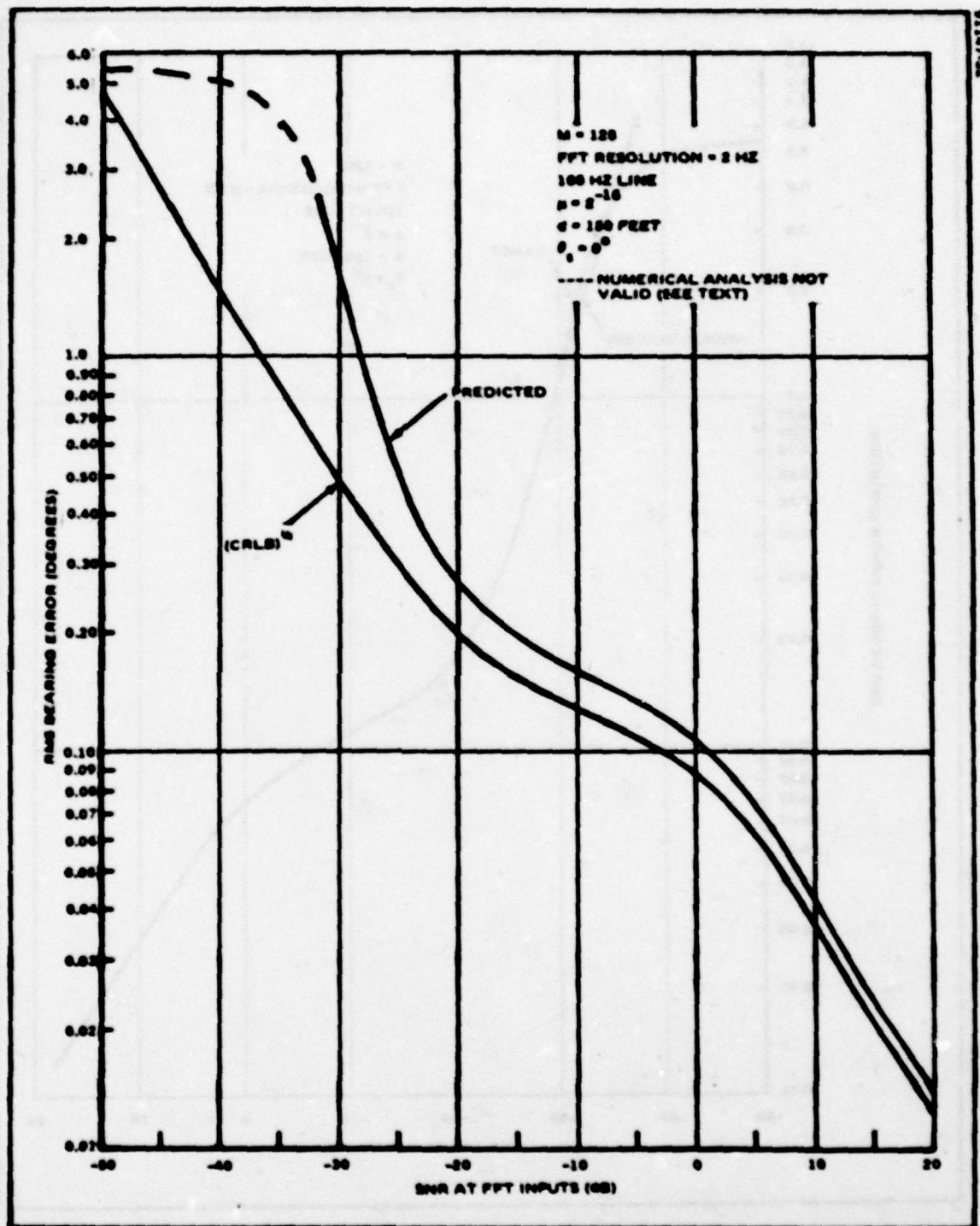
9

Figure 2-3: Comparison Of Adaptive Tracker Bearing Estimate And Cramer-Rao Lower Bound

where

θ_s = actual target bearing

ω_o = narrowband line frequency

k = index of FFT bin containing signal

M = FFT size

T_s = sample rate

This bias decreases as the FFT resolution is made finer. Since the maximum error, given adequate SNR to select the bin nearest the signal, is one-half of an FFT bin, the bias is proportional to the ratio of FFT resolution to center frequency,

$$|B_{max}| \approx \left(\frac{\Omega_R/2}{\omega_o - \Omega_R/2}\right)\left(\Theta_s\right)_{max} \tag{9}$$

where

$(\theta_s)_{max}$ = largest bearing angle considered

Ω_R = FFT resolution

This relationship can be used to set the FFT resolution for acceptable bias. Note that the estimate is unbiased for targets at broadside.

The rms bearing error of a narrowband adaptive tracker with a composite target is shown in Figure 2-4 as a function of the narrowband signal to background noise ratio for various levels of broadband signal. The presence of broadband noise from the same target can significantly improve the narrowband estimate, particularly when its power exceeds that of the narrowband component. The tracker here is a 128 tap filter with FFT resolution of 2 Hz and a weight update coefficient, μ, of 2^{-16}. The array has 150 ft between phase centers, and the target is at 0° bearing with a 100 Hz line and a flat broadband spectrum. As in section 2.1, these results are valid only when the correct FFT bin is selected. Also shown in the figure are the results of computer simulations, which verify the analytical predictions.

By noting the performance of the tracker in Figure 2-4 at low narrowband SNR for moderate to high broadband SNR, that is when most target energy is broadband, it appears that the narrowband tracker is a good estimator of the bearing of a broadband target. However, the analyses here assume that the delay between phase centers is always an integer number of sample intervals, an assumption necessary in the uncorrelated noise case. For correlated noise and non-integer delays, this may change somewhat. Further analysis and simulation would be required to conclude that the narrowband tracker can always be used for broadband signals.
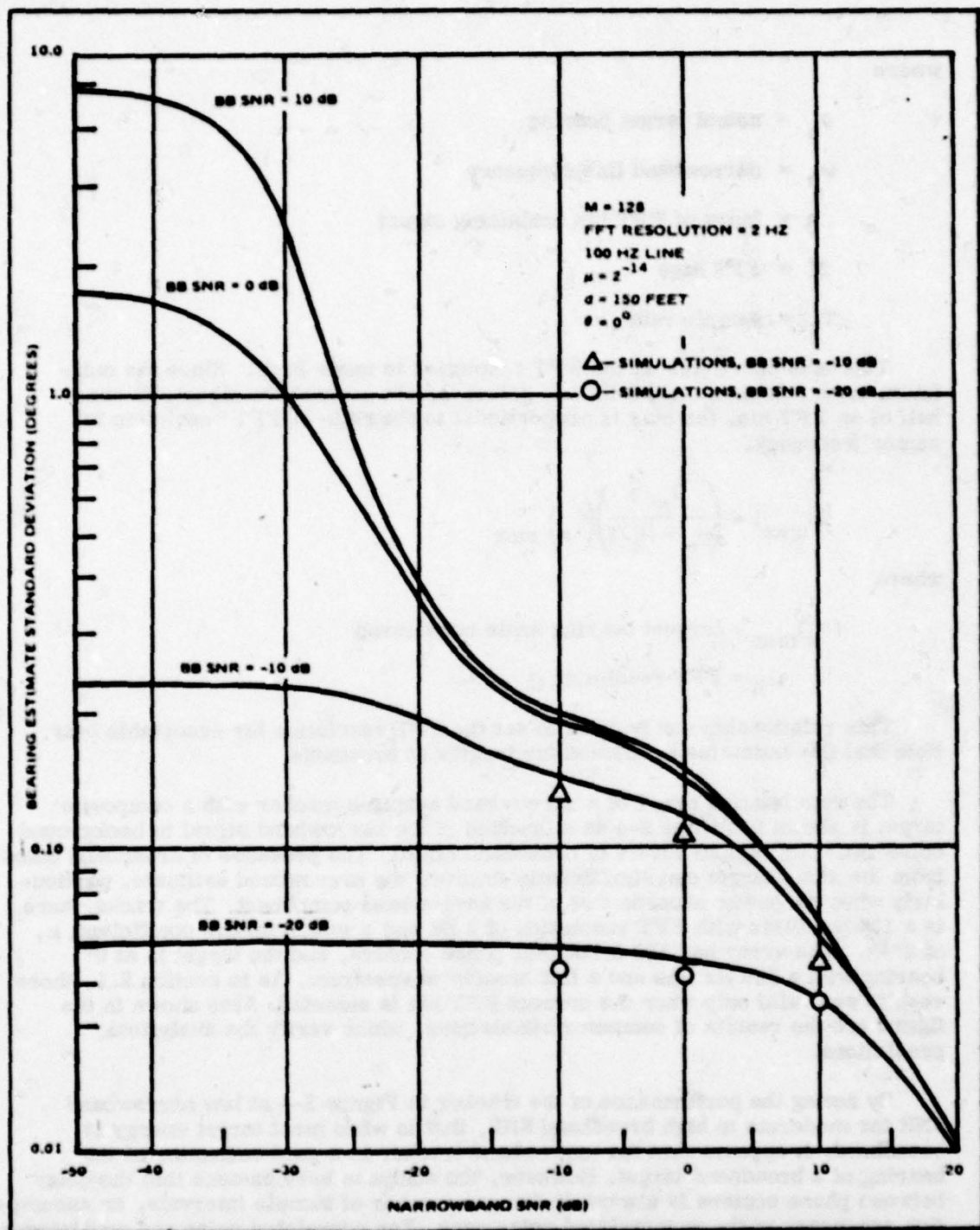
11

Figure 2-4: RMS Bearing Error For Narrowband Adaptive Tracker And Target
With Broadband And Narrowband Radiated Noise.

The approximation developed in Appendix A for the rms bearing error with a narrowband signal only, (A-46), is equally valid here when the parameter, β^2, is replaced by (D-6) from Appendix D, although the complexity of the latter makes the approximation less useful.

2.3 Performance Of The Narrowband Adaptive Tracker With A Narrowband Target And Broadband Interference. The analyses and simulations in section 2.1 and 2.2 consider a target in a noise field that is uncorrelated between array halves. A realistic environment could be expected to include directional sources other than the target, referred to as interferences. Appendix D, using the results of Appendix C, considers the effects of a single broadband interference on the performance of a narrowband tracker with a narrowband target. The weight statistics developed in Appendix C represent this situation when the bearing angles of the broadband and narrowband components are not equal. The mapping of the weight statistics to bearing is identical to that described in section 3.2. The results, however, differ significantly.

When a broadband interference of moderate strength relative to the narrowband target is present, the dominant effect is a bias in the bearing estimate toward the interference. For angles within $\pm 10^O$ of broadside, this bias is given in Appendix D as

$$B \approx \left(\frac{\omega_o M T_s}{2\pi k} - 1 \right) \theta_s - \frac{M T_s}{2\pi k}\frac{c}{d} \arctan \left[\frac{\sin\left[\omega_o \frac{d}{c}\sin\theta_s - \frac{2\pi k}{M T_s}\frac{d}{c}\sin\theta_I \right]}{\lambda + \cos\left[\omega_o \frac{d}{c}\sin\theta_s - \frac{2\pi}{M T_s}\frac{d}{c}\sin\theta_I \right]} \right] \tag{10}$$

where

θ_s = target bearing

θ_I = interference bearing

λ = signal to interference ratio in FFT bin

ω_o = target frequency

k = index of FFT bin nearest the signal

d = distance between half array phase centers

c = speed of sound

M = FFT size

T_s = sample rate

The first term is due to non-bin centering of the signal, and will typically be negligible in comparison to the second term. The bias can also be computed numerically by integrating over the phase density, as described in section 2.1, and

in Appendix D. When this is done, curves like those shown in Figure 2-5 result. This figure shows the bias in a particular narrowband adaptive tracker as a function of the signal-to-noise ratio (SNR) of a target at 0°, with an interference at 4° for four interference-to-noise ratios (INR). When the SNR is low in comparison to the INR in the FFT bin, the estimate is very nearly the interference angle while at high SNR, the estimate is essentially unbiased. The results of computer simulations are also shown in Figure 2-5, and show excellent agreements.

This result should not be considered as unique to the narrowband adaptive tracker, but will be typical of trackers of this generic type that extract phase information from FFT outputs. This suggests that, at least in part, the disappointing performance experienced with many existing narrowband trackers may be due to the commulative bias effect of numerous broadband directional sources such as own ship and distant shipping.

The variance of the tracker with a broadband interference has also been determined using the numerical integrations of the phase density described in Appendix D, and the results for a particular example are shown in Figure 2-6. The signal is a 100 Hz line received by an array with 150 ft between phase centers, and emanating from a target of 4° bearing. The single broadband interference is located at 0°. The 128 tap adaptive tracker uses an FFT resolution of 2 Hz and a weight update coefficient of 2^{-14}. The standard deviation of the bearing error is plotted as a function of SNR for four values of interference-to-noise ratio. Any evaluation of tracking performance must consider both Figure 2-5, the bias, and 2-6, the standard deviation, simultaneously. For example, while a +10 dB interference gives very low standard deviation at low SNR from Figure 2-6, the estimate is severely biased, from Figure 2-5. A reasonable performance measure is the root mean square error, given by the square root of the sum of the square of the bias and the variance. It is interesting to note that at high SNR, when the bias is negligible, the interference has the effect of increasing the variance of the estimate. Results of computer simulations of this adaptive tracker are also shown on Figure 2-6, and verify the analytical predictions.

2.4 Performance Of The Broadband Adaptive Tracker With Incorrect A Priori Assumptions On Input Spectra. The broadband adaptive tracker has been suggested as an alternative to conventional split beam correlator trackers because of several potential advantages stemming from the adaptive characteristics. One of these possible advantages is that the adaptive filter does not require a priori knowledge of the signal and noise statistics, but estimates these dynamically during operation. Conventional split beam trackers, on the other hand, require the input signal and noise spectra in order to optimize their performance (see, for example, [2] or [3]). The goal of this analysis is to determine, at least for some simple cases, whether or not the adaptive tracker is more tolerant of spectral variation about those assumed a priori than the split beam tracker (SBT).

The approach is as follows. A signal and noise spectrum is assumed a priori, and the weighting filter for the SBT is set using these spectra. Then, with the input spectra matching the a priori assumptions the variance of the bearing estimate for the adaptive tracker and SBT are computed analytically. Either the input noise or signal spectrum is then varied without changing the weighting filter of the SBT, and the variances recomputed. The ratio of the variances with correct and incorrect a priori knowledge gives the change in performance of the two trackers. These are then used to determine which of the two is less susceptible to the changing inputs.
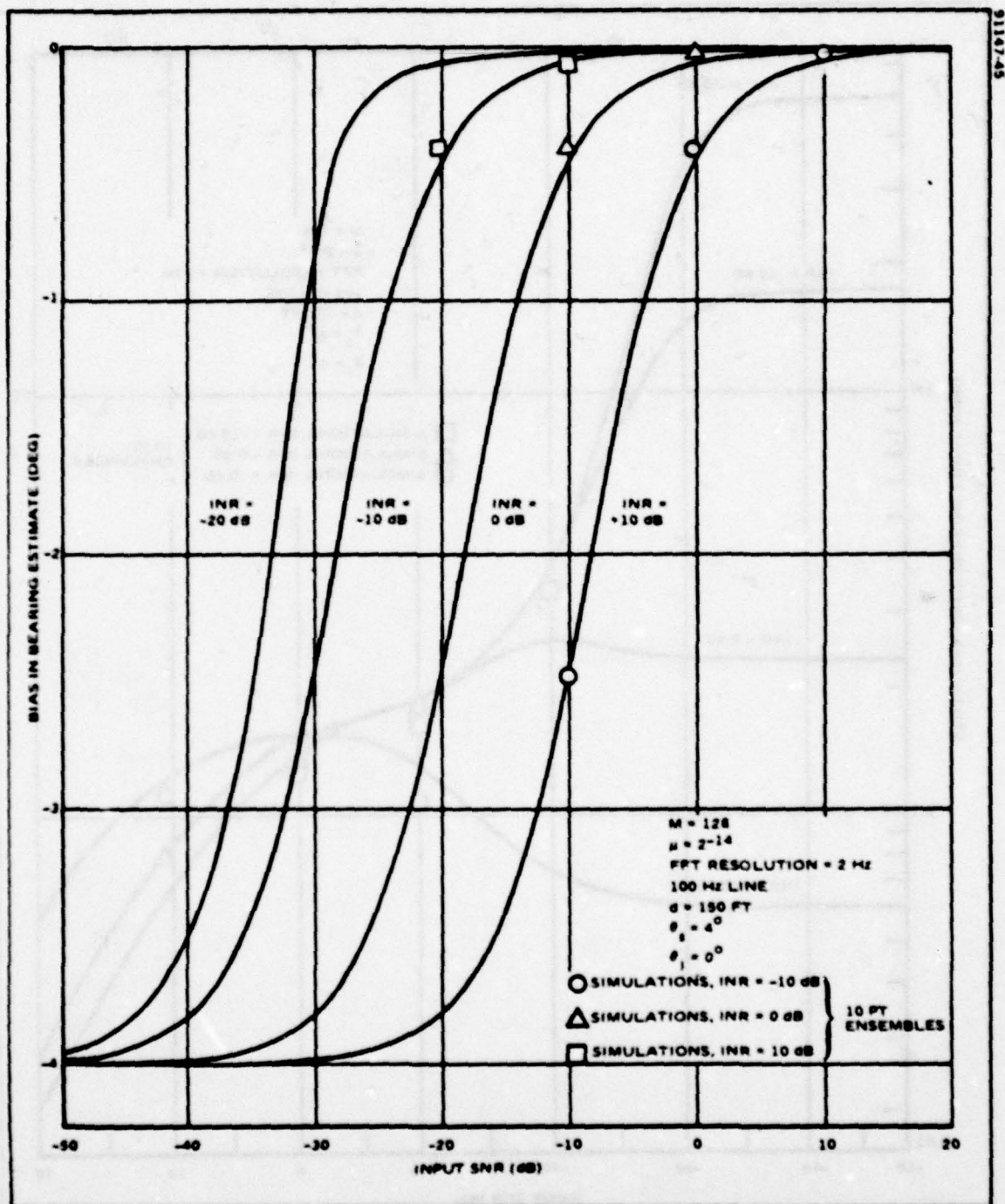
14

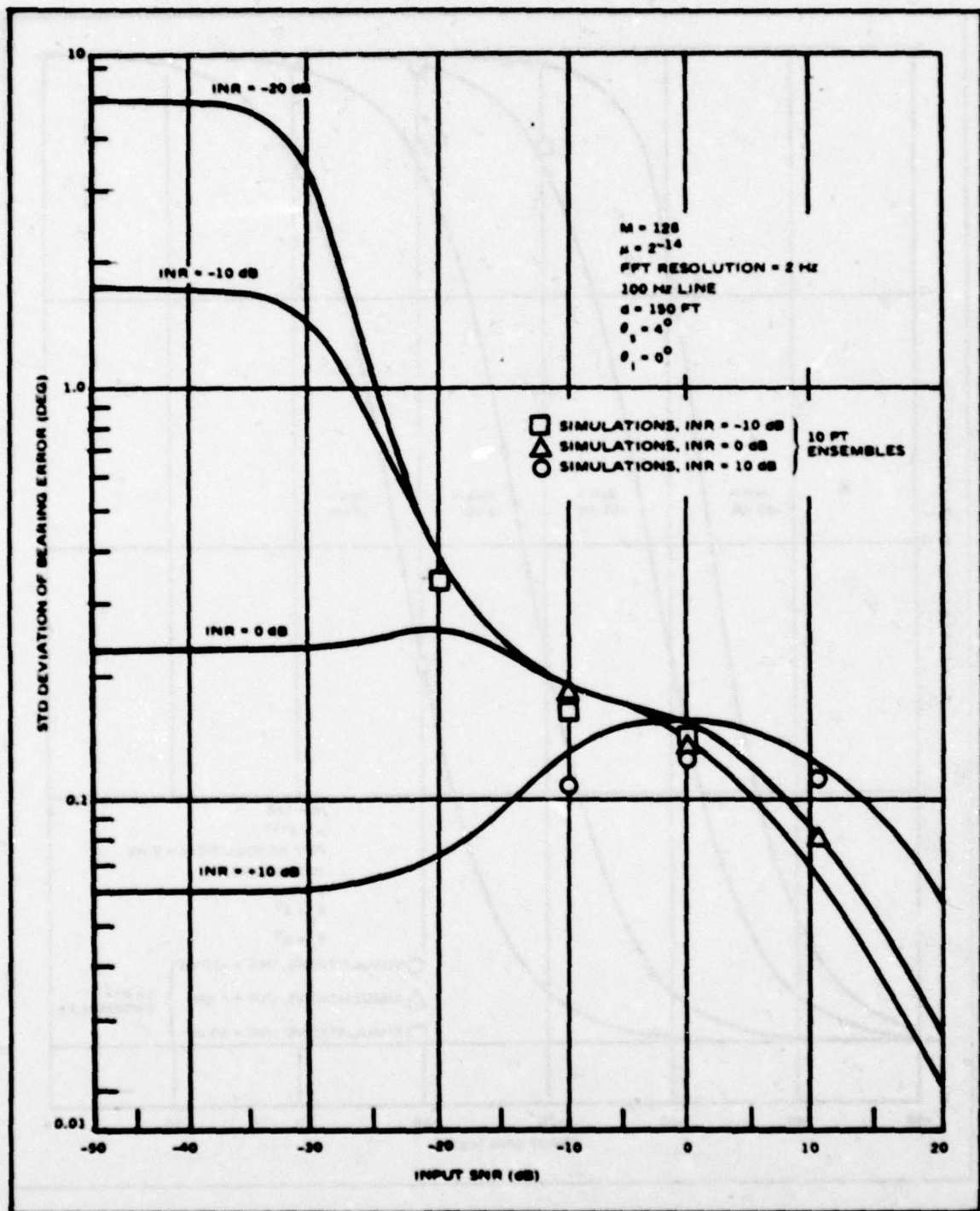**Figure 2-5: Bias In The Narrowband Adaptive Tracker Due To Broadband Interference**

Figure 2-6: RMS Bearing Error For The Narrowband Adaptive Filter In the
Presence Of A Broadband Interference.

In Appendix 4 of [1], the mean and variance of the transfer function of a continuous adpative filter was derived under the condition of equal signal and noise bands. This was done by resolving the inputs into descrete frequency bins, and applying a single tap complex adaptive filter in each bin, as discussed in Appendix 3 of [1]. The transfer functions are obtained as the limit of the discrete case. This approach depends upon the independence of the individual frequency bins. The resulting transfer function can be used to obtain the impulse response of the adaptive filter, $h(\tau)$.

The angle, θ, is to be estimated by determining the value of τ for which the impulse response, $h(\tau)$, is a maximum. This is an estimate of the delay between arrivals of the signal wavefront at the half array phase centers, and can be converted to a bearing estimate, $\hat{\theta}$, using

$$\tau = \frac{d}{c} \sin \hat{\theta} . \tag{11}$$

The value of θ for which $h(\tau)$ is peaked corresponds to the value for which the derivative of $h(\tau)$ with respect to θ is zero. In the neighborhood of the zero crossing the derivative of the impulse response is approximately linear. The fluctuations in the derivative of the transfer function then map through the linear function to provide an estimate of the mean square error in the angle estimate. Thus the mean value of the derivative of the transfer function, the standard deviation of the derivative of the transfer function, and the slope of the mean of the derivative of the transfer function are required, at the point where $\hat{\theta} = \theta$. Then the errors in the transfer function can be mapped into the errors in one's ability to extract the peak of the transfer function as follows:

$$\text{Var}^{1/2}[\hat{\theta}] = \frac{\text{Var}^{1/2}\left[\frac{\partial h(\tau)}{\partial \tau}\right]}{\frac{\partial E\left[\frac{\partial h(\tau)}{\partial \tau}\right]}{\partial \theta}}\Bigg|_{\tau = \frac{d}{c} \sin \hat{\theta}} \tag{12}$$

This approach is motivated by the treatment of BDI split beam trackers by MacDonald and Schultheiss in Reference [2].

In Appendix E, the adaptive tracker is compared with the conventional split beam tracker, using MacDonald and Schultheiss' results.[2] These results require a priori assumptions regarding the signal and noise spectra. The a priori signal and noise spectra are denoted $S_{sa}(\omega)$ and $S_{na}(\omega)$, respectively, not necessarily equal to the actual spectra.

The effects of incorrect a priori assumptions on the performance of the split beam tracker are examined in several specific cases. This is done by comparing the variance of the bearing estimate under actual conditions with the case when a priori assumptions are true. The performance of the adaptive filter under both conditions is also computed. In order to maintain the same time constant for the adaptive tracker, the power at the input is normalized to unit power (equivalent to an AGC).

17

The two special cases shown in Figure 2-7 are studied in detail. In case 1, the signal and noise spectra are assumed a priori to be flat over a bound 0 to ω_a with levels L_s and L_n, respectively. The actual noise spectrum is as assumed, but the actual signal spectrum differs in level from the assumed in the region from ω_s to ω_a. The analysis is performed at low signal-to-noise ratio. It is shown in Appendix E that at low SNR, the performance of the SBT and the adaptive tracker changes in the same way with changing signal spectrum. This is due primarily to the low SNR, since the adaptive filter is responding mostly to the noise input under the minimum mean square error criterion.

The second case shown in Figure 2-7 uses the same a priori assumptions as case 1, but the actual noise spectrum differs from the assumed, and the signal spectrum matches the assumptions. The noise spectrum differs in level in the region ω_n to ω_a. In this case, the analysis of Appendix E shows considerable difference between two trackers. As the noise decreases in the region ω_n to ω_a, the performance of both trackers improves, but the adaptive tracker improves more rapidly since it can adapt to better take advantage of the reduced noise. As the noise increases, both trackers degrade, and except for very small changes in level, the adaptive tracker degrades more slowly.

The two trackers can be compared in terms of a performance ratio, D, given by

$$D = \frac{Var(\hat{\theta})/V_0}{D^2(\hat{\theta})/D_0} \tag{13}$$

where

$\quad$ $Var(\hat{\theta})$ = variance of adaptive tracker estimate with actual input spectra

$\quad$ V_0 = variance of adaptive tracker estimate if a priori assumptions were true

$\quad$ $D^2(\hat{\theta})$ = variance of SBT estimate with weighting filter set using a priori assumptions, but actual spectra

$\quad$ D_0 = variance of SBT estimate with weighting function for assumed spectra, if assumptions were true

The numerator and denominator represent the change in performance as the noise spectrum varies from the assumed (note that when either is greater than unity, the performance improves with the change in spectrum). Therefore, when $D > 1$, the split beam tracker has responded more favorably to the change (i.e., it has degraded less or improved more), while $D < 1$ favors the adaptive tracker. Figure 2-8 shows D plotted as a function of

$$K_n = \frac{L_{n1}}{L_n} \quad \frac{\text{actual noise level in } \omega_n \text{ to } \omega_a}{\text{assumed noise level in } \omega_n \text{ to } \omega_a}$$
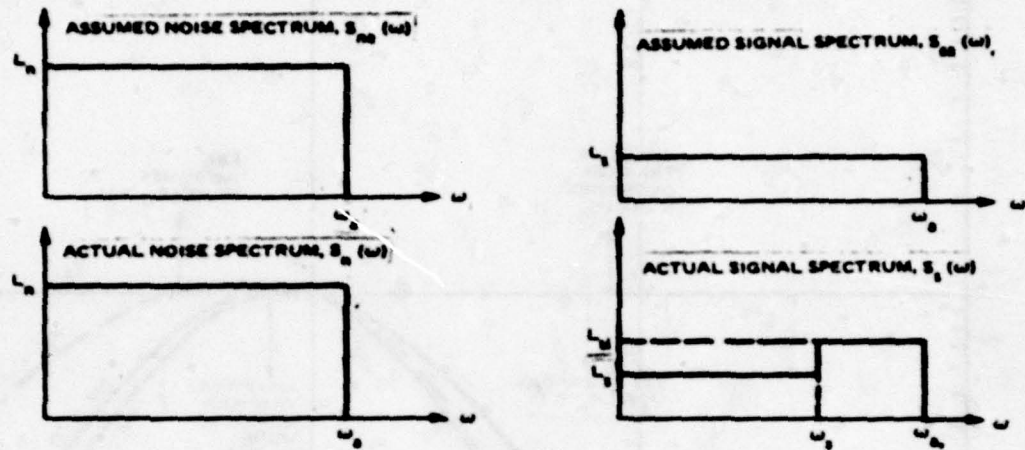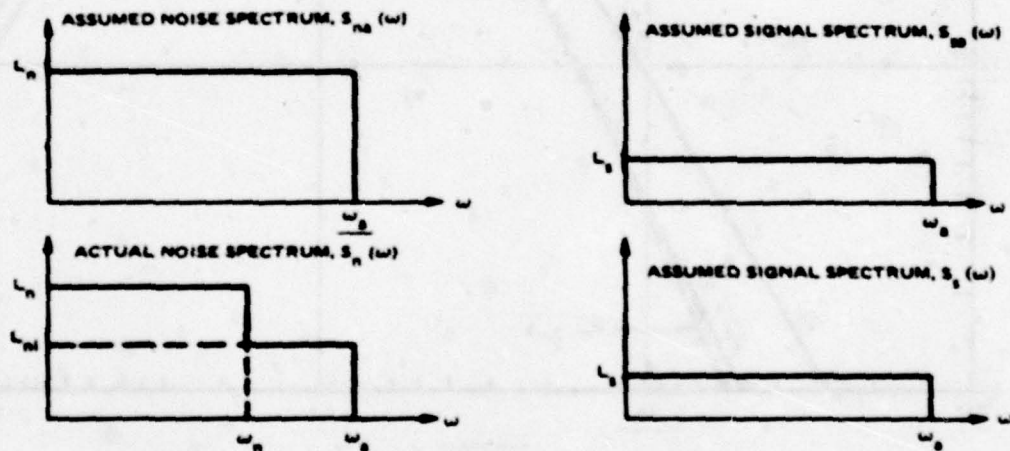
Figure 2-7: Cases Of Incorrect A Priori Input Spectra Considered In Adaptive Tracker Study
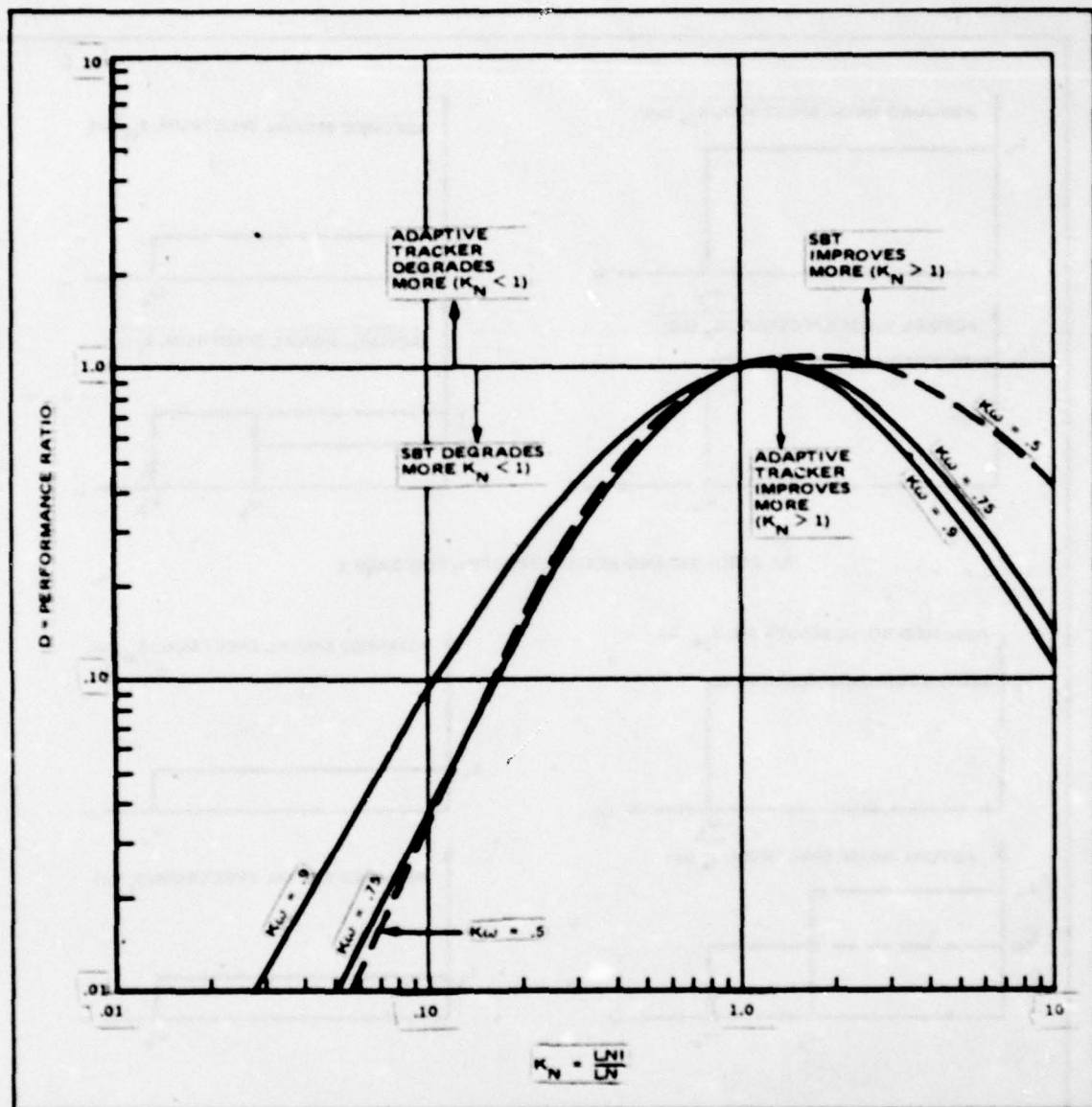
Figure 2-8: Comparison For The Performance Of The Adaptive Tracker And Conventional SBT With Incorrect A Priori Assumptions

This is plotted for several values of K_ω, where

$$K_w = \frac{\omega_n}{\omega_a}$$

is a measure of the size of the region in which the assumptions are invalid. As mentioned above, for $K_n < 1$ and for K_n significantly greater than 1, the adaptive tracker yields superior performance ($D<1$). When the noise level differs significantly from that assumed, the advantage of the adaptive tracker can be great.

For small increases in the noise level, the SBT shows a slight advantage over the adaptive tracker, as shown for K_n slightly greater than one in Figure 2-8. It is shown in Appendix E that the advantage is at most on the order of 0.5 dB. This must be compared with the much larger advantages of the adaptive filter for other values of K_n. Further, it should be noted that when $K_\omega < 0.5$ the a priori assumptions as to spectra shape are improving with decreasing K_ω. The worst case situation for spectral shape is then $K_\omega = 0.5$. With this in mind, the appendix shows that increases in the noise up to about 3 dB favor the SBT, but beyond that, the adaptive tracker is superior. The adaptive tracker appears then to offer significant immunity to changing input spectra relative to the SBT for most spectral variations studied, which the SBT offers only a slight relative advantage when the change is a small increase in noise.

2.5 Performance Of The Broadband Adaptive Tracker In The Presense Of A Broadband Interference. The first phase of the Adaptive Tracking System Study considered the performance of the broadband adaptive tracker with a single broadband directional source, the target. [1] This was done by using the frequency domain model of the tracker to develop expressions for the mean and variance of the adaptive filter weights. These frequency domain weights were then transformed to give the second order statistics of the time domain weights, or impulse response of the filter. The delay between half array phase centers was extracted from the impulse response by determining the location of the maximum. The weight vector statistics must therefore be mapped into the mean and variance in the determination of the peak.

This was done using the method used by McDonald and Schultheiss. [6] The value of the peak corresponds to the value for which the derivative of the impulse response with respect to bearing is zero. Near the zero crossing, the derivative, $h'(t)$, is approximately linear. The fluctuations in the derivative than map through the slope of the derivative, $\partial[h'(t)]/\partial\theta$, to the fluctuations in the zero crossing, or peak selection process. The variance in the bearing estimate is then

$$\mathrm{Var}^{1/2}[\hat{\theta}] = \left. \frac{\mathrm{Var}^{1/2}\left[\frac{\partial h(\tau)}{\partial \tau}\right]}{\frac{\partial E[\partial h(\tau)/\partial \tau]}{\partial \theta}} \right|_{\tau = t_z} \tag{14}$$

where $h(\tau)$ is the impulse response of the adaptive tracker and t_z is the location of the zero crossing.

Two cases were considered, a continuous realization of the adaptive filter, and a discrete, or sampled, version. The continuous case was analyzed by determining the mean and covariance functions of a continuous frequency domain tracker as the limitting case of the discrete tracker. Fourier transforms then yielded the statistics of the impulse response required to evaluate (14). The results of the analysis was primarily of value as a means of comparison with the Cramer-Rao Lower Bound (CRLB) on the variance of any estimator with the same observation. In practice however, the adaptive tracker is discrete in time, and interpolation must be used to determine the location of the peak between discrete taps. The interpolation significantly increases the variance above that obtained using a continuous adaptive filter. This, then, is the more realistic performance measure from a practical point of view.

Appendix F repeats the analysis of the variance of the bearing estimate of a broadband target, but includes a single white, broadband interference at another bearing. The derivation of the mean and variance of the adaptive filter weights uses the frequency domain model and the results of Appendix V of [1], which gave the mean and variance of the frequency domain weights. The weight variance is of the same form as in the absense of interference, but with the signal power replaced by the combined signal plus interference power,

$$\text{Var}\left[W_k(\infty)\right] = \frac{\mu M \sigma_n^2 \left[M \sigma_n^2 + 2M \left(\sigma_s^2 + \sigma_I^2 \right) \right]}{M \left(\sigma_s^2 + \sigma_I^2 + \sigma_n^2 \right) 2 - 2 \mu M \left(\sigma_s^2 + \sigma_I^2 + \sigma_n^2 \right)} \tag{15}$$

where

$W_k(\infty) = $ steady state weight in k^{th} FFT bin

$M = $ number of adaptive filter taps

$\mu = $ weight update coefficient

$\sigma_n^2 = $ noise power

$\sigma_s^2 = $ signal power

$\sigma_I^2 = $ interference power

The mean steady state weight in the kth bin is

$$E[W_k(\infty)] = \frac{1}{\sigma_s^2 + \sigma_I^2 + \sigma_n^2} \left[\sigma_s^2 e^{-j\frac{2\pi}{m}\Delta k} + \sigma_I^2 e^{-j\frac{2\pi}{m}\gamma k} \right] \tag{16}$$

where Δ and γ are the delays between half array phase centers expressed in units of the sample interval for signal and interference, respectively.

This expression, (16), points out the primary difference between the cases of interference and no interference. When (16) is inverse transformed, it yeilds the sum of two unimodal functions, with their peaks located at $t = \Delta T_S$ and $t = \gamma T_S$. If the signal and interference correlation functions are narrow in comparison to the distance between the peaks, the resulting adaptive tracker inpulse response will be bimodal, with both peaks biased somewhat toward each other. In this case, if it is possible to identify the signal peak, either through previous tracking history, or a priori knowledge, it will be possible to obtain a relatively unbiased estimate of target bearing, although the variance will be increased by the interference power. On the other hand, if the correlation functions are wide relative to the distance between the peaks, the resulting weight vector may be unimodal, with the peak somewhat between the correct delays corresponding to signal and interference. In this case, only a biased estimate is possible.

Expressions for the variance of the adaptive tracker bearing (or delay) estimate are developed in Appendix F as a function of the location at which the zero crossing occurs. This is done both for the continuous and the discrete adaptive filter. In both cases, the expressions are somewhat more complicated than the target only case, and yield little insight without numerical evaluation. Further, it is not possible to determine the location of the peak or peaks in the inpulse response explicitly. This must be done numerically on the computer, then the resulting location of the peak substituted into the variance expressions for evaluation. The appendix presents the required expressions for evaluation, but numerical computation of the results has not been completed. This will be carried out as part of Phase 3 of the study.

2.6 Adaptive Tracking Of Moving Broadband Targets. As mentioned in the introduction, one of the reasons for studying the adaptive tracker structure of Figure 1-1 is that it seemed possible that the dynamic adjustment of the tracker weights to a minimum mean square error criterion would yield some advantage over conventional tracker when the target is moving. Appendix G considers this possibility by analytically comparing the adaptive tracker and a conventional first order split beam tracker with a broadband target at low SNR whose bearing is changing linearly with time.

Using the expression for the mean weight vector at low SNR with a moving target developed in Appendix VI of reference [1], and assuming an exponential correlation function for the tracker signal input, it is possible to develop closed form expressions for the mean weights of the adaptive tracker. These results are derived in Addenda GI and GII of Appendix G. By taking limits to obtain steady state results, then determining the location of the peak of the mean weight vector, an expression for the lag of the adaptive is

$$\text{Lag} = \left[\frac{c}{bc\delta + \ln\left(1 - \mu\sigma_n^2\right)}\right] \ln \left[\frac{bc\delta\left[1 - \left(1 - \mu\sigma_n^2\right)\rho^{c\delta}\right]}{-\ln\left(1 - \mu\sigma_n^2\right)\left[\left(1 - \mu\sigma_n^2\right)\left(\rho^{-c\delta} - \rho^{c\delta}\right)\right]}\right] \quad (17)$$

where

c = linear rate of change of delay between half array phase centers

σ_δ^2 = signal power

σ_n^2 = noise power

$\rho = e^{-b}$ = exponential correlation function of signal

b = bandwidth of signal

δ = algorithm sample time

μ = weight update coefficient of adaptive filter

When $\mu\sigma_n^2 \gg bc\delta$, then this is approximately given by

$$\text{Lag} \approx \frac{0.69c}{\mu\sigma_n^2 - bc\delta} \quad (18)$$

In sections 2.4 and 2.5, and in Appendix IV of [1], a method of determining the variance of the delay or bearing, estimate from the mean and variance of the adaptive tracker weights was described. This mapping, used by McDonald and Schultheiss [6] in their analysis of conventional split beam trackers, gives the estimate variances as

$$\text{Var}^{1/2}\left[\hat{\theta}\right] = \frac{\text{Var}^{1/2}\left[\dfrac{\partial h(t)}{\partial t}\right]}{\dfrac{\partial}{\partial\theta}\left[E\,\dfrac{\partial h(t)}{\partial t}\right]}\Bigg|_{t = t_p} \quad (19)$$

with $h(t)$ the adaptive tracker weight function and t_p the location of the peak. To obtain the statistics of the derivative required by (19), it is necessary to have not only the mean weight vector, but its variance. Appendix G assumes small signal-to-noise ratio, and that the variance does not differ significantly from the noise-only case at low SNR. The variance used in (19) is therefore the

24

"null hypothesis" variance. With this approach the variance in the delay estimate is found to be

$$\text{Var}^{1/2}[\hat{t}_p] = \frac{\sigma_n^2}{\sigma_s^2} \sqrt{\mu\sigma_n^2 \left[\rho^{c\delta} + \frac{1-\rho^{c\delta}}{\mu\sigma_n^2} \right]} \frac{1}{\sqrt{2}} \frac{\delta}{1-\rho\delta} \tag{20}$$

This result agrees with previous results [1] for the static case when $c \longrightarrow 0$, and demonstrates the expected behavior with SNR, rate (c), and bandwidth.

The lag and variance of the conventional split beam tracker are determined using a linearized mathematical model described in Appendix G. Using the results of this analysis, the design parameters of the conventional tracker and the adaptive tracker are selected so that the two have equal lags for a particular dynamical input. This allows the two trackers to be compared in terms of the delay variance for equal lags. The ratio of the variance in the delay estimate from the adaptive tracker to that of the conventional tracker is, for $bc\delta \ll \mu\sigma_n^2$

$$R = \frac{\text{Var}^{1/2}(\hat{t}_{af})}{\text{Var}^{1/2}(\hat{t}_{sbt})} = \sqrt{0.69} \left[\rho^{c\delta} + \frac{1-\rho^{c\delta}}{\mu\sigma_n^2} \right] \tag{21}$$

which, when $\mu\sigma_n^2$ is small, can be further approximated as

$$R \approx \sqrt{0.69} \left[1 + \frac{bc\delta}{\mu\sigma_n^2} \right] \geq \sqrt{0.69} \tag{22}$$

Therefore, since this analysis assumes that $bc\delta \ll \mu\sigma_n^2$, the adaptive filter bearing variance is 0.69 times as large (or 1.6 dB better) than the split beam tracker.

It must be reiterated that this analysis includes assumptions whose validity in a practical adaptive tracker configuration have not yet been verified by simulation. During the next phase of this study, simulations will be performed, and the analysis refined, if necessary.

SECTION 3.0
CONCLUSIONS

3.0 CONCLUSIONS AND RELATIONSHIP TO PHASE 3

The feasibility of an adaptive filter as a generic split beam bearing tracker has been supported by detailed investigations into certain of its properties. In particular, it has been shown that the static bearing estimation and dynamic tracking performance are comparable to or better than conventional systems, without having to know the a priori spectral and temporal information needed to properly design a fixed parameter device. The advantages of the adaptive filter tracker are most apparently in the realm of real world sensitivity. In an ideal environment, conventional systems are satisfactory. Yet in actual applications they sometimes produce disappointing performance. The adaptive tracker may provide the additional environmental estimates required to perform closer to the analytical predictions. Thus the third phase of the study will emphasize the use of taped sea data to drive simulations under as many situations as possible. Analyses will stress the inclusion of adverse environmental effects as extensions of the analyses already performed. For example, higher order dynamics, multipaths, and array effects such as beam steering and preformed beam handover will be examined.

A key conclusion of the study of broadband plane wave interference is the bias effect produced on narrowband tracker bearing estimates. Broadband components from different directions within the narrowband of the target energy do not impact on the variance of the estimate anywhere near as significantly as they do on the mean value. This effect may be the limitation in performance for many current narrowband systems. The adaptive tracker, which performs both narrowband and broadband tracking simultaneously from the same set of weight values, may automatically resolve this problem. Since the data to be employed initially is from a towed line array this effect will be studied early in the third phase.

At the conclusion of Phase 3 sufficient real world examination will have been performed to decide whether or not a subsequent sea test of the resulting adaptive filter bearing tracker would be warranted.

REFERENCES

[1] P. L. Feintuch, F. A. Reed, and N. J. Bershad, "Final Report on Phase 1 of the Adaptive Tracking System Study," October 1978, Hughes Aircraft Company Final Report FR78-11-1345, prepared for the Naval Sea Systems Command Code 06H1

[2] J. B. Thomas, "An Introduction to Statistical Communication Theory," New York; John Wiley and Sons, Inc. (1969)

[3] A. J. Viterbi, "Principles of Coherent Communication," New York; McGraw-Hill Book Company (1966)

[4] A. Papoulis, "Probability, Random Variables, and Stochastic Processes," New York; McGraw-Hill Book Company (1965)

[5] H. L. VanTrees, "Detection, Estimation, and Modulation Theory, Part I," New York; John Wiley and Sons, Inc. (1968)

[6] V. H. MacDonald and P. M. Schultheiss, "Optimum Passive Bearing Estimation in a Spatially Incoherent Noise Environment," J. Acoustical Society of America, Vol. 46, No. 1, 1969

[7] G. Clifford Carter, "Time Delay Estimation," Naval Underwater System Center Technical Report #TR-5335, April 1976

APPENDIX A

Appendix A

Bearing Estimation Performance with Stationary Narrowband Signals

During the first phase of this study, the time domain adaptive tracker configuration shown in Figure A-1 was selected for split beam bearing estimation with narrowband signals. The inputs for the narrowband bearing estimation problem can be modeled as

$$d(t) = \sigma_s e^{j\omega_0(t-\tau)} + n_d(t)$$

$$x(t) = \sigma_s e^{j\omega_0(t)} + n_x(t)$$

(A-1)

where n_d and n_x are independent zero mean, white gaussian random processes with power σ^2.

If the target is in the same horizontal plane as the split array phase centers, then

$$\tau = \frac{d}{c} \sin \theta \qquad (A-2)$$

with d the distance between phase center, c the speed of sound, and θ the bearing of the target relative to a normal line to a vertical plane through both phase centers.

It was shown during Phase 1 that the steady state time domain weight vector for these inputs is a sampled sinusoid with a phase shift, $\phi = \omega_0\tau$. To extract this phase angle, the weight vector is Fast Fourier Transformed, and the bin with the largest magnitude chosen as that containing
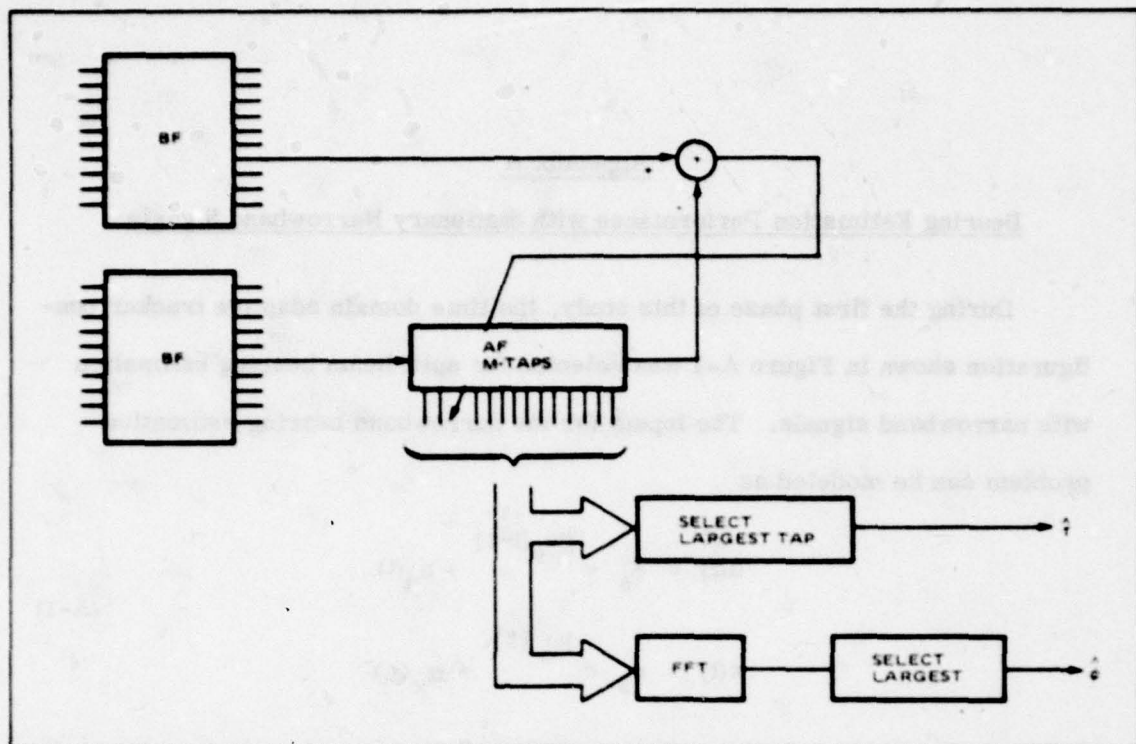
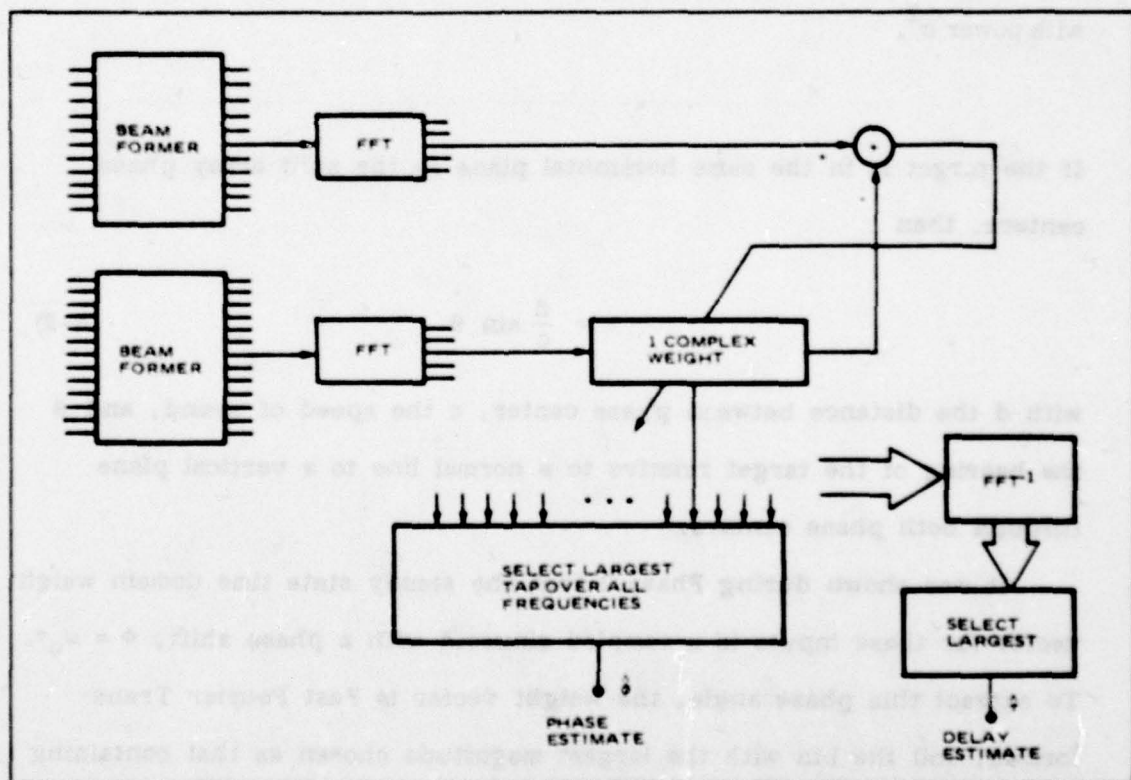**Figure A-1. Split-Beam Adaptive Bearing Estimator Structure**

Figure A-2. Frequency Domain Equivalent Model of System in Figure A-1

the signal. The phase of this bin, which is corrupted by background and algorithm noise, is the estimate of the phase angle.

In order to convert this phase estimate, $\hat{\phi}$, to a bearing estimate, $\hat{\theta}$, it is necessary to know the frequency of the signal, which is not known a priori and must be estimated. This could be done by interpolating between the discrete FFT bins to determine the frequency of the sinusoid. However, it is assumed here that the FFT bins are sufficiently closely spaced that the center frequency of the bin with the largest magnitude is taken as the frequency estimate, $\hat{\omega}_o$. The bearing estimate is then given by

$$\hat{\theta} = \sin^{-1}\left(\frac{c}{d\hat{\omega}_o}\hat{\phi}\right) \tag{A-3}$$

The analysis that follows utilizes the frequency domain model for the adaptive filter shown in Figure A-2. During the first phase of this study, it was shown that this frequency domain configuration behaved equivalently to the time domain filter for broadband inputs, provided the FFT time window is large. The behavior was essentially the same both in transient and steady states.

Mean and Variance of the Frequency Domain Weights

The primary advantage of the frequency domain model for the narrowband tracker shown in Figure A-2 is that it is possible to compute the mean and variance of the weight vector with signal present. This is not possible in general for the time domain realization of the adaptive tracker. In Appendix III of reference [1], the mean and variance of the frequency domain weights were determined for a broadband input signal. Certain results of that appendix can be used here to address the narrow-

A-3

band case under the assumptions that (a) the input sequences are gaussian, (b) the two split array noise outputs are uncorrelated, and (c) both sequences are uncorrelated in time. These assumptions certainly apply to the model given in (A-1). The reference also made the assumption that the inputs were zero mean, which is not true here (the inputs have a time varying, non-zero mean). However, the results used do not require this assumption.

Using the input model given in (A-1). The reference also made the assumption of Figure A-2, the inputs to the single complex tap filter in the kth FFT bin are

$$X_k(m) = \sum_{\ell=0}^{M-1} X[(\ell-mM)T_s] e^{-j\frac{2\pi}{M}\ell k}$$

$$D_k(m) = \sum_{\ell=0}^{M-1} d[(\ell-mM)T_s] e^{-j\frac{2\pi}{M}\ell k} \tag{A-4}$$

or

$$X_k(m) = \sigma_s \frac{\sin\left[\frac{M}{2}\left(\frac{2\pi}{M}k - \omega_o T_s\right)\right]}{\sin\left[\frac{1}{2}\left(\frac{2\pi}{M}k - \omega_o T_s\right)\right]} e^{j\frac{M-1}{2}\left(\frac{2\pi k}{M} - \omega_o T_s\right)}$$

$$+ N_{kx}(m)$$

$$\tag{A-5}$$

$$D_k(m) = \sigma_s \frac{\sin\left[\frac{M}{2}\left(\frac{2\pi}{M}k - \omega_o T_s\right)\right]}{\sin\left[\frac{1}{2}\left(\frac{2\pi}{M}k - \omega_o T_s\right)\right]} e^{-j\omega_o \tau} e^{j\frac{M-1}{2}\left(\frac{2\pi k}{M} - \omega_o T_s\right)}$$

$$+ N_{kd}(m)$$

Note that

$$E\,[N_{kx}(m)] \;=\; E\,[N_{kd}(m)] \;=\; 0$$

$$E\,[N_{kx}(m)\,N_{kd}(m)] \;=\; 0$$

and, for $k \neq o$ or $M/2$,

$$E\,[N_{kx}(m)\,N_{kx}^{*}(p)] = \begin{cases} 0 \;,\; p \neq m \\ M^{2}\,\sigma_{n}^{2} \;,\; p = m \end{cases} \qquad (A-6)$$

It is assumed that the signal is not in the bins $k=o$ or $k=M/2$.

Assuming that the initial weight is zero, from [1], Appendix III, the mean weight is given by

$$E\,[W(n+1)] \;=\; \mu \sum_{m=0}^{n} E[D(m)X^{*}(m)] \prod_{k=m+1}^{n} E[1-\mu|X(k)|^{2}] \qquad (A-7)$$

where, using (A-6),

$$E[D(m)X^{*}(m)] \;=\; |G(k,\omega_{o})|^{2}\sigma_{s}^{2}\,e^{-j\omega_{o}\tau}$$

$$E[\,|X(k)|^{2}] \;=\; |G(k,\omega_{o})|^{2}\sigma_{s}^{2} + M\sigma_{n}^{2}$$

with

$$G(k,\omega_{o}) \;=\; \frac{\sin\left[\dfrac{M}{2}\left(\dfrac{2\pi}{M}\,k - \omega_{o}T_{s}\right)\right]}{\sin\left[\dfrac{1}{2}\left(\dfrac{2\pi}{M}\,k - \omega_{o}T_{s}\right)\right]}\,e^{j\frac{M-1}{2}\left(\dfrac{2\pi}{M}\,k - \omega_{o}T_{s}\right)}$$

Substituting gives

$$E[W(n+1)] = |G(k,\omega_o)|^2 \sigma_s^2 \, \frac{1 - \left[1 - \mu\left(|G(k,\omega_o)|^2 \, \sigma_s^2 + M\sigma_n^2\right)\right]^{n+1}}{|G(k,\omega_o)|^2 \sigma_s^2 + M\sigma_n^2} \cdot e^{-j\omega_o\tau}$$

The steady state mean weight is then
(A-8)

$$E[W(\infty)] = \frac{|G(k,\omega_o)|^2 \, \sigma_s^2}{|G(k,\omega_o)|^2 \sigma_s^2 + M\sigma_n^2} \, e^{-j\omega_o\tau}$$
(A-9)

Again, using Appendix III of reference [1], with the initial weight zero, the mean square weight is

$$E[|W(n+1)|^2] = \mu^2 \sum_{n=0}^{n} E|F(m)|^2 + 2\mu^2 \sum_{m=0}^{n} \sum_{q=0}^{m-1} E[F(m)F^*(q)]$$
(A-10)

with

$$F(m) = D(m)X(m) \prod_{k=m+1}^{n} [1 - \mu|X(k)|^2]$$
(A-11)

It is shown in [1] that,

$$E|F(m)|^2 = E[|D(m)X(m)|^2] \prod_{p=m+1}^{n} E\left\{[1 - \mu|X(p)|^2]^2\right\}$$
(A-12)

Using the gaussian assumption, it is easily shown that

$$E[|d(m)X(m)|^2] = |G(k,\omega_o)|^4 \, \sigma_s^4 + 2M|G(k,\omega_o)|^2 \sigma_s^2 \sigma_n^2 + M^2\sigma_n^4$$
(A-13)

A-6

and

$$E[1 - \mu|X(p)|^2]^2 = 1 - 2\mu[|G(k,\omega_o)|^2 \sigma_s^2 + M\sigma_n^2] + \mu^2[|G(k,\omega_o)|^4 \sigma_s^4$$
$$+ 2M^2\sigma_n^4$$
$$+ 4|G(k,\omega_o)|^2 M\sigma_s^2 \sigma_n^2] \qquad (A\text{-}14)$$

Substituting this in the first sum of (A-11) and closing the sum,

$$\mu^2 \sum_{m=0}^{n} E[F(m)]^2 + \mu \frac{(|G(k,\omega_o)|^2 \sigma_s^2 + M\sigma_n^2)^2}{2(|G(k,\omega_o)|^2 + M\sigma_n^2) - \mu(|G(k,\omega_o)|^4 \sigma_s^4 + 2M^2\sigma_n^4 + 4|G(k,\omega_o)|^2 M\sigma_d^2 \sigma_n^2)}$$

$$\cdot \left[1 - (1 - 2\mu(|G(k,\omega_o)|^2 \sigma_s^2 + M\sigma_n^2) + \mu^2(|G(k,\omega_o)|^4 \sigma_s^4 + 2M^2\sigma_s^2 \sigma_n^2 \right.$$

$$\left. + 4|G(k,\omega_o)|^2 M\sigma_s^2 \sigma_n^2))^{n+1} \right] \qquad (A\text{-}15)$$

Returning to reference [1],

$$E[F(m)F^*(q)] = E\left\{ \prod_{p=m+1}^{n} \prod_{r=m+1}^{n} [1 - \mu|X(p)|^2][1 - \mu|X(r)|^2] \right\}$$

$$E\left\{ D^*(q)X(q) \right\} \cdot E\left\{ D(m)X^*(m)[1 - \mu|X(m)|^2] \right\} \qquad (A\text{-}16)$$

$$\prod_{v=q+1}^{m-1} E[1 - \mu|X(v)|^2]$$

A-7

The first factor is available using (A-14), and it is readily shown that

$$E[D^*(q) X(q)] = |G(k,\omega_o)|^2 \sigma_s^2 e^{j\omega_o \tau} \tag{A-17}$$

and

$$E[D(m) X^*(m)[1 - \mu|X(m)|^2] = |G(k,\omega_o)|^2 \sigma_s^2 e^{-j\omega_o \tau}$$
$$[1 - \mu(|G(k,\omega_o)|^2 \sigma_s^2 + 2M\sigma_n^2)] \tag{A-18}$$

Finally, using (A-14) from above,

$$\prod_{r=q+1}^{m-1} E[1 - \mu|X(r)|^2] = [1 - \mu(|G(k,\omega_o)|^2 \sigma_s^2 + M\sigma_n^2)]^{m-q-1} \tag{A-19}$$

Substituting (A-14), (A-17), (A-18) and (A-19) into (A-16), gives

$$\mu^2 \sum_{m=0}^{n} \sum_{q=0}^{m-1} E[F(m)F^*(q)] = \mu^2 |G(k,\omega_o)|^2 [1 - \mu(|G(k,\omega_o)|^2 \sigma_s^2 + 2M\sigma_n^2)]\sigma_s^4$$

$$\sum_{m=0}^{n} \left\{ [1-2\mu(|G(k,\omega_o)|^2 \sigma_s^2 + M\sigma_n^2) + \mu^2(|G(k,\omega_o)|^4 \sigma_s^4 + 2M^2\sigma_n^2 \right.$$
$$\left. + 4|G(k,\omega_o)|^2 M\sigma_s^2 \sigma_n^2)]^{n-m} \cdot \sum_{q=0}^{m-1} [1 - \mu(|G(k,\omega_o)|^2 \sigma_s^2 + M\sigma_n^2)]^{m-q-1} \right\}$$

$$(A-20)$$

Closing the sums gives

$$\mu^2 \sum_{m=0}^{n} \sum_{q=0}^{m-1} E\{F(m)F^*(q)\} = \frac{|G(k,\omega_o)|^4 \sigma_s^4 [1-\mu(|G(k,\omega_o)|^2\sigma_s^2+M\sigma_n^2)]}{(|G(k,\omega_o)|^2 \sigma_s^2 + M\sigma_n^2)}$$

$$\cdot \left\{ \frac{\left[\begin{array}{l}[1-2\mu(|G(k,\omega_o)|^2\sigma_s^2 + M\sigma_n^2) + \mu^2(|G(k,\omega_o)|^4\sigma_s^4 + 2M^2\sigma_n^4 \\ +4|G(k,\omega_o)|^2 M\sigma_s^2\sigma_n^2]^{n+1} - [1-\mu(|G(k,\omega_o)|^2 + M\sigma_n^2]^{n+1}\end{array}\right]}{\left[\begin{array}{l}(|G(k,\omega_o)|^2\sigma_s^2 + M\sigma_n^2) - \mu(|G(k,\omega_o)|^4\sigma_s^4 + 2M^2\sigma_n^4 \\ + 4|G(k,\omega_o)|^2 M\sigma_s^2\sigma_n^2\end{array}\right]} \right.$$

$$\left. - \frac{[1-2\mu(|G(k,\omega_o)|^2\sigma_s^2+M\sigma_n^2) + \mu^2(|G(k,\omega_o)|^4\sigma_s^4 + 2M^2\sigma_n^4 + 4|G(k,\omega_o)|^2 M\sigma_s^2\sigma_n^2]^{n+1} - 1}{2(|G(k,\omega_o)|^2\sigma_s^2+M\sigma_n^2) - \mu(|G(k,\omega_o)|^4\sigma_s^4 + 2M^2\sigma_n^4 + 4|G(k,\omega_o)|^2 M\sigma_s^2\sigma_n^2} \right\} \tag{A-21}$$

To obtain the steady state weight, the limit of (A-15) and (A-21) is taken as

$n \to \infty$ and the results summed. Under the conditions, given in (A-24),

$$E\{|W(\infty)|^2\} = \frac{1}{2(|G(k,\omega_o)|^2\sigma_s^2 + M\sigma_n^2) - \mu(|G(k,\omega_o)|^4\sigma_s^4 + 2M^2\sigma_n^4 + 4|G(k,\omega_o)|^2 M\sigma_s^2\sigma_n^2)}$$

$$\cdot \left\{ \mu(|G(k,\omega_o)|^2\sigma_s^2 + M\sigma_n^2)^2 \right.$$

$$\left. + \frac{2|G(k,\omega_o)|^4\sigma_s^4(1 - \mu(|G(k,\omega_o)|^2\sigma_s^2 + 2M\sigma_n^2)}{|G(k,\omega_o)|^2\sigma_s^2 + M\sigma_n^2} \right\} \tag{A-22}$$

A-9

To obtain the variance of the weight, subtract the magnitude squared of the steady state mean weight, with the result that

$$\text{Var}\left[W(\infty)\right] = \frac{\left(2\mu M\sigma_n^2 \left[|G(k,\omega_o)|^4\sigma_s^4 + |G(k,\omega_o)|^2 M\sigma_s^2\sigma_n^2 + M^2\sigma_n^4\right]\right)\left(\mu(|G(k,\omega_o)|^2\sigma_s^2 + M\sigma_n^2) - \mu M^4\sigma_n^8\right)}{\left(|G(k,\omega_o)|^2\sigma_s^2 + M\sigma_n^2\right)^2\left[2\left(|G(k,\omega_o)|^2\sigma_s^2 + M\sigma_n^2\right) - \mu\left(|G(k,\omega_o)|^4\sigma_s^4 + |G(k,\omega_o)|^2 M\sigma_s^2\sigma_n^2 + 2M^2\sigma_n^4\right)\right]} \quad \text{(A-23)}$$

These statistics of the weight vector allow numerical evaluation of the bearing estimation bias and variance.

It is important to note the convergence conditions for these results. The steady state mean and variance, (A-9) and (A-23), follow from (A-8) and A-22). respectively, if

$$\left| 1 - \mu\left(|G(k,\omega_o)|^2 \sigma_s^2 - M\sigma_n^2\right) \right| < 1$$

and

$$\left| 1 - 2\mu(|G(k,\omega_o)|^2\sigma_s^2 + M\sigma_n^2) + \mu^2(|G(k,\omega_o)|^4\sigma_s^4 + 4|G(k,\omega_o)|^2 M\sigma_s^2\sigma_n^2 + M^2\sigma_n^4) \right| < 1$$

Defining the signal-to-noise ratio in the bin as

$$\gamma = \frac{|G(k\,\omega_o)|^2\sigma_s^2}{M\sigma_n^2}$$

these requirements lead to the following sufficient conditions;

$$0 < \mu M\sigma_n^2 \,(\gamma + 1) < 1 \quad \text{(A-24)}$$

A-10

and

$$\mu M q_n^2 (\gamma^2 + 4\gamma + 2) < 2(\gamma + 1)$$

These conditions will be important in evaluating the variance of the bearing estimate in the section to follow.

BIAS AND VARIANCE OF THE BEARING ESTIMATE

The estimation process consists of extracting the phase from the FFT bin with the largest magnitude, so it is necessary to obtain the density of the phase in each FFT bin. Because the input statistics are gaussian and a large number of iterations of the weight recursion equation can be assumed, the frequency domain weights may be regarded as complex gaussian random variables. Therefore, the density of the phase of the kth frequency domain weight can be obtained by transforming the two dimensional gaussian density of the real and imaginary parts of W_k to polar coordinates. This gives [2]

$$f_{R,\phi}(r,\phi) = \frac{1}{2\pi\sigma^2 r^2} \exp\left\{ -\frac{1}{2\sigma^2}(r^2 + a^2 - 2ar\cos(\phi - \omega_o \frac{d}{c}\sin\theta)) \right\}$$

with

$$R = |W_k|, \ \phi = \arg(W_k), \ \sigma^2 = \frac{1}{2}\text{Var}[W_k], \ a = |E(W_k)| \qquad (A-25)$$

The phase density is obtained by integrating with respect to r: [2]

$$f_\phi(\phi) = \frac{\exp(-a^2/2\sigma^2)}{2\pi} + \frac{a\cos\left(\phi - \omega_o \frac{d}{c}\sin\theta\right)}{2(2\pi)^{\frac{1}{2}}\sigma} \exp\left[-\frac{a^2}{2\sigma^2}\sin^2\left(\phi - \omega_o \frac{d}{c}\sin\theta\right)\right]$$

$$\cdot \left[1 + \operatorname{erf}\left(\frac{a\cos\left(\phi - \omega_o \frac{d}{c}\sin\theta\right)}{\sqrt{2}\sigma}\right)\right]$$

$$\operatorname{erf}(x) \triangleq \frac{2}{\pi^{\frac{1}{2}}} \int_0^x e^{-z^2} dz \tag{A-26}$$

The variance of the phase can be obtained by numerical integration of (A-26).

The result is parametric in

$$\beta^2 = \frac{a^2}{2\sigma^2}$$

which for the adaptive tracker is given by

$$\beta^2 = \frac{|G(k,\omega_o)|^4 \sigma_s^4 \left(2(|G(k,\omega_o)|^2 \sigma_s^2 + M\sigma_n^2) - \mu(|G(k,\omega_o)|^4 \sigma_s^4 + 4|G(k,\omega_o)|^2 M\sigma_s^2\sigma_n^2 + 2M^2\sigma_n^4)\right)}{2\mu M\sigma_n^2 \left(|G(k,\omega_o)|^2 \sigma_s^2 + M\sigma_n^2\right)\left(|G(k,\omega_o)|^4 \sigma_s^4 + |G(k,\omega_o)|^2 M\sigma_s^2\sigma_n^2 + M^2\sigma_n^4\right)}$$

where

$$G(k,\omega_o)^2 = \frac{\sin^2\left[\pi k - \frac{\omega_o M \tau_s}{2}\right]}{\sin^2\left[\frac{\pi k}{M} - \frac{\omega_o \tau_s}{2}\right]} \tag{A-27}$$

Suppose that the signal-to-noise ratio in the kth bin is denoted by

$$\gamma = \frac{|G(k,\omega_o)|^2 \sigma_s^2}{M\sigma_n^2}$$

Then

$$\beta^2 = \mu^{-1} \frac{\gamma^2 (2(\gamma+1) - \mu M\sigma_n^2 (\gamma^2 + 4\gamma + 2))(\gamma+1)}{(2\gamma^3 + 4\gamma^2 + 4\gamma + 1)\left[|G(k,\omega_o)|^2 \sigma_s^2 + M\sigma_n^2\right]} \tag{A-28}$$

When a steady state weight exists, that is, when the convergence conditions of (A-24) are met, this quantity is positive, as required. The time constant of the filter is

$$\tau_I = \left[\mu \left(|G(k,\omega_o)|^2 \sigma_s^2 + M \sigma_n^2 \right) \right]^{-1}$$

so

$$\beta^2 = \frac{\gamma^2 \left(2(\gamma+1) - \mu M \sigma_n^2 (\gamma^2 + 4\gamma + 2)\right)(\gamma+1)}{(2\gamma^3 + 4\gamma^2 + 4\gamma + 1)} \tau_I \qquad \text{(A-29)}$$

At high signal to noise ratio, this is approximately

$$\beta^2 \approx \frac{\gamma^3 (2\gamma - \mu M \sigma_n^2 \gamma^2)}{2\gamma^3} \tau_I$$

$$\approx \gamma \tau_I - \frac{\mu M \sigma_n^2 \gamma^2}{2 \mu M \sigma_n^2 (\gamma+1)} \approx (\tau_I - \tfrac{1}{2}) \gamma, \quad \gamma \gg 1 \qquad \text{(A-30)}$$

In most practical applications, $\tau_I \gg 1$, so

$$\beta^2 \approx \tau_I \gamma, \quad \gamma \gg 1$$

A special case of particular interest is when the time domain input is real, that is, (A-1) is replaced by

$$d(t) = \sigma_s \sin[\omega_o(t-\tau)] + N_d(t) \qquad \text{(A-31)}$$

$$x(t) = \sigma_s \sin(\omega_o t) + N_x(t)$$

For a real sinusoidal input, the FFT power gain is no longer given by (A-27), and the expressions for the variance are considerably more complicated. For example, while for the complex case,

$$\sum_{N=0}^{M-1} \sum_{M=0}^{M-1} e^{j\omega_0(nTs-\tau)} \; e^{j\omega_0 MT_s} \; e^{-j\frac{2\pi}{M}(n-m)k} = \left|G(k,\omega_0)\right|^2 e^{-j\omega_0\tau}$$

the real case gives

$$\sum_{n=0}^{M-1} \sum_{m=0}^{M-1} \sin\left[\omega_0(nT_s-\tau)\right] \sin\left[\omega_0 mT_s\right] e^{-j\frac{2\pi}{M}(n-m)k}$$

$$= \frac{1}{4}\left|G(k,\omega_0)\right|^2 e^{-j\omega_0\tau} + \frac{1}{4}\left|G(-k,\omega_0)\right|^2 e^{j\omega_0\tau}$$

$$+ \frac{1}{2}\left|G(k,\omega_0)\right|\left|G(-k,\omega_0)\right| \cos\left[\phi - (M-1)\omega_0 T_s\right]$$

Fortunately, when ω_0 is near bin center, the results given above hold if $\left|G(k,\omega_0)\right|^2$ is replaced by

$$\left|G_r(k,\omega_0)\right|^2 = \frac{1}{2}\left|G(k,\omega_0)\right|^2 \qquad\qquad (A-32)$$

and the signal power is appropriately adjusted.

Of interest are the statistics of $\hat{\theta}$ rather than that of the phase. The bearing estimate is given by

$$\hat{\theta} = \sin^{-1}\left(\frac{c}{\dot{\omega}_0 d}\dot{\phi}\right)$$

where $\hat{\omega}_0$ is the center frequency of the bin with the largest magnitude. Assuming that sufficient integration is used to assure selection of the bin closest to the signal, call it bin k,

$$\hat{\theta} = \sin^{-1}\left(\frac{cM\tau_s}{2\pi kd}\phi_k\right)$$

with ϕ_k the phase of the kth bin. Then

$$E\,[\hat{\theta}] = \int_{-\pi}^{\pi} \sin^{-1}\left(\frac{cM\tau_s}{2\pi kd}\phi\right) f_{\phi_k}(\phi)\,d\phi$$

$$E\,[\hat{\theta}^2] = \int_{-\pi}^{\pi}\left[\sin^{-1}\left(\frac{cM\tau_s}{2\pi kd}\phi\right)\right]^2 f_{\phi_k}(\phi)\,d\phi \qquad \text{(A-33)}$$

and

$$\text{Var}\,[\hat{\theta}] = E\,[\hat{\theta}^2] - E^2\,[\hat{\theta}].$$

While these integrals cannot be evaluated explicitly, they are readily evaluated numerically on the computer.

Some care is required in interpreting the bearing statistics determined by this method due to the modulo 2π assumption inherent in the derivation of the phase density. The bearing estimate given by

$$\theta = \sin^{-1}\left(\frac{cM\tau_s}{2\pi kd}\phi_k\right)$$

has considered ϕ_k to be on $[-\pi, \pi)$, that is, modulo 2π, so assuming the principal value of the arc sine, the bearing estimate is restricted to

$$|\theta| \leqslant \sin^{-1}\left(\frac{cM\tau_s}{2\pi kd}\pi\right)$$

Typically, the distance between phase centers, d, is many wavelengths, so

$$\frac{cM\tau_s}{2kd} \ll 1$$

and

$$|\hat{\theta}| \ll \pi$$

For a given split array beam, the estimate is limited to some small fraction of 180°. This presents no practical difficulty, since bearing trackers generally use a beam steered near the target. However, it does impact the interpretation of the bearing error statistics computed by the above method.

Suppose the actual bearing angle is θ degrees, where θ is such that

$$\left|\frac{\omega_o d}{c}\sin\theta\right| < \pi$$

This corresponds to the "correct" value of ϕ_k being on $[-\pi, \pi)$, just as interpreted above. Now, a sufficiently large fluctuation in the weight, W_k, can cause the phase angle to change more than a half cycle, to say, $\phi_k + \Delta\phi$. This should correspond to a bearing

$$\hat{\theta} = \sin^{-1}\left(\frac{cM\tau_s}{2\pi kd}(\phi_k + \Delta\phi)\right)$$

but by the modulo 2π interpretation of ϕ_k,

$$\hat{\theta} = \sin^{-1}\left(\frac{cM\tau_s}{2\pi kd}\alpha\right), \alpha\epsilon[-\pi\pi).$$

The statistics of the bearing estimate as derived above do not, therefore, reflect the true bearing error statistics when the phase makes frequent excursions of more than π radians. This is similar to the consideration of cycle skipping in the analysis of phase errors in phase locked loops[3].

The phase density, (A-26), is shown in Figure A-3 as a function of the parameter β^2. It can be seen that for the parameter $\beta^2 > 1$, the density is essentially zero near $\phi = \pm \pi$, so such excursions are unlikely. Under this condition, the bearing estimate statistics evaluated by the method given above should be valid. Figure A-4 shows the standard deviation of ϕ as a function β^2, computed numerically from (A-26). For $\beta^2 = 1$, the phase standard deviation is 48°. If θ is small, this give a bearing error standard deviation of approximately $(48 \, c/\omega_o d)$. This is a nominal upper bound on the range over which the results of this section are valid.

Figure A-5 shows the predicted rms bearing error for a particular real adaptive tracker, computed as described above. The split array has 150 ft between phase centers, and the signal is a 100 Hz real sinusoid embedded in white gaussian noise. The FFT has 128 points and a resolution of 2 Hz, so the signal is centered in the 50th bin. The figure shows the rms bearing error as a function of the signal-to-noise ratio at the FFT input for various values of the weight feedback coefficient, μ. In keeping with the comments of the preceding paragraph, the curve is valid for rms bearing error of less than 2.54°. Further, the curves are only plotted over the range of signal-to-noise ratio for which the stability conditions of the preceding section are met accounting for the endpoints on the curves for $\mu = 2^{-11}$, 2^{-12}, and 2^{-13}. Computer simulations over 10 ensembles are also shown on the figure, supporting the analytical predictions.
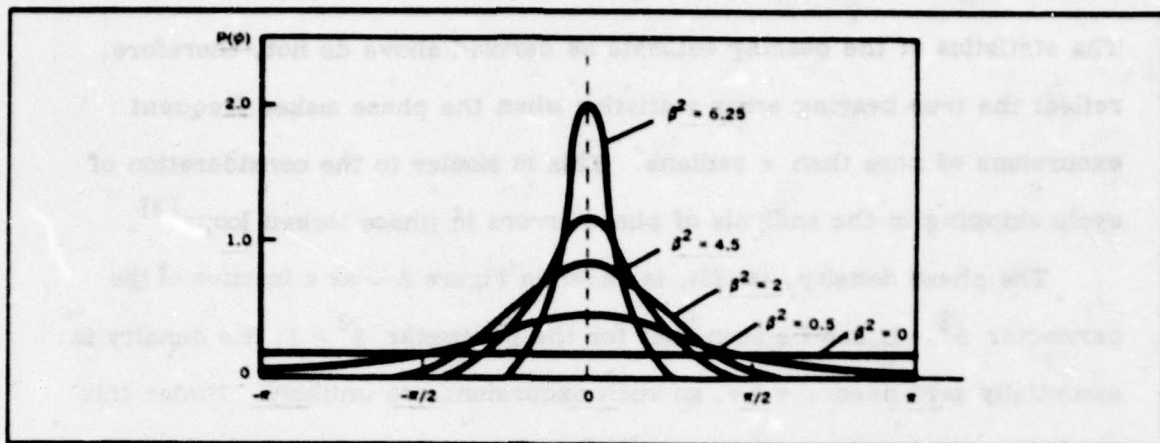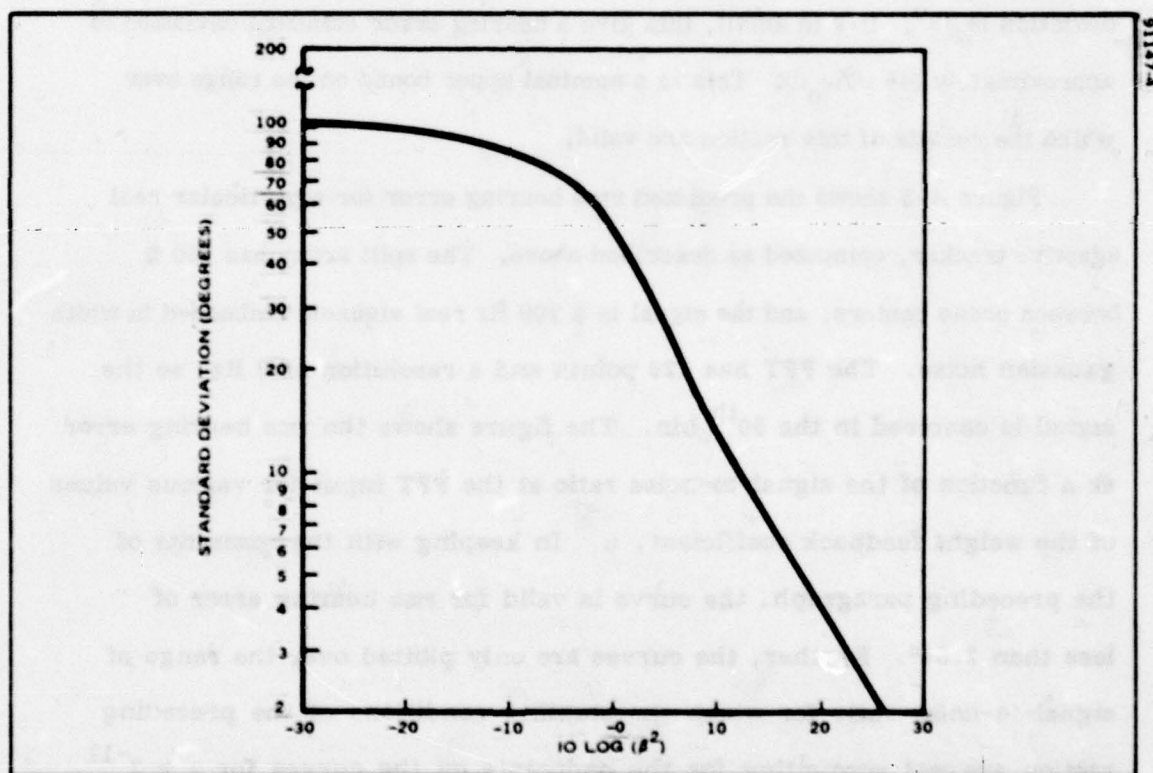
Figure A-3. Phase Density for Various Values of β^2

Figure A-4. Standard Deviation of Phase for Density of Figure 3
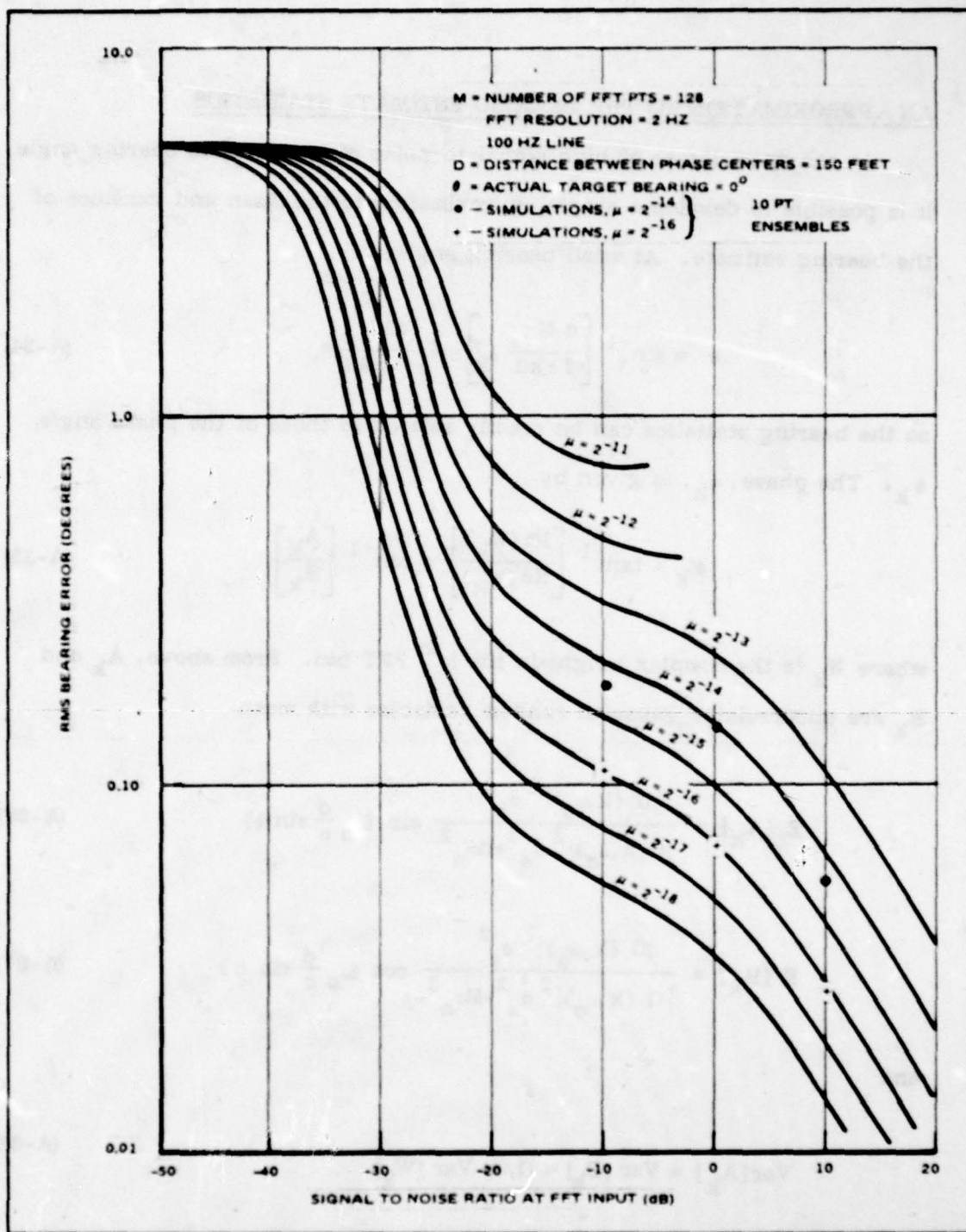
A-18

Figure A-5. Predicted RMS Bearing Error

AN APPROXIMATION TO THE BEARING ESTIMATE STATISTICS

In the special case of high signal-to-noise ratio and small bearing angle, it is possible to develop a simple approximation to the mean and variance of the bearing estimate. At small bearing angles

$$\hat{\theta} = \sin^{-1}\left[\frac{c\,M\,\tau_s}{2\pi kd}\phi_k\right] \approx \frac{cMT_s}{2\pi kd}\phi_k \qquad (A-34)$$

so the bearing statistics can be readily related to those of the phase angle ϕ_k. The phase, ϕ_k, is given by

$$\phi_k = \tan^{-1}\left[\frac{Im(W_k)}{Re(W_k)}\right] = \tan^{-1}\left[\frac{A_k}{B_k}\right] \qquad (A-35)$$

where W_k is the complex weight in the kth FFT bin. From above, A_k and B_k are uncorrelated gaussian random variables with mean

$$E[A_k] = \frac{|G(k\omega_o)|^2\sigma_s^2}{|G(k,\omega_o)|^2\sigma_s^2 + M\sigma_n^2}\sin\left(\omega_o\frac{d}{c}\sin\theta\right) \qquad (A-36)$$

$$E[B_k] = \frac{|G(k,\omega_o)|^2\sigma_s^2}{|G(k\omega_o)|^2\sigma_s^2 + M\sigma_n^2}\cos\left(\omega_o\frac{d}{c}\sin\theta\right) \qquad (A-37)$$

and

$$(A-38)$$

$$Var[A_k] = Var[B_k] = (1/2)\,Var[W_k]$$

where $Var[W_k]$ is given in (A-23).

It is possible to approximate the expectation of a function of two random variables, $g(x,y)$, given the joint density function of x and y, $p_{xy}(x,y)$, by expanding $g(x,y)$ in a Taylor series.

$$g(x,y) = g(a,b) + \left[\frac{\partial g}{\partial x}(x-a) + \frac{\partial g}{\partial y}(y-b) \right] + \frac{1}{2!} \left[\frac{\partial g^2}{\partial x^2}(x-a)^2 \right.$$

$$\left. + 2 \frac{\partial g^2}{\partial x \partial y}(x-a)(y-b) + \frac{\partial g^2}{\partial y^2}(y-a)^2 \right] + \dots \qquad (A-39)$$

where

$$\frac{\partial g^n}{\partial x^{n-r} \partial x^r} = \left. \frac{\partial g^{n}(x,y)}{\partial x^{n-r} \partial y^r} \right|_{\substack{x=a \\ y=b}}$$

If $a = \eta_x$ and $b = \eta_y$, the means of x and y, the joint density $p_{xy}(x,y)$ is concentrated near (η_x, η_y), and $g(x,y)$ is smooth in the vicinity of (η_x, η_y), then $E[g(x,y)]$ can be approximated by retaining second order terms in (A-39) giving[4]

$$E[g(x,y)] \approx g(\eta_x, \eta_y) + \frac{1}{2} \left(\sigma_x^2 \frac{\partial^2 g}{\partial x^2} + 2 \mu_{xy} \frac{\partial^2 g}{\partial x \partial y} + \sigma_y^2 \frac{\partial^2 g}{\partial y^2} \right)_{\substack{x=\eta_x \\ y=\eta_y}} \qquad (A-40)$$

with $\mu_{xy} = E[(x - \eta_x)(y - \eta_y)]$. Similarly, by expanding $g^2(x,y)$ in a Taylor series and retaining only second order terms, it can be shown that[4]

$$\sigma^2_{g(x,y)} \approx \left. \left(\frac{\partial g}{\partial x} \right)^2 \sigma_x^2 + \left(\frac{\partial g}{\partial y} \right)^2 \sigma_y^2 + 2 \frac{\partial g}{\partial x} \frac{\partial g}{\partial y} \mu_{xy} \right|_{\substack{x=\eta_x \\ y=\eta_y}} \qquad (A-41)$$

The case of interest here is $g(x,y) = \tan^{-1}\left(\frac{y}{x}\right)$ with $y = A_k$, $x = B_k$, so

$$n_y = E[y] = C_1 \sin\left(\frac{\omega_o d}{c}\sin\theta\right), \quad n_x = E(x) = C_1\cos\left(\frac{\omega_o d}{c}\sin\theta\right) \quad (A-42)$$

$$\sigma_x^2 = \sigma_y^2 = \text{Var}[A_k], \quad \mu_{xy} = 0, \quad \text{and} \quad C_1 = \frac{\left|G(k,\omega_o)\right|^2 \sigma_s^2}{\left|G(k,\omega_o)\right|^2 \sigma_s^2 + M\sigma_\eta^2} .$$

To evaluate these approximations, we need the derivatives $\partial g/\partial x$, $\partial g/\partial y$, $\partial^2 g/\partial x^2$, $\partial^2 g/\partial y^2$ are needed.

Care must be taken in the interpretation of $g(x,y)$ if the result is to be valid for $\theta \epsilon [-\pi, \pi]$. This is due to the fact that

$$a = \tan^{-1}(a)$$

is generally assumed to return $a \epsilon [-\frac{\pi}{2}, \frac{\pi}{2}]$. The estimator, on the other hand, returns $\hat{\theta} \epsilon [-\pi, \pi]$ by recognizing the signs of x and y. Therefore, $g(x,y)$ is properly defined as

$$g(x,y) = {}^*\tan^{-1}\left(\frac{y}{x}\right)$$

where ${}^*\tan(\cdot)$ includes the quadrant resolution using the signs of x and y. Using n_x, n_y, σ_x and σ_y from (A-42), the derivatives in (A-40) and (A-41) are

$$\frac{\partial g}{\partial x} = -\frac{C_1\sin\lambda}{(C_1^2\sin^2\lambda + C_1^2\cos^2\lambda)} = -\frac{\sin\lambda}{C_1}$$

$$\frac{\partial g}{\partial y} = \frac{C_1\cos\lambda}{(C_1^2\sin^2\lambda + C_1^2\cos^2\lambda)} = \frac{\cos\lambda}{C_1}$$

$$\frac{\partial^2 g}{\partial x^2} = \frac{2(C_1\cos\lambda)C_1\sin\lambda}{(C_1^2\sin^2\lambda + C_1^2\sin^2\lambda)^2} = \frac{\sin 2\lambda}{C_1^2} \qquad (A-43)$$

$$\frac{\partial^2 g}{\partial y^2} = -\frac{\sin 2\lambda}{C_1^2}, \quad \lambda = \omega_o\frac{d}{c}\sin\theta$$

Therefore,

$$E[\phi_k] \approx \tan^{-1}\left[\frac{C_1 \sin\lambda}{C_1 \cos\lambda}\right] + \frac{1}{2}\frac{1}{C_1^2}\left[\sigma_x^2 \sin 2\lambda - \sigma_y^2 \sin 2\lambda\right] = \frac{\omega_o d}{c}\sin\theta \quad \text{(A-44)}$$

and

$$\text{Var}[\phi_k] = \frac{\sigma_x^2}{C_1^2}\sin^2\lambda + \frac{\sigma_y^2}{C_1^2}\cos^2\lambda = \frac{\sigma_x^2}{C_1^2} \quad \text{(A-45)}$$

Using the small bearing angle approximation, (A-34), we get

$$E[\dot{\theta}] \approx \frac{kMT_s}{2\pi kd} E[\phi_k]$$

and, using the definition of β from (A-29),

$$\text{Var}[\dot{\theta}] \approx \frac{M^2 T_s^2}{(2\pi k)^2}\frac{C^2}{d^2}\frac{1}{2\beta^2} \quad \text{(A-46)}$$

$$= \frac{M^2 T_s^2}{(2\pi k)^2}\frac{C^2}{d^2}\frac{(2\gamma^3 + 4\gamma^2 + 4\gamma + 1)}{\gamma^2[2(\gamma + 1) - \mu M \sigma_n^2(\gamma^2 + 4\gamma + 2)](\gamma + 1)\tau_I}$$

This approximation is compared with the numerically evaluated r.m.s. bearing error for a particular real adaptive filter in Figures A-6 through A-8. The tracker uses a 128 point FFT with two Hz resolution. The 100 Hz real sinusoidal signal embedded in white noise is centered in the 50th FFT bin. The results are given for three values of μ, and, as before, the curves are only plotted over the range of SNR for which the filter is stable. The target bearing is zero degrees. As can be seen, the approximation, (A-46), gives excellent
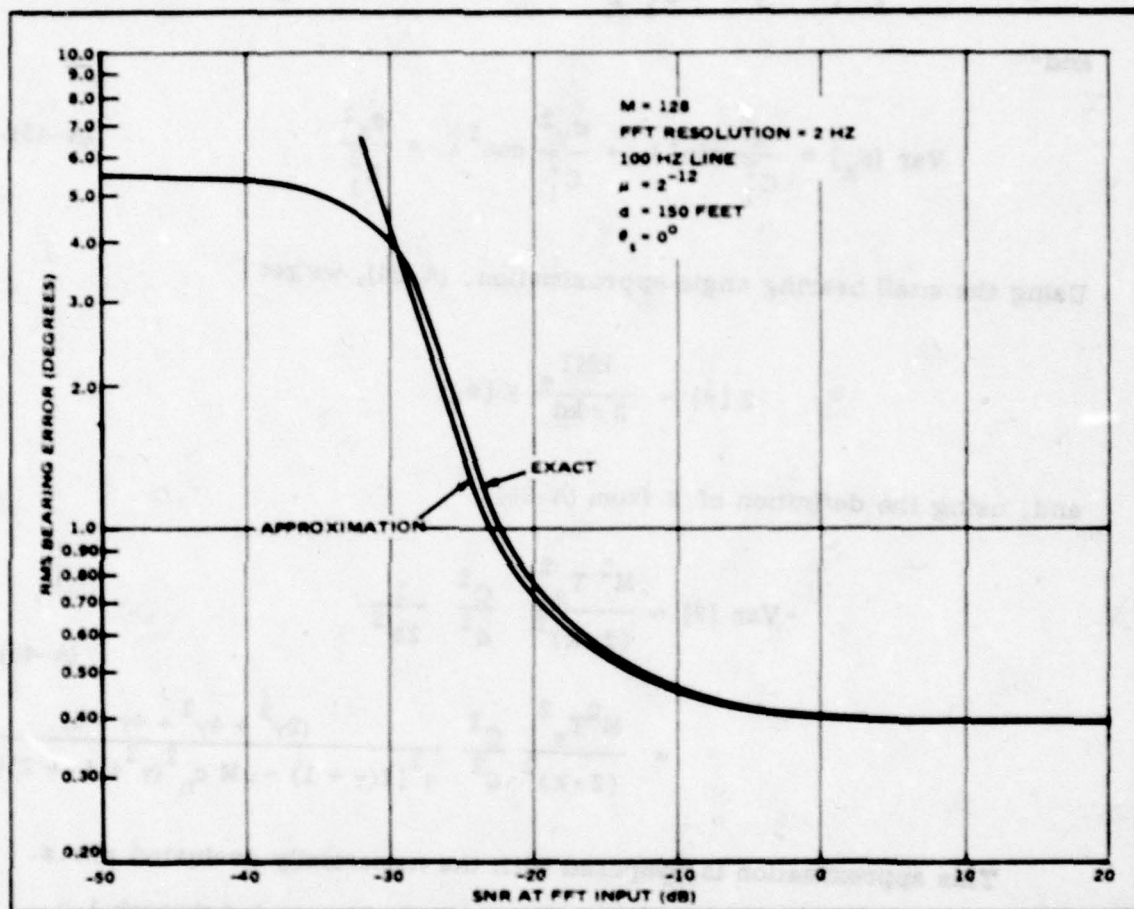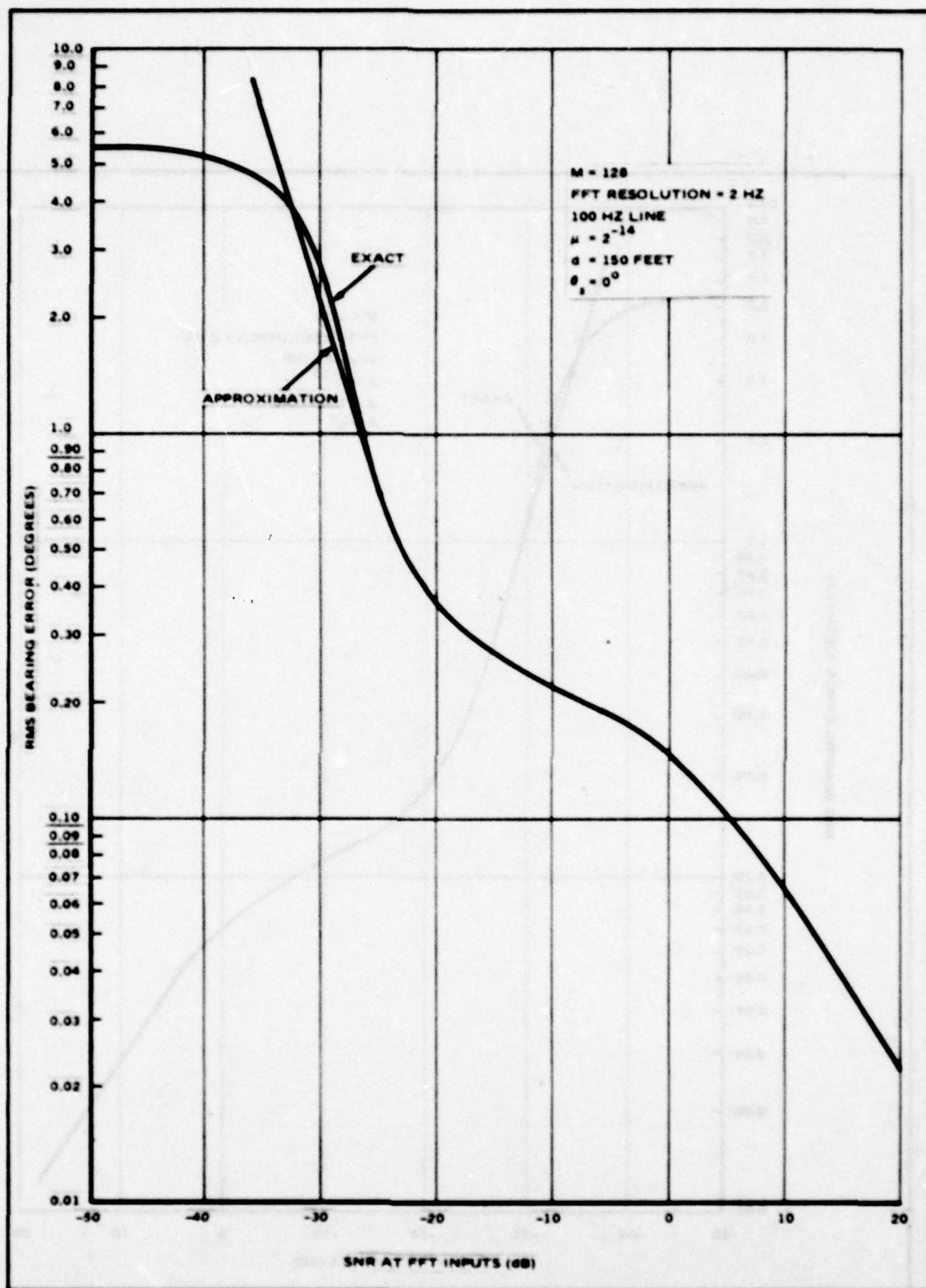
A-23

Figure A-6. Comparison of Predicted RMS Bearing Error With Approximation

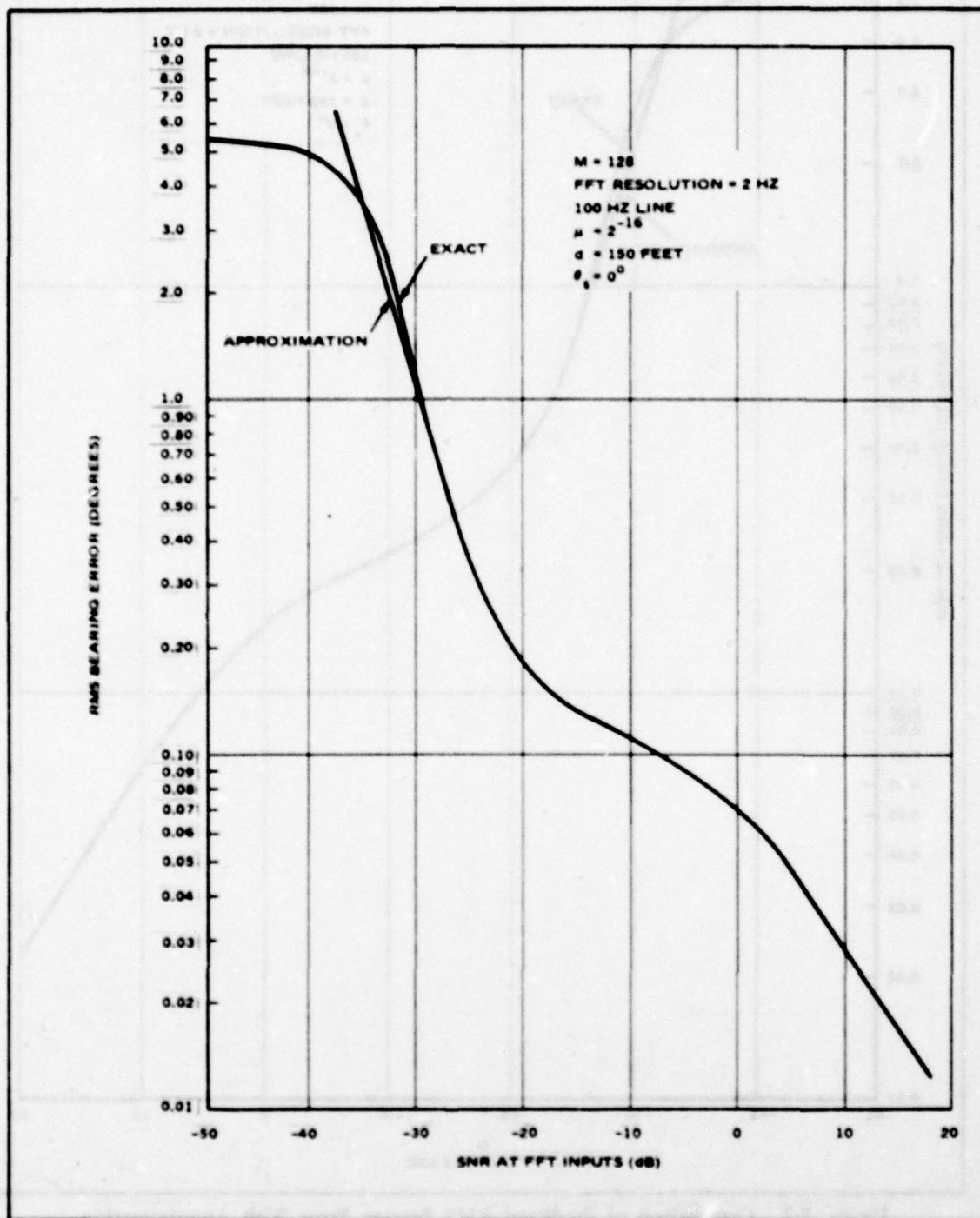Figure A-7. Comparison of Predicted RMS Bearing Error With Approximation

A-25

Figure A-8. Comparison of Predicted RMS Bearing Error with Approximation

A-26

agreement with the numerical computation over the range for which the analysis is valid, that is, for standard deviation less than 2.54 degrees. This suggests that for small bearing angles, the numerical computation can be avoided.

SIMULATIONS OF THE NARROWBAND ADAPTIVE TRACKER

Simulations of the narrowband case were performed for two array configurations, each with a different signal frequency embedded in white Gaussian noise. A vernier FFT with a resolution of 2 Hz is positioned around the location of the narrowband signal, with the signal centered in one of the frequency bins. The phase of that bin is extracted and converted to a bearing estimate. The computer calculates the mean and variance of the estimate using a sliding window, and generates a plot of the estimate vs. time.

The simulation model is a PDP-11/70 computer implementation of the tracker, driven by pseudo-random noise and signal generators designed to simulate environments of interest, as shown in Figure A-9. Three independent pseudo-random gaussian noise (PRGN) generators provide independent background noise for the simulated half array outputs and the broadband signal. These are each passed through a finite impulse response filter with selectable response, allowing simulations of various signal and noise spectra. The inter-array delay can be injected either as a fixed value, or can vary with time. In addition, a sinusoidal signal component can be added to the simulated array output, with the appropriate phase shift between array halves. The model also includes the capability to plot the resulting estimates, and to compute second order statistics using a sliding window technique.

The first array simulated has 150 feet between phase centers, and a 100 Hz line emanating from a target at 0° bearing relative to broadside. The vernier 16 point FFT is positioned such that the line is centered in FFT bin number four.

GAUSSIAN PR NOISE GENERATOR

FIR FILTER

SIMULATED LEFT HALF ARRAY OUTPUT

GAUSSIAN PR NOISE GENERATOR

FIR FILTER

TIME DELAY (FIXED OR TIME VARYING)

SINE WAVE GENERATOR

PHASE SHIFT (FIXED OR TIME VARYING)

GAUSSIAN PR NOISE GENERATOR

FIR FILTER

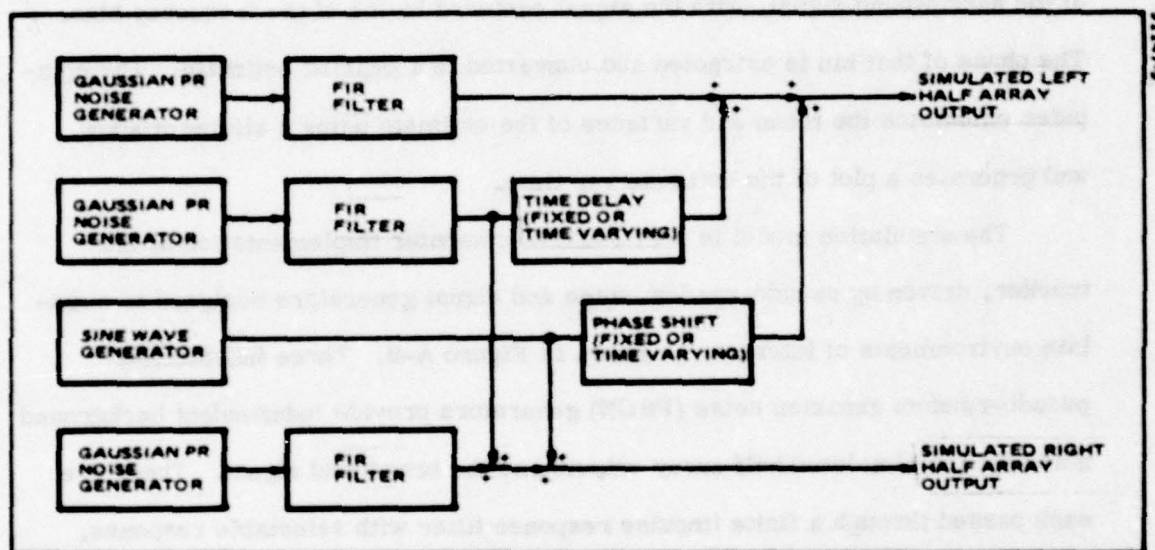SIMULATED RIGHT HALF ARRAY OUTPUT

Figure A-9. Simulation Model For Adaptive Tracker Inputs

A-28

Figures A-10 through A-12 show the bearing estimate vs time for a feedback coefficient, μ, of 2^{-12} and input signal-to-noise ratios of 9, -1, and -11 dB. The input SNR is measured in the entire FFT input band, and the selection of μ yields a time constant of 128 seconds for the adaptive filter. The simulations are approximately 8 time constants in duration. Figures A-13 through A-16 show the same data for $\mu = 2^{-14}$ and SNRs of 9, -1, -11, and -21 dB. In this case, the time constant is 512 seconds, so the runs are about 2 time constants long. Figure A-17 compares the simulation results with theoretically predicted values. In all cases, the statistics were computed over the 270 most recent estimates.

The other array simulated has 75 feet between phase centers and a 600 Hz signal from a target at broadside. As above, the 16 point FFT is positioned such that the signal is bin-centered in frequency bin number four. Figures A-18 through A-20 show the bearing estimate vs time for $\mu = 2^{-10}$ and SNRs of 10, 0, and -10 dB. The time constant is 32 seconds, and the simulations are about 31 time constants in duration. Figures A-21 through A-23 give the results for $\mu = 2^{-12}$, and for the same SNRs, corresponding to a 128 second time constant and a run duration of 8 time constants. The results for $\mu = 2^{-14}$, with SNR's of 10, 0, -10, and -20 dB, respectively, are shown in Figures A-24 through A-27. These have a time constant of 512 seconds and simulation length of approximately 4 time constants. The simulation results are compared to the theoretical predictions (computed as described earlier) in Figure A-28, where statistics were computed over the 200 most recent estimates.

Finally, simulation runs were made using the tracker configuration used in the predictions of Figure A-5. Since the analysis has assumed that the FFT bin containing the signal is selected for phase extraction, it was felt that the best

Figure A-10. Bearing Estimate Versus Time For NB Tracker

Figure A-11. Bearing Estimate Versus Time

A-31

Figure A-12. Bearing Estimate Versus Time

A-32

Figure A-13. Bearing Estimate Versus Time

A-33

Figure A-14. Bearing Estimate Versus Time

A-34

Figure A-15. Bearing Estimate Versus Time

A-35
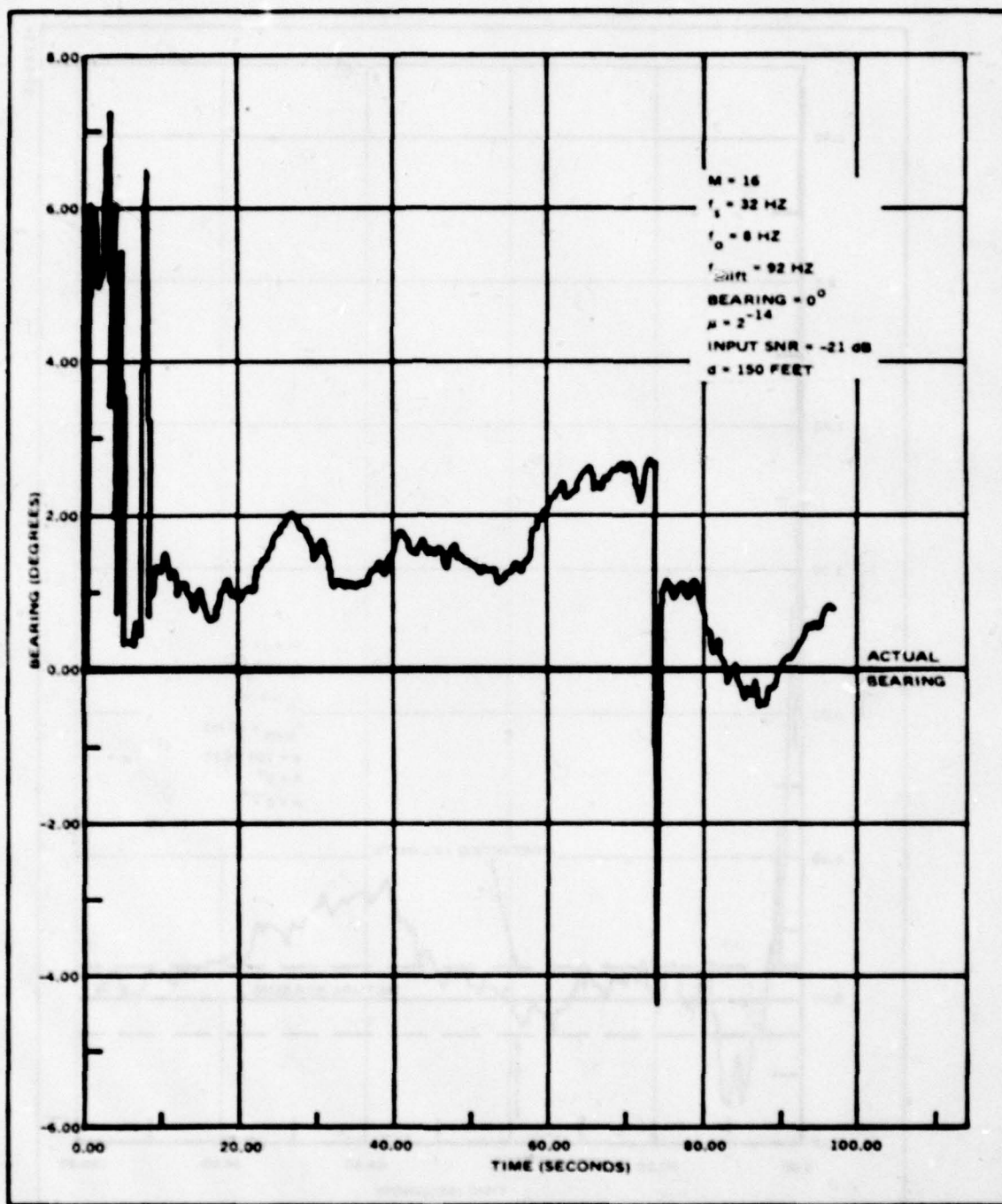
Figure A-16. Bearing Estimate Versus Time

The chart shows Bearing (Degrees) on the vertical axis from -6.00 to 8.00 versus Time (Seconds) on the horizontal axis from 0.00 to 100.00. Parameters listed:

M = 16
f_s = 32 HZ
f_o = 8 HZ
f_shift = 92 HZ
BEARING = 0°
μ = 2^{-14}
INPUT SNR = -21 dB
d = 150 FEET

ACTUAL BEARING
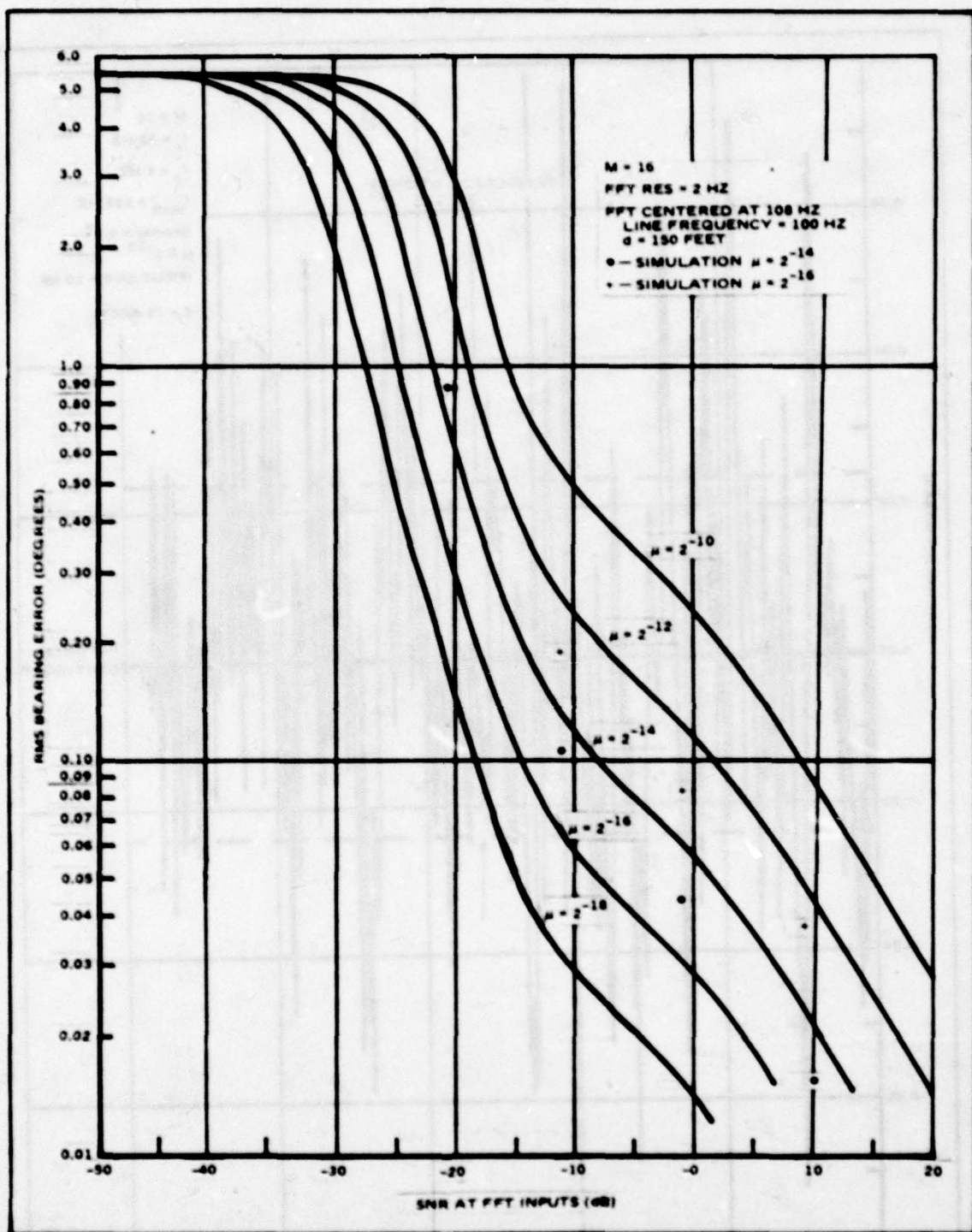
Figure A-17. Comparison of Simulations with Predicted Results for RMS Bearing Error
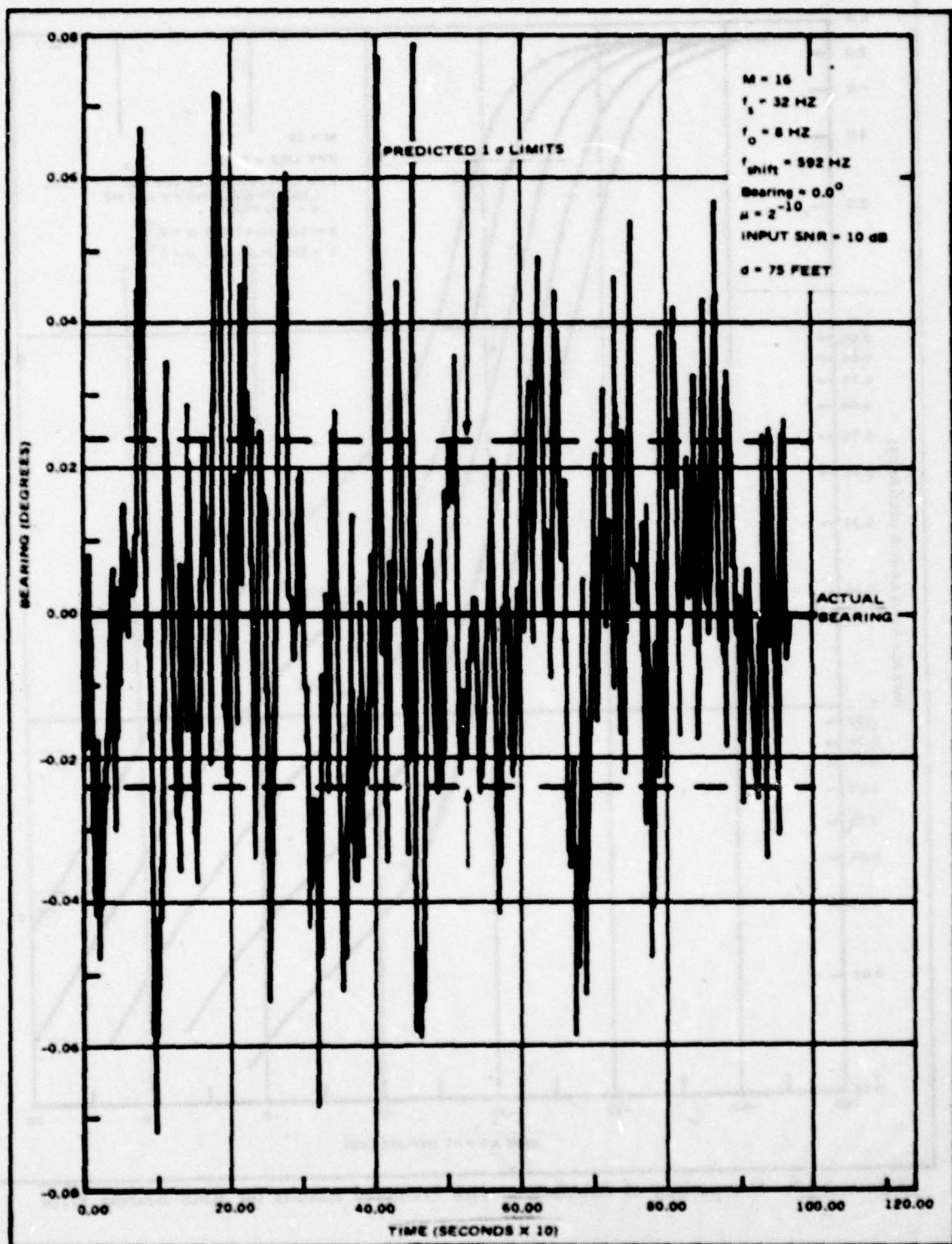
Figure A-18. Bearing Estimate Versus Time
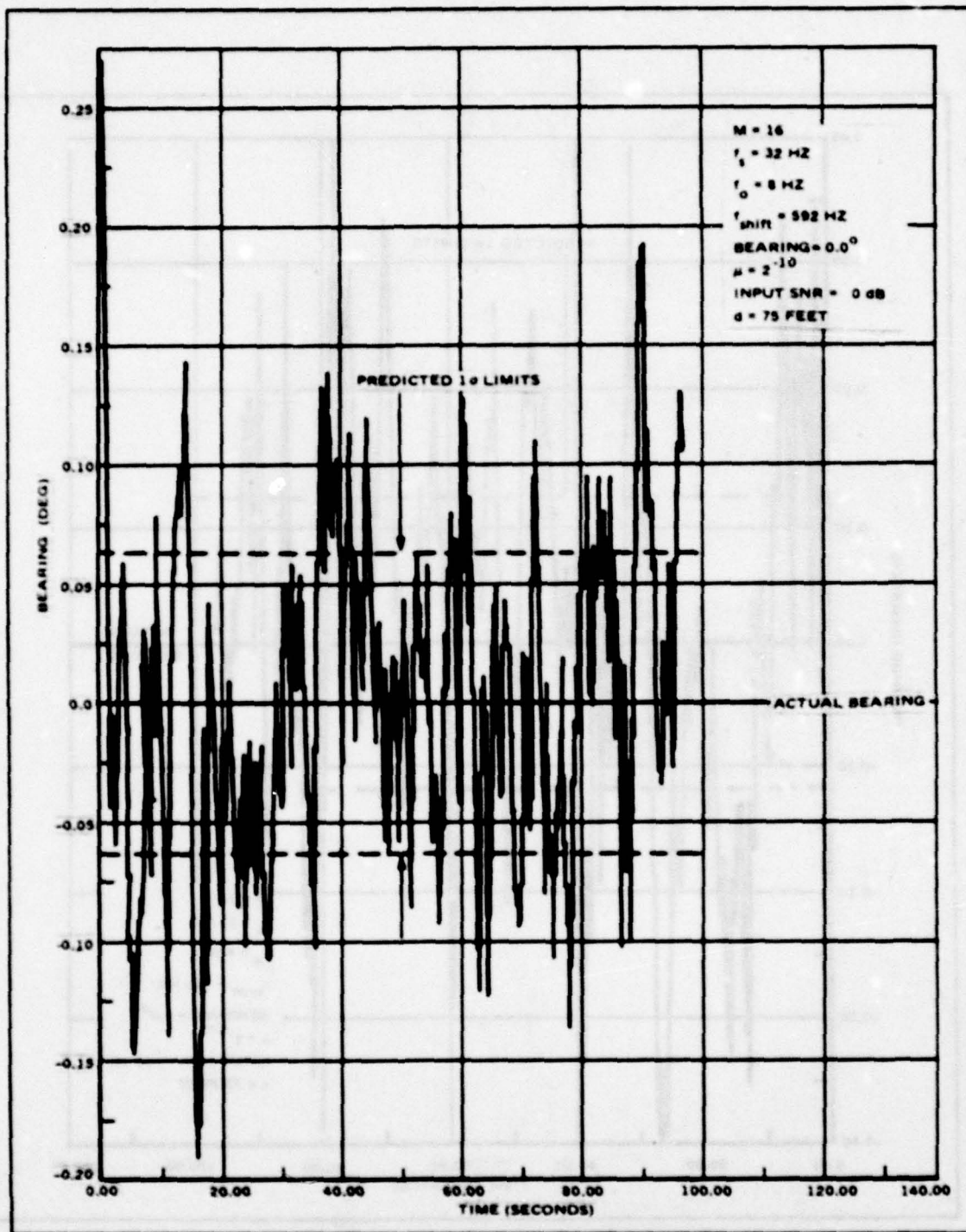
Figure A-19. Bearing Estimate vs Time

A-39
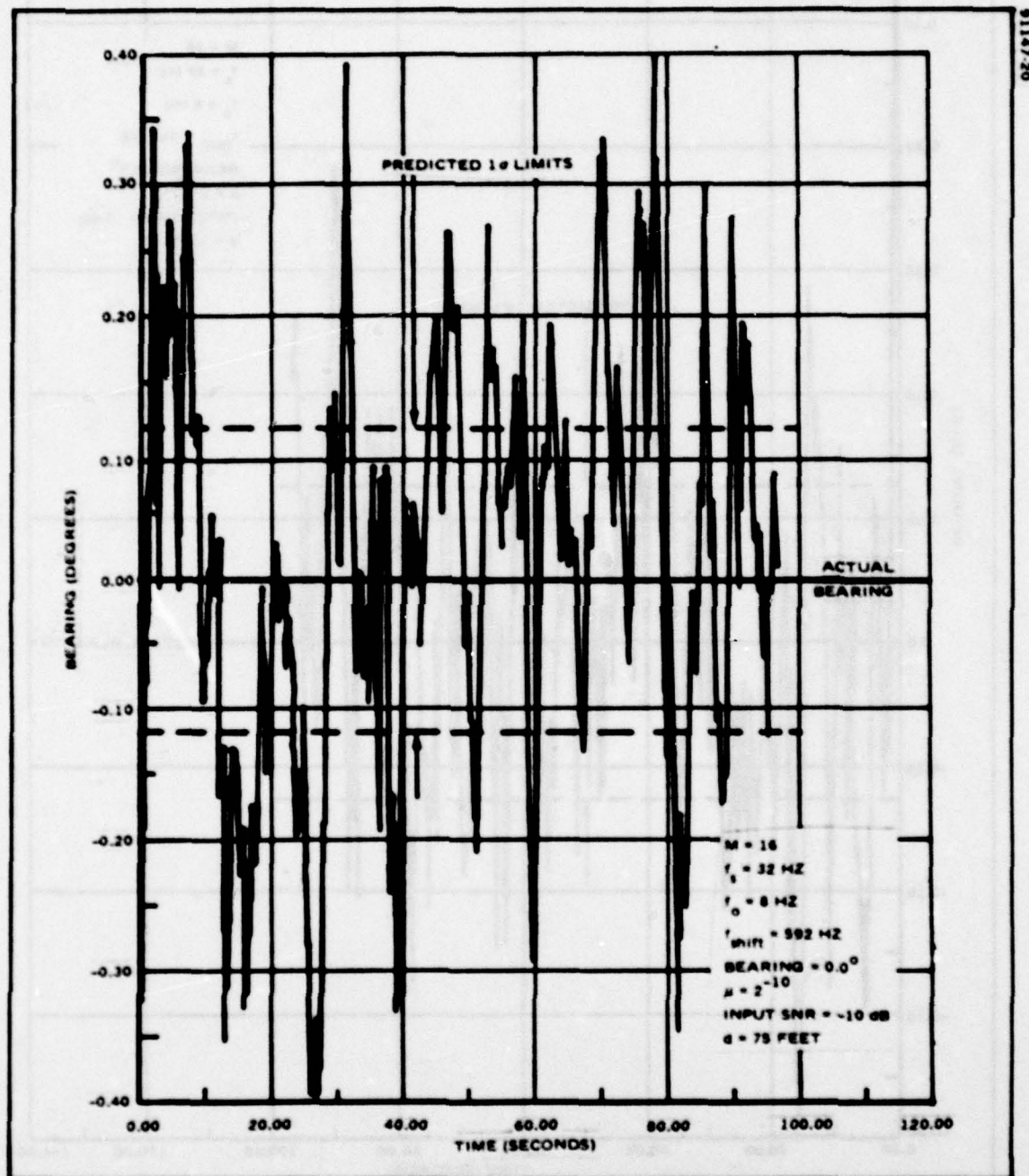
Figure A-20. Bearing Estimate Versus Time
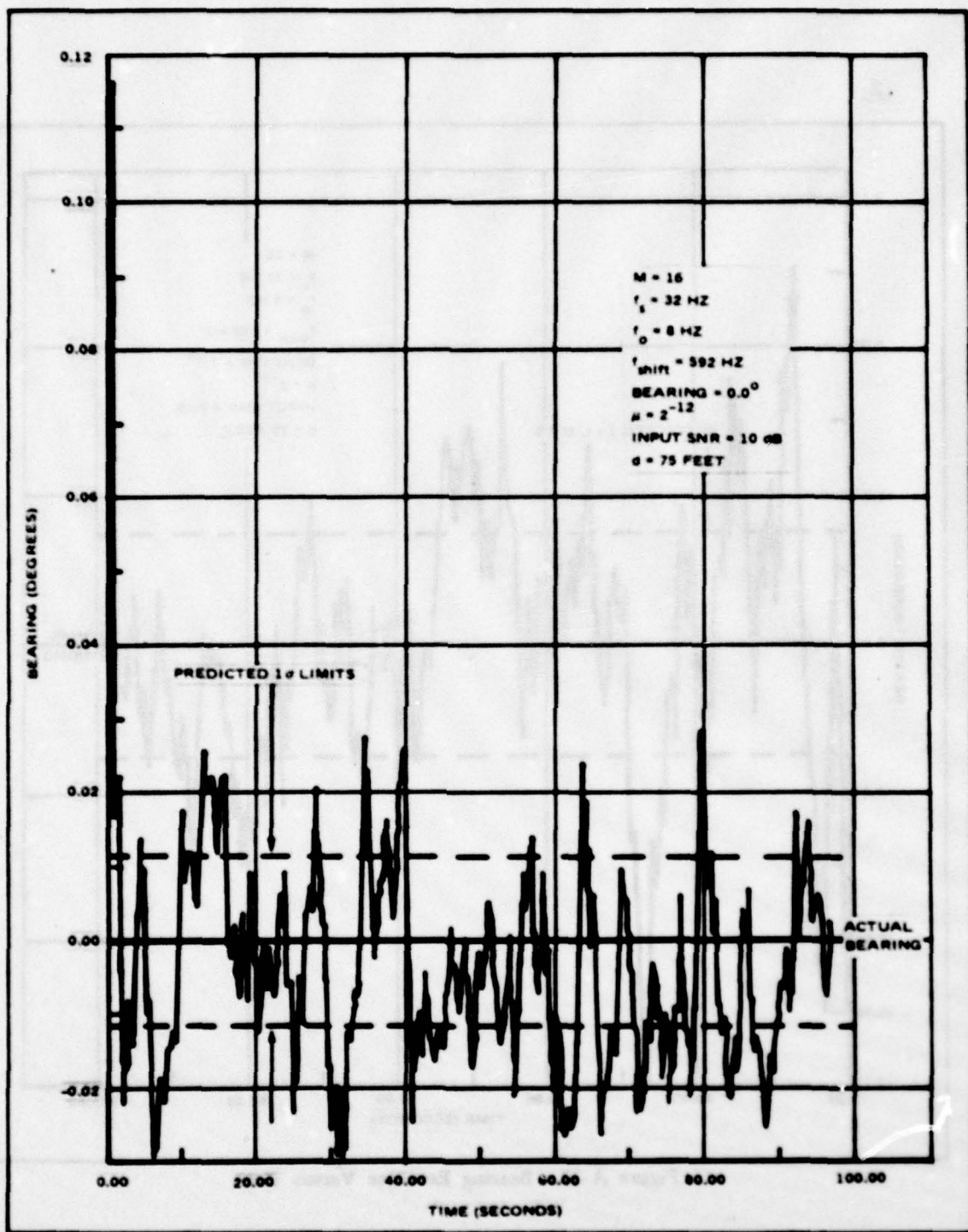
Figure A-21. Bearing Estimate Versus Time

A-41

M = 16
f_s = 32 HZ
f_o = 8 HZ
f_shift = 592 HZ
BEARING = 0.0°
μ = 2^{-12}
INPUT SNR = 0 dB
d = 75 FEET

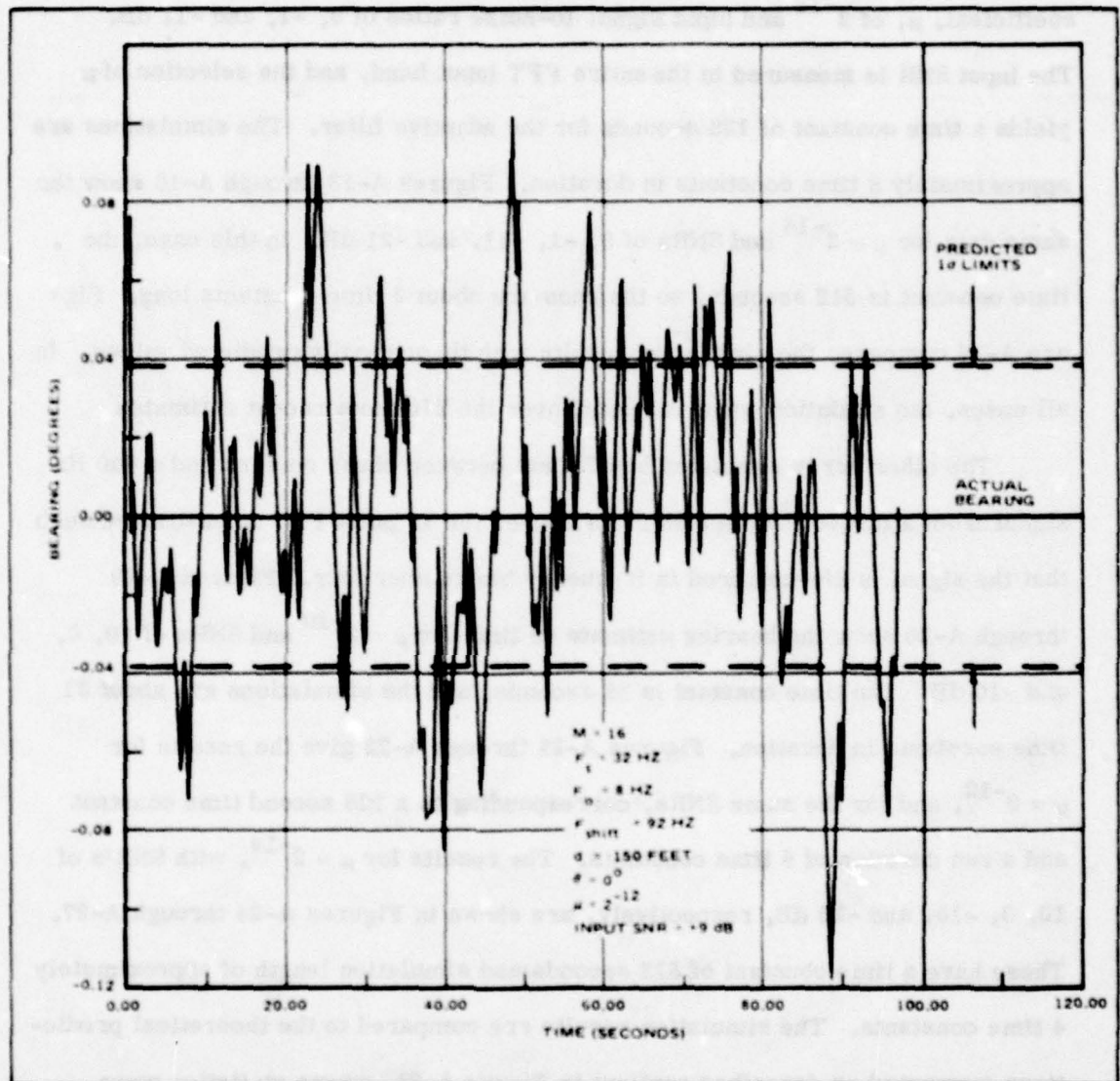PREDICTED 1σ LIMITS

ACTUAL BEARING

BEARING (DEGREES)
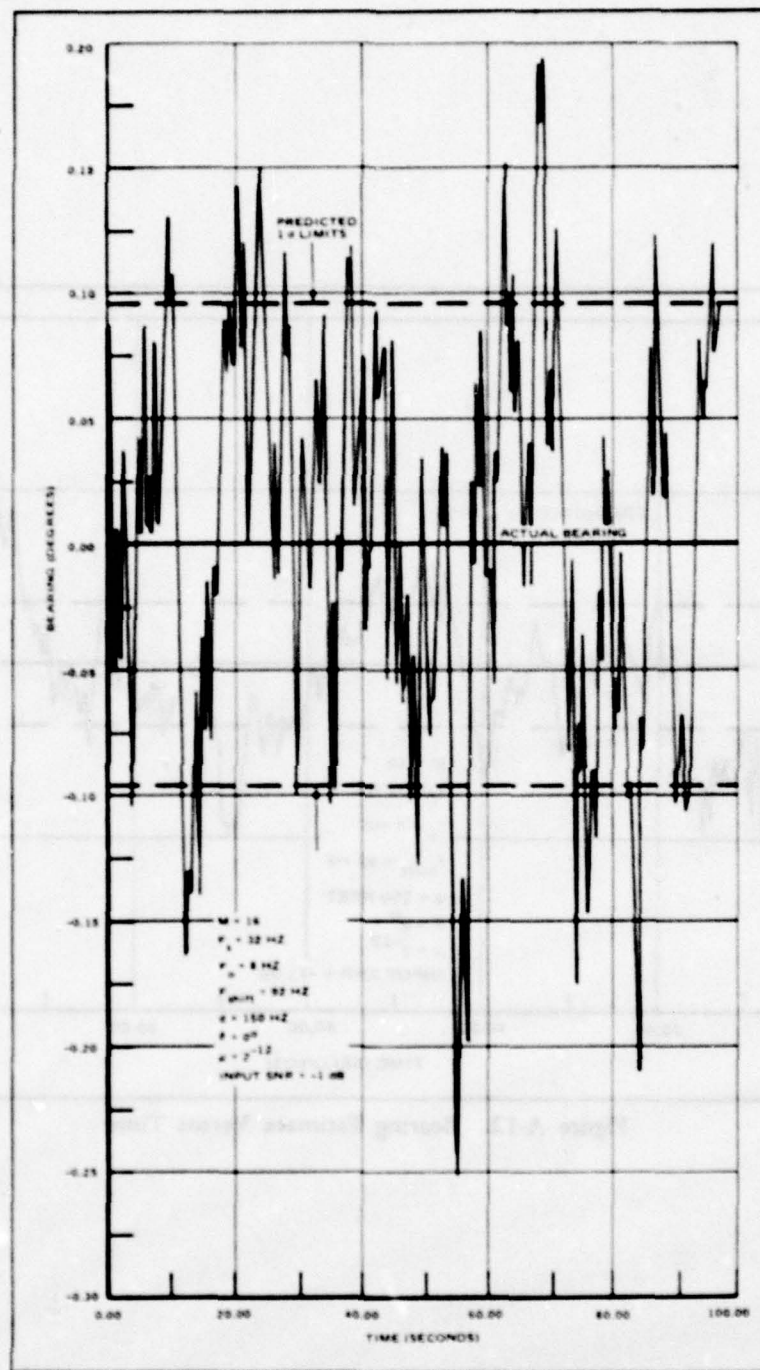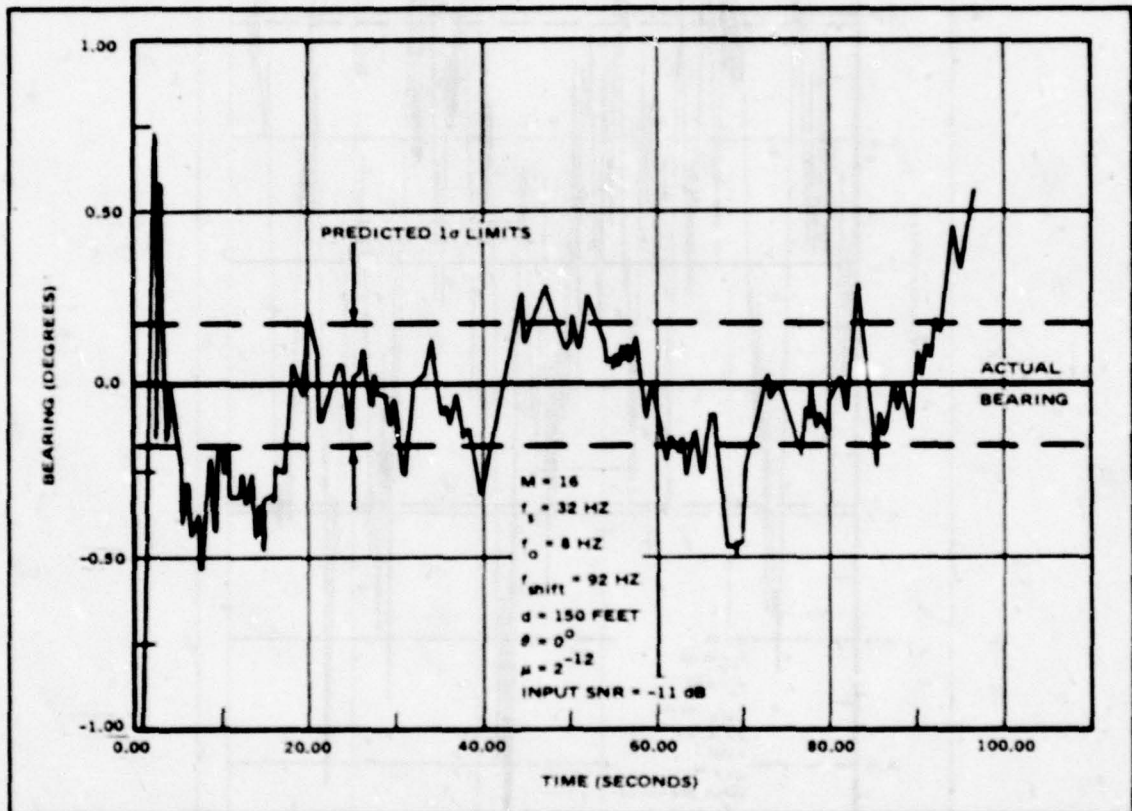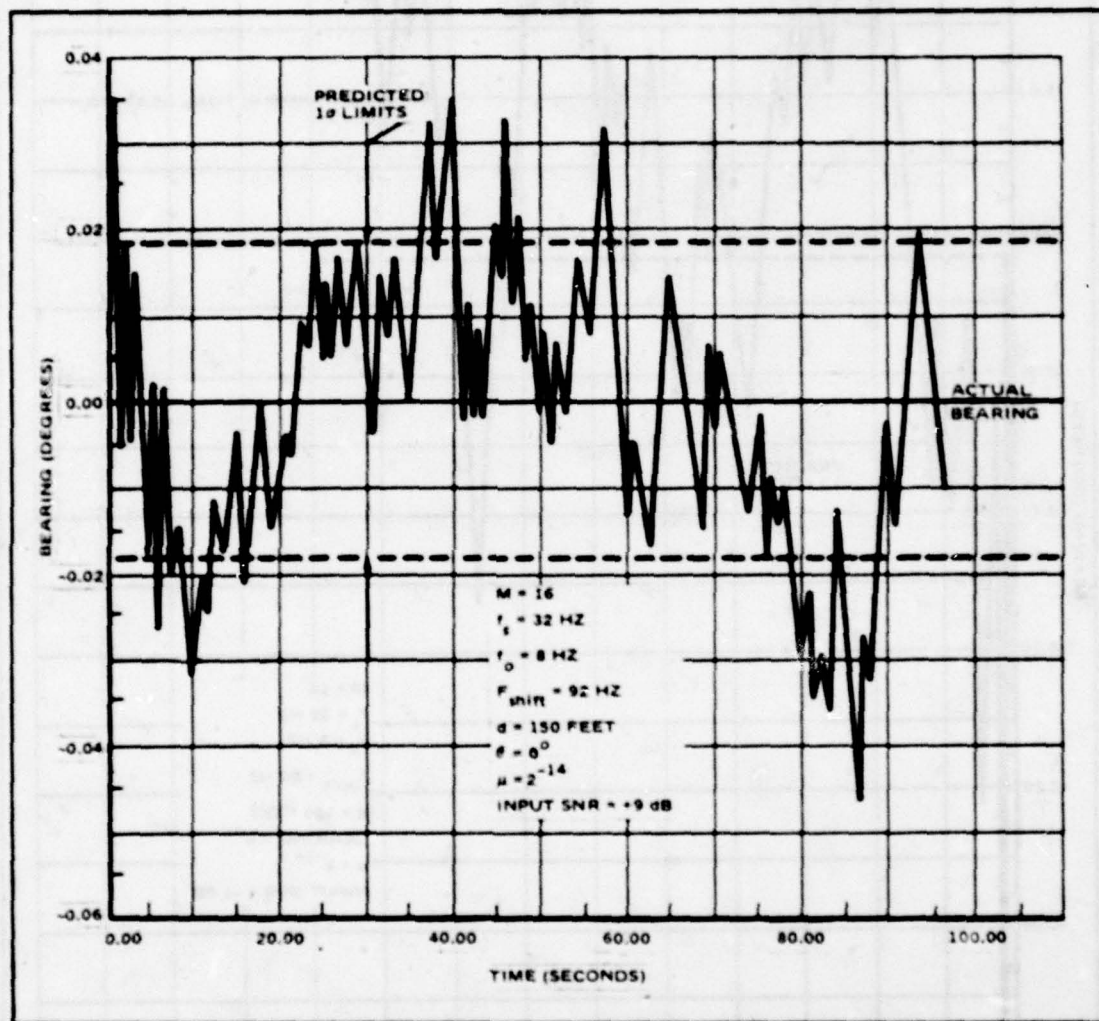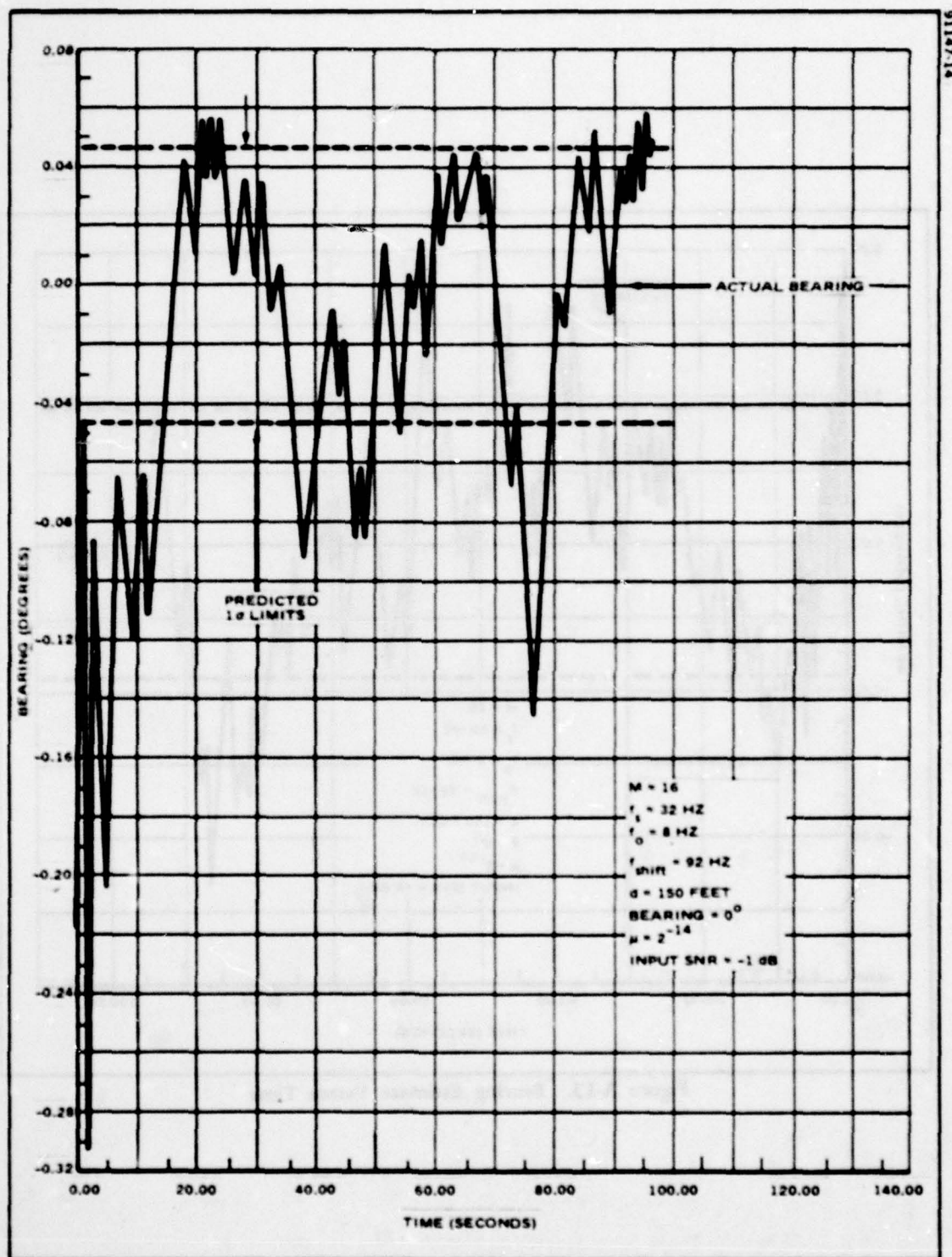
TIME (SECONDS)
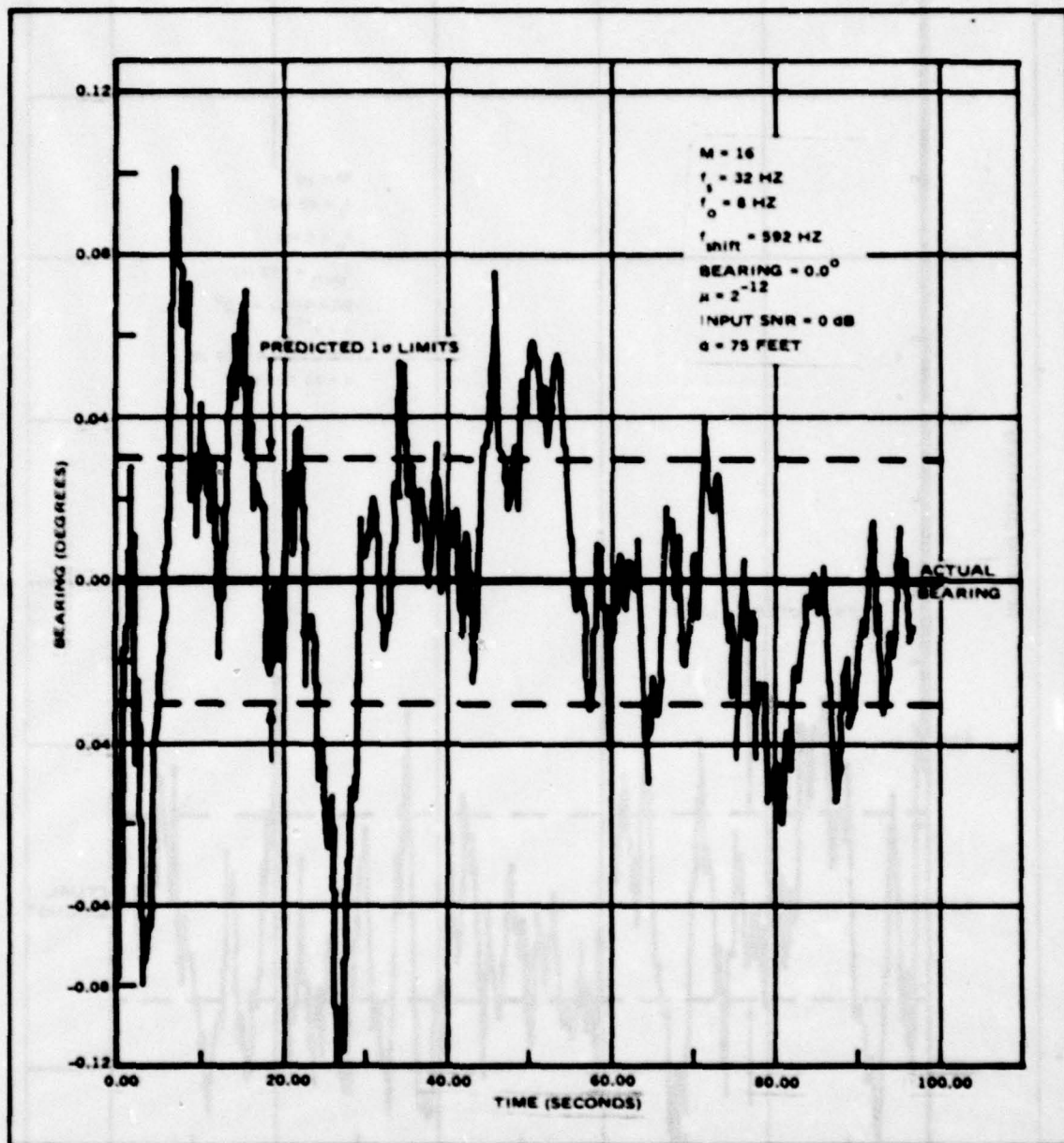
Figure A-22. Bearing Estimate Versus Time
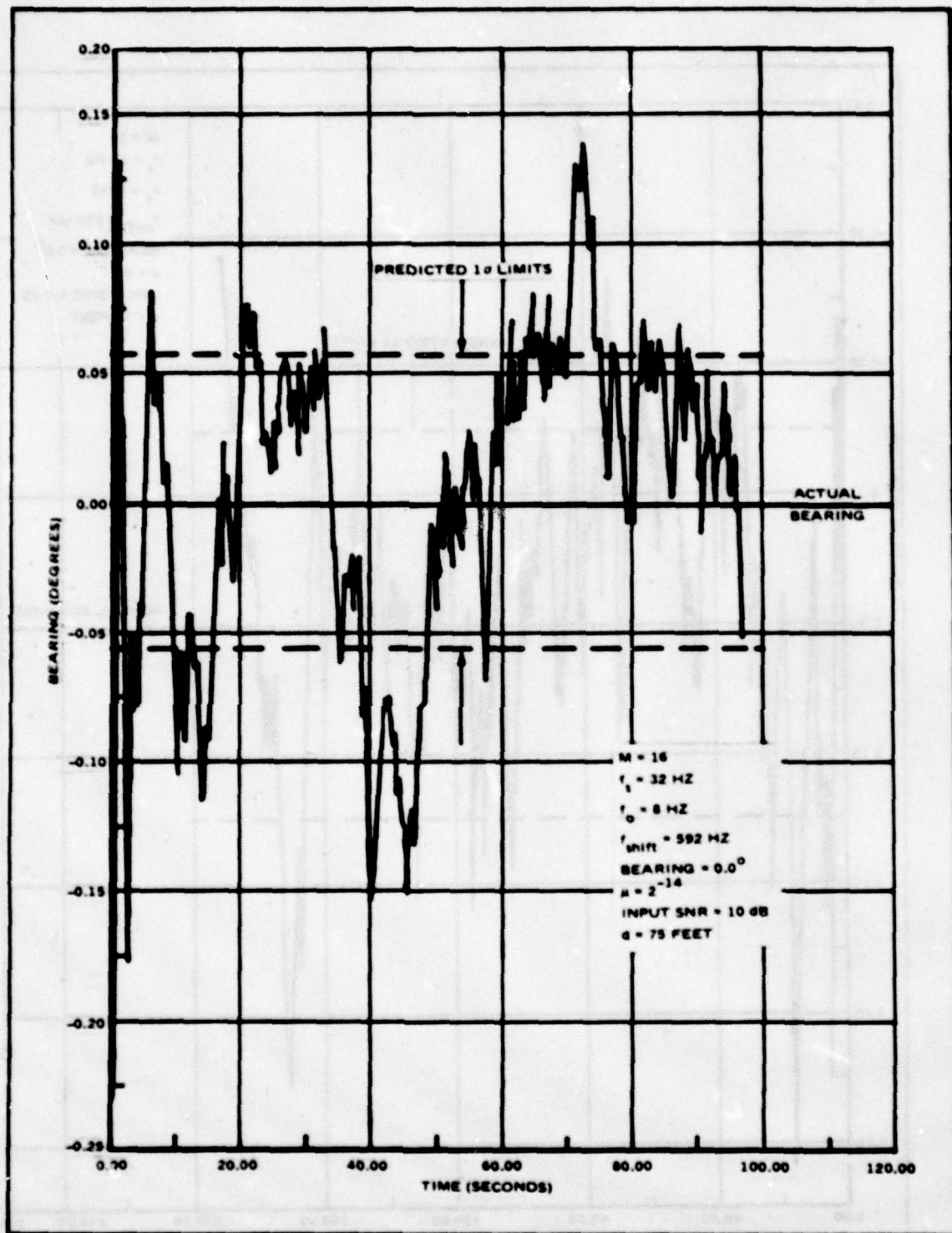
Figure A-24. Bearing Estimate Versus Time

A-43

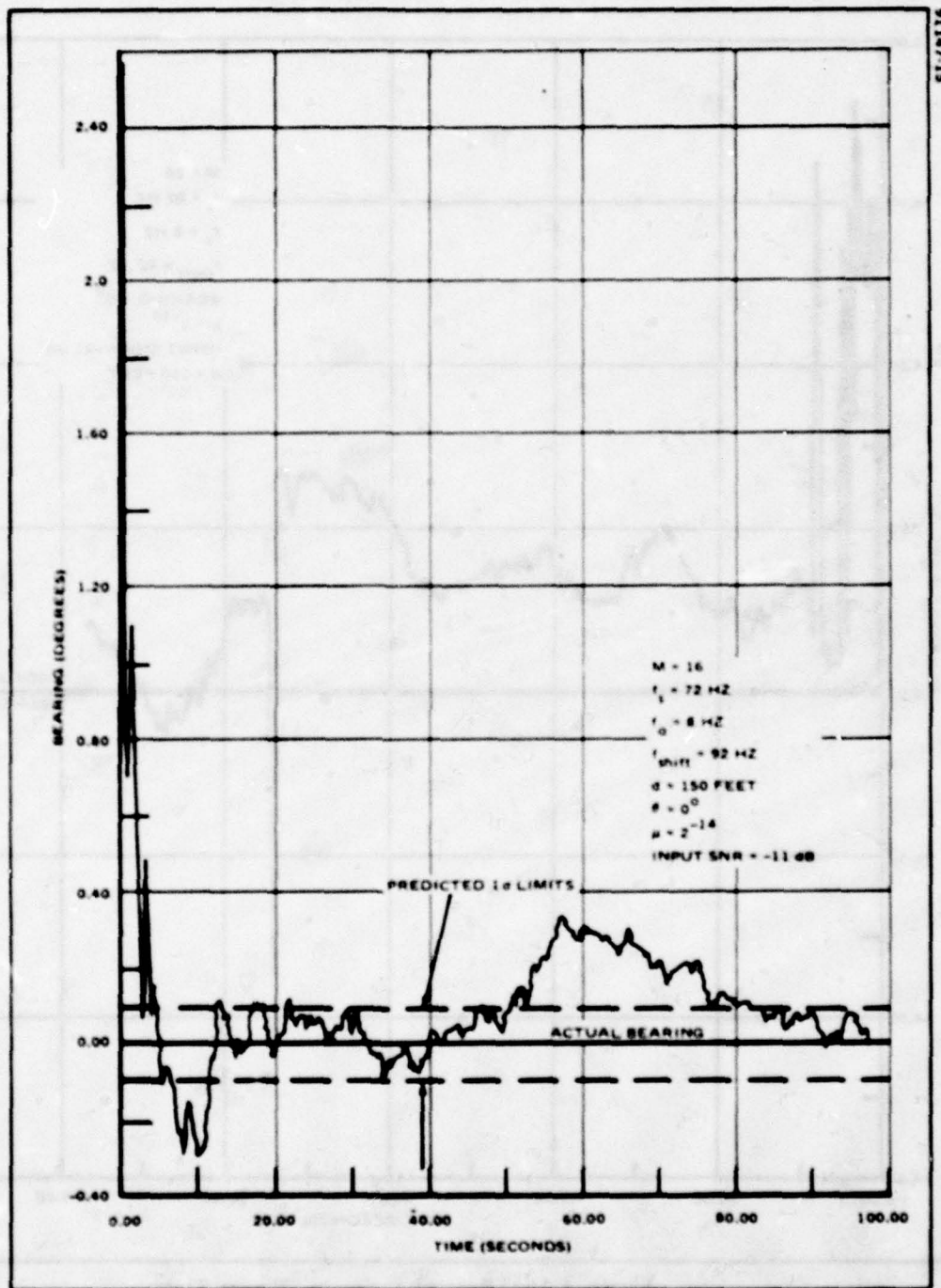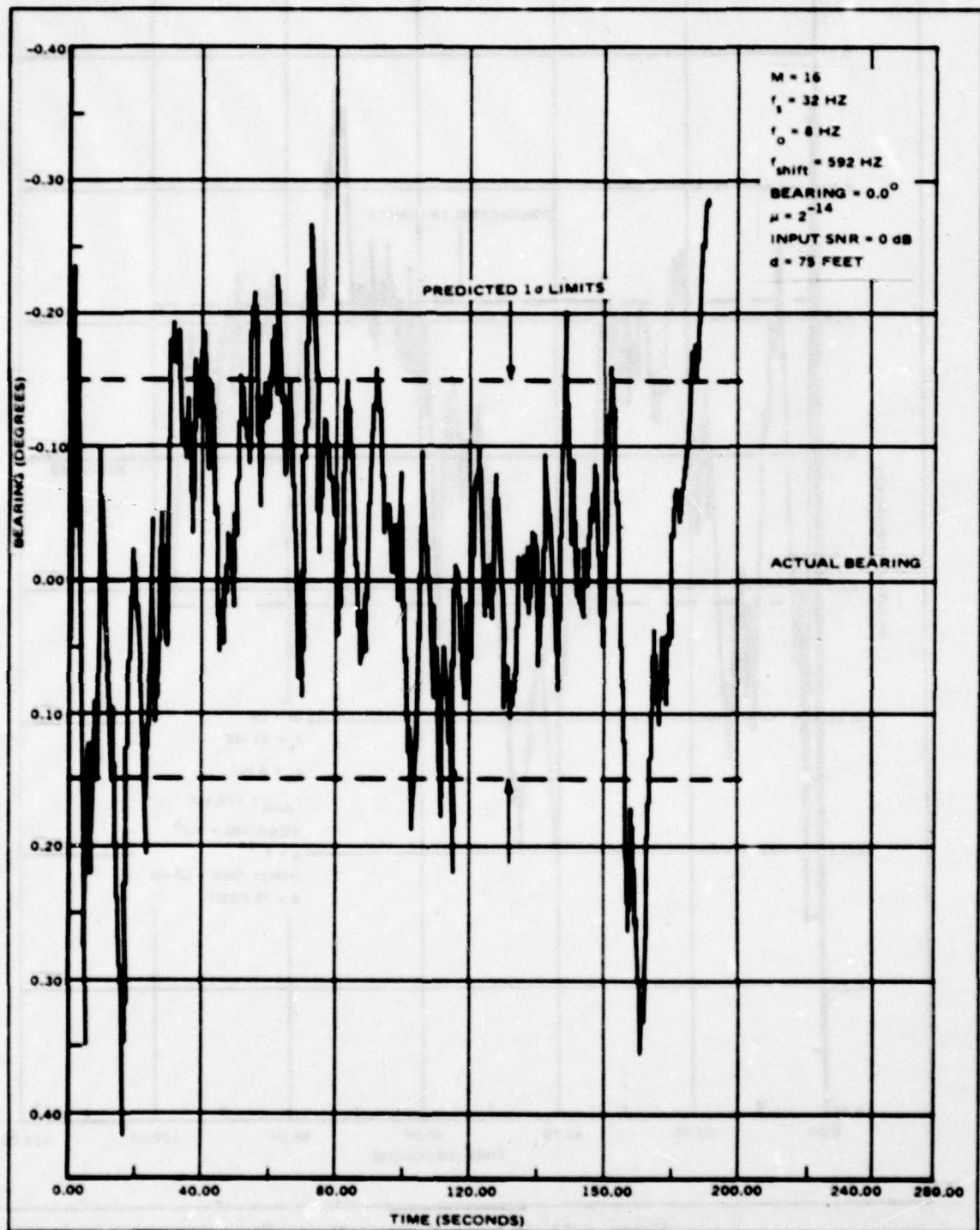Figure A·25.   Bearing Estimate Versus Time

A-44
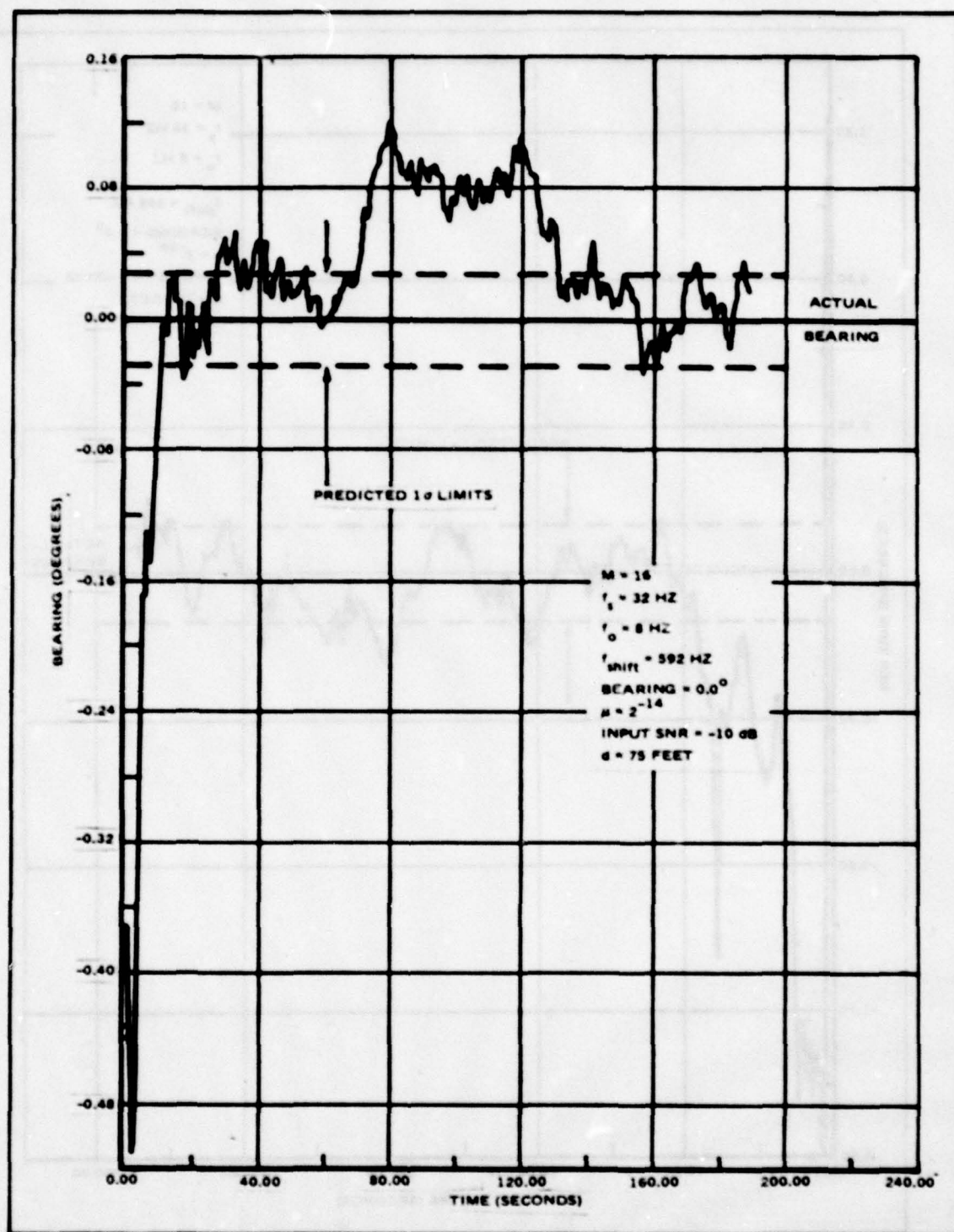
Figure A-26. Bearing Estimate Versus Time

A-45
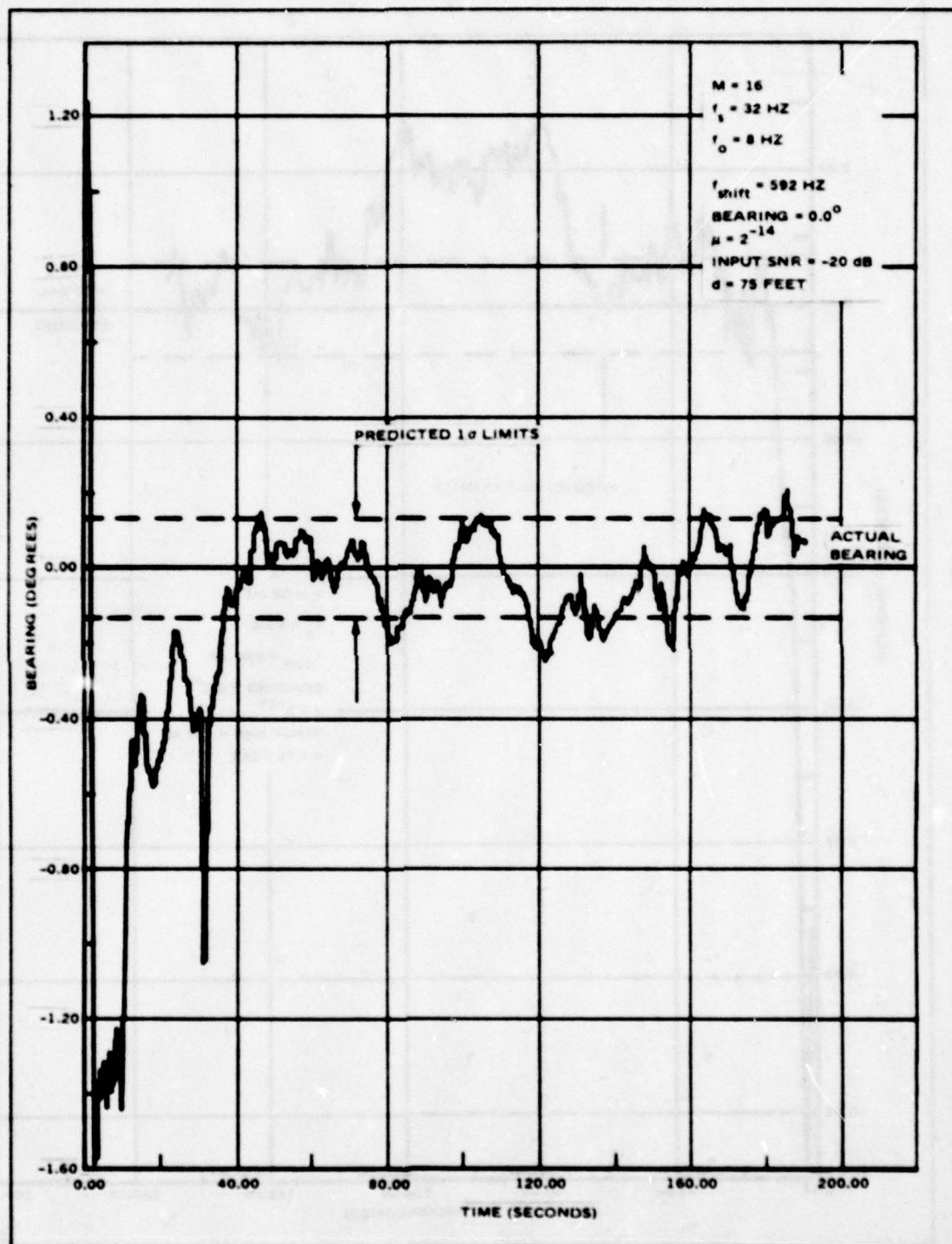
Figure A-27. Bearing Estimate Versus Time
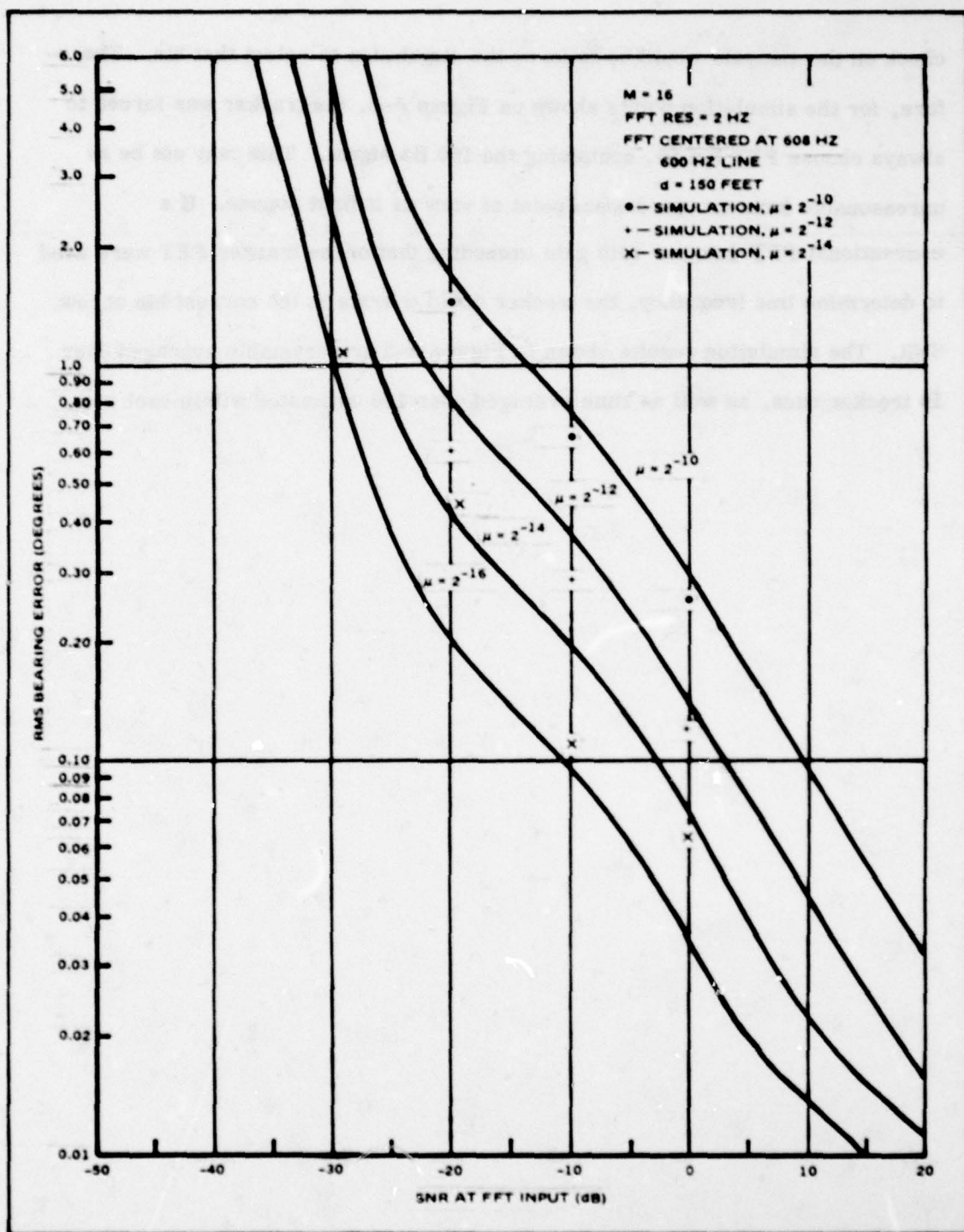
Figure A-28. Comparison of Simulations With Predicted Results For RMS Bearing Error

check on the analysis would be to force the simulation to select that bin. There-
fore, for the simulation points shown on Figure A-5, the tracker was forced to
always choose FFT bin 50, containing the 100 Hz signal. This may not be as
unreasonable from an operational point of view as it first sounds. If a
conventional FFT detector with gain exceeding that of the tracker FFT were used
to determine line frequency, the tracker could operate in the correct bin at low
SNR. The simulation results shown in Figure A-5 are ensemble averaged over
10 tracker runs, as well as time averaged over 190 estimates within each run.
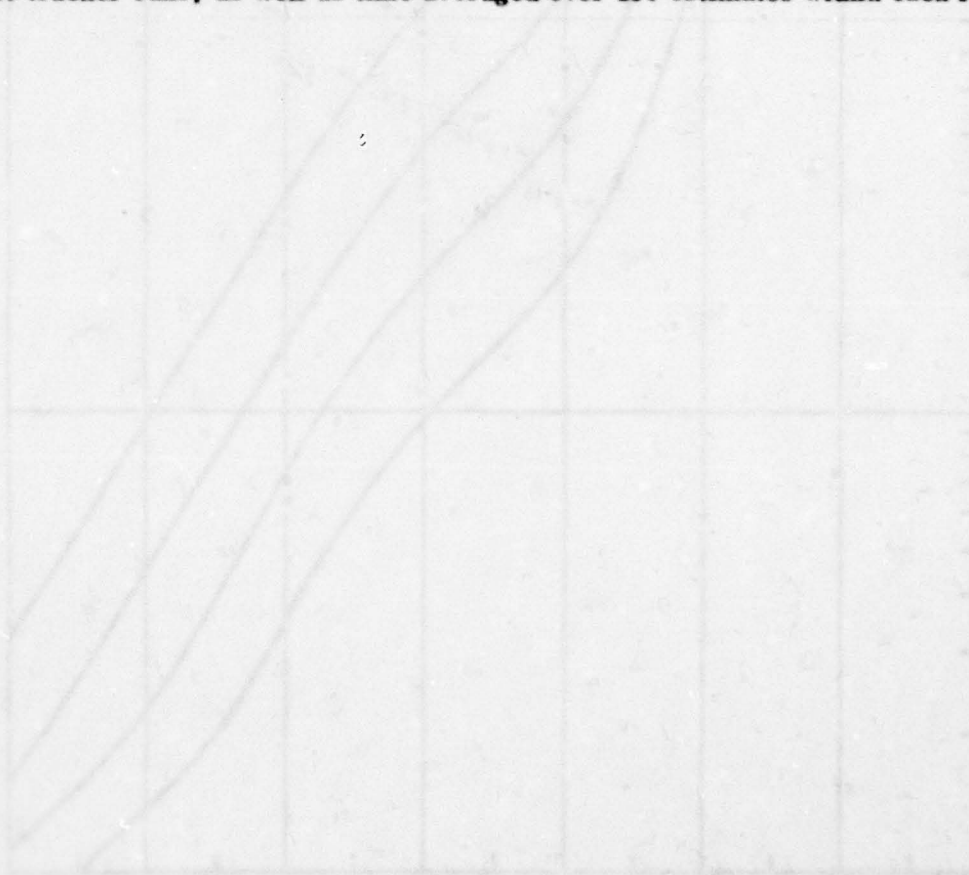
APPENDIX B

Appendix B

Comparison of NB Adaptive Tracker Performance with the
Cramer-Rao Lower Bound

The *Cramer-Rao Lower Bound* (CRLB) is a lower bound on the variance
of any estimate of a parameter given a particular set of observations. For
the estimation of multiple parameters, or the estimation of a particular
parameter when others are unknown (and, hence, must be estimated) the
CRLB can be determined using Fisher's information matrix.[5] Let $\underline{Z}$ be a
vector of observations and $\underline{A}$ be a vector of parameters to be estimated,
where

$$\underline{A} = [A_1, A_2, \cdots A_K]^T \qquad \text{(B-1)}$$

Fisher's information matrix is a K X K matrix given by

$$J = - E[\nabla_{\underline{A}} (\nabla_{\underline{A}}^T [\ln P_{z/a} (Z/A)])] \qquad \text{(B-2)}$$

where

$$P_{z/a}(Z/A) = \text{conditional density of } Z \text{ given } A$$

and

$$\nabla_{\underline{A}} f = \left[\frac{\partial f}{\partial A_1} \cdots\cdots \frac{\partial f}{\partial A_k}\right]^T \qquad \text{(B-3)}$$

Any unbiased estimate of A_i satisfies

$$\text{Var}\left[\hat{A}_i(\underline{z}) - A_i\right] \geq J^{ii} \qquad \text{(B-4)}$$

where J^{ii} is the ii^{th} element of J^{-1}.

Let the 2N dimensional observation vector for the narrowband bearing estimation problem in the kth frequency bin be given by

$$\underline{Z}_k = [D_k(1), X_k(1), ---- D_k(N), X_k(n)]^T \qquad \text{(B-5)}$$

where D_k and X_k are the FFT outputs in the bin closet to the signal as defined in (A-5). Assume that the signal amplitude, σ_s, frequency, ω_o, and bearing, θ, are unknown and to be estimated. Then

$$\underline{A} = [\sigma_s, \omega_o, \theta]^T \qquad \text{(B-6)}$$

Using the mean and variance of D_k and X_k from (A-7), and the gaussian input assumption, the conditional density of $\underline{Z}$ given $\underline{A}$ is

$$P_{\underline{Z}_k|A}(\underline{z}_k|\underline{A}) = \pi^{-2N}(M\sigma_n^2)^{-2N} \exp\left\{-\frac{1}{M\sigma_n^2}(\underline{z}_k - \underline{\mu}(\underline{A}))^+(\underline{z}_k - \underline{\mu}(\underline{A}))\right\} \qquad \text{(B-7)}$$

where + denotes complex conjugate transpose and

$$\underline{\mu}(\underline{A}) = E[\underline{Z}|\underline{A}] = \sigma_s S(k, \omega_o)\left[e^{-j\omega_o \frac{d}{c}\sin\theta}, 1, ---- e^{-j\omega_o \frac{d}{c}\sin\theta}, 1\right]^T$$

with

$$S(k, \omega_o) = \frac{\sin\left[\pi k - \frac{M\omega_o T_s}{2}\right]}{\sin\left[\frac{\pi k}{M} - \frac{\omega_o T_s}{2}\right]} e^{j\frac{M-1}{M}\left|\pi k - \frac{M\omega_o T_s}{2}\right|} \qquad \text{(B-8)}$$

B-2

Therefore,

$$\log P_{\underline{Z}_k|\underline{\Delta}}(\underline{\zeta}_k|\underline{\Delta}) = C_2 - \frac{1}{M\sigma_n^2}(\underline{\zeta}_k - \underline{\mu}(\underline{\Delta}))^+ (\underline{\zeta}_k - \underline{\mu}(\underline{\Delta})) \tag{B-9}$$

with C_2 a constant. Since $(\underline{\zeta}_k - \underline{\mu}(\underline{\Delta}))^+ (\underline{\zeta}_k - \underline{\mu}(\underline{\Delta}))$ is a Hermitian form,

$$\nabla_A \log P_{\underline{Z}_k|\underline{\Delta}}(\underline{\zeta}_k|\underline{\Delta}) = \frac{1}{M\sigma_n^2} 2\mathrm{Re}\left[(\underline{\zeta}_k - \underline{\mu}(\underline{\Delta}))^+ \nabla_A \underline{\mu}(\underline{\Delta})\right] \tag{B-10}$$

We want

$$J = -E[\nabla_A(\nabla_A^T \log P_{\underline{Z}_k|A}(\underline{\zeta}_k|\underline{\Delta}))]$$

$$= -E\left[\nabla_A\left(\frac{1}{M\sigma_n^2}\right)\mathrm{Re}\left[(\underline{\zeta}_k - \underline{\mu}(\underline{\Delta}))^+ \nabla_A(\underline{\mu}(\underline{\Delta}))\right]\right] -$$

$$= -\frac{2}{M\sigma_n^2}\mathrm{Re}\, E\left[\nabla_A(\nabla^+ \underline{\mu}(\underline{\Delta}))\underline{\zeta}_k - \nabla(\nabla^+ \underline{\mu}(\underline{\Delta}))\right.$$

$$\left. - (\nabla\underline{\mu}(\underline{\Delta}))(\nabla^+\underline{\mu}(\underline{\Delta}))\right]$$

$$= -\frac{2}{M\sigma_n^2}\mathrm{Re}\left[\nabla(\nabla^+\underline{\mu}(\underline{\Delta}))\underline{\mu}(\underline{\Delta}) - \nabla(\nabla^+\underline{\mu}(\underline{\Delta}))\underline{\mu}(\underline{\Delta})\right.$$

$$\left. - (\nabla\underline{\mu}(\underline{\Delta}))(\nabla^+\underline{\mu}(\underline{\Delta}))\right] \tag{B-11}$$

giving

$$J = \frac{2}{M\sigma_n^2}\mathrm{Re}\left[\nabla(\underline{\mu}(\underline{\Delta}))\nabla^+(\underline{\mu}(\underline{\Delta}))\right] \tag{B-12}$$

B-3

Now, observe that

$$\nabla \underline{\mu}(\underline{\Delta}) = \left[\frac{\partial}{\partial \sigma_s} \underline{\mu}(\underline{\Delta}) \quad \frac{\partial}{\partial \omega_o} \underline{\mu}(\underline{\Delta}) \quad \frac{\partial}{\partial \theta} \underline{\mu}(\underline{\Delta}) \right]^T \tag{B-13}$$

so that

$$J = \frac{2}{M\sigma_n^2} Re \begin{bmatrix} \left| \frac{\partial}{\partial \sigma_s} \underline{\mu}(\underline{\Delta}) \right|^2 & \left(\frac{\partial}{\partial \sigma_s} \underline{\mu}(\underline{\Delta}) \right)^T \left(\frac{\partial}{\partial \omega_o} \underline{\mu}(\underline{\Delta}) \right)^* & \left(\frac{\partial}{\partial \sigma_s} \underline{\mu}(\underline{\Delta}) \right)^T \left(\frac{\partial}{\partial \theta} \underline{\mu}(\underline{\Delta}) \right)^* \\ \left(\frac{\partial}{\partial \omega_o} \underline{\mu}(\underline{\Delta}) \right)^T \left(\frac{\partial}{\partial \sigma_s} \underline{\mu}(\underline{\Delta}) \right)^* & \left| \frac{\partial}{\partial \omega_o} \underline{\mu}(\underline{\Delta}) \right|^2 & \left(\frac{\partial}{\partial \omega_o} \underline{\mu}(\underline{\Delta}) \right)^T \left(\frac{\partial}{\partial \theta} \underline{\mu}(\underline{\Delta}) \right)^* \\ \left(\frac{\partial}{\partial \theta} \underline{\mu}(\underline{\Delta}) \right)^T \left(\frac{\partial}{\partial \sigma} \underline{\mu}(\underline{\Delta}) \right)^* & \left(\frac{\partial}{\partial \theta} \underline{\mu}(\underline{\Delta}) \right)^T \left(\frac{\partial}{\partial \omega_o} \underline{\mu}(\underline{\Delta}) \right)^* & \left| \frac{\partial}{\partial \theta} \underline{\mu}(\underline{\Delta}) \right|^2 \end{bmatrix}$$

$$= \frac{2}{M\sigma_n^2} Re \begin{bmatrix} \sum_{i=1}^{2N} \left| \frac{\partial}{\partial \sigma_s} \mu_i \right|^2 & \sum_{i=1}^{2N} \left(\frac{\partial}{\partial \sigma_s} \mu_i \right) \left(\frac{\partial}{\partial \omega_o} \mu_i \right)^* & \sum_{i=1}^{2N} \left(\frac{\partial}{\partial \sigma_s} \mu_i \right) \left(\frac{\partial}{\partial \theta} \mu_i \right)^* \\ \sum_{i=1}^{2N} \left(\frac{\partial}{\partial \omega_o} \mu_i \right) \left(\frac{\partial}{\partial \sigma_s} \mu_i \right)^* & \sum_{i=1}^{2N} \left| \frac{\partial}{\partial \omega_o} \mu_i \right|^2 & \sum_{i=1}^{2N} \left(\frac{\partial}{\partial \omega_o} \mu_i \right) \left(\frac{\partial}{\partial \theta} \mu_i \right)^* \\ \sum_{i=1}^{2N} \left(\frac{\partial}{\partial \theta} \mu_i \right) \left(\frac{\partial}{\partial \sigma_s} \mu_i \right)^* & \sum_{i=1}^{2N} \left(\frac{\partial}{\partial \theta} \mu_i \right) \left(\frac{\partial}{\partial \omega_o} \mu_i \right)^* & \sum_{i=1}^{2N} \left| \frac{\partial}{\partial \theta} \mu_i \right|^2 \end{bmatrix} \tag{B-14}$$

Note that this matrix is Hermitian and denote its ijth element as a_{ij}.

The elements of J can be found by considering the derivatives

$$\frac{\partial}{\partial \sigma_s} E D_k(n) = \frac{1}{\sigma_s} E D_k(n) , \frac{\partial}{\partial \sigma_s} E X_k(n) = \frac{1}{\sigma_s} EX_k(n)$$

$$\frac{\partial}{\partial \omega_o} E D_k(n) = \left[j \frac{d}{c} \sin\theta + \frac{\partial S(k,\omega_o)}{\partial \omega_o} S^{-1}(k,\omega_o) \right] E D_k(n)$$

$$\frac{\partial}{\partial \omega_o} E X_k(n) = \frac{\partial S(k,\omega_o)}{\partial \omega_o} S^{-1}(k,\omega_o) E X_k(n) \qquad (B-15)$$

$$\frac{\partial}{\partial \theta} E D_k(n) = j\omega_o \frac{d}{c} \cos\theta \, E D_k(n), \frac{\partial}{\partial \theta} E X_k(n) = 0$$

Substitution of these derivatives to yield the elements α_{ij} gives

$$\alpha_{11} = 2N \, S^2$$

$$\alpha_{12} = \alpha_{21}^* = N \, S^2 \, \sigma_s^2 \left[-j\frac{d}{c}\sin\theta + 2\left[\frac{\partial S(k,\omega_o)}{\partial \omega_o} S^{-1}(k,\omega_o)\right]^* \right]$$

$$\qquad (B-16)$$

$$\alpha_{13} = \alpha_{31}^* = -jNS^2 \sigma_s \, \omega_o \frac{d}{c} \cos\theta$$

$$\alpha_{22} = N \, S^2 \sigma_s^2 \left[2\left| \frac{\partial S(k,\omega_o)}{\partial \omega_o} \right| S^{-1}(k,\omega_o)|^2 + \frac{d^2}{c^2}\sin^2\theta \right.$$

$$\left. + 2\frac{d}{c}\sin\theta \, \mathrm{Im}\left(\frac{\partial S(k,\omega_o)}{\partial \omega_o} S^{-1}(k,\omega_o)\right) \right]$$

$$\alpha_{23} = \alpha_{32}^* = N \, S^2 \sigma_s^2 \left[\frac{d^2}{c^2} \, \omega_o \sin\theta \cos\theta - j\omega_o \frac{d}{c}\cos\theta \frac{\partial S(k,\omega_o)}{\partial \omega_o} S^{-1}(k,\omega_o) \right]$$

and

$$\alpha_{33} = N \, S^2 \sigma_s^2 \, \omega_o^2 \frac{d^2}{c^2} \cos^2\theta$$

where

$$S^2 = |S(k,\omega_o)|^2. \text{ Then the elements of J are}$$

$$J_{11} = \frac{4}{M\sigma_n^2} N \, S^2$$

$$J_{12} = J_{21} = \frac{4}{Mq_n^2} N S^2 \sigma_s \, \text{Re} \left[\frac{\partial S(k,\omega_o)}{\partial \omega_o} S^{-1}(k,\omega_o) \right]$$

$$J_{13} = J_{31} = 0 \tag{B-17}$$

$$J_{22} = \frac{2}{Mq_n^2} N S^2 \sigma_s^2 \left[2 \left| \frac{\partial S(k,\omega_o)}{\partial \omega_o} S^{-1}(k,\omega_o) \right|^2 + \frac{d^2}{c^2} \sin^2 \theta \right.$$

$$\left. + 2 \frac{d}{c} \sin\theta \, \text{Im} \left(\frac{\partial S(k,\omega_o)}{\partial \omega_o} S^{-1}(k,\omega_o) \right) \right]$$

$$J_{23} = \frac{2}{Mq_n^2} N S^2 \sigma_s^2 \left[\frac{d^2}{c^2} \omega_o \sin\theta \cos\theta + \omega_o \frac{d}{c} \cos\theta \, \text{Im} \left(\frac{\partial S(k,\omega_o)}{\partial \omega_o} S^{-1}(k,\omega_o) \right) \right]$$

$$J_{33} = \frac{2}{Mq_n^2} N S^2 \sigma_s^2 \omega_o^2 \frac{d^2}{c^2} \cos^2 \theta$$

The term of interest is J^{33}, the i=3, j=3 element of J^{-1}, since

$$\text{Var} \left[\hat{A}_3 (Z) - A_3 \right] = \text{Var} \left[\dot{\hat{\theta}} (\underline{Z}) - \theta \right] \geq J^{33} \tag{B-18}$$

This element is given by

$$J^{33} = \frac{J_{11} J_{22} - J_{12}^2}{J_{11} (J_{22} J_{33} - J_{23}^2) - J_{12} (J_{21} J_{33} - J_{31} J_{23}) + J_{13} (J_{21} J_{32} - J_{22} J_{31})} \tag{B-19}$$

where, substituting from (B-17), after some algebra

$$J_{11}(J_{26}J_{33} - J_{23}^2) = \frac{16\,N^3 S^6 \sigma_s^4}{M^3 \sigma_n^6}\left[\omega_o^2\,\frac{d^2}{c^2}\cos^2\theta\left|\frac{\partial S(k,\omega_o)}{\partial\omega_o}S^{-1}(k,\omega_o)\right|^2\right.$$

$$\left. + \omega_o^2\,\frac{d^2}{c^2}\cos^2\theta\left(\mathrm{Re}\,\frac{\partial S(k,\omega_o)}{\partial\omega_o}S^{-1}(k,\omega_o)\right)^2\omega_o^2\right]$$

$$J_{12}(J_{21}J_{33} - J_{33}J_{23}) = \frac{32N^3 S^6 \sigma_s^4}{M^3\sigma_n^6}\left[\omega_o^2\,\frac{d^2}{c^2}\cos^2\theta\,\mathrm{Re}\left(\frac{\partial S(k,\omega_o)}{\partial\omega_o}S^{-1}(k,\omega_o)\right)\right]$$

$$J_{13}(J_{21}J_{32} - J_{22}J_{31}) = 0 \tag{B-20}$$

$$J_{11}J_{21} - J_{12}^2 = \frac{8N^2 S^4 \sigma_s^2}{M^2\sigma_n^4}\left[2\left(\mathrm{Im}\left(\frac{\partial S(k,\omega_o)}{\partial\omega_o}S^{-1}(k,\omega_o)\right)\right)^2\right.$$

$$\left. + \frac{d^2}{c^2}\sin^2\theta + 2\frac{d}{c}\sin\theta\left(\mathrm{Im}\left(\frac{\partial S(k,\omega_o)}{\partial\omega_o}S^{-1}(k,\omega_o)\right)\right)\right]$$

Therefore

$$J^{33} = \frac{M\sigma_n^2}{2NS^2\sigma_s^2\,\omega_o^2\,\frac{d^2}{c^2}\cos^2\theta}\left[1 + \frac{1}{I(s)}\,\frac{d}{c}\,\sin\theta + \frac{1}{2I(s)}\frac{d^2}{c^2}\sin^2\theta\right] \tag{B-21}$$

where

$$I(s) = \mathrm{Im}\left[\frac{\partial S(k,\omega_o)}{\partial\omega_o}S^{-1}(k,\omega_o)\right]$$

Then J^{33}, which is the CRLB for the bearing estimate, is

$$J^{33} = \frac{M\sigma_n^2}{NS^2\sigma_s^2 \omega_o^2 \frac{d^2}{c^2}\cos^2\theta}\left[1 + \frac{2}{(M-1)T_s}\frac{d}{c}\sin\theta\left[1 + \frac{1}{(M-1)T_s}\frac{d}{c}\sin\theta\right]\right] \quad (B-24)$$

This can be expressed in terms of the signal to noise ratio in the bin

$$\gamma = \frac{S^2\sigma_s^2}{M\sigma_n^2} = \frac{|S(k,\omega_o)|^2\sigma_s^2}{M\sigma_s^2} \quad (B-25)$$

so that

$$\text{Var}\,[\hat{\theta} - \theta] \geq \frac{1}{\gamma N\omega_o^2\frac{d^2}{c^2}\cos^2\theta}\left[1 + \frac{2}{(M-1)T_s}\frac{d}{c}\sin\theta\left[1 + \frac{1}{(M-1)T_s}\frac{d}{c}\sin\theta\right]\right] \quad (B-26)$$

It is interesting to compare this result with the high SNR approximation for the variance of the adaptive tracker bearing estimate, (A-46) developed in the preceding section. For small bearing angles and high SNR, the variance is

$$\text{Var}\,[\hat{\theta}] \approx \frac{M^2T_s^2}{(2\pi k)^2}\frac{c^2}{d^2}\frac{1}{2\gamma\tau_I} \quad (B-27)$$

where, under the same assumptions, (B-26) reduces to

$$\text{Var}\,[\hat{\theta} - \theta] \geq \frac{c^2}{\omega_o^2 d^2}\frac{1}{\gamma N} \quad (B-28)$$

B-9

But

$$\frac{\partial}{\partial \omega_o} S(k, \omega_o) = \frac{\partial}{\partial \omega_o} \left[\frac{\sin\left(\pi k - \frac{M \omega_o T_s}{2}\right)}{\sin\left(\frac{\pi k}{M} - \frac{\omega_o T_s}{2}\right)} e^{j\frac{M-1}{M}\left(\pi k - \frac{M \omega_o T_s}{2}\right)} \right]$$

$$= \left[\frac{1}{\sin^2\left(\frac{\pi k}{M} - \frac{\omega_o T_s}{2}\right)} \right] \left\{ -\frac{T_s}{2} \left[\cos\left(\frac{\pi k}{M} - \frac{\omega_o T_s}{2}\right) \right] \right.$$

$$\left[\sin\left(\pi k - \frac{M \omega_o T_s}{2}\right) e^{j\frac{M-1}{M}\left(\pi k - \frac{M \omega_o T_s}{2}\right)} \right]$$

$$+ \left[\sin\left(\frac{\pi k}{M} - \frac{\omega_o T_s}{2}\right) \right] \left[\frac{MT_s}{2} \cos\left(\pi k - \frac{M \omega_o T_s}{2}\right) e^{j\frac{M-1}{M}\left(\pi k - \frac{M \omega_o T_s}{2}\right)} \right.$$

$$\left. \left. + j\frac{(M-1)T_s}{2} \sin\left(\pi k - \frac{M \omega_o T_s}{2}\right) e^{j\frac{M-1}{M}\left(\pi k - \frac{M \omega_o T_s}{2}\right)} \right] \right\}$$

$$\hspace{12cm} \text{(B-22)}$$

$$= -\frac{T_s}{2} \left[\sec\left(\frac{\pi k}{M} - \frac{\omega_o T_s}{2}\right) \right] S(k, \omega_o)$$

$$+ \frac{MT_s}{2} \left[\sec\left(\pi k - \frac{M \omega_o T_s}{2}\right) S(k, \omega_o) \right] + j\frac{(M-1)T_s}{2} S(k, \omega_o)$$

Then,

$$\text{Im}\left[\frac{\partial S(k, \omega_o)}{\partial \omega_o} S(k, \omega_o) \right] = \text{Im}\left[-\frac{T_s}{2} \sec\left(\frac{\pi k}{M} - \frac{\omega_o T_s}{2}\right) + \frac{MT_s}{2} \sec\left(\pi k - \frac{M \omega_o T_s}{2}\right) \right.$$

$$\left. + j\frac{(M-1)T_s}{2} \right]$$

$$= \frac{(M-1)T_s}{2} \hspace{6cm} \text{(B-23)}$$

Since MT_s/k is the estimate of ω_0, it can be seen that there is a correspondence between the time constant of the adaptive filter, in iterations, and the total number of observations of the FFT output in the CRLB as would be expected. Just as in the case of the comparison of the adaptive tracker with the CRLB for broadband inputs,[1] it is necessary to resolve the relationship between N and τ_I. The method applied in the broadband analysis, specifically, the incorporation of an exponentially decay term in the large SNR approximation, also works well here.

The mean weight, given a zero initial weight, can be written as a function of time as

$$E[W_k(n)] = E[W_k][1 - e^{-n/\tau_I}] \qquad (B-29)$$

where n is the number of filter iterations and $E[W_k]$ is the steady state mean weight. The variance has approximately half the time constant, so we can assume that after one or so time constants, the transient response of the variance may be neglected. Then incorporating this change in the derivation of (A-46) gives

$$\text{Var}\,[\hat{\theta}(n)] \approx \frac{M^2 T_s^2}{(2\pi k)^2} \frac{c^2}{d^2} \frac{1}{2\gamma\tau_I}\left[1 - e^{-n/\tau_I}\right]^{-2} \qquad (B-30)$$

The parameter n corresponds exactly to the number of FFT outputs processed by the filter, that is, to N in the CRLB. Then

$$\frac{\text{Var}\,[\hat{\theta}(n)]}{\text{CRLB}} = \frac{N}{2\tau_I}\left[1 - e^{-N/\tau_I}\right]^{-2} \qquad \begin{array}{l} SNR \gg 1 \\ \theta \ll 1 \end{array} \qquad (B-31)$$

B-10

It is assumed here that the FFT resolution is sufficiently fine that $\omega_o \approx 2\pi k/MT_s$. This ratio is plotted as a function of the ratio N/τ_I in Figure B-1. It can be seen that the minimum occurs at $N/\tau_I = 1.25$, and that the ratio is 1.228 at the minimum. Therefore, at high SNR, the adaptive tracker is degraded approximately 0.45 dB from the CRLB. The relative performance at low SNR must be determined numerically as described earlier. Whether or not the ratio $N/\tau_I = 1.25$ yields the best relative performance at low signal to noise ratios and at other bearing angles must be determined numerically.

Figures B-2 through B-4 compare the performance of a particular real input narrowband adaptive tracker with the CRLB for a 100 Hz real sinusoidal signal from a target at 0°. The FFT size is 128 points and the resolution is 2 Hz. The distance between the split array phase centers is 150 feet. Three values of the feedback coefficient, μ, are shown, and the curves only plotted in the stable range of the filter. The dashed portions of the predicted rms error curves represent the range in which the numerical analysis is not valid.

It can be seen that above an input SNR of -20 dB, corresponding nominally to a 0 dB SNR in the bin, the ratio of the predicted rms error to the square root of CRLB is on the order of 1.15 to 1.5 if μ is small enough. This agrees well with the ratio of 1.228 developed by approximation above.
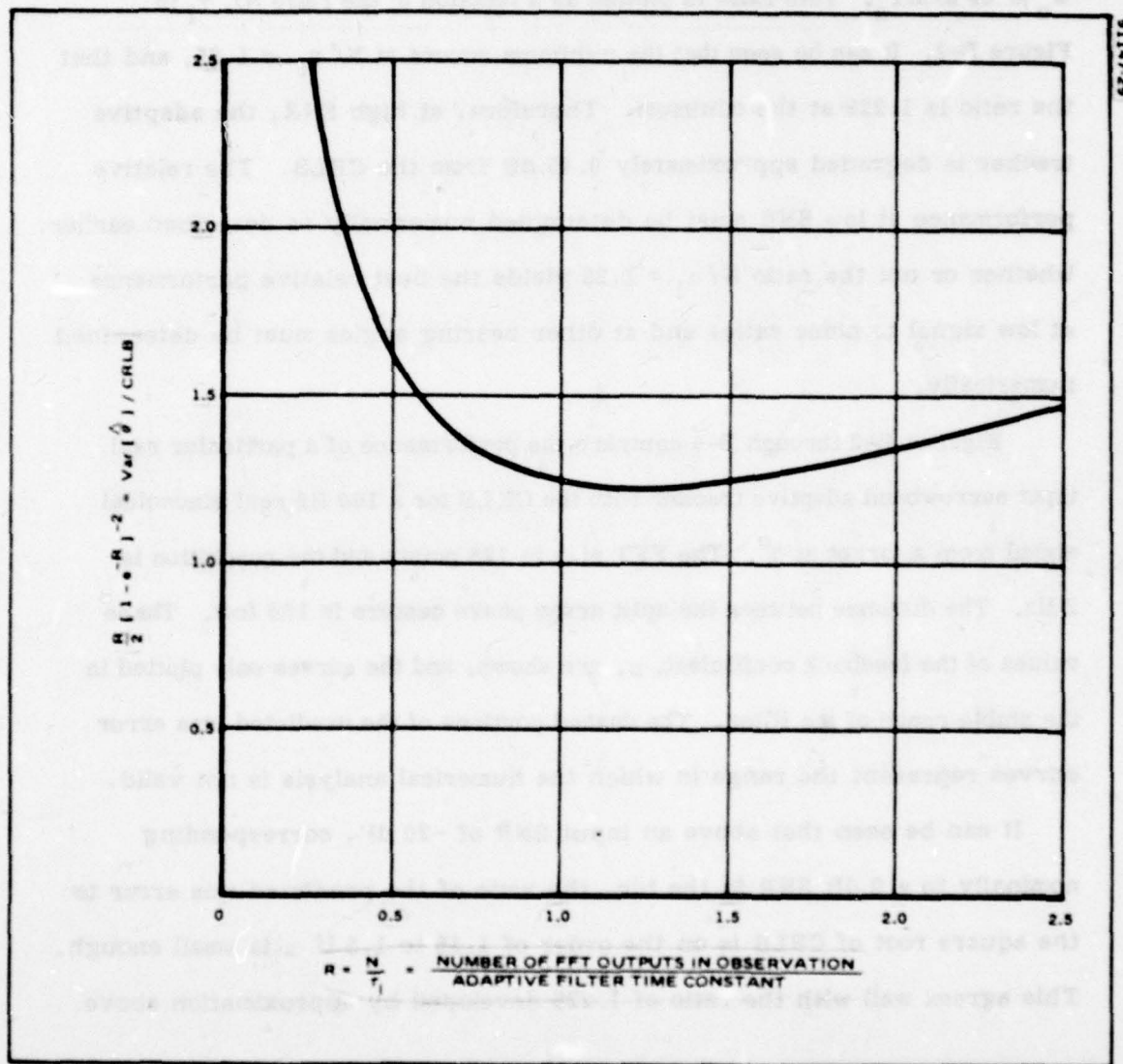
Figure B-1. Ratio of Adaptive Tracker Bearing Estimation Error Variance to Cramer Rao Lower Bound (High SNR, target near $\theta = 0^o$)

1·0

1·1

1·25   1·4

2·5

2·2

2·0

1·8

1·6
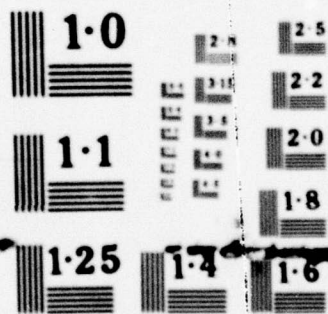
NATIONAL BUREAU OF STANDARDS
MICROCOPY RESOLUTION TEST CHART
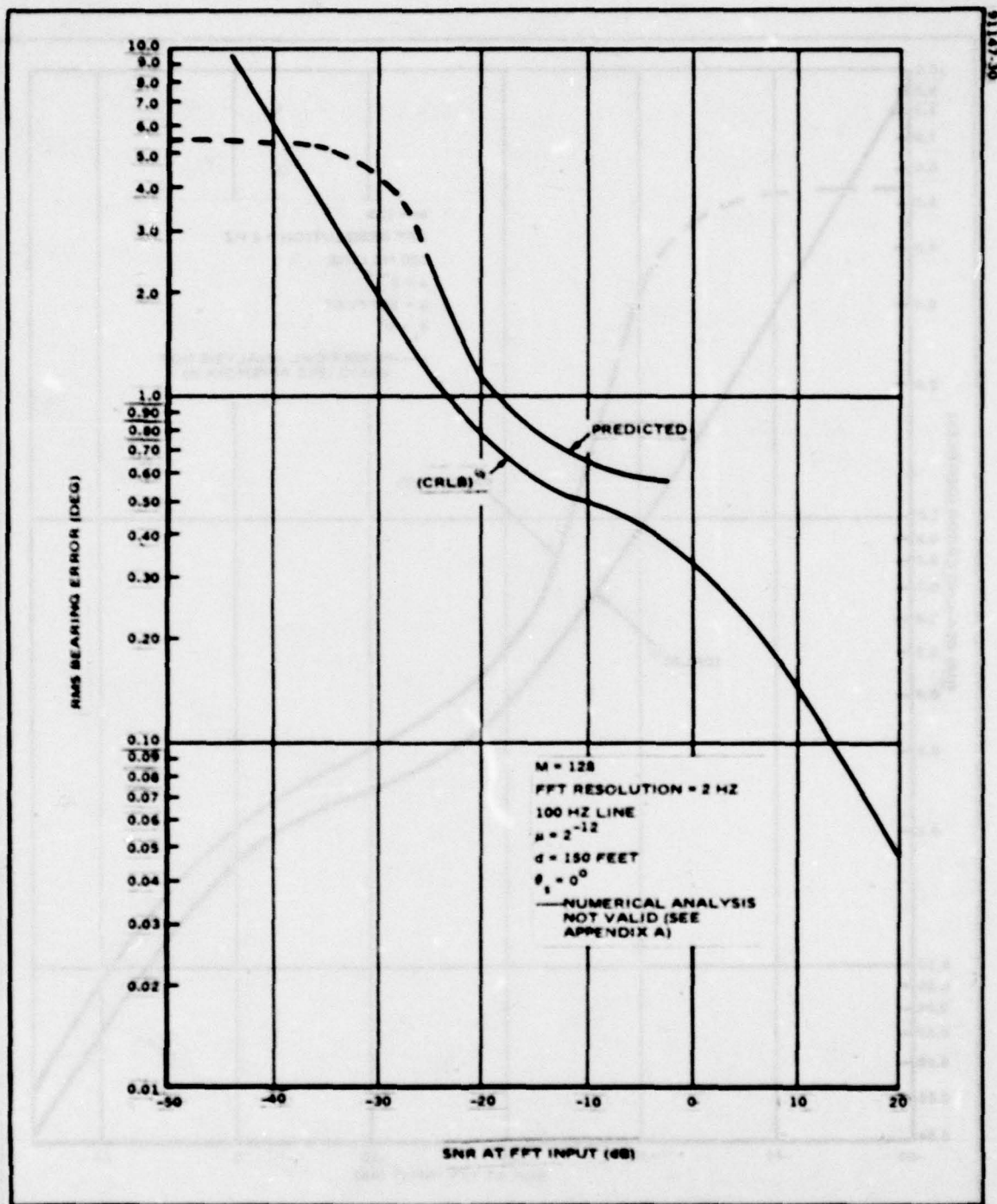
Figure B-2. Comparison of Predicted RMS Bearing Error with Cramer-RAO Lower Bound

B-13
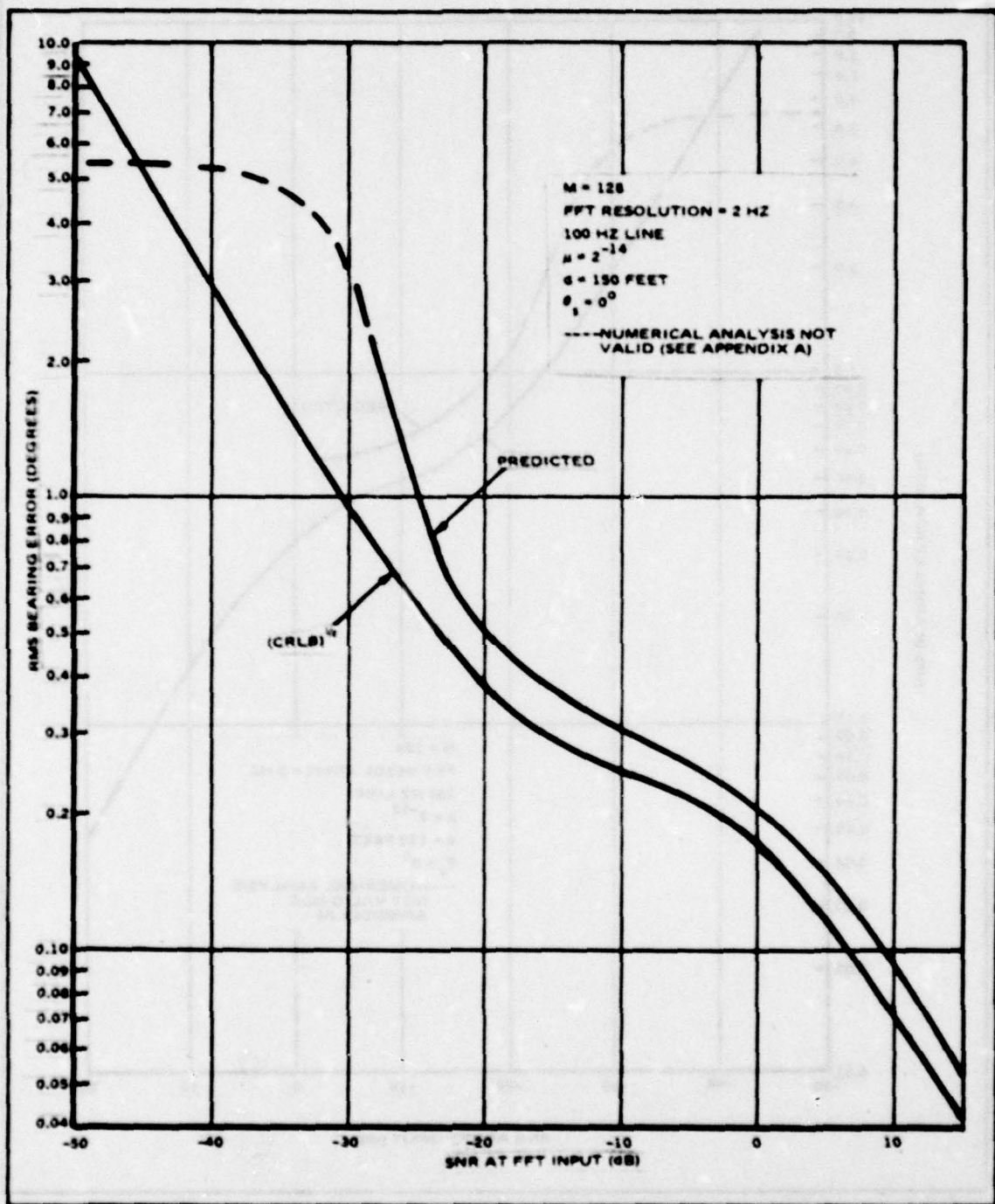
Figure B-3. Comparison of Predicted RMS Bearing Error with Cramer-RAO Lower Bound

APPENDIX C

Appendix C

Mean and Variance of the Adaptive Tracker Weights for Simultaneous Broadband and Narrowband Directional Source

The adaptive filter configuration of Figure C-1 has been proposed as an alternative to conventional split beam trackers as part of the Adaptive Tracking System Study [1]. In this approach, the split array outputs are provided as the primary and reference inputs to the adaptive filter. In the case of broadband signals, the bearing of the target is determined by extracting the time delay of the target wavefront between array halves from the time domain weight vector. [1] This is done by locating the peak of the weight vector, its location corresponding to the delay. For narrowband signals, the phase shift between array halves is extracted from the Fast Fourier Transform (FFT) of the weight vector and converted to bearing. [2]

Previous results have considered the mean and variance of these estimates for broadband signal only [1] and narrowband signal only in Appendix A. It is now desired to consider (1) single targets with both broadband and narrowband components, and (2) simultaneous broadband and narrowband sources from different directions, one the target of interest and one an interference. Analysis of the adaptive tracker performance in this case requires determination of the mean and variance of the weight vector with these inputs.

These statistics are developed in this Appendix by using the frequency domain realization of the algorithm, as done in Appendix A for narrowband signals only.

Analysis

Let the left and right half array inputs to the adaptive tracker be

$$d(t) = \sigma_s e^{j\omega_0(t-\tau_1)} + b(t - \tau_2) + n_d(t)$$

$$x(t) = \sigma_s e^{j\omega_0 t} + b(t) + n_x(t)$$

<div align="right">(C-1)</div>

where n_x, n_d, and b are independent, zero mean, white gaussian random processes. The delay, τ_1, is the delay of the narrowband signal between array halves, given by

$$\tau_1 = \frac{d}{c} \sin \theta_s$$

<div align="right">(C-2)</div>

and τ_2 the delay associated with the broadband signal,

$$\tau_2 = \frac{d}{c} \sin \theta_b$$

<div align="right">(C-3)</div>

where

d = distance between array centers

c = speed of sound

θ_s = bearing angle of narrowband source

θ_b = bearing angle of broadband source

It is assumed that the targets are in the same horizontal plane as the array centers, and that τ_2 is an integer multiple of the sample interval of the algorithm, T_s, that is

$$\tau_2 = \Delta T_s$$

<div align="right">(C-4)</div>

<div align="right">C-2</div>

Reference [1] considered the mean and variance of the weight vector of the adaptive tracker by utilizing a frequency domain model for the adaptive filter. This has been shown to behave equivalently to the time domain adaptive filter when the FFT time window is large. Appendix A extended these results to the case of a narrowband input signal. The assumptions necessary to use these results here are: (a) gaussian input sequences, (b) noise uncorrelated between split array outputs, and (c) frequency domain input sequences uncorrelated in time. It is shown in below that (a) and (b) are true and that (c) is approximately true for large FFT sizes.

The inputs to the single complex tap adaptive filter in the kth FFT bin are

$$X_k(n) = \sum_{\ell=0}^{m-1} x[(\ell - nM) T_s] e^{-j\frac{2\pi}{M}\ell k}$$ (C-5)

and

$$D_k(n) = \sum_{\ell=0}^{m-1} d[(\ell - nM) T_s] e^{-j\frac{2\pi}{M}\ell k}$$

The FFT is assumed to be performed with no redundancy and no gap between successive time records. These can be written as

$$X_k(n) = G(k, \omega_o) \sigma_s + N_{xk}(n) + B_{xk}(n)$$ (C-6)

and

$$D_k(n) = G(k, \omega_o) \sigma_s e^{-j\omega_o \tau_1} + N_{dk}(n) + B_{dk}(n)$$

where N_{xk}, B_{xk}, N_{dk}, and B_{dk} are the transforms of n_x, $b(t)$, n_d, and $b(t - \tau_2)$, respectively, and

$$G(k, \omega_o) = \frac{\sin\left[\frac{M}{2}(\frac{2\pi}{M} k - \omega_o T_s)\right]}{\sin\left[\frac{1}{2}(\frac{2\pi}{M} k - \omega_o T_s)\right]} e^{j\frac{M-1}{2}\left(\frac{2\pi}{M}k - \omega_o T_s\right)} e^{j\omega_o n M T_s} \quad (C-7)$$

It is assumed that $k \neq 0$, $M/2$ since the results differ in these bins. It was shown in reference [1] that for $k \neq 0$, $M/2$,

$$E[N_{xk}] = E[N_{dk}] = 0$$

$$E[N_{xk}N_{dk}] = 0 \quad (C-8)$$

and

$$E[N_{xk}(m)N_{xk}^*(p)] = \begin{cases} 0, & p \neq m \\ M\sigma_{nx}^2, & p = m \end{cases}$$

$$\quad (C-9)$$

$$E[N_{dk}(m)N_{dk}^*(p)] = \begin{cases} 0, & p \neq m \\ M\sigma_{nd}^2, & p = m \end{cases}$$

It is also easily shown that

$$E[B_{dk}(m)] = E[B_{xk}(m)] = 0$$

$$E[B_{xk}(m)B_{xk}^*(p)] = E[B_{dk}(m)B_{dk}^*(p)] = \begin{cases} 0, & p \neq m \\ M\sigma_b^2, & p = m \end{cases}$$

However,

$$E[B_{dk}(m)B_{xk}^*(p)] = \sum_{\ell=0}^{M-1}\sum_{q=0}^{M-1} E\{b[(\ell-mM)T_s]\, b[(q-pm)T_s-\tau_2]\} e^{-j\frac{2\pi}{M}(\ell-q)k}$$

$$= \sigma_b^2 \sum_{\ell=0}^{M-1}\sum_{q=0}^{M-1} \delta[(\ell-q)T_s + (m-p)MT_s - \tau_2] e^{-j\frac{2\pi}{M}(\ell-q)k} \quad (C-10)$$

Given the range of ℓ and q, if $|n-p| > 1$, then the expectation is zero. If $m = p$, then

$$E[B_{dk}(m)B_{xk}^*(p)] = \sigma_b^2(M-\Delta)e^{-j\frac{2\pi}{M}\Delta k} \tag{C-11}$$

and if $|m-p| = 1$

$$E[B_{dk}(m)B_{xk}^*(p)] = \sigma_b^2 \Delta e^{-j\frac{2\pi}{M}(M-\Delta)k} \tag{C-12}$$

The input samples to the single tap filter in the kth bin are not, therefore, uncorrelated as assumed in [1]. However, the correlation coefficient between adjacent samples ($|m-p| = 1$) is

$$p = \frac{\Delta}{m-\Delta} \tag{C-13}$$

Therefore, if $M >> \Delta$, the input sequence is approximately uncorrelated, and we the results of Appendix III, reference [2] apply.

From [2], the mean weight in the kth bin can be written as

$$E[W(n+1)] = \mu \sum_{m=0}^{n} E[D_k(m)X_k^*(m)] \prod_{k=m+1}^{n} E[1-\mu|X(k)|^2] \tag{C-14}$$

Using the above model,

$$E[D_k(m)X_k^*(m)] = |G(k,\omega_0)|^2 \sigma_s^2 e^{-j\omega_0 t_1} + (M-\Delta)\sigma_b^2 e^{-j\frac{2\pi}{M}\Delta k} \tag{C-15}$$

and

$$E[|X_k(m)|^2] = |G(k,\omega_0)|^2 \sigma_s^2 + M\sigma_b^2 + M\sigma_n^2$$

Substituting in (C-15) gives

$$E[W(n+1)] = \frac{1-\left[1-\mu(|G(k,\omega_0)|^2\sigma_s^2 + M(\sigma_n^2+\sigma_b^2))\right]^{n+1}}{|G(k,\omega_0)|^2\sigma_s^2 + M(\sigma_n^2+\sigma_b^2)}$$

$$\cdot \left[|G(k,\omega_0)|^2\sigma_s^2 e^{-j\omega_0 t_1} + (M-\Delta)\sigma_b^2 e^{-j\frac{2\pi}{M}\Delta k}\right] \tag{C-16}$$

Under the condition that $\left|1-\mu\left(|G(k,\omega_0)|^2 G_s^2 + M(\sigma_n^2+\sigma_b^2)\right)\right| < 1$,

C-5

this gives a steady state mean weight of

$$E[W(\infty)] = \frac{1}{|G(k,\omega_o)|^2 \sigma_s^2 + M(\sigma_n^2 + \sigma_b^2)} \left[|G(k,\omega_o)|^2 \sigma_s^2 e^{-j\omega_o \tau} 1 \right.$$

$$\left. + (M-\Delta)\sigma_b^2 e^{-j\frac{2\pi}{M}\Delta k} \right] \tag{C-17}$$

To compute the mean square weight, use the results of Appendix III of [1],

$$E\left[|W(n+1)|^2\right] = \mu^2 \sum_{m=0}^{n} E|F(m)|^2 + 2\mu^2 R_e \left(\sum_{M=0}^{n} \sum_{q=0}^{m-1} E[F(m)F^*(q)] \right)$$

$$\tag{C-18}$$

and

$$F(m) = D_k(m) X_k(m) \prod_{\ell=m+1}^{n} \left[1 - \mu \, |X_k(\ell)|^2 \right]$$

Reference [1] also gives

$$E|F(m)|^2 = E\left[\left|D_k(m)\, X_k(n)\right|^2\right] \prod_{p=m+1}^{n} E\left\{\left[1 - \mu\left|X_k(p)\right|^2\right]^2\right\} \quad \text{(C-19)}$$

With considerable algebra, it can be shown that

$$E\left[\left|D_k(m)\, X_k(m)\right|^2\right] = \left[|G|^2\, \sigma_s^2 + M(\sigma_n^2 + \sigma_b^2)\right]^2$$

$$+ (M - \Delta)^2\, \sigma_b^4 + \left|S(M, \Delta)\right|^2 \sigma_b^4$$

$$+ 2\mathrm{Re}\left[G^2\, S^*(M, \Delta)\, \sigma_s^2 \sigma_b^2\, e^{-j\left[\omega_o \tau_1 - \frac{2\pi}{M}\Delta k\right]}\right]$$

$$+ 2\mathrm{Re}\left[|G|^2\, (M - \Delta)\, \sigma_s^2 \sigma_b^2 \right.$$

$$\left. \cdot e^{j\left[\omega_o \tau_1 - \frac{2\pi}{M}\Delta k\right]}\right] = A_1 \quad \text{(C-20)}$$

and

$$E\left[1 - \mu\left|X_K(p)\right|^2\right]^2 = 1 - A_4 \quad \text{(C-21)}$$

where

$$A_4 = 2\mu\left[|G|^2\sigma_s^2 + M\left(\sigma_b^2 + \sigma_n^2\right)\right] - {}^2\left[|G|^4\sigma_s^4 + 2M^2\left(\sigma_n^2 + \sigma_b^2\right)^2\right.$$

$$\left. + 4|G|^2\, M\sigma_s^2\left(\sigma_n^2 + \sigma_b^2\right)\right) \quad \text{(C-22)}$$

with

$$\left| G \right|^2 = \left| G(k, \omega_o) \right|^2$$

Therefore

$$\mu^2 \sum_{m=0}^{n} E\left[\left| F(m) \right|^2 \right] = \mu^2 A_1 \frac{1 - (1 - A_4)^{n+1}}{A_4} \qquad (C-23)$$

and if $\left| A_4 \right| < 1$, this goes to

$$\mu \sum_{M=0}^{\infty} E\left[\left| F(n) \right|^2 \right] = \mu^2 \frac{A_1}{A_4} \qquad (C-24)$$

To evaluate the second term of (C-18), the evaluation of $E\left[F_k(m) \, F_K^*(m) \right]$ is required [1].

$$E\left[F_k(m) \, F_k^*(q) \right] = E\left[D_k^*(q) \, X_k(q) \right]$$

$$\cdot E\left\{ D_k(m) \, X_k^*(m) \left[1 - \mu \left| X_k(n) \right|^2 \right] \right.$$

$$\cdot \prod_{v=q+1}^{m-1} E\left[1 - \mu \left| X_k(v) \right|^2 \right]$$

$$\cdot E\left\{ \prod_{p=m+1}^{n} \prod_{v=m+1}^{n} \left[1 - \mu \left| X_k(p) \right|^2 \right] \right.$$

$$\left. \left. \left[1 - \mu \left| X_k(q) \right|^2 \right] \right\} \right. \qquad (C-25)$$

C-8

Again, it can be shown that

$$E \left[D_k^*(q) \, X_k(q) \right] = \left\{ E \left[D_k(q) \, X_k^*(q) \right] \right\}^*$$

$$= |G|^2 \, \sigma_s^2 \, e^{j\omega_o \tau_1} + (M - \Delta) \, \sigma_b^2 \, e^{j\frac{2\pi}{M}\Delta k}$$

$$= A_2^*$$

$$E \left[1 - \mu \left| X_k(v) \right|^2 \right] = 1 - \mu P_T \tag{C-26}$$

where

$$P_T = |G|^2 \, \sigma_s^2 + M \left(\sigma_n^2 + \sigma_b^2 \right)$$

Finally, with considerable computation, it can be shown that

$$E \left[D_K(m) \, X_k^*(m)(1 - \mu \left| X_k(m) \right|^2) \right] = A_2 -$$

$$- \mu \left\{ A_2 \left[|G|^2 \sigma_s^2 + 2M(\sigma_n^2 + \sigma_b^2) \right] \right.$$

$$+ |G|^2 \, (M - \Delta) \, \sigma_s^2 \sigma_b^2 \, e^{-j\frac{2\pi}{M}\Delta k}$$

$$+ |G|^2 \, |S(M,\Delta)| \, \sigma_s^2 \sigma_b^2 \, e^{-j\frac{2\pi}{M}\Delta k} \, e^{-j(M-1)\omega_o \tau s} \right\}$$

$$\tag{C-27}$$

Therefore

$$E\left[F_k(m) \ F_k^*(q)\right] = A_2^* \left[A_2 - \mu \left\{A_2 \left[|G|^2 \sigma_s^2 + 2M(\sigma_n^2 + \sigma_b^2)^2\right]\right.\right.$$

$$+ |G|^2 (M - \Delta) \ \sigma_s^2 \sigma_b^2 \ e^{-j\frac{2\pi}{M}\Delta k}$$

$$\left.\left.+ |G|^2 | S(M, \Delta)| \ \sigma_s^2 \sigma_b^2 \ e^{-j\frac{2\pi}{M}\Delta k} \ e^{j(M-1)\omega_o T_s}\right\}\right]$$

$$[1 - \mu \ P_T]^{m-q-1} \ [1 - A_4]^{n-m} \tag{C-28}$$

Substituting this in (C-25) and closing the sums gives

$$\sum_{m=0}^{n} \ \sum_{q=0}^{m-1} \ E \ [F_k(m) \ F_k^*(q)] = \frac{A_2^* A_7}{\mu P_T} \left\{\frac{(1 - \mu P_T)^{n+1} - (1 - A_4)^{n+1}}{\mu P_T - A_4}\right.$$

$$\left.+ \frac{1 - [1 - A_4]^{n+1}}{A_4}\right\} \tag{C-29}$$

If $\mu P_T < 1$ and $|A_4| < 1$, as $n \rightarrow \infty$, this goes to

$$\sum_{m=0}^{\infty} \ \sum_{q=0}^{m-1} \ E \ [F_k(n) \ F_k^*(q)] = \frac{A_2^* A_7}{\mu P_T A_4} \tag{C-30}$$

The mean square weight in steady state is therefore

$$E\left[\,|W(\infty)|^2\,\right] \;=\; \mu^2 \frac{A_1}{A_4}$$

$$+\; 2\mu^2\, R_e\left\{\frac{1}{\mu P_T A_4}\left[\,|A_2|^2\left[1-\mu(\,|G|^2\sigma_s^2+2M(\sigma_n^2+\sigma_b^2)\right]-\mu A_2^* A_3\,\right]\right\}$$

$$\overline{\hspace{3cm}}\text{(C-31)}$$

with

$$A_3 \;=\; |G|^2\,(m-\Delta)\,\sigma_s^2\sigma_b^2\,e^{-j\frac{2\pi}{M}\Delta k}$$

$$+\; |G|^2\, S(M,\Delta)\,\sigma_s^2\sigma_b^2\,e^{-j\frac{2\pi}{M}\Delta k}\,e^{j(M-1)\omega_o T_s}$$

To obtain the variance, subtract $\left|E[W(\infty)]\right|^2$, and obtain

$$\text{Var }\{W(\infty)\} \;=\; \frac{\mu P_T^2 A_1 + 2|A_2|^2 P_T\left|\left(1-\mu(\,|G|^2\sigma_s^2 + 2M(\sigma_n^2+\sigma_b^2)\right)\right) - 2\mu A_6\right| - |A_2|^2 A_5}{P_T^2 A_5} \quad \text{(C-32)}$$

where

$$P_T \;=\; |G|^2\,\sigma_s^2 + M\left(\sigma_n^2 + \sigma_b^2\right)$$

$$A_1 = P_T^2 + (M - \Delta)^2 \sigma_b^4 + |S(M, \Delta)|^2 \sigma_b^4$$

$$+ 2|G|^2 (M - \Delta) \sigma_s^2 \sigma_b^2 \cos\left[\omega_0 \tau_1 - \frac{2\pi}{M}\Delta k\right]$$

$$+ 2|G|^2 |S(M, \Delta)| \sigma_s^2 \sigma_b^2 \cos\left[\omega_0 \tau_1 - \frac{2\pi}{M}\Delta k + \omega_0 (M - 1) T_s\right]$$

$$A_2 = |G|^2 \sigma_s^2 e^{-j\omega_0 \tau_1} + (M - \Delta) \sigma_b^2 e^{-j\frac{2\pi}{M}\Delta k}$$

$$A_6 = |G|^2 \sigma_s^2 \left\{ (M - \Delta)^2 \sigma_b^4 + (M - \Delta)|S(M, \Delta)| \sigma_b^4 \cos\left[(M - 1)\omega_0 T_s\right] \right.$$

$$+ |G|^2 (M - \Delta) \sigma_s^2 \sigma_b^2 \cos\left[\omega_0 \tau_1 - \frac{2\pi}{M}\Delta k\right]$$

$$+ |G|^2 |S(M, \Delta)| \sigma_s^2 \sigma_b^2 \cos\left[\omega_0 \tau_1 - \frac{2\pi}{M}\Delta k + (M - 1) \omega_0 T_s\right]$$

$$A_5 = 2P_T - \mu \left[|G|^4 \sigma_s^4 + 2M^2 (\sigma_n^2 + \sigma_b^2)^2 + 4|G|^2 M \sigma_s^2 (\sigma_n^2 + \sigma_b^2) \right]$$

When either $\sigma_s^2 = 0$ or $\sigma_b^2 = 0$, this checks with previous results.

In most cases of interest, either the tracker will be implemented in the time domain, so that no windowing occurs, or $M \gg \Delta$, so windowing is negligible. In that case

$$M - \Delta \approx M$$

and

$$S(M, \Delta) \approx 0$$

C-12

Therefore

$$A_1 = P_T^2 + M^2 \sigma_b^4 + 2|G|^2 M \sigma_s^2 \sigma_b^2 \cos \left[\omega_o \tau_1 - \frac{2\pi}{M} \Delta k \right]$$

$$A_2 = |G|^2 \sigma_s^2 e^{-j \omega_o \tau_1} + M \sigma_b^2 e^{-j \frac{2\pi}{M} \Delta k}$$

$$A_6 = |G|^2 \sigma_s^2 \left\{ M^2 \sigma_b^4 + |G|^2 M \sigma_s^2 \cos \left[\omega_o \tau_1 - \frac{2\pi}{M} \Delta k \right] \right\} \tag{C-33}$$

and A_5 is unchanged. This can be rewritten as

$$\text{Var}[W(\infty)] \approx \frac{\mu \left[\begin{array}{l} 2|G|^6 M \sigma_s^6 \left(\sigma_n^2 + \sigma_b^2 \right) + \left[|G|^4 M^2 \sigma_s^4 + |G|^2 M^3 \sigma_s^2 \left(\sigma_n^2 + \sigma_b^2 \right) \right] \left[4 \left(\sigma_n^2 + \sigma_b^2 \right)^2 - 2\sigma_b^4 \right] \\ + M^4 \left(\sigma_n^2 + \sigma_b^2 \right)^2 \left(\sigma_n^4 + 2 \sigma_n^2 \sigma_b^2 \right) \\ - 2|G|^2 M \sigma_s^2 \sigma_b^2 \left[|G|^4 \sigma_s^4 + |G|^2 M \sigma_s^2 \left(\sigma_n^2 + \sigma_b^2 \right) + M^2 \left(\sigma_n^2 + \sigma_b^2 \right)^2 \right] \cos \left[\omega_o \tau_1 - \frac{2\pi}{M} \Delta k \right] \end{array} \right]}{\left[\left(|G|^2 \sigma_s^2 + M \left(\sigma_n^2 + \sigma_b^2 \right) \right)^2 \left(2 \left(|G|^2 \sigma_s^2 + M \left(\sigma_n^2 + \sigma_b^2 \right) \right) \right. \right.} \tag{C-34}$$

$$\left. \left. - \mu \left(|G|^4 \sigma_s^4 + 2M^2 \left(\sigma_n^2 + \sigma_b^2 \right)^2 + 4|G|^2 M \sigma_s^2 \left(\sigma_n^2 + \sigma_b^2 \right) \right) \right) \right]$$

Note that the cosine term vanishes whenever $\omega_o \tau_1 = 2\Delta k/M$, which happens when the broadband and narrowband energy come from the same direction and the narrowband signal is bin centered.

Summary

Expressions for the mean and variance of the complex weight of the frequency domain adaptive tracker in the presence of simultaneous broadband and narrowband directional sources at arbitrary bearing angles have been developed.

These results allow determination of:

(1) Performance of narrowband adaptive tracker algorithm for targets with broadband and narrowband components by the method of Appendix A.

(2) Effect of broadband interference on narrowband tracker by the same method.

(3) Performance of the broadband tracker algorithm for targets with narrowband components using the method of [1].

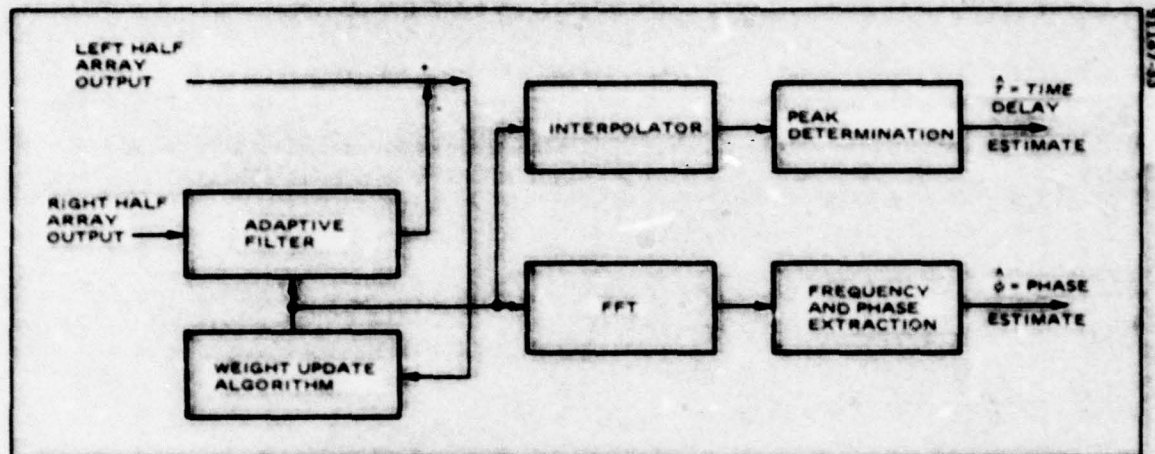(4) Effects of narrowband interference on the broadband tracker by the same methods.

Figure C-1. Adaptive Tracker Structure.

APPENDIX D

Appendix D

Statistics of Narrowband Adaptive Tracker Bearing Estimate with Simultaneous Broadband and Narrowband Directional Sources

During Phase 1 of the Adaptive Tracking System Study, the adaptive filter configuration of Figure C-1 has been proposed as a means of determining the bearing of a narrowband source. The outputs of the two split arrays provide the reference and primary inputs of the adaptive filter. When only the narrowband target and the uncorrelated hydrophone noise are present, the mean weight vector converges to a sampled sinusoid at the same frequency as the narrowband source with a phase shift

$$\phi = \omega_c \frac{d}{c} \sin \theta_s \qquad (D-1)$$

where ω_0 is the source frequency, θ_s is the source bearing angle, d the distance between array phase centers, and c the speed of sound. It is assumed that the target is in the same horizontal plane as the array phase centers. To extract this phase angle, the weight vector is Fast Fourier Transformed, and the bin with the largest magnitude chosen as that containing the signal. The phase of this bin, which is corrupted by background and algorithm noise, is the estimate of the phase angle.

In order to convert this phase estimate, $\hat{\phi}$, to a bearing estimate, $\hat{\theta}$, it is necessary to know the frequency of the signal, which is not known a priori and must be estimated. This could be done by interpolating between the discrete FFT bins to determine the frequency of the sinusoid. However, it is assumed here that the FFT bins are sufficiently closely spaced that the center frequency of the

D-1

bin with the largest magnitude is taken as the frequency estimate, $\widehat{\omega}_o$. The bearing estimate is then given by

$$\widehat{\theta} = \sin^{-1}\left(\frac{c}{d\widehat{\omega}_o}\,\widehat{\phi}\right) \tag{D-2}$$

Appendix A developed the mean and variance of the bearing estimate of such a tracker when the narrowband source is the only directional component in the noise field. Considered herein is the case when a broadband directional source is also present. When located at an angle different from the narrowband source this may represent a broadband interference, while the broadband source at the same angle as the narrowband source models a single target with components of both types. In Appendix A, the mean and variance of the bearing estimate for the narrowband adaptive tracker with a sinusoidal signal was determined as follows:

(1) Derive the mean and standard deviation of the FFT of the time domain weight vector.

(2) Based upon the large number of iterations required in the adaptive algorithm, assume that the FFT of the weights are complex gaussian random variables.

(3) Transform the weights to polar coordinates, then integrate out the magnitude, yielding the density of the phase of each FFT bin.

(4) Using numerical integration, obtain the mean and variance of the bearing estimate from the phase density.

The density of the phase in the kth FFT bin, ϕ_k, was shown to be

$$f_{\phi}(\phi_k) = \frac{\exp(-\beta^2)}{2\pi} + \frac{\beta\cos(\phi_k - \psi)}{2\pi^{\frac{1}{2}}}\exp\left[-\beta^2\sin^2(\phi_k - \psi)\right]\left[1 + \text{erf}\left(\beta\cos(\phi_k - \psi)\right)\right] \tag{D-3}$$

where

$$\text{erf}(x) \triangleq \frac{2}{\pi^{1/2}} \int_0^x e^{-z^2} \, dz, \quad x \geq 0$$

$$\text{erf}(x) \triangleq -\text{erf}(|x|), \quad x < 0$$

$$\beta^2 = \frac{|E(W_k)|^2}{\text{Var}(W_k)}$$

$$\psi = \arg\left(\frac{\text{Im}\{E(W_k)\}}{\text{Re}\{E(W_k)\}}\right)$$

and

$$W_k = \text{FFT of weight vector in } k^{th} \text{ FFT bin.}$$

This result is equally valid in the case where the both broadband and narrowband directional components are present. From [2], when both are present, the mean and variance of the weights in the kth FFT bin in steady state is:

$$E\left[W_k\right] = \frac{1}{P_T^2}\left[|G|^2 \sigma_s^2 e^{-j\omega_0 \tau_1} + M\sigma_b^2 e^{-j\frac{2\pi}{M}\Delta k}\right] \tag{D-4}$$

and

$$\text{Var}\left[W_k\right] = \frac{\mu\left[\begin{array}{l} 2|G|^6 M\sigma_s^6\left(\sigma_n^2+\sigma_b^2\right) + \left[|G|^4 M^2 \sigma_s^4 + |G|^2 M^3 \sigma_s^2\left(\sigma_n^2+\sigma_b^2\right)\right]\left[4\left(\sigma_n^2+\sigma_b^2\right)^2 - 2\sigma_b^4\right] \\ + M^4\left(\sigma_n^2+\sigma_b^2\right)^2\left(\sigma_n^4 + 2\sigma_n^2\sigma_b^2\right) \\ -2|G|^2 M\sigma_s^2\sigma_b^2\left[|G|^4\sigma_s^4 + |G|^2 M\sigma_s^2\left(\sigma_n^2+\sigma_b^2\right) + M^2\left(\sigma_n^2+\sigma_b^2\right)^2\right]\cos\left[\omega_0 \tau_1 - \frac{2\pi}{M}\Delta k\right]\end{array}\right]}{\left(|G|^2\sigma_s^2 + M\left(\sigma_n^2+\sigma_b^2\right)\right)^2\left[2\left(|G|^2\sigma_s^2 + M\left(\sigma_n^2+\sigma_b^2\right)\right) - \mu\left(|G|^4\sigma_s^4 + 2|G|^2 M\sigma_s^2\left(\sigma_n^2-\sigma_b^2\right) + 4M^2\left(\sigma_n^2+\sigma_b^2\right)^2\right)\right]}$$

$$\tag{D-5}$$

Therefore, for this case,

$$
\beta^2 = \frac{\mu^{-1}\left[|G|^4\sigma_s^4 + M^2\sigma_b^4 + 2|G|^2 M\sigma_s^2\sigma_b^2\cos\left[\omega_0\tau_1 - \frac{2\pi}{M}\,\Delta k\right]\right]\left[2P_T - \mu\left(|G|^4\sigma_s^4 + 2|G|^2 M\sigma_s^2\left(\sigma_n^2+\sigma_b^2\right) + 4M^2\left(\sigma_n^2+\sigma_b^2\right)^2\right)\right]}{\begin{bmatrix} 2|G|^6 M\sigma_s^2\left(\sigma_n^2+\sigma_b^2\right) + \left[|G|^4 M\sigma_s^4 + |G|^2 M^3\sigma_s^2\left(\sigma_n^2+\sigma_b^2\right)\right]\left[4\left(\sigma_n^2+\sigma_v^2\right)^2 - 2\sigma_b^4\right] \\[4pt] + M^4\left(\sigma_n^2+\sigma_b^2\right)^2\left(\sigma_n^4+2\sigma_n^2\sigma_b^2\right) \\[4pt] -2|G|^2 M\sigma_s^2\sigma_b^2\left[|G|^4\sigma_s^4 + |G|^2 M\sigma_s^2\left(\sigma_n^2+\sigma_b^2\right) + M^2\left(\sigma_n^2+\sigma_b^2\right)^2\right]\cos\left[\omega_0\tau_1 - \frac{2\pi}{M}\,\Delta k\right] \end{bmatrix}}
$$

(D-6)

and

$$
\Psi = \tan^{-1}\left[\frac{|G|^2\sigma_s^2\sin\omega_0\tau_1 + M\sigma_b^2\sin\left(\frac{2\pi}{M}\,\Delta k\right)}{|G|^2\sigma_s^2\cos\omega_0\tau_1 + M\sigma_b^2\cos\left(\frac{2\pi}{M}\,\Delta k\right)}\right]
$$

(D-7)

In these expressions

μ = adaptive filter feedback coefficient

σ_s^2 = power in narrowband directional component

σ_b^2 = variance of broadband directional component

σ_n^2 = variance of noise

M = no. of adaptive filter taps = no. of FFT bins

$$
|G|^2 = |G(k,W_0)|^2 = \frac{\sin^2\left[\pi k - \frac{M\omega_0 T_s}{2}\right]}{\sin^2\left[\frac{\pi k}{M} - \frac{\omega_0 T_s}{2}\right]}
$$

(D-8)

D-4

T_s = algorithm sample rate

ω_0 = radian frequency of narrowband component

$$\tau_1 = \frac{d}{c} \sin \theta_s \quad , \quad \Delta T_s = \frac{d}{c} \sin \theta_b \tag{D-9}$$

τ_1 = delay in narrowband signal between array phase centers

ΔT_s = delay in broadband signal between array phase centers

Δ = integer

d = distance between array phase centers

c = speed of sound

θ_s = bearing angle of narrowband source

θ_b = bearing angle of broadband source

It is assumed that the directional sources are in the same horizontal plane as the array phase centers.

The bearing estimate [1] is then

$$\hat{\theta} = \sin^{-1}\left[\frac{cMT_s}{2\pi kc}\phi_{max}\right] \tag{D-10}$$

where ϕ_{max} is the phase of the bin with the largest magnitude. Therefore,

$$E\left[\hat{\theta}\right] = \int_{-\pi}^{\pi} \sin^{-1}\left[\frac{cMT_s}{2\pi kd}\phi_{max}\right] f_{\phi_{max}}(\phi_{max}) \, d\phi_{max} \tag{D-11}$$

$$E\left[\hat{\theta}^2\right] = \int_{-\pi}^{\pi} \left[\sin^{-1}\left[\frac{cMT_s}{2\pi kd}\phi_{max}\right]\right] f_{\phi_{max}}(\phi_{max}) \, d\phi_{max} \tag{D-12}$$

D-5

and

$$\text{Var}\left[\hat{\theta}\right] = E\left[\hat{\theta}^2\right] - E^2\left[\hat{\theta}\right] \tag{D-13}$$

The density, $f_{\phi_{max}}$, is that of the phase in the bin with the largest magnitude. While these integrals cannot be evaluated explicitly, they can be evaluated numerically on the computer. Care must be taken in the interpretation of these results due to the modulo 2π assumption inherent in the derivation of the phase density (see pages 15 and 22 of Appendix A).

The density given in (D-3) is even about $(\phi - \gamma) = 0$, so that

$$E(\phi - \gamma) = E\left[\phi\right] - \gamma = 0$$

or

$$E\left[\phi\right] = \gamma$$

Since the estimate of interest is the bearing of the narrowband source, the "correct" phase angle is $\phi_s = \omega_0 \tau_1$. Expression (20) can be written as

$$\gamma = \arctan\left[\frac{\sin \omega_0 \tau_1 + \lambda^{-1} \sin\left(\frac{2\pi}{M}\Delta k\right)}{\cos \omega_0 \tau_1 + \lambda^{-1} \sin\left(\frac{2\pi}{M}\Delta k\right)}\right] \tag{D-14}$$

with λ the signal-to-interference ratio in the FFT bin, given by

$$\lambda = \frac{|G(k, \omega_0)|^2 \sigma_s^2}{(M-\Delta) \sigma_b^2} \tag{D-15}$$

The bias in the phase angle is $E(\phi - \omega_0 \tau_1) = \gamma - \omega_0 \tau_1$. By a trigonometric identity

$$\tan\left[\omega_0 \tau_1 - \gamma\right] = \frac{\tan \omega_0 \tau_1 - \tan \gamma}{1 + \tan \omega_0 \tau_1 \tan \gamma} \tag{D-16}$$

Substituting (24) and (22) and solving for $\omega_0 \tau_1 - \gamma$ gives

$$B = \omega_0 \tau_1 - \gamma = \arctan\left[\frac{\sin\left(\omega_0\tau_1 - \frac{2\pi}{M}\Delta k\right)}{\lambda + \cos\left(\omega_0\tau - \frac{2\pi}{M}\Delta k\right)}\right] \tag{D-17}$$

This gives the bias in the phase angle of the FFT bin containing the signal as a function of the time delays associated with the broadband and narrowband signals. Figure D-1 shows this function plotted against the difference $(\omega_0\tau_1 - 2\pi$ to $M\Delta k)$ for various values of the signal-to-interference ratio, λ. For angles from $-0°$ to $-180°$, it can be seen from (25) that the function is odd about $0°$.

When the apparent bearing angle of the target is small, then the bearing estimate is

$$\hat{\theta}_s = \arcsin\left[\frac{MTs}{2\pi k}\frac{C}{d}\phi\right] \approx \frac{MTs}{2\pi k}\frac{C}{d}\phi \tag{D-18}$$

Then the bias in the narrowband bearing estimate is

$$B = E\left[\hat{\theta}_s - \theta_s\right] \approx \frac{MTs}{2\pi k}\frac{c}{d}\gamma - \theta_s$$

$$\approx -\frac{MTs}{2\pi k}\frac{c}{d}\arctan\left[\frac{\sin\left(\omega_0\tau_1 - \frac{2\pi}{M}\Delta k\right)}{\lambda + \cos\left(\omega_0\tau_1 - \frac{2\pi}{M}\Delta k\right)}\right] + \frac{MTs}{2\pi k}\frac{c}{d}\omega_0\tau_1 - \theta_s$$

$$\approx \left(\frac{\omega_0 MTs}{2\pi k} - 1\right)\theta_s - \frac{MTs}{2\pi k}\frac{c}{d}\arctan\left[\frac{\sin\left(\omega_0\tau_1 - \frac{2\pi}{M}\Delta k\right)}{\lambda + \cos\left(\omega_0\tau_1 - \frac{2\pi}{M}\Delta k\right)}\right] \tag{D-19}$$

The first term is a bias occurring when the narrowband component is not bin centered, and becomes negligible as the resolution of the FFT increases. The second term is just expression (D-17) multiplied by the factor $(MTsc/2\pi kd)$.

To obtain some feel for the magnitude of the bias to be expected in the narrowband bearing estimate due to broadband interference, consider an array with 75 feet between phase centers, operating on a 600 Hz sinusoid, which is bin centered in the FFT. In this case,

$$\left(\frac{MTs}{2\pi k}\frac{c}{d}\right) = 0.0178$$

that is, a $10°$ bias in phase ϕ, represents only a $0.178°$ bias in bearing. Then to interpret Figure D-1 for this array, the scales on the axes are multiplied by 0.0178. Hence, for an interference 3 dB below the narrowband component in the FFT bin, the bias is at most $(0.0178 \times 30°) = 0.531°$, while for an interference 12 dB down, the bias is at most $0.0637°$.
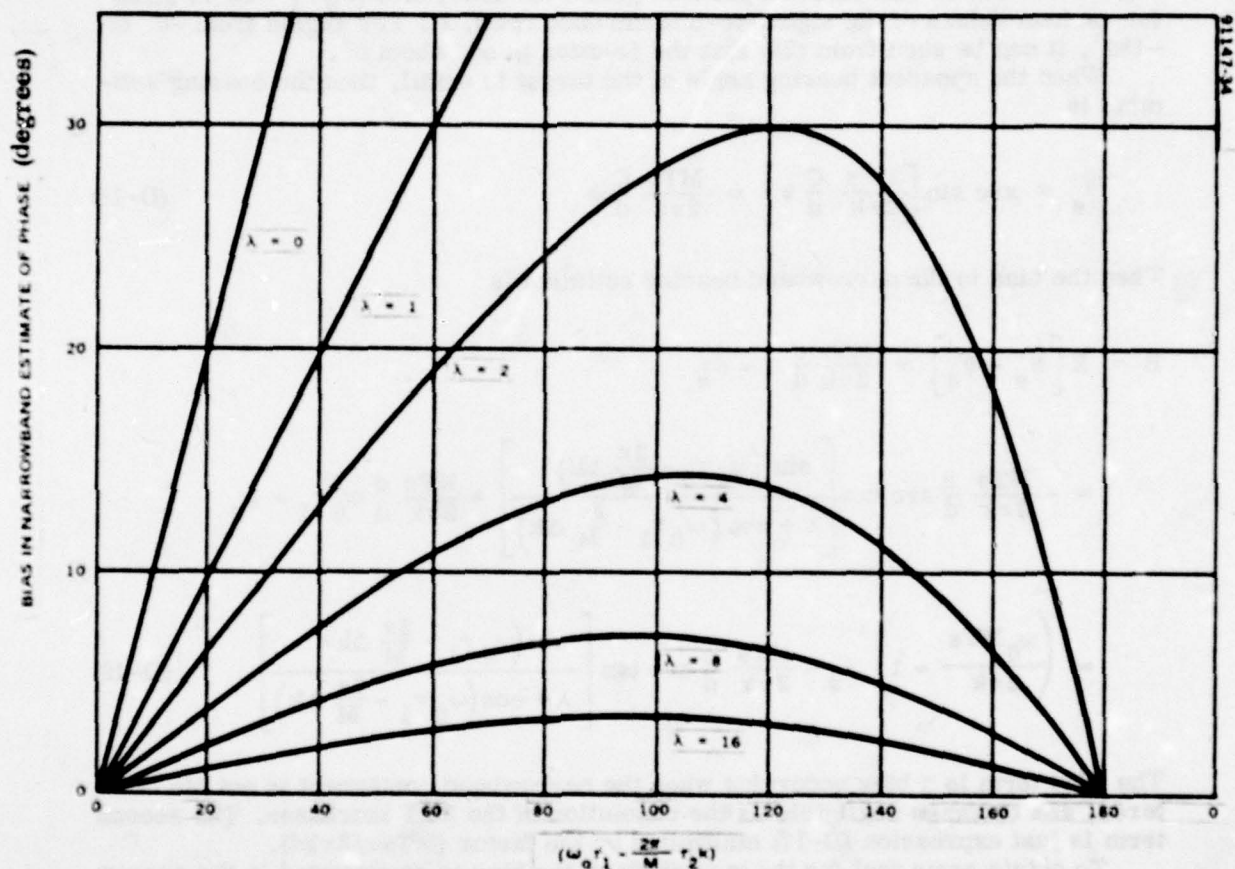
Figure D-1. Bias in Phase Estimate for Adaptive Tracker with Broadband and Narrowband Targets

The following observations should be noted:

1. The apparent immunity of the estimate to large bearing bias errors is primarily due to the fact that the bearing estimate is ambiguous beyond $\pm \pi c / \omega_0 d$ radians, so all estimates are interpreted in this range.

2. When the signal to interference ratio in dB is negative, the bias is between $(1/2)(\theta_s - \theta_b)$ and $(\theta_s - \theta_b)$. For even moderately positive signal to interference ratios, the bias is considerably smaller than $(1/2)(\theta_s - \theta_b)$.

3. This analysis has not included any array response. To include array response, the relative array gains for the narrowband and broadband components would be incorporated in the signal to interference ratio, λ.

4. There is no reason to expect the behavior of this narrowband estimator to differ significantly from any other narrowband split beam estimator that extracts a bearing estimate from the phase difference in an FFT bin containing the signal.

5. From (D-19), it can be seen that a bias occurs when ever the line frequency is not bin centered. This bias has two components, one due to using the bin center as the frequency estimate, and one due to a bias of the phase of the FFT bin. This bias exists even when the broadband and narrowband sources are colocated, as in the case of a target with the broadband and narrowband radiated noise. Increasing the resolution of the FFT reduces this bias.

Figures D-2 through D-4 show the variance of the bearing estimate for the narrowband adaptive tracker with a target having both broadband and narrowband
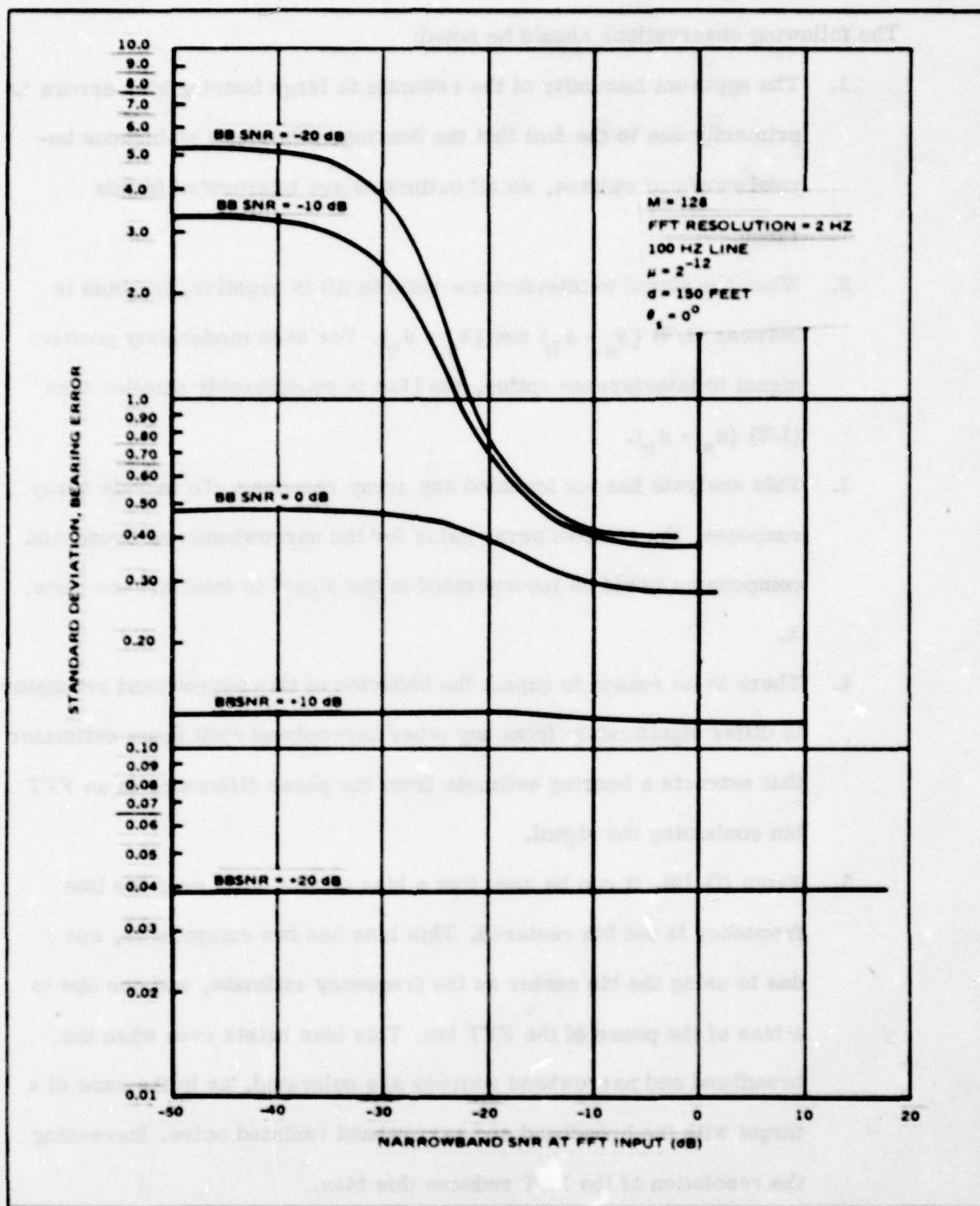
Figure D-2. Standard Deviation of Bearing Error Versus Narrowband SNR for Various Broadband SNR
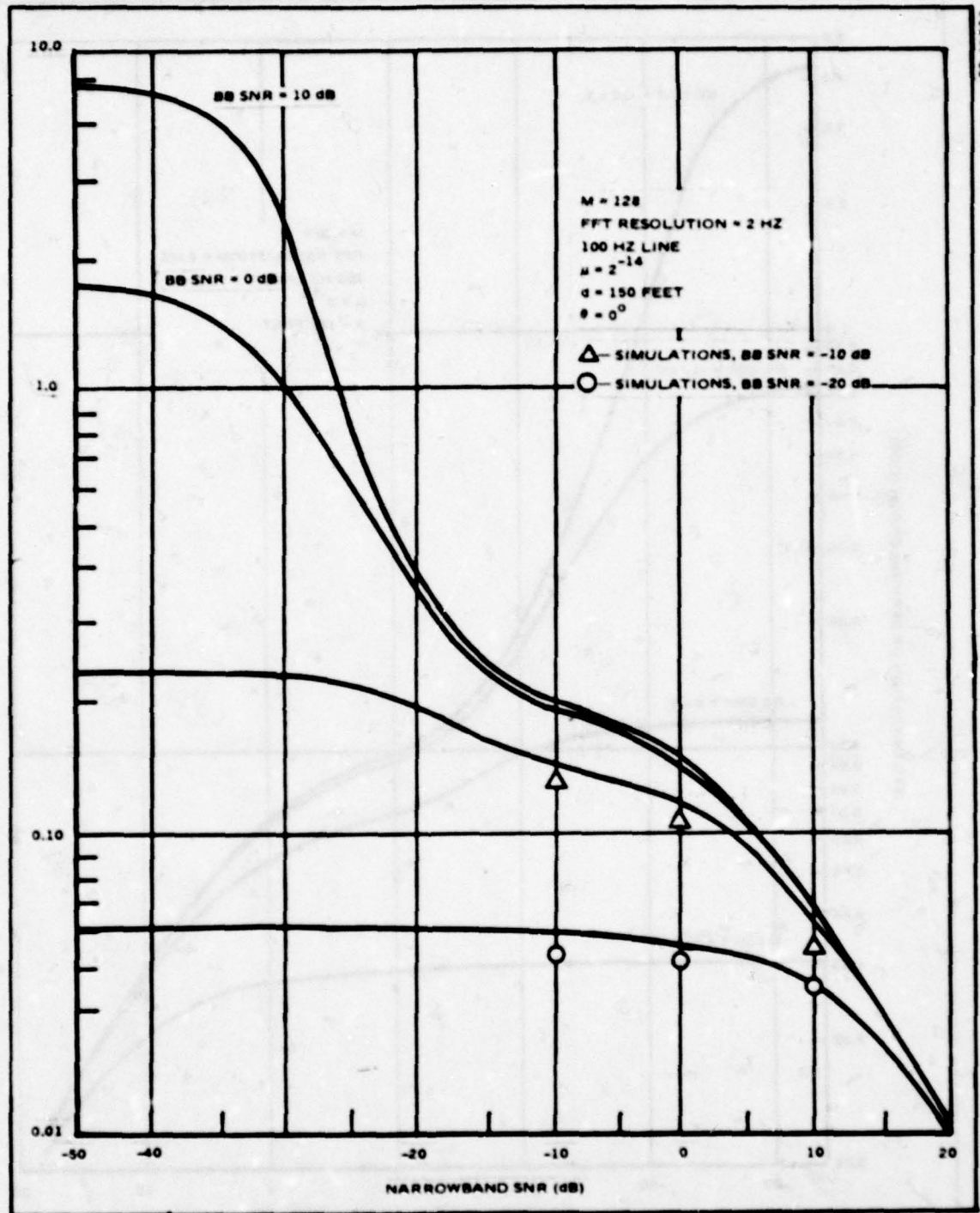
Figure D-3. Standard Deviation of Bearing Error Versus Narrowband SNR for Various BB SNR
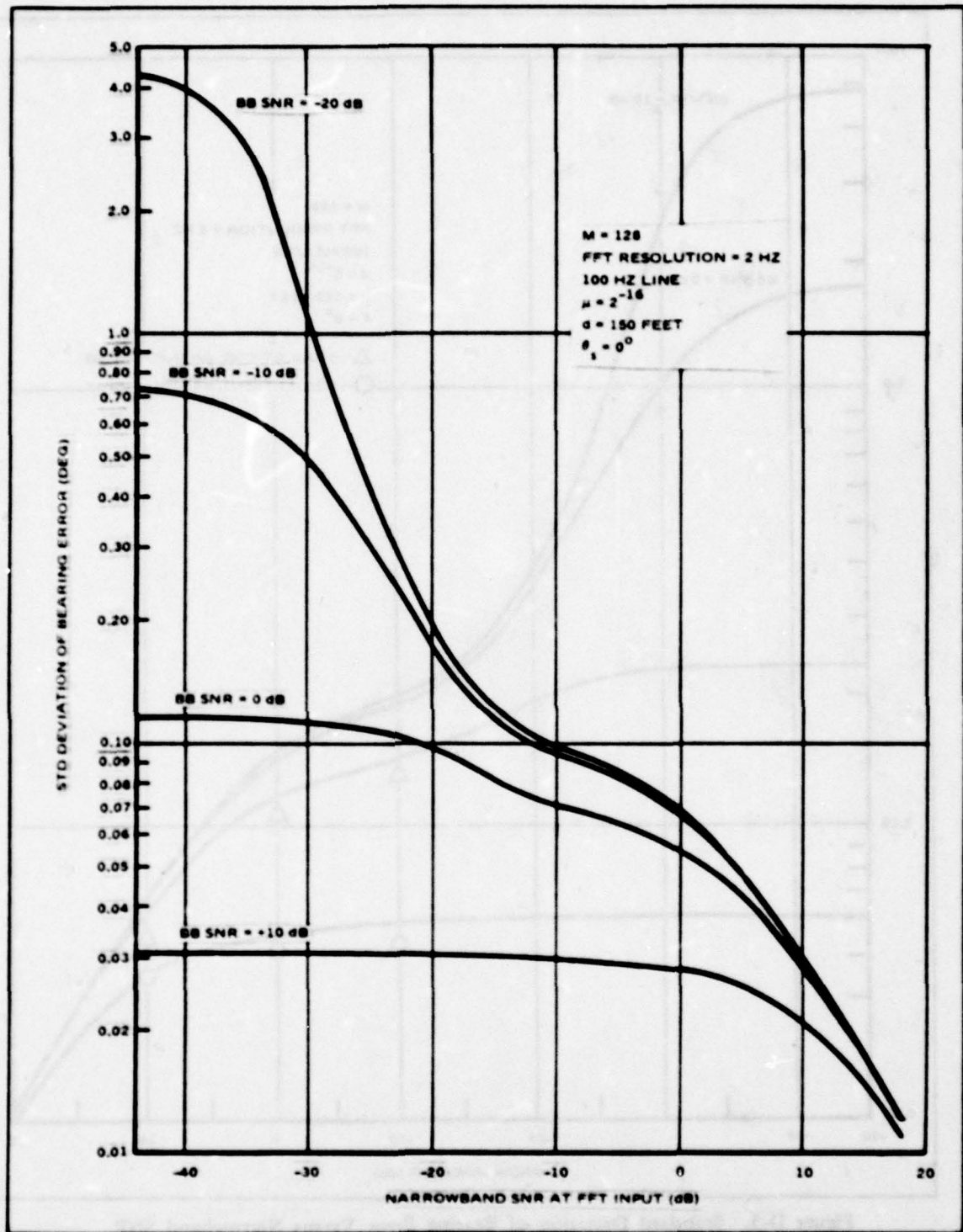
Figure D-4. Standard Deviation of Bearing Error Verus Narrowband SNR for Various Broadband SNR

components, determined by the numerical method above. The narrowband component is bin centered, so that the estimate is unbiased. The simulation utilizes a 0 to 256 Hz band with a 2 Hz FFT resolution, and an array with 150 ft between phase centers. The variance is plotted as a function of the ratio of narrowband signal power to background noise (narrowband SNR) for various values of broadband signal power to noise ratio (broadband SNR). The plots only extend over the range of parameters for which the filter is stable. Plots for $\mu = 2^{-12}$, 2^{-14}, and 2^{-16} are given in Figures D-2, D-3, and D-4, respectively. In all cases, the target is at $0°$ azimuth. Figure 2 shows several points from computer simulations at $\mu = 2^{-14}$ which verify the analytical results.

As noted earlier, the analyses leading to the expressions (D-4) and (D-5) assume that the correct FFT bin, i.e., the one containing the narrowband component, is chosen for bearing extraction. This selection is based upon the FFT bin having the largest magnitude. When both narrowband and broadband components are present, the total broadband energy (signal plus noise) may result in choice of the incorrect bin. While the narrowband tracker does show the ability to determine bearing from broadband signals, this incorrect selection does change the statistics of the estimate, as the estimate depends on bin number, via (D-10). In the simulation results shown in Figure D-3, the algorithm has been forced to choose the correct bin, regardless of narrowband to broadband power ratio, in order to verify the results of the analysis. Therefore, when the narrowband to total broadband power ratio in the FFT bin is less than about 10 dB, the curves are not valid unless some other means of determining the correct bin is available. For example, an additional FFT with post-FFT integration might be used to identify the bin containing the narrowband line.

The analysis described above can also be used to assess the performance of the narrowband adaptive tracker with a narrowband target and a broadband interference in a different direction. Figures D-5 through D-8 show the effect of a broadband interference at $2°$ and $4°$ in bearing, on the bearing estimate for a narrowband target at $0°$. The configuration of the tracker is identical to that used in Figure D-3 with $\mu = 2^{-14}$. Figures D-5 and D-6 show the standard deviation and bias of the estimate for the interference at $2°$, while Figures D-7 and D-8 give the same information for an interference at $4°$. As would be expected [2], when the interference power in the FFT bin is significant relative to the power of the target line, the estimate is biased toward the interference. Additionally, Figures D-5 and D-7 show that for sufficiently high SNR, the presence of a broadband interference may increase the variance of the estimate. This increase in variance appears to occur in a range of SNR where bias due to the interference is no longer significant. At lower SNR, the variance of the estimate is reduced with increasing interference power, while the bias becomes significant (i.e., the output is a "good" estimate of the interference bearing). The SNR at which the transition from variance decreasing with INR to variance increasing with INR appears to decrease with increasing separation between target and interference.

Figures D-9 and D-11 show the variance of the estimate for the same tracker configuration when the target is at $2°$ and $4°$ respectively, and the interference is at $0°$ and Figures D-10 and D-12 show the bias for the same situation. These curves show the results of simulations of the device under the same input conditions.
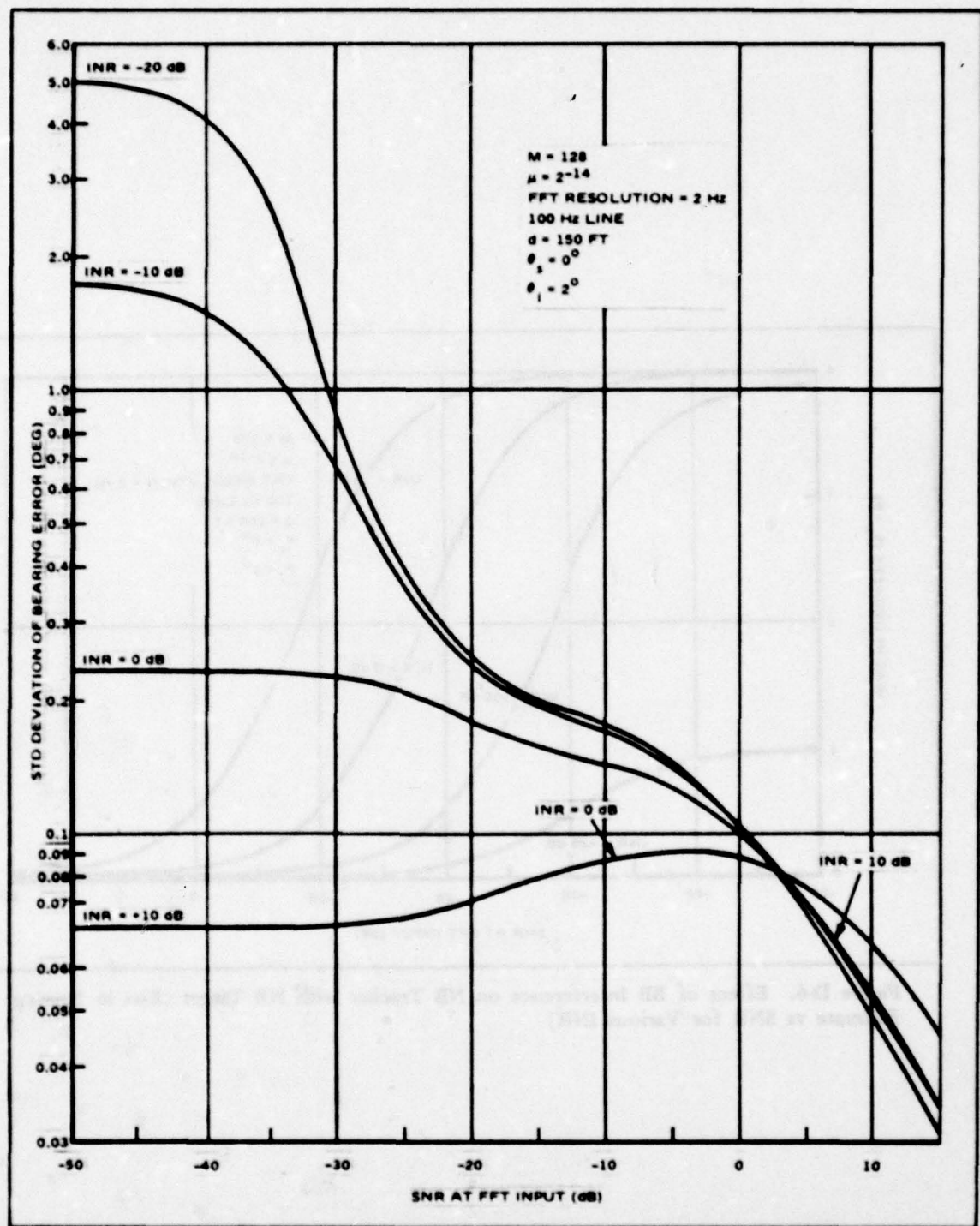
Figure D-5. Effect of BB Interference on NB Tracker with NB Target

D-15

Figure D-6. Effect of BB Interference on NB Tracker with NB Target (Bias in Bearing Estimate vs SNR for Various INR)

Figure D-7. Effect of BB Interference on NB Tracker with NB Target (Std Deviation of Bearing Error vs SNR for Various INR)

Figure D-8. Effect of BB Interference on NB Tracker with NB Target (Bias in Bearing Estimate vs SNR for Various INR)
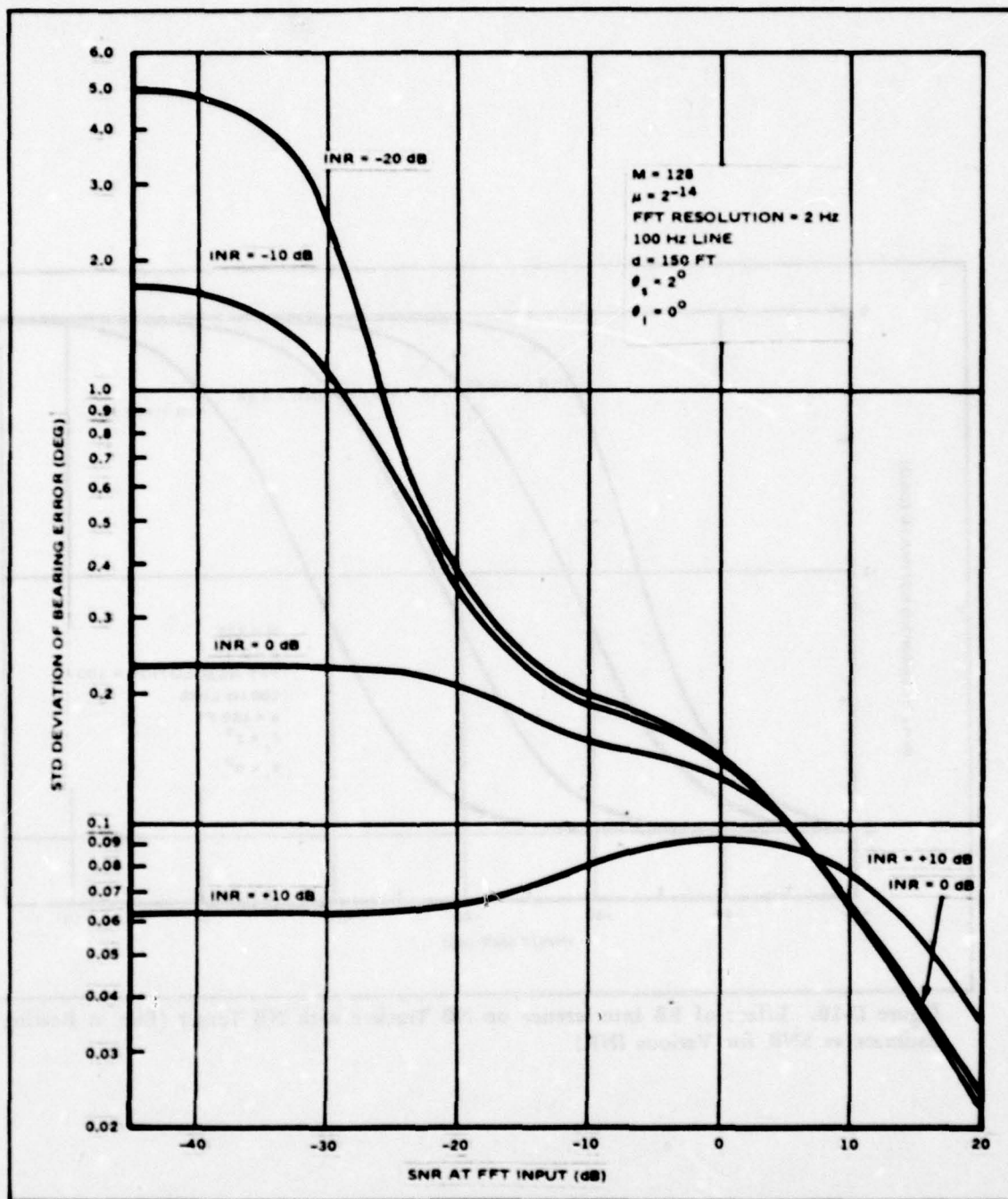
Figure D-9. Effect of BB Interference on NB Tracker with NB Target (Std Deviation of Bearing Error vs SNR for Various INR)
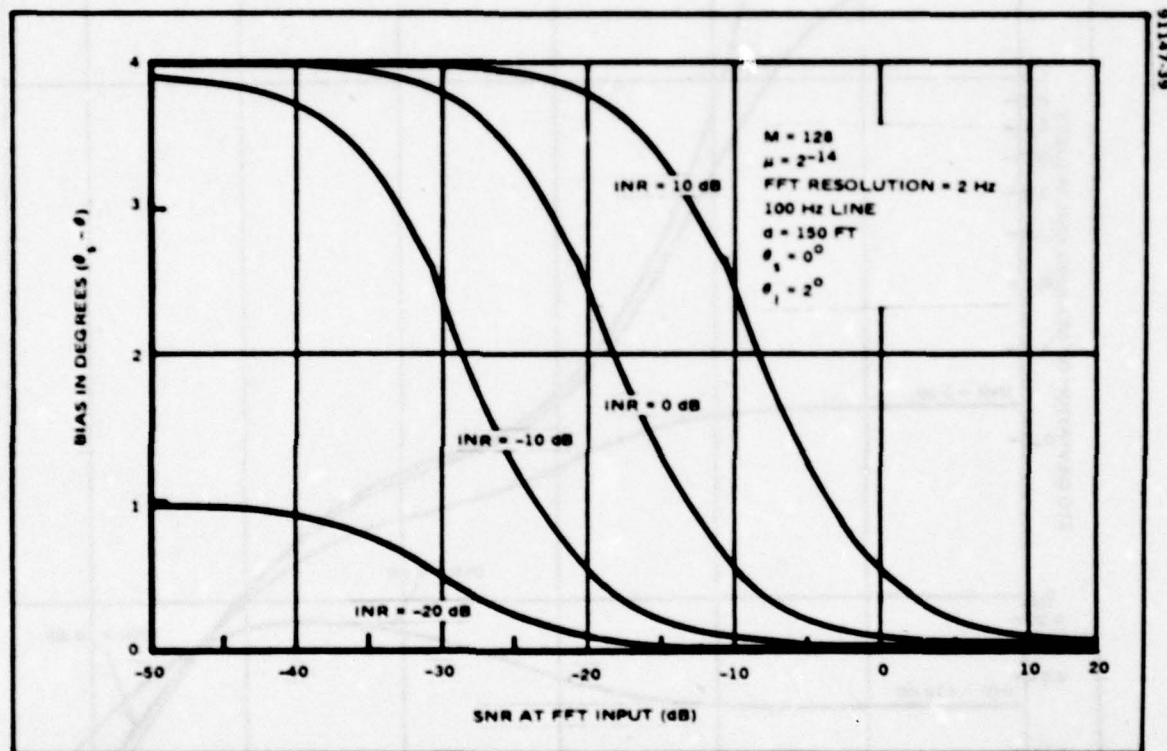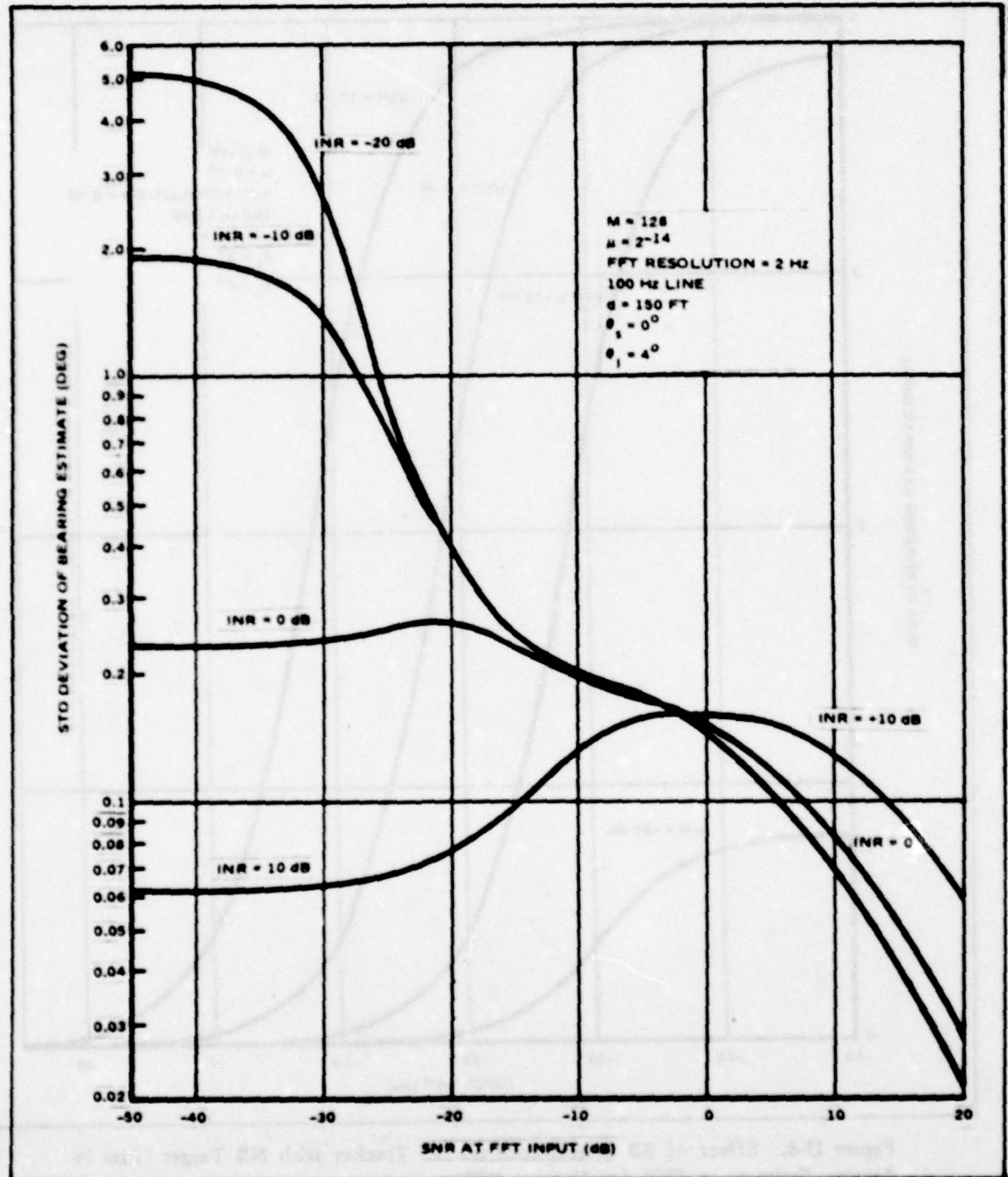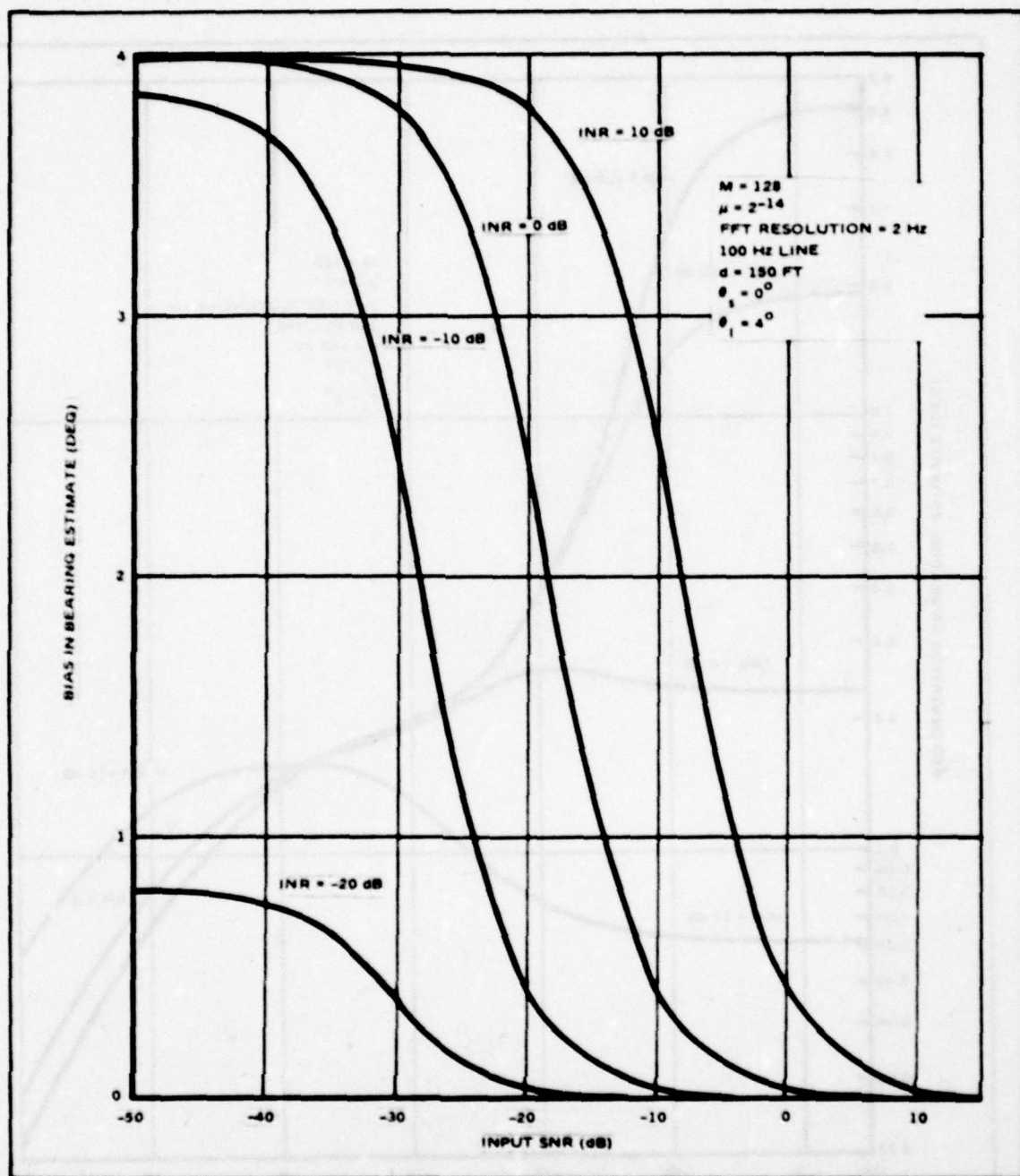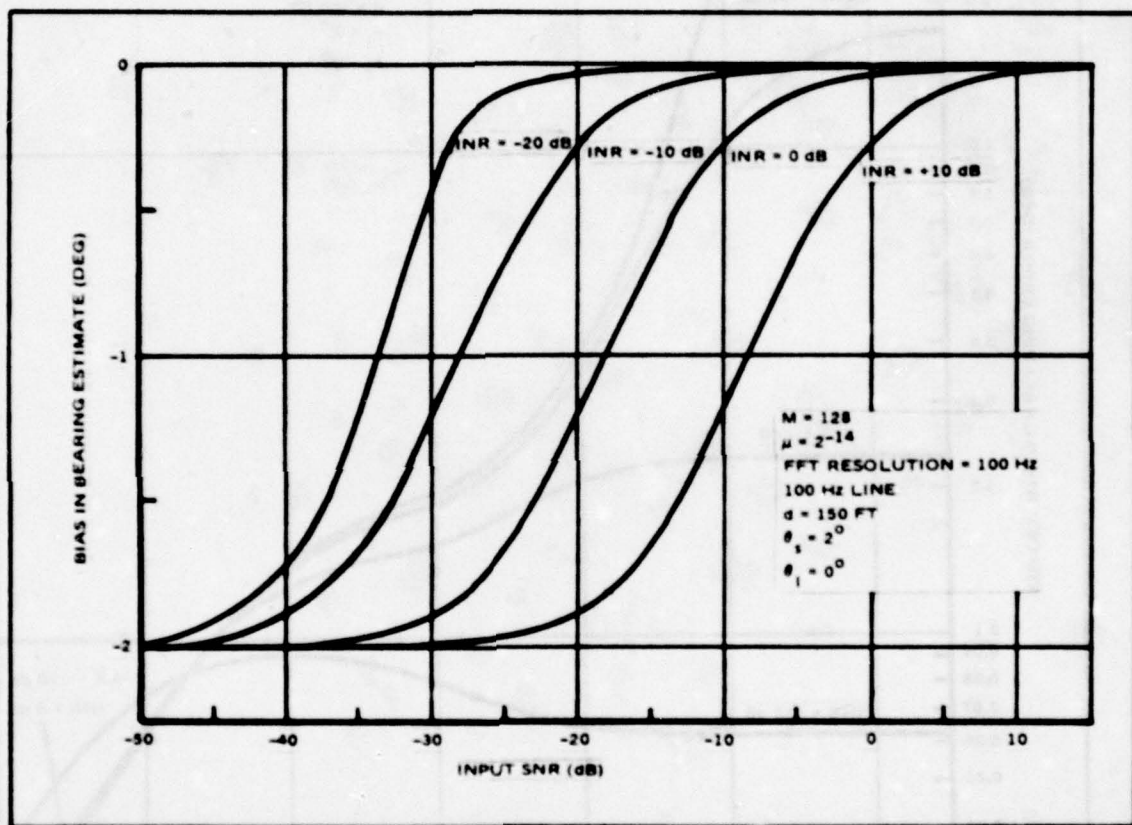
Figure D-10. Effect of BB Interference on NB Tracker with NB Target (Bias in Bearing Estimate vs SNR for Various INR)
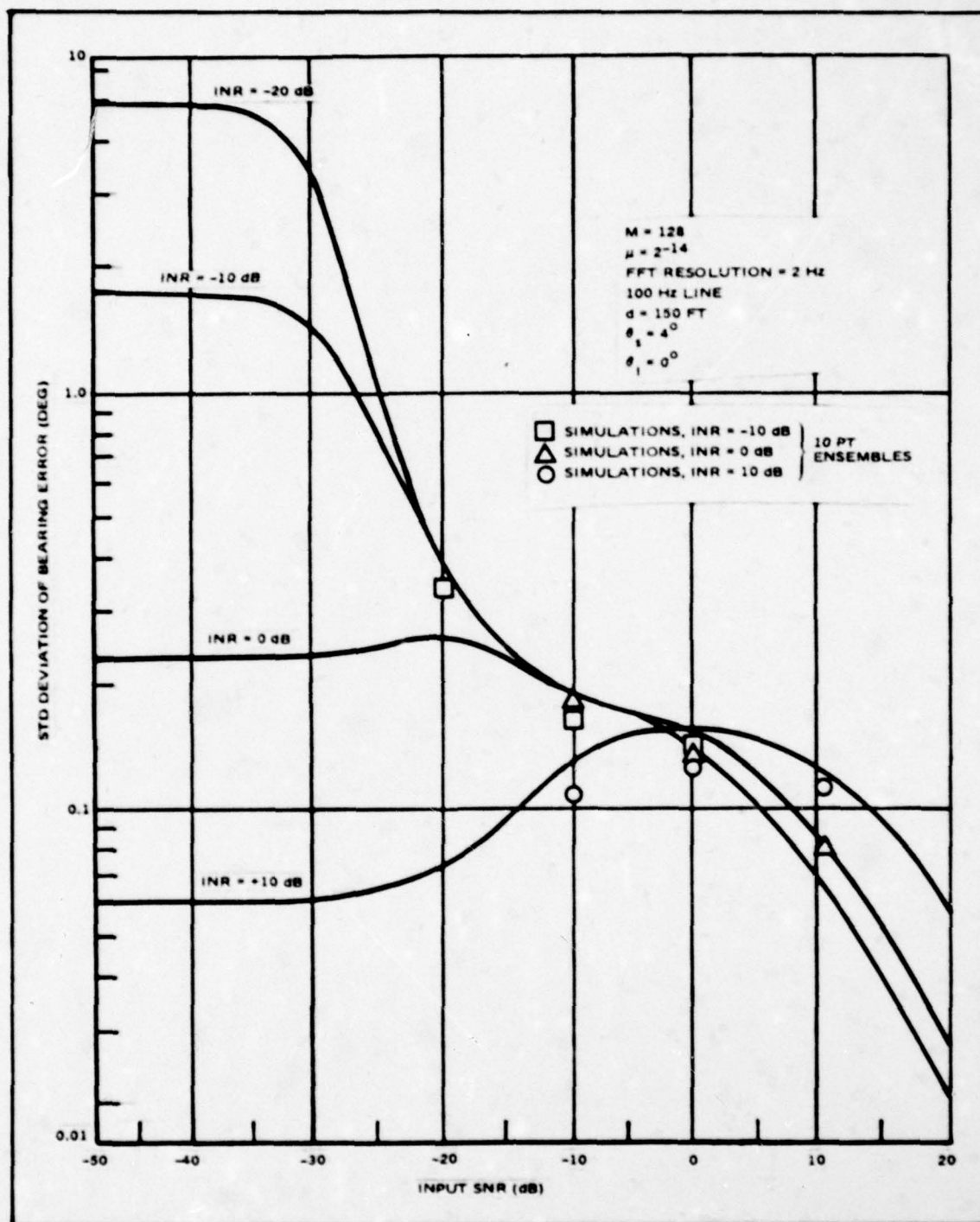
Figure D-11. Effect of BB Interference on NB Tracker (NB Target) (Std Deviation of Bearing Error vs SNR for Various INR)

APPENDIX E

Appendix E

Comparison of an Adaptive Tracker and a Split Beam Tracker
With Incorrect a Priori Assumptions on Input Spectra

The broadband adaptive tracker[1] has been suggested as an alternative to conventional split beam correlator trackers because of several potential advantages stemming from the adaptive characteristics. One of these possible advantages is that the adaptive filter does not require a priori knowledge of the signal and noise statistics, but estimates these dynamically during operation. Conventional split beam trackers, on the other hand, require the input signal and noise spectra in order to optimize their performance (see, for example, [6] or [7]). The goal of this analysis is to determine, at least for some simple cases, whether or not the adaptive tracker (ADT) is more tolerant of spectral variation about those assumed a priori than the split beam tracker (SBT).

The approach is as follows. A signal and noise spectrum is assumed a priori, and the weighting filter for the SBT is set using these spectra. Then, with the input spectra matching the a priori assumptions the variance of the bearing estimate for the ADT and SBT are computed analytically. Either the input noise or signal spectrum is then varied without changing the weighting filter of the SBT, and the variances recomputed. The ratio of the variances with correct and incorrect a priori knowledge gives the change in performance of the two trackers. These are then used to determine which of the two is less susceptible to

E-1

changing inputs. In this report, the assumed signal and noise spectra are flat over the input band of the tracker. The case in which the actual spectra are of some general shape is so complicated that it yields little insight. The most detailed results are for the specific examples in which actual spectra differ from the assumed only in level in some portion of the input band.

Analysis:

Let the split inputs to the tracker be

$$x_L(t) = S(t - \frac{d}{c} \sin \Theta) + n_L(t)$$

$$x_R(t) = S(t) + n_R(t) \tag{E-1}$$

where $S(t)$, $n_L(t)$, and $n_R(t)$ are independent, zero mean gaussian random processes with power spectral densities $S_s(\omega)$ and $S_n(\omega)$ (n_L and n_R have identical power spectra). Also, let

d = distance between half array phase centers

c = speed of sound

Θ = angle between plane wavefront and axis of phase centers.

In Appendix 4 of [1], the mean and variance of the transfer function of a continuous adaptive filter is derived under the condition of equal signal and noise bands. This was done by resolving the inputs into discrete frequency bins, and applying a single tap complex adaptive filter in each bin, as discussed in Appendix 3 of [1]. The transfer functions are obtained as

the limit of the discrete case. This approach depends upon the independence of the individual frequency bins. The resulting transfer function an be used to obtain the impulse response of the adaptive filter, $h(\tau)$.

The angle, Θ, is to be estimated by determining the value of τ for which the impulse response, $h(\tau)$, is a maximum. This is an estimate of the delay between arrivals of the signal wavefront at the half array phase centers, and can be converted to a bearing estimate, $\hat{\Theta}$, using

$$\tau = \frac{d}{c} \sin \hat{\Theta} . \tag{E-2}$$

The value of Θ for which $h(\tau)$ is peaked corresponds to the value for which the derivative of $h(\tau)$ with respect to Θ is zero. In the neighborhood of the zero crossing the derivative of the impulse response is approximately linear. The fluctuations in the derivative of the transfer function then map through the linear function to provide an estimate of the mean square error in the angle estimate. Thus the mean value of the derivative of the transfer function, the standard deviation of the derivative of the transfer function, and the slope of the mean of the derivative of the transfer function are required, at the point where $\hat{\Theta} = \Theta$. Then the errors in the transfer function can be mapped into the errors in one's ability to extract the peak of the transfer function as follows:

$$\text{Var}^{1/2}[\Theta] = \left. \frac{\text{Var}^{1/2}\left[\dfrac{\partial h(\tau)}{\partial \tau}\right]}{\dfrac{\partial E\left[\dfrac{\partial h(\tau)}{\partial \tau}\right]}{\partial \theta}} \right|_{\tau = \frac{d}{c} \sin \Theta} \tag{E-3}$$

This approach is motivated by the treatment of BDI split beam trackers by MacDonald and Schultheiss in Reference [2].

We want to compare the adaptive tracker with the conventional split beam tracker, which can be done using MacDonald and Schultheiss' results.[6] These results require a priori assumptions regarding the signal and noise spectra. The a priori signal and noise spectra will be denoted $S_{sa}(\omega)$ and $S_{na}(\omega)$, respectively, not necessarily equal to the actual spectra.

Here, we will examine the effect of incorrect a priori assumptions on the performance of the split beam tracker in several cases. This will be done by comparing the variance of the bearing estimate under actual conditions with the case when a priori assumptions are true. The performance of the adaptive filter under both conditions will also be computed. In order to maintain the same time constant for the ADT, the power at the input is normalized (equivalent to an AGC) such that

$$\int_{-\infty}^{\infty} [S_s(\omega) + S_n(\omega)] \, d\omega = \int_{-\infty}^{\infty} [S_{sa}(\omega) + S_{na}(\omega)] \, d\omega \qquad (E-4)$$

Case 1: Signal spectrum differing from a priori assumptions. Suppose that the assumed spectra are

$$S_{na}(\omega) = \begin{cases} Ln & |\omega| \le \omega_a \\ 0 & \text{Otherwise} \end{cases}$$

(E-5)

$$S_{sa}(\omega) = \begin{cases} Ls & |\omega| \le \omega_a \\ 0 & \text{Otherwise} \end{cases}$$

while the actual spectra are $L_n(\omega) = L_{na}(\omega)$ and

$$L_s(\omega) = \begin{cases} L_s & |\omega| \le \omega_s, \; \omega_s < \omega_a \\ L_{s1} & \omega_s \le |\omega| \le \omega_a \\ 0 & \text{Otherwise} \end{cases}$$

(E-6)

These spectra are illustrated in Figure E-1, where K_1 is selected to satisfy (E-4), so that

$$2\omega_a(L_s + L_n) = 2[\omega_s K_1(L_s + L_n) + (\omega_a - \omega_s) K_1(L_{s1} + L_n)] \quad \text{(E-7)}$$

or

$$K_1 = \frac{(L_s + L_n)\,\omega_a}{\omega_s(L_s + L_n) + (\omega_a - \omega_s)(L_{s1} + L_n)}$$

The results cited in reference [1] lead to the following statistics for the transfer function of the adaptive filter;

E-5
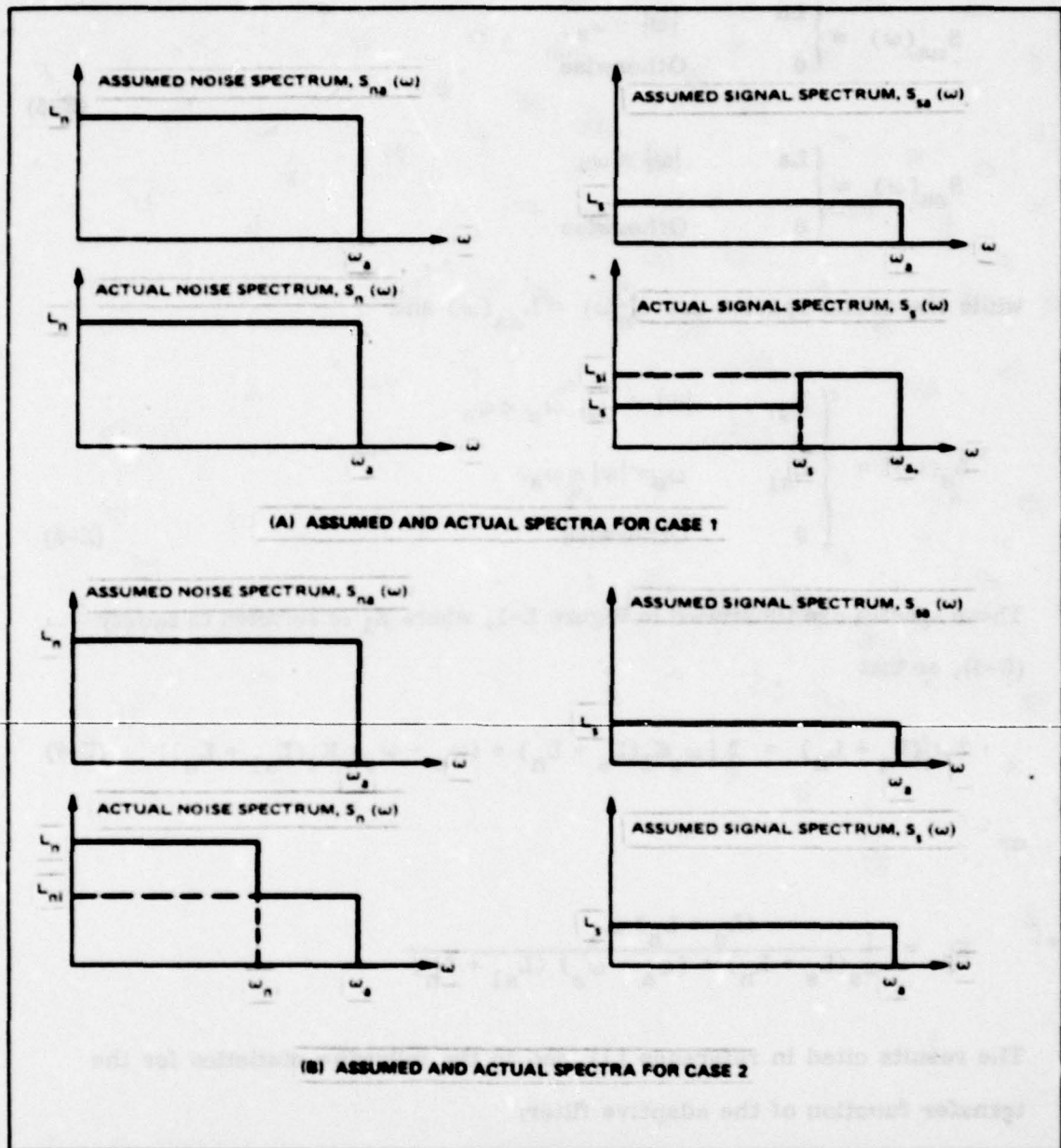
Figure E-1. Input Spectra for Analysis of Adaptive and Conventional Split Beam Trackers

$$
E\left[H(\omega)\right] = \begin{cases} \dfrac{L_s}{L_s + L_n}\, e^{-j\frac{\omega d}{c}\sin\theta} & |\omega| \leq \omega_c \\[4mm] \dfrac{L_{s1}}{L_{s1} + L_n}\, e^{-j\frac{\omega d}{c}\sin\theta} & \omega_s \leq |\omega| \leq \omega_a \\[4mm] 0 & \text{Otherwise} \end{cases} \tag{E-8}
$$

and

$$
\text{Cov}\left[H(\omega)\right] \approx \begin{cases} \dfrac{2\pi\mu K_1 L_n\,[2L_s + L_n]}{(L_s + L_n)(2 - 2\mu K_1(L_s + L_n)}\,\delta\,(\omega_1 - \omega_2), & |\omega_1 - \omega_2| \leq \omega_2 \\[4mm] \dfrac{2\pi\mu K_1 L_n\,[2L_{s1} + L_n]}{(L_{s1} + L_n)(2 - 2\mu K_1(L_{s1} + L_n))}\,\delta\,(\omega_1 - \omega_2), & \omega_s < |\omega_1 - \omega_2| \leq \omega_n \\[4mm] 0, & \text{otherwise} \end{cases} \tag{E-9}
$$

Then

$$
\text{Var}\left[\frac{\partial h(\tau)}{\partial\tau}\right] = \frac{1}{\pi}\frac{\mu K_1 L_n\,[2L_s + L_n]}{(L_s + L_n)\,(2 - 2\mu(L_s + L_n)}\left[\frac{\omega_s^3}{3}\right]
$$

$$
+ \frac{1}{\pi}\frac{\mu K_1 L_n\,[2L_{s1} + L_n]}{(L_{s1} + L_n)(2 - 2\mu(L_{s1} + L_n))}\left[\frac{\omega_a^3 - \omega_s^3}{3}\right] \tag{E-10}
$$

and

$$
\left.\frac{\partial E\,[\partial h(\tau)/\partial\tau]}{\partial\Theta}\right|_{\tau=\frac{d}{c}\sin\theta} = \frac{d}{c}\cos\frac{1}{\pi}\left\{\frac{L_s}{L_s + L_n}\left(\frac{\omega_s^3}{3}\right)\right.
$$

$$
\left. + \frac{L_{s1}}{L_{s1} + L_n}\left(\frac{\omega_a^3 - \omega_s^3}{3}\right)\right\} \tag{E-11}
$$

E-7

Therefore, the variance of the bearing estimate is, using (3),

$$\text{Var}[\hat{\theta}] = \frac{C^2 \pi}{d^2 \cos^2 \Theta} \frac{\dfrac{\mu K_1 L_n (2L_s + L_n)}{(L_s + L_n)(2 - 2\mu(L_s + L_n))} \left[\dfrac{\omega_s^3}{3}\right] + \dfrac{\mu K_1 L_n (2L_{s1} + L_n)}{(L_s + L_n)(2 - 2\mu(L_{s1} + L_n))} \left[\dfrac{\omega_a^3 - \omega_s^3}{3}\right]}{\left[\dfrac{L_s}{L_s + L_n}\left(\dfrac{\omega_s^3}{3}\right) + \dfrac{L_{s1}}{L_{s1} + L_n}\left(\dfrac{\omega_a^3 - \omega_s^3}{3}\right)\right]^2} \tag{E-12}$$

If the a priori assumptions were true, then the variance would

$$V_o = \frac{C^2 \pi}{d^2 \cos^2 \Theta} \frac{\dfrac{L_n (2L_s + L_n)}{(L_s + L_n)(2 - 2\mu(L_s + L_n))}\left[\dfrac{\omega_a^3}{3}\right]}{\left(\dfrac{L_s}{L_s + L_n}\right)^2 \left(\dfrac{\omega_a^3}{3}\right)^2} \tag{E-13}$$

Factoring this out of (12) gives

$$\text{Var}[\hat{\theta}] = V_o \left[K_1 \frac{1 + \left(\dfrac{\omega_s^3 - \omega_a^3}{\omega_a^3}\right) + \dfrac{(2_{Ls1} + L_n)(L_s + L_n)(2 - 2\mu(L_s + L_n))}{(2L_s + L_n)(L_{s1} + L_n)(2 - 2\mu(L_{s1} + L_n))}\left(\dfrac{\omega_a^3 - \omega_s^3}{3}\right)}{\left[1 + \left(\dfrac{\omega_s^2 - \omega_a^3}{\omega_a^3}\right) + \dfrac{L_{s1}(L_s + L_n)}{L_s(L_{s1} + L_n)}\left(\dfrac{\omega_a^3 - \omega_s^3}{\omega_a^3}\right)\right]^2} \right] \tag{E-14}$$

We are primarily interested in the small SNR case, where $L_s \ll L_n$ and $L_{s1} \ll L_n$, so $K_1 \approx 1$ and

$$\text{Var}[\hat{\theta}] \approx V_o \left[\left(1 + \left(\frac{L_{s1}}{L_s} - 1\right)\left(\frac{\omega_a^3 - \omega_s^3}{\omega_a^3}\right)\right)\right] \tag{E-15}$$

A special case is when $L_{s1} = 0$, so that the signal spectrum is narrower than assumed. In this case

$$\text{Var}\,[\hat{\theta}] = V_o \left[\frac{1 + \left(\dfrac{(L_s + L_n)\,(2 - 2\mu(L_s + L_n))}{(2L_s + L_n)\,(2 - 2\mu L_n)} - 1 \right) \dfrac{\omega_a^3 - \omega_s^3}{\omega_a^3}}{\left[1 - \left(\dfrac{\omega_a^3 - \omega_s^3}{\omega_a^2} \right) \right]^2} \right] \tag{E-16}$$

At low SNR, this gives

$$\text{Var}\,[\hat{\theta}] \approx V_o \left[1 - \left(\frac{\omega_a^3 - \omega_s^3}{\omega_a^3} \right) \right]^{-2} \tag{E-17}$$

This is to be compared with the split beam tracker under the same circumstances. From MacDonald and Schutheiss,[6] the variance of the split beam tracker (SBT) bearing estimate is given by

$$D^2(\Theta) = \frac{2\pi c^2}{Td^2 \cos^2\Theta} \left[\frac{\displaystyle\int_{-\infty}^{\infty} |H(\omega)|^4 \,[S_n^2(\omega) + 2 S_n(\omega)\,S_s(\omega)]\,\omega^2\,d\omega}{\left[\displaystyle\int_{-\infty}^{\infty} |H(\omega)|^2 \,S_s(\omega)\,\omega^2\,d\omega \right]^2} \right] \tag{E-18}$$

where $H(\omega)$ is a weighting function given by

$$|H(\omega)|^2 = \frac{S_{sa}(\omega)/S_{na}^2(\omega)}{1 + 2 S_{sa}(\omega)/S_{na}(\omega)} \tag{E-19}$$

E-9

Using (E-5) and (E-6), we obtain

$$\int_{-\infty}^{\infty} |H(\omega)|^2 \, S_s(\omega) \, \omega^2 \, d\omega \; = \; + \frac{(2K_1 L_s^2/L_n^2)\, \omega_s^3}{(1 + 2L_s/L_n)^3} + \frac{2K_1 L_s L_{s1}/L_n^2}{1 + L_{s1}/L_n} \left[\frac{\omega_a^3 - \omega_s^3}{3} \right]$$

(E-20)

and

$$\int_{-\infty}^{\infty} |H(\omega)|^4 \, [S_n^2(\omega) + 2S_n(\omega)\, S_s(\omega)] \; \omega^2 \, d\omega$$

$$= \frac{2K_1^2 L_s^2/L_n^2}{1 + 2L_s/L_n} \left[\frac{\omega_s^3}{3} \right] + \frac{4K_1^2 L_s^2/L_n^2 \, [1 + 2L_{s1}/L_n]}{[1 + 2L_s/L_n]^2} \left[\frac{\omega_a^3 - \omega_s^3}{3} \right]$$

(E-21)

Then

$$D^2(\Theta) \; = \; \frac{2\pi c^2}{Td^2 \cos^2 \Theta} \left[\frac{\dfrac{2L_s^2/L_n^2}{1 + 2L_s/L_n} \left[\dfrac{\omega_s^3}{3} \right] + \dfrac{L_s^2/L_n^2 \, [1 + 2L_{s1}/L_n]}{[1 + 2L_s/L_n]^2} \left[\dfrac{\omega_a^3 - \omega_s^3}{3} \right]}{\left[\dfrac{2L_s^2/L_n^2}{1 + 2L_s/L_n} \, \dfrac{\omega_s^3}{3} + \dfrac{2L_s L_{s1}/L_n^2}{1 + L_{s1}/L_n} \left(\dfrac{\omega_a^3 - \omega_s^3}{3} \right) \right]^2} \right]$$

(E-22)

Note that when the prior assumptions are true, the variance is

$$D_o^2 \; = \; \frac{2\pi c^2}{Td^2 \cos^2 \Theta} \frac{\dfrac{2L_s^2/L_n^2}{1 + 2L_s/L_n} \left[\dfrac{\omega_a^3}{3} \right]}{\left(\dfrac{2L_s^2/L_n^2}{1 + 2L_s/L_n} \left[\dfrac{\omega_a^3}{3} \right] \right)^2}$$

(E-23)

so factoring this out of (E-22) yields

$$D^2(\Theta) = D_o^2 \left[\frac{1 - \left(\dfrac{\omega_a^3 - \omega_s^3}{\omega_a^3} \right) + \dfrac{[1 + 2L_{s1}/L_n]}{[1 + 2L_s/L_n]} \left(\dfrac{\omega_a^3 - \omega_s^3}{\omega_a^3} \right)^2}{1 - \left(\dfrac{\omega_a^3 - \omega_s^3}{\omega_a^3} \right) + \dfrac{L_{s1}(1 + 2L_s/L_n)}{L_s(1 + 2L_{s1}/L_n)} \left(\dfrac{\omega_a^3 - \omega_s^3}{\omega_a^3} \right)^2} \right]$$

(E-24)

At low SNR we get

$$D^2(\Theta) \approx D_o^2 \left[\frac{1}{\left[1 + \left(\dfrac{L_{s1}}{L_s} - 1 \right) \left(\dfrac{\omega_a^3 - \omega_s^3}{\omega_a^3} \right) \right]^2} \right]$$

(E-25)

In the special case of $L_{s1} = 0$,

$$D^2(\Theta) = D_o^2 \left[\frac{1 - \dfrac{2L_s/L_n}{1 + 2L_s/L_n} \left(\dfrac{\omega_a^3 - \omega_s^3}{\omega_a^3} \right)}{\left[1 - \left(\dfrac{\omega_a^3 - \omega_s^3}{\omega_a^3} \right) \right]^2} \right]$$

(E-26)

which gives, for small SNR,

$$D^2(\Theta) \approx D_o^2 \left\{ 1 - \left[\left(\frac{\omega_a^3 - \omega_s^3}{\omega_a^3} \right) \right]^{-2} \right\}$$

(E-27)

Comparing (E-15) with (E-25), and (E-17) with (E-27) for the case when $L_{s1} = 0$, it can be seen that at low SNR, the SBT and the adaptive tracker degrade in the same way from the case when the a priori assumptions are true.

Case 2: Noise spectrum differing from a priori assumptions.

Here, the a priori assumptions are the same as in case 1, but the actual spectra are, as shown in Figure E-1,

$$S_s(\omega) = S_{sa}(\omega)$$

and

$$S_n(\omega) = \begin{cases} L_n, & |\omega| \leq \omega_n \\ L_{n1}, & \omega_n < |\omega| \leq \omega_a \\ 0, & \text{otherwise} \end{cases} \tag{E-28}$$

This is a straightforward extension of case 1, giving

$$\text{Var}(\Theta) = \frac{c^2}{d^2 \cos^2 \theta} \frac{\frac{\mu K_2 L_n (2L_s + L_n)}{(L_s + L_n)(2 - 2\mu(L_s + L_n)]} \left(\frac{\omega_n^3}{3}\right) + \frac{\mu K_2 L_{n1}(2L_s + L_{n1})}{(L_s + L_{n1})(2 - 2\mu(L_s + L_{n1})]} \left(\frac{\omega_a^3 - \omega_n^3}{3}\right)}{\left[\frac{L_s}{L_s + L_n} \left(\frac{\omega_n^3}{3}\right) + \frac{L_s}{L_s + L_{n1}} \left(\frac{\omega_a^3 - \omega_n^3}{3}\right) \right]^2}$$

$$\tag{E-29}$$

Were the a priori assumptions valid, the variance would be V_o, given in (E-13), above, so

$$\mathrm{Var}(\Theta) = V_o \left[K_2 \frac{1 + \left(\frac{\omega_n^3 - \omega_a^3}{\omega_a^3}\right) + \frac{L_{n1}(2L_s + L_{n1})(L_s + L_n)(2 - 2\mu(L_s + L_n))}{L_n(2L_s + L_n)(L_s + L_{n1})(2 - 2\mu(L_s + L_{n1}))} \left(\frac{\omega_a^3 - \omega_n^3}{\omega_a^3}\right)}{\left[1 + \left(\frac{\omega_a^2 - \omega_a^3}{\omega_a^3}\right) + \frac{L_s + L_n}{L_s + L_{n1}} \left(\frac{\omega_a^3 - \omega_n^3}{\omega_a^3}\right) \right]^2} \right] \quad \text{(E-30)}$$

As in Case 1, we are interested mainly in the low SNR case where $L_s \ll L_n$ and $L_s \ll L_{n1}$, so

$$\mathrm{Var}(\hat{\Theta}) = V_o K_2 \left[1 + \left(\frac{L_n}{L_{n1}} - 1\right) \left(\frac{\omega_a^3 - \omega_n^3}{\omega_a^3}\right) \right]^{-2} \left[1 + \left(\frac{L_{n1}}{L_n} - 1\right) \left(\frac{\omega_a^3 - \omega_n^3}{\omega_a^3}\right) \right] \quad \text{(E-31)}$$

In this case, K_2 is selected such that

$$2(L_s + L_n) \omega_a = 2K_2 \left[(L_s + L_n) \omega_a + (L_s + L_{n1})(\omega_a - \omega_n) \right]$$

$$K_2 = \frac{(L_s + L_n) \omega_a}{(L_s + L_n) \omega_a + (L_s + L_{n1})(\omega_a - \omega_n)}$$

At small SNR,

$$K_2 \approx \frac{L_n \omega_a}{L_{n1}(\omega_a - \omega_n) + L_n \omega_n} \quad \text{(E-32)}$$

$$\text{Var}(\hat{\Theta}) \approx V_o \left[\frac{\omega_n}{\omega_o} \cdot \frac{L_{n1}}{L_n} \left(\frac{\omega_a - \omega_n}{\omega_a} \right) \right]^{-1} \left[1 + \left(\frac{L_{n1}}{L_n} - 1 \right) \left(\frac{\omega_a^3 - \omega_n^3}{\omega_a^3} \right) \right] \left[1 + \left(\frac{L_n}{L_{n1}} - 1 \right) \left(\frac{\omega_a^3 - \omega_n^3}{\omega_n^3} \right) \right]^{-2} \quad \text{(E-33)}$$

For the SBT, we obtain

$$D^2(\Theta) = \frac{2\pi c^2}{Td^2 \cos^2\theta} \left[\frac{\dfrac{2L_s^2/L_n^2}{1 + 2L_s/L_n} \left(\dfrac{\omega_n^3}{3} \right) + \dfrac{2L_s^2 L_{n1}^2/L_n^4 \; [1 + 2L_s/L_{n1}]}{[1 + 2L_s/L_n]^2} \left(\dfrac{\omega_a^3 - \omega_n^3}{3} \right)}{\left[\dfrac{2L_s^2/L_n^2}{1 + 2L_s/L_n} \left(\dfrac{\omega_a^3}{3} \right) \right]^2} \right]$$

$$= D_o^2 \left[1 - \left(\frac{\omega_a^3 - \omega_n^3}{\omega_a^3} \right) + \frac{L_{n1}^2 \, [1 + 2L_s/L_{n1}]}{L_n^2 \, [1 + 2L_s/L_n]} \left(\frac{\omega_a^3 - \omega_n^3}{\omega_a^3} \right) \right] \quad \text{(E-34)}$$

At small SNR, this gives

$$D^2(\Theta) \approx D_o^2 \left[1 + \left(\frac{L_{n1}^2}{L_n^2} - 1 \right) \left(\frac{\omega_a^3 - \omega_n^3}{\omega_a^3} \right) \right] \quad \text{(E-35)}$$

For convenience, let

$$K_n = \frac{L_{n1}}{L_n} \qquad \text{and} \qquad K_\omega = \frac{\omega_n}{\omega_a}$$

E-14

so

$$Var(\Theta) = V_o [K_\omega + K_n (1 - K_\omega)]^{-1} [1 + (K_n - 1)(1 - K_\omega^3)]$$

$$\cdot [1 + (K_n^{-1} - 1)(1 - K_\omega^3)]^{-2} \tag{E-36}$$

and

$$D^2(\Theta) = D_o^2 [1 + (K_n^2 - 1)(1 - K_\omega^3)] = D_o^2 K_D \tag{E-37}$$

From (E-37), it can be seen that for all values of K_ω less than unity, the variance of the SBT bearing estimate is monotonically increasing in K_n. Hence when the actual noise in the band ω_n to ω_a is less than assumed, the SBT performs better, while if there is more noise, it degrades. It should also be observed that incorrect a priori assumptions as to the noise spectrum affects only the variance of the correlation function, not the mean, while affecting both the mean and the variance of the ADT weights. Figure E-2 shows the performance factor, K_D, plotted as a function of K_n for various values of K. When K_D is greater than unity the variance increases, while it decreases for K_D less than one.

The parametric behavior of the ADT is not so obvious from (E-36). By definition, the variance of the estimate is V_o when $K_n = 1$, and it can be shown that

$$\left. \frac{\partial}{\partial K_n} Var(\Theta) \right|_{K_n=1} = V_o [2 + K_\omega - 3K_\omega^3]$$

This is positive for all values of $K_\omega \in [0,1]$, so, at least in the vicinity of $K_n = 1$ (a priori, assumptions approximately true), the variance of the ADT estimate increases with K_n. Further.
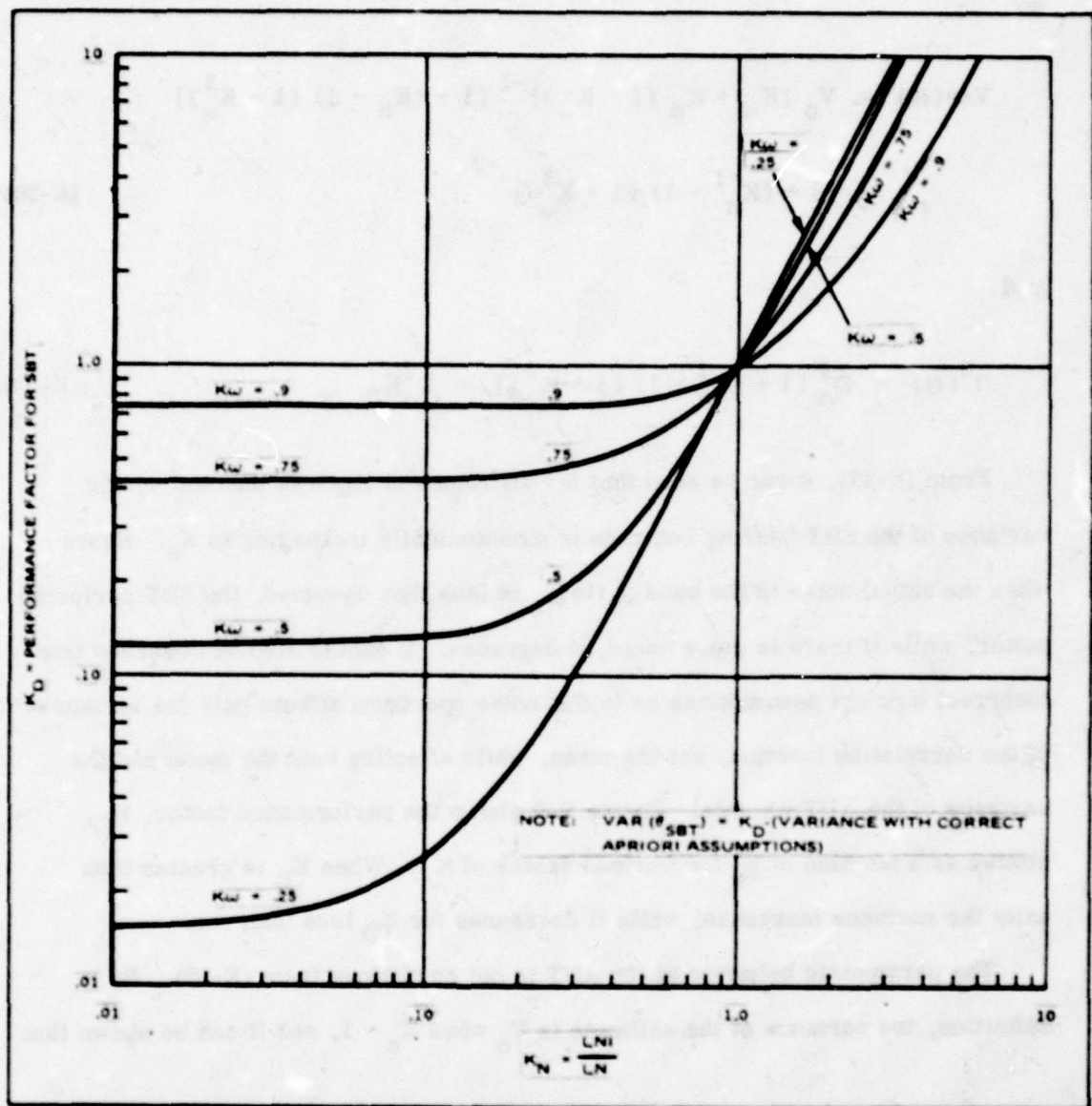
Figure E-2. Change in Variance of Split Beams Tracker Bearing Estimate with Incorrect Apriori Noise Spectrum Input

$$\text{Var}(\hat{\Theta}) \approx V_o \frac{1 - K_\omega^3}{(1 - K_\omega) K_\omega^6} \geq V_o \frac{1}{K_\omega^6} \geq V_o$$

so for large K_n, the ADT degrades from its performance when a priori assumptions are true. Finally, as $K_n \to 0$,

$$\text{Var}(\Theta) \to 0$$

Figure E-3 show the performance factor for the ADT

$$K_v = [K_\omega + K_n (1-K_\omega)]^{-1} [1 + (K_n - 1)(1-K_\omega^3)] \cdot [1 + (K_n^{-1}-1)(1-K_\omega^3)]^{-2}$$

plotted as a function of K_n for various values of K_ω. It can be seen that, as in the case of the SBT, the variance of the estimate increases with K_n.

In order to compare the way in which the two trackers degrade, consider the ratio of their variances at low SNR.

$$R = \frac{\text{Var}(\Theta)}{D^2(\Theta)} = \frac{V_o}{D_o^2} [1 + (K_n - 1)(1 - K_\omega)]^{-1}$$

$$\cdot [1 + (K_n^2 - 1)(1 - K_\omega^3)]^{-1} [1 + (K_n - 1)(1 - K_\omega^3)]$$

$$\cdot [1 + (K_n^{-1} - 1)(1 - K_n^3)]^{-2} \cdot$$

so that

$$R = \frac{V_o}{D_o^2} D$$

NOTE: VAN (θ_{ADT}) = K_V (VARIANCE WITH FLAT INPUT SPECTRA)
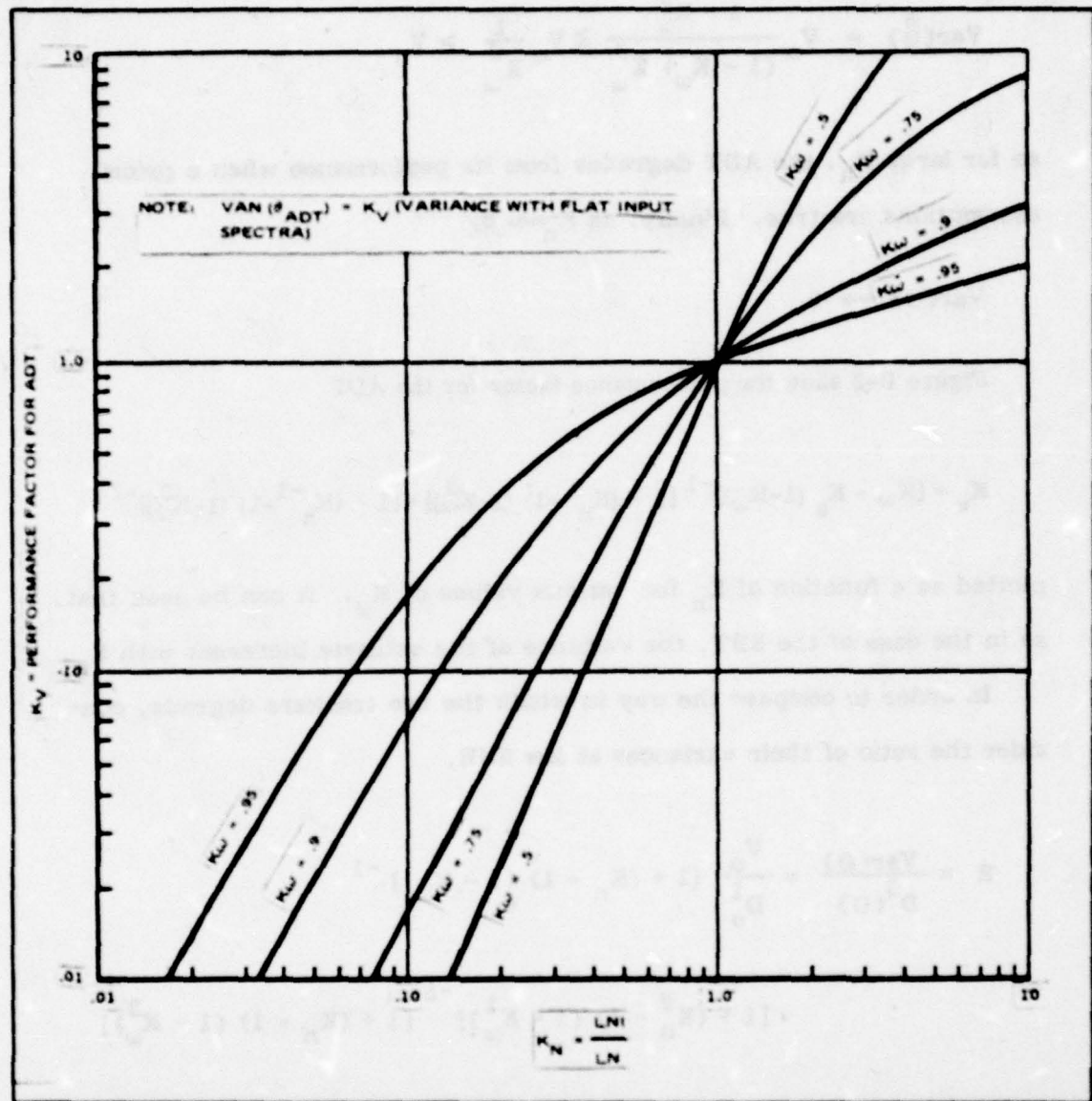
Figure E-3. Change in Variance of Adaptive Tracker Bearing Estimator with Changes in Noise Spectrum.

For $K_n < 1$, when both trackers degrade from the variance with correct a priori assumptions, $D < 1$ indicates that the ADT is less susceptible to degradation. When $K_n > 1$, where both traders improve performance, $D < 1$ indicates that the ADT has improved more than the SBT. It can be shown that

(1) if $K_n \leq 1$, $\qquad\qquad$ $D \leq 1$

(2) as $K_n \rightarrow \infty$, $\qquad\qquad$ $D \rightarrow 0$

(3) as $K_n \rightarrow 0$, $\qquad\qquad$ $D \rightarrow 0$

(4) $\left. \dfrac{\partial D}{\partial K_n} \right|_{K_n = 1} \geq 0$

Therefore, for $K_n < 1$ and for large K_n, the adaptive tracker degrades less severely than the SBT, but by (E-4), the ADT is superior at least for some values of K_n greater than, but close to, one.

Figure E-4 shows the performance ratio, D, plotted as a function of K_n for various values of K_n. The value of D is less than one except in a region extending from $K_n = 1$ to some value of $K_n = K_{no}$, where $K_n > 1$. The value of K_{no} appears to be inversely proportional to K_ω. In the region where the SBT is superior, it's advantage is slight, while the ADT may be significantly better than the SBT for values of $K_n < 1$ and $K_n > K_{no}$. Figure E-5 shows the magnitude and location of the maximum of D as a function of K_ω. At most, the ADT bearing estimate is degraded 0.53 dB from that of the SBT, while it is clear from Figure E-5 that the ADT can offer very significant advantages for other values of K_n. For reasonable
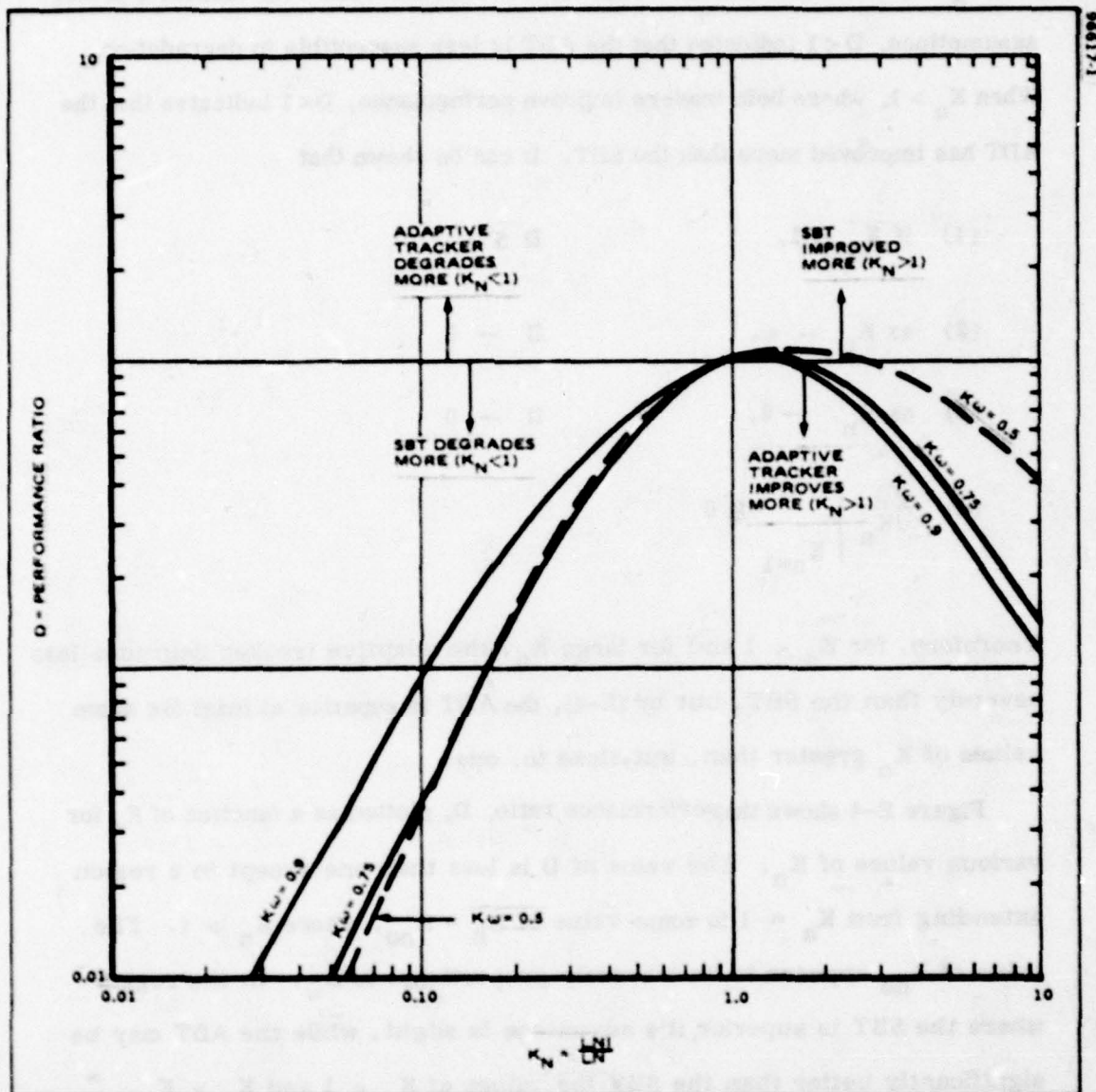
Figure E-4. Comparison of Change in SBT/ADT Performance with Changing Noise Spectrum
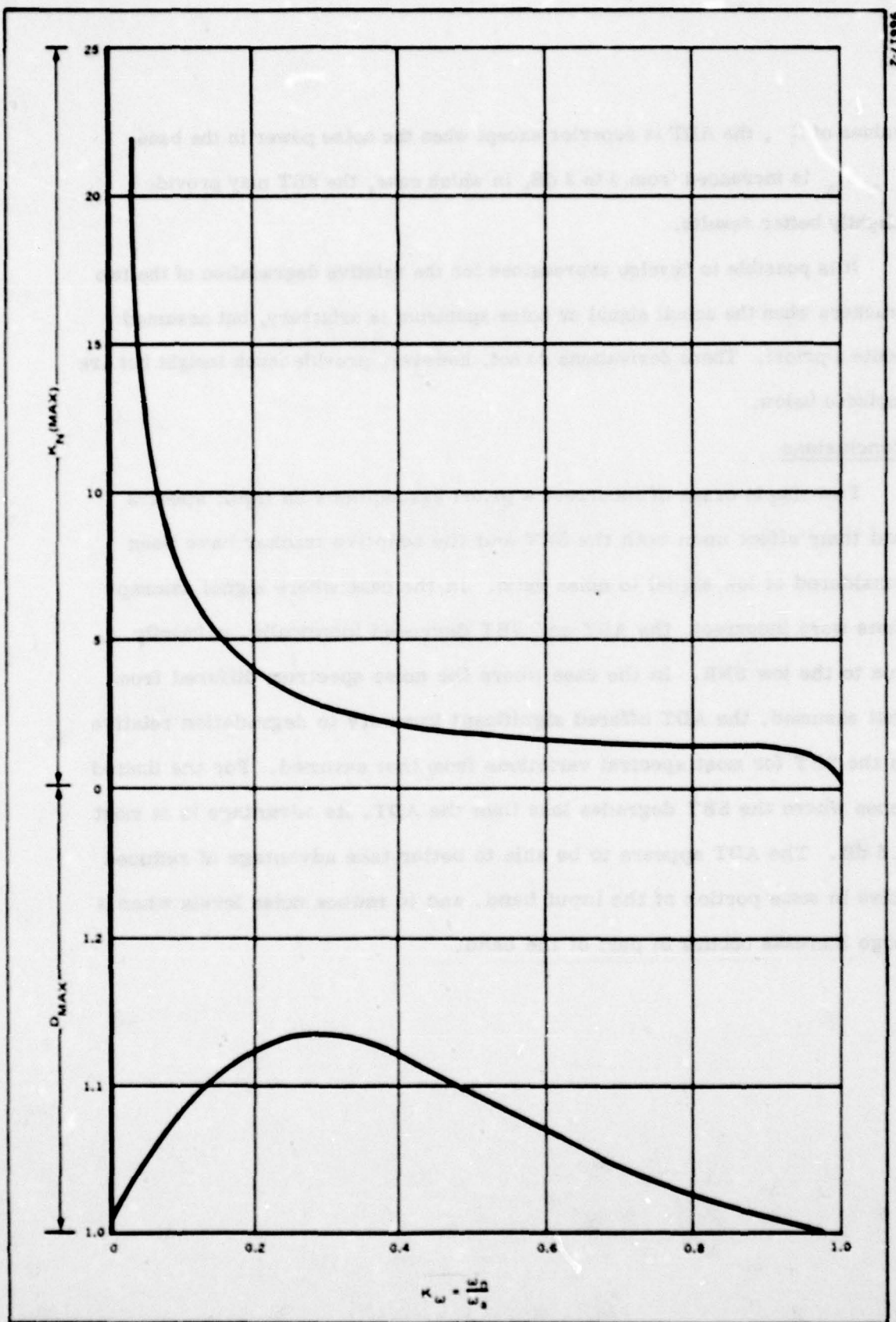
Figure E-5. Maximum Value and Location of Maximum of the Performance Ratio, D

E-21

values of K_n, the ADT is superior except when the noise power in the band is increased from 0 to 3 dB, in which case, the SBT may provide slightly better results.

It is possible to develop expressions for the relative degradation of the two trackers when the actual signal or noise spectrum is arbitrary, but assumed white a priori. These derivations do not, however, provide much insight but are included below.

Conclusions

Two simple cases of incorrect a priori assumptions on input spectra and their effect upon both the SBT and the adaptive tracker have been considered at low signal to noise ratio. In the case where signal assumptions were incorrect, the ADT and SBT degraded identically, primarily due to the low SNR. In the case where the noise spectrum differed from that assumed, the ADT offered significant immunity to degradation relative to the SBT for most spectral variations from that assumed. For the limited cases where the SBT degrades less than the ADT, its advantage is at most 0.5 dB. The ADT appears to be able to better take advantage of reduced noise in some portion of the input band, and to reduce noise levels when a large increase occurs in part of the band.

STATISTICS OF FREQUENCY DOMAIN WEIGHT VECTOR FOR NON-FLAT INPUT SIGNAL AND NOISE

In Appendix IV of reference [1], the statistics of a frequency domain weight vector of a continuous adaptive filter were developed for signal and noise spectra that are flat between two frequencies, ω_L and ω_u, that is

$$S_s(\omega) = \begin{cases} P_s, & |\omega| \epsilon [\omega_L, \ \omega_u] \\ 0, & \text{otherwise} \end{cases}$$

$$S_n(\omega) = \begin{cases} P_n, & |\omega| \epsilon [\omega_L, \ \omega_u] \\ 0, & \text{otherwise} \end{cases}$$

The statistics of the transfer function of the adaptive filter, $H(\dot{\omega})$, in these cases are

$$E[H(\omega)] = \frac{P_s}{P_s + P_n} e^{-j\omega \frac{d}{c} \sin \Theta}$$

$$E[H(\omega_1) H^*(\omega_2)] = \frac{2\pi\mu P_n [2P_s + P_n]}{(P_s + P_n)(2 - 2\mu(P_s + P_n))} \delta(\omega_1 - \omega_1)$$

$$+ \left(\frac{P_s}{P_s + P_n}\right)^2 e^{-j(\omega_1 - \omega_2)\frac{d}{c}\sin\theta}$$

In this appendix, these statistics are developed for signal spectrum, $S_s(\omega)$, and noise spectrum $S_n(\omega)$, symmetric and band limited to $[\omega_L, \omega_u]$ as follows. A stepwise approximation to the signal spectrum is constructed as

$$S_s(N, \omega) = S_s(\omega_k), \qquad \omega \epsilon [\omega_k, \omega_{k+1}), \qquad k = 0, 1, \ldots N$$

where

$$\omega_L = \omega_0 < \omega_1 < \cdots < \omega_H = \omega_u.$$

Similarly,

$$S_n(N, \omega) = S_n(\omega_k), \qquad \omega \epsilon [\omega_k, \omega_{k+1}), \qquad k = 0, 1, \ldots N$$

Using the results from reference [1] on each of these intervals, the statistics of the adaptive filter transfer function are

$$E[H(N, \omega)] = \frac{S_s(\omega_k)}{S_s(\omega_r) + S_n(\omega_r)} e^{-j\omega \frac{d}{c} \sin \Theta}, \omega \epsilon [\omega_k, \omega_{k+1}]$$

$$E[H(N, \omega_1) H^*(N, \omega_2)] = \frac{2 \pi \mu S_n(\omega_k) [2 S_s(\omega_k) + S_n(\omega_k)]}{[S_s(\omega_k) + L_n(\omega_k)][2 - 2(S_s(\omega_k) + S_n(\omega_k))]]}$$

$$\cdot \delta(\omega_1 - \omega_2) + \left(\frac{S_s(\omega_k)}{S_s(\sigma_k) + \sigma_n(\omega_k)} \right)^2$$

$$\cdot e^{-j(\omega_1 - \omega_2) \frac{d}{c} \sin \theta}, \quad (\omega_1 - \omega_2) \epsilon (\omega_k, \omega_{k+1})$$

To compute the variance of the bearing error for the adaptive tracker, we require

$$\text{Var} \left[\frac{\partial h(\tau)}{\partial \tau} \right]$$

and

$$\frac{\partial E \left[\partial h(\tau)/dt \right]}{\partial \Theta} \Bigg|_{\tau = \frac{d}{c} \sin \Theta}$$

Again applying the results of Appendix IV of reference [1], we get

$$\text{Var} \left[\frac{\partial h(\tau)}{\partial \tau} \right] =$$

$$\frac{2}{(2\pi)^2} \sum_{k=0}^{N} \frac{(2\pi) \mu S_n(\omega_k)[2 S_s(\omega_k) + S_n(\omega_k)]}{[S_s(\omega_k) + S_n(\omega_k)][2 - 2\mu(S_s(\omega_k) + S_n(\omega_k)]}$$

$$\cdot \left[\frac{\omega_{k+1}^3 - \omega_k^3}{3} \right]$$

and

$$\frac{\partial E \left[\partial h(\tau)/dt \right]}{\partial \Theta} \Bigg|_{\tau = \frac{d}{c} \sin}$$

$$= \sum_{K=0}^{N} \left(\frac{d}{c} \cos \theta \right) \frac{1}{\pi} \frac{S_s(\omega_k)}{S_s(\omega_k) + S_n(\omega_k)} \left[\frac{\omega_{k+1}^3 - \omega_k^3}{3} \right]$$

Note that these are both Riemann sums, with

$$\left[\frac{\omega_{k+1}^3 - \omega_k^3}{3} \right] \rightarrow \frac{1}{3} d\omega^3 = \omega^2 d\omega$$

so as $N \to \infty$ with $\omega_o = \omega_L$ and $\omega_N = \omega_u$, we get

$$\text{Var}\left[\frac{\partial h(\tau)}{\partial \tau}\right] = \frac{1}{(\pi)} \int_{\omega_L}^{\omega_u} \frac{\mu S_n(\omega)[2 S_s(\omega) + S_n(\omega)]}{[S_s(\omega) + S_n(\omega)][2 - 2\mu(S_s(\omega) + S_n(\omega)]} \omega^2 d\omega$$

and

$$\left. \frac{\partial E[\partial h(\tau)/\partial \tau]}{\partial \Theta} \right|_{\tau = \frac{d}{c}\sin\Theta} = \frac{d}{\pi c}\cos\Theta \int_{\omega_L}^{\omega_n} \frac{S_s(\omega)}{S_s(\omega) + S_n(\omega)} \omega^2 d\omega$$

COMPARISON OF THE ADT AND SBT WITH ASSUMED WHITE SIGNAL AND NOISE, AND GENERAL SIGNAL SPECTRUM

Let the a priori assumptions for signal and noise be as in Case 1, and let

$$S_n(\omega) = S_{na}(\omega)$$

with $S_s(\omega)$ symmetric and equal to zero for $|\omega| > \omega_a$. From the appendix, under small, signal to noise ratio conditions ($S_s(\omega) \ll S_n(\omega)$ each ω), we have

$$\text{Var} \left| \frac{\partial h(\tau)}{\partial \tau} \right| \approx \frac{1}{\pi} \int \mu S_n(\omega) \omega^2 d\omega$$

$$= \frac{1}{\pi} 2 \mu L_n \left| \frac{\omega_a^3}{3} \right|$$

and

$$\frac{\partial E[\partial h(\tau)/\partial \tau]}{\partial \theta} \Bigg|_{\tau = \frac{d}{c} \sin \theta} \approx \frac{d}{\pi c} \cos \theta \int \frac{S_s(\omega)}{S_n(\omega)} \omega^2 d\omega$$

$$= \frac{d}{\pi c} \cos \theta \frac{1}{Ln} \int S_s(\omega) \omega^2 d\omega$$

The variance of the adaptive tracker bearing estimate is then, from (3),

$$\text{Var}[\hat{\theta}] \approx \frac{c^2 \pi}{d^2 \cos^2 \theta} \left[2 \mu L_n^3 \left| \frac{\omega_a^3}{3} \right| \left(\int S_s(\omega) \omega^2 d\omega \right)^{-2} \right]$$

If the prior assumptions were true, the variance would be

$$V_0 \approx \frac{c^2 \pi}{d^2 \cos^2\theta} \frac{1}{2} \mu L_s^{-2} L_n^3 \left[\frac{\omega_a^3}{3}\right]^{-1}$$

so factoring this out of the above gives

$$Var(\hat{\theta}) \approx \frac{c^2 \pi}{d^2 \cos^2\theta} \left[\frac{1}{2}\mu L_s^{-2} L_n^3 \left[\frac{\omega_a^3}{3}\right]^{-1} \right.$$

$$\left. \left\{ 4L_s^2 \left[\frac{\omega_a^3}{3}\right]^2 \left(\int S_s(\omega)\omega^2 d\omega\right)^{-2} \right\} \right]$$

$$= V_0 \left[\left(\frac{2L_s \omega_a^3}{3}\right)^2 \left(\int S_s(\omega)\omega^2 d\omega\right)^{-2} \right]$$

We can use equations (18) and (19) to obtain the variance for the SBT under the same conditions, where

$$\int_{-\infty}^{\infty} |H(\omega)|^2 S_s(\omega)\omega^2 d\omega = \frac{L_s/L_n^2}{1 + 2L_s/L_n} \int S_s(\omega)\omega^2 d\omega$$

and

$$\int_{-\infty}^{\infty} |H(\omega)|^4 [S_n^2(\omega) + 2S_n(\omega)S_s(\omega)] d\omega \approx \left(\frac{L_s/L_n}{1 + 2L_s/L_n}\right)^2$$

$$\left[\frac{2L_n^2\omega_a^3}{3} + 2L_n \int S_s(\omega)\omega^2 d\omega\right]$$

Therefore,

$$D^2(\theta) \approx \frac{2\pi c^2}{Td^2 \cos^2\theta} \left[\frac{\frac{2L_n^2 \omega_a^3}{3} + 2L_n \int S_s(\omega)\omega^2 d\omega}{\left(\int S_s(\omega)\omega^2 d\omega \right)^2} \right]$$

If the a priori assumptions were true, the value of $D^2(\theta)$ would be

$$D_o^2 \approx \frac{2\pi c^2}{Td^2 \cos^2\theta} \left(\frac{2L_n^2 \omega_a^3/3 + 4L_n L_s \omega_a^3/3}{4L_s^2 (\omega_a^3/3)^2} \right)$$

$$= \frac{2\pi c^2}{Td^2 \cos^2\theta} \left(\frac{\omega_a^3}{3} \right)^{-1} \left(\frac{2L_s^2/L_n^2}{1 + 2L_s/L_n} \right)^{-1}$$

which, under small SNR assumptions, is

$$D_o^2 \approx \frac{2\pi c^2}{Td^2 \cos^2\theta} \left(\frac{\omega_a^3}{3} \right)^{-1} \left(\frac{2L_s^2}{L_n^2} \right)^{-1}$$

Then, at low SNR

$$D^2(\theta) \approx \frac{2\pi c^2}{Td^2 \cos^2\theta} \left[\left(\frac{\omega_a^3}{3}\right)^{-1} \frac{L_n^2}{2L_s^2} \left\{\left(\frac{2\omega_a^3 L_s}{3}\right)^2 \left(\int S_s(\omega)\,\omega^2 d\omega\right)^{-2}\right.\right.$$

$$\left.\left. + \frac{2L_s^2 \omega_a^3}{3L_n} \left(\int S_s(\omega)\,\omega^2 d\omega\right)^{-1}\right\}\right]$$

$$= D_o^2 \left[\left(\frac{2\omega_a^3 L_s}{3}\right)^2 \left(\int S_s(\omega)\,\omega^2 d\omega\right)^{-2}\right.$$

$$\left. + \frac{2\omega_a^3 L_s^2}{3L_n} \left(\int S_s(\omega)\,\omega^2 d\omega\right)^{-1}\right]$$

$$= D_o^2 \left[\left(\frac{2\omega_a^3 L_s}{3}\right)^2 \left(\int S_s(\omega)\,\omega^2 d\omega\right)^{-2}\right]$$

At low SNR, then, the adaptive tracker and SBT degrade the same way
under incorrect a priori signal assumptions.

COMPARISON OF THE ADT AND SBT WITH ASSUMED WHITE SIGNAL AND NOISE AND GENERAL NOISE SPECTRUM

Let the a priori assumptions be as in Case II, but let

$$S_s(\omega) = S_{sa}(\omega)$$

and let $S_n(\omega)$ be a symmetric spectrum band limited to $|\omega| \leq \omega_a$. Proceeding as in Appendix II, under small SNR,

$$\text{Var}\left[\frac{\partial h(\tau)}{\partial \tau}\right] \approx \frac{1}{\pi}\int \mu S_n(\omega)\omega^2 d\omega = \frac{1}{\pi}\mu\int S_n(\omega)\omega^2 d\omega$$

and

$$\frac{\partial E\left[\partial h(\tau)/\partial \tau\right]}{\partial \theta}\bigg|_{\tau=\frac{d}{c}\sin\theta} \approx \frac{d}{\pi c}\cos\theta\int\frac{S_s(\omega)}{S_n(\omega)}\omega^2 d\omega$$

$$= \frac{d}{\pi c}\cos\theta\ L_s\int\frac{1}{S_n(\omega)}\omega^2 d\omega$$

Then

$$\text{Var}(\hat{\theta}) \approx \frac{c^2\pi}{d^2\cos^2\theta}\left[\frac{\mu}{L_s^2}\int S_n(\omega)\omega^2 d\omega\left(\int\frac{1}{S_n(\omega)}\omega^2 d\omega\right)^{-2}\right]$$

$$= \frac{c^2\pi}{d^2\cos^2\theta}\left[\frac{1}{2}\mu L_s^{-2}L_n^3\left(\frac{\omega_a^3}{3}\right)^{-1}\right]\left[2\frac{1}{L_n^3}\left[\frac{\omega_a^3}{3}\right]\int S_n(\omega)\omega^2 d\omega\left(\int\frac{1}{S_n(\omega)}\omega^2 d\omega\right)^{-2}\right]$$

$$= V_o\left[\frac{2}{L_n^3}\frac{\omega_a^3}{3}\int S_n(\omega)\omega^2 d\omega\left(\int\frac{1}{S_n(\omega)}\omega^2 d\omega\right)^{-2}\right]$$

Similarly, the variance for the SBT is as follows:

$$\int_{-\infty}^{\infty} |H(\omega)|^2\, S_s(\omega)\, \omega^2\, d\omega \approx \frac{L_s/L_n^2}{1 + 2L_s/L_n} \int S_s(\omega)\, \omega^2 d\omega$$

$$= \frac{2L_s^2/L_n^2}{1 + 2L_s/L_n} \left[\frac{\omega_a^3}{3} \right]$$

$$\int_{-\infty}^{\infty} |H(\omega)|^4\, [S_n^2(\omega) + 2S_n(\omega)\, S_s(\omega)]\, d\omega \approx$$

$$\left(\frac{L_s/L_n^2}{1+2L_s/L_n} \right)^2 \left[\int S_n^2(\omega)\, \omega^2 d\omega + 2L_s \int S_n(\omega)\, \omega^2 d\omega \right]$$

$$D^2(\theta) \approx \frac{2\pi c^2}{Td^2 \cos^2\theta}\, \frac{1}{4L_s^2} \left[\frac{\omega_a^3}{3} \right]^{-2} \left[\int S_n^2(\omega)\, \omega^2 d\omega + 2L_s \int S_n(\omega)\, \omega^2 d\omega \right]$$

$$= \frac{2\pi c^2}{Td^2 \cos^2\theta} \left(\frac{\omega_a^3}{3} \right)^{-1} \left(\frac{2L_s^2}{L_m^2} \right)^{-1}$$

$$\left[\frac{1}{2} \left(\frac{\omega_a^3}{3} \right)^{-1} \frac{1}{L_n^2} \left[\int S_n^2(\omega)\, \omega^2 d\omega + 2L_s \int S_n(\omega)\, \omega^2 d\omega \right] \right]$$

$$= D_o^2 \left[\frac{1}{2} \left(\frac{\omega_a^3}{3} \right)^{-1} \frac{1}{L_n^2} \left\{ \int S_n^2(\omega)\, \omega^2\, d\omega + 2L_s \int S_n(\omega)\, \omega^2\, d\omega \right\} \right]$$

$$\approx \ D_o^2 \left[\frac{1}{2} \left(\frac{\omega_a^3}{3} \right)^{-1} \frac{1}{L_n^2} \int S_n^2(\omega)\,\omega^2\,d\omega \right] \qquad , \text{ Small SNR}$$

Therefore,

$$\frac{\text{Var}(\hat{\theta})}{D^2(\theta)} \approx \frac{V_o}{D_o^2} \left\{ \frac{4}{L_n} \left(\frac{\omega_a^3}{3} \right)^2 \int S_n(\omega)\,\omega^2\,d\omega \left[\int \frac{1}{S_n(\omega)}\,\omega^2\,d\omega \right]^{-2} \right.$$

$$\left. \left[\int S_n^2(\omega)\,\omega^2\,d\omega \right]^{-1} \right\}$$
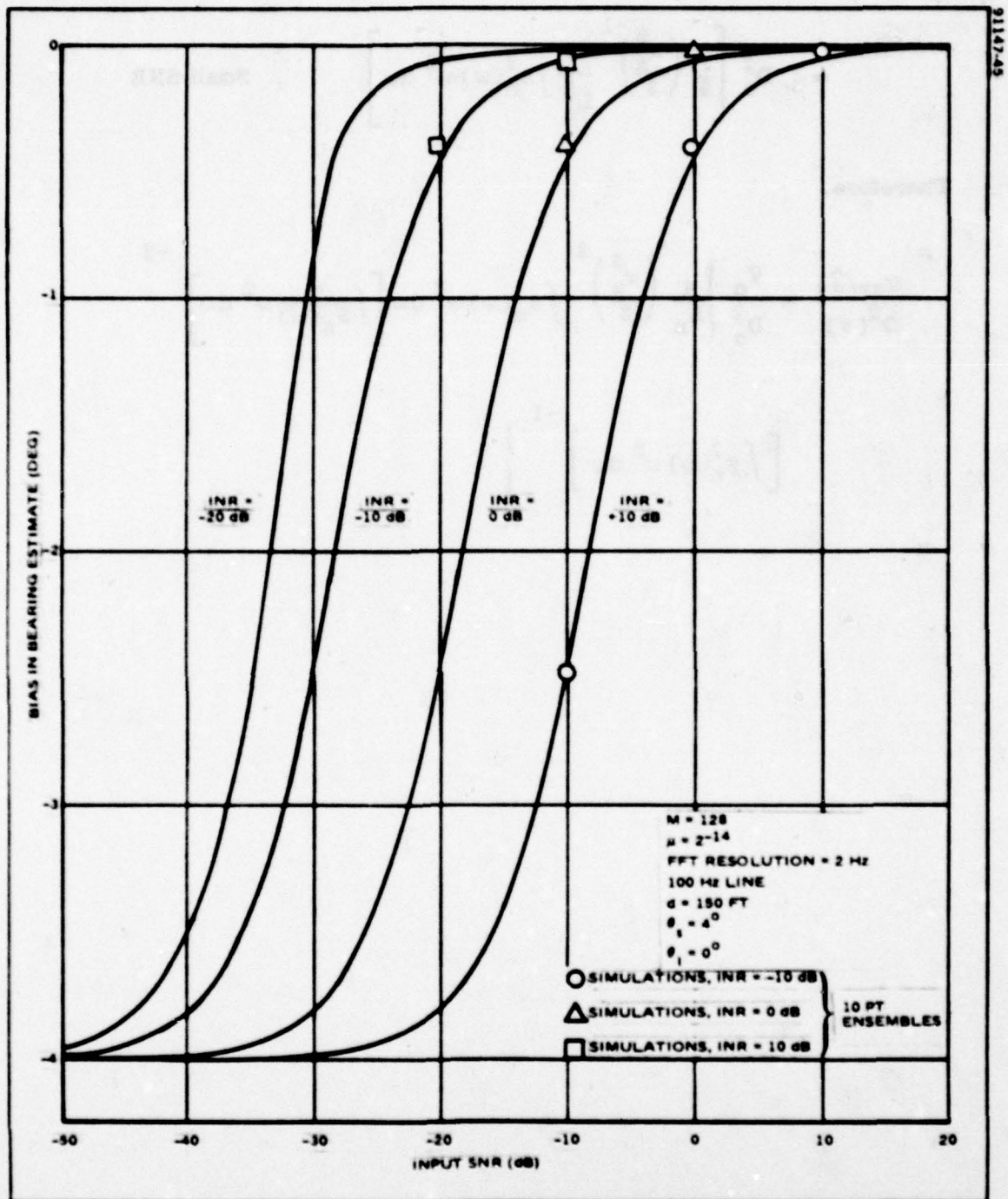
Figure D-12. Effect of BB Interference on NB Tracker (NB Target) (Bias in Bearing Estimate vs SNR for Various INR)

APPENDIX F

Appendix F

Broadband Bearing Estimating in the Presence of an Interference

During the first phase of this study, the performance of the adaptive tracker with a broadband input signal was analyzed. In this section, the ground work for an analysis of the effect of a single broadband interference plus ambient noise on the bearing estimate for a broadband target is developed. Here a broadband interference refers to a directional point source radiating broadband noise, generally separated from the target in azimuth. The approach to the analysis of the adaptive tracker performance in the presence of an interference will be a direct extension of the method used in the analysis for broadband interference in the first phase of this study. The analysis will initially utilize a continuous version of the adaptive filter, as shown in Figure F-1. By analogy with the frequency domain model of Figure A-2, it is possible to determine the mean and variance of the continuous weight function in the presence of interference. As before, the time delay estimate between split arrays is extracted by locating the peak of the weight function.

A crucial difference between the signal only and signal plus interference case is that in the latter, the weight function may have two peaks, one at the signal delay and the other corresponding to the delay in the interference between split arrays. Moreover, there may be only a single peak located between the two delays. When two peaks occur, the estimate will be unbiased if we select the correct (signal) peak. If only a single peak occurs between the two delays, then the estimate will be biased.

As in Appendix IV of reference [1], and in [6], the variance in the determination of the location of the peak is

$$Var^{\frac{1}{2}}[\tau] = \frac{Var^{\frac{1}{2}}\left[\frac{\partial h(t)}{\partial t}\right]}{\frac{\partial}{\partial t}\ E\ [h(t)]}\Bigg|_{t=\tau_p} \tag{F-1}$$

where $h(t)$ is the weight function, $\hat{\tau}$ is the estimate of the peak location, and τ_p is the location of the peak in the mean weight function. This result can be easily converted to a bearing error for a given array.

Just as in the analysis of the signal only broadband case, the array is treated as two omnidirectional point sensors located at the phase centers of the split arrays. This model is valid when the signal and interference are near the MRA, so that the response of the half arrays are nearly invariant with frequency.

Determination of Mean and Variance of Weight Vector in the Presence of Broadband Interference

For the broadband signal plus interference, the time domain inputs to the adaptive tracker can be modeled as

$$\begin{aligned} x(t) &= s(t) + n_x(t) \\ d(t) &= s(t - \Delta T_s) + i(t - \gamma T_s) + n_d(t) \end{aligned} \tag{F-2}$$

where $s(t)$, $i(t)$, $n_x(t)$, and $n_d(t)$ are zero mean, stationary random processes, uncorrelated in time and independent of each other. Let the delay between the two inputs for signal and interference, ΔT_s and γT_s, be multiples of the sampling interval, T_s.

The mean and variance of the weight vector can be analyzed using the frequency domain model for the adaptive filter shown in Figure F-1. An FFT is performed on both $x(t)$ and $d(t)$ every RT_s seconds, so that each frequency

domain filter iterates every RT_s seconds. With M the FFT size, $R = M$ corresponds to FFT processing without overlapping or gaps between time windows, $R < M$ corresponds to overlapping FFTs and $R > M$ indicates gap processing.

The ith input to the adaptive filter in the kth FFT bin is given by

$$X_k(i) = \sum_{p=0}^{M-1} \left\{ s[(p+iR)T_s] + i\,[(p+iR)T_s] + n_x[(p+iR)T_s] \right\} e^{-j\frac{2\pi}{M}pk}$$

and

$$D_k(i) = \sum_{p=0}^{M-1} \left\{ s[(p+iR-\Delta)T_s] + i[(p+iR-\gamma)T_s] \right.$$

$$\left. + n_d[(p+iR)T_s] \right\} e^{-j\frac{2\pi}{M}pk} \tag{F-3}$$

Using the results of reference [1], Appendix III, the mean square value of the weight in the kth FFT bin is defined by

$$E[|W_k(n+1)|^2] = \mu^2 \sum_{m=0}^{n} E|F_k(m)|^2 + 2\mu^2 \sum_{m=0}^{n} \sum_{q=0}^{m-1} E[F_k(m)F_k^*(q)] \tag{F-4}$$

where

$$F_k(m) = D_k(m)X_k(m) \prod_{\ell=m+1}^{n} [1 - \mu |X_k(k)|^2] \tag{F-5}$$

The single sum is treated first.

$$E[|F_k(m)|^2] = E\left\{|D_k(m)\,X_k(m)|^2 \prod_{p=m+1}^{n} \prod_{q=m+1}^{n} [1-\mu|X_k(p)|^2]\right.$$

$$\left. \cdot [1-\mu|X_k(q)|^2]\right\} \qquad (F-6)$$

$$= E[|D_k(m)\,X_k(m)|^2] \prod_{p=m+1}^{n} E\left\{[1-\mu|X_k(p)|^2]\right\}^2$$

The expectation separates because the terms in the product involve inputs at later times, which are uncorrelated. Using the gaussian assumption,

$$E[|D_k(m)\,X_k(m)|^2] = E\{|D_k(m)|^2\}\,E\{|X_k(m)|^2\} + E\{D_x(m)X_k^*(m)\}$$

$$E\{D_x^*(m)\,X_k(m)\} + E\{D_k(m)X_d(m)\}E\{D_k^*(m)X_k^*(m)\} \qquad (F-7)$$

From reference [1], Appendix II,

$$E[|D_k(m)|^2] = E[|X_k(m)|^2] = M(\sigma_s^2 + \sigma_s^2 + \sigma_n^2)$$

and

$$E[D_k(m)X_k^*(m)] = (E[D_k^*(m)\,X_k(m)])^* = (M-\Delta)\,\sigma_s^2\,e^{-j\frac{2\pi}{M}\Delta k}$$

$$+ (M-\gamma)\,\sigma_I^2\,e^{-j\frac{2\pi}{M}\gamma k} \qquad (F-8)$$

We also need $\left| E\{D_k(m) \, X(m)\} \right|^2$. Consider the signal contribution.

$$E\left\{ \sum_{n=0}^{M-1} \sum_{m=0}^{M-1} s[(n+iR)T_s] s[(n+R-\Delta)T_s] \right\} = \sum_n \sum_m \sigma_s^2 \, \delta_{n,m-\Delta} \, e^{-j\frac{2\pi}{M}(n+m)k}$$

$$= \sum_{n=0}^{M-1} \sum_{m'=-\Delta}^{M-\Delta-1} \delta_{n,m'} \, \sigma_s^2 \, e^{-j\frac{2\pi}{M}(n+m'+\Delta)k}$$

$$= \sum_{n=0}^{M-\Delta-1} \sigma_s^2 \, e^{-j\frac{2\pi}{M}\Delta k} \, e^{-j\frac{2\pi}{M}nk}$$

$$= S(M,\Delta) \, \sigma_s^2 \, e^{-j\frac{2\pi}{M}\Delta k} \qquad (F-9)$$

with

$$S(M,\Delta) = \frac{\sin 2\pi k \left(\frac{M-\Delta}{M}\right)}{\sin 2\pi k/m} \, e^{j2\pi \left(\frac{M-1}{M}\right)k}$$

By analogy with the signal term,

$$E[|D_k(m)X_k(m)|^2] = M^2(\sigma_s^2 + \sigma_I^2 + \sigma_n^2)$$

$$+ \left| (M-\Delta)\sigma_s^2 \, e^{-j\frac{2\pi}{M}\Delta k} + (M-\gamma)\sigma_I^2 \, e^{-j\frac{2\pi}{M}\gamma k} \right|^2$$

$$+ \left| S(M,\Delta) \, e^{j\frac{2\pi}{M}\Delta k} \, \sigma_s^2 + S(M,\gamma) \, e^{j\frac{2\pi}{M}\gamma k} \, \sigma_I^2 \right|^2 \qquad (F-10)$$

We also need

$$E[1-\mu |X_k(p)|^2]^2 = 1 - 2\mu E |X_k(p)|^2 + \mu^2 E|X_k(p)|^4 \qquad (F-11)$$

where

$$E[|X_k(p)|^4] = 2E^2(|X_k(p)|^2) + E[X_k^2(p)] E[(X_k^*(p))^2] \qquad (F-12)$$

But,

$$E[X_k^2(p)] = \sum_{n=0}^{M-1} \sigma_s^2 + \sigma_n^2 + \sigma_I^2) e^{-j\frac{2\pi}{M} 2n} = \begin{cases} M(\sigma_s^2 + \sigma_n^2 + \sigma_I^2), & k=0 \\ 0, & \text{otherwise} \end{cases} \qquad (F-13)$$

$$E[1-\mu |X_k(p)|^2]^2 = \begin{cases} 1-2\mu M(\sigma_s^2 + \sigma_I^2 + \sigma_n^2) + 2\mu^2 M^2\left(\sigma_s^2 + \sigma_I^2 + \sigma_n^2\right)^2, & k\neq 0, M/2 \\ 1-2\mu M(\sigma_s^2 + \sigma_I^2 + \sigma_n^2) + 3\mu^2 M^2(\sigma_s^2 + \sigma_I^2 + \sigma_n^2), & k=0, M/2 \end{cases} \qquad (F-14)$$

Therefore,

$$\mu^2 \sum_{m=0}^{n} E[|F(m)|^2] = \frac{\mu A_1}{P_T(2-2\mu P_T)} \left[1 - (1-2\mu P_T + 2\mu^2 P_T^2)^{n+1}\right] \qquad (F-15)$$

where

$$A_1 = P_T^2 + \left| (M-\Delta) \sigma_s^2 e^{-j\frac{2\pi}{M} \Delta k} + (M-\gamma) \sigma_I^2 e^{-j\frac{2\pi}{M} \gamma k} \right|^2$$

$$+ \left| S(M,\Delta) \sigma_s^2 + S(M,\gamma) \sigma_I^2 \right|^2$$

and

$$P_T = M (\sigma_s^2 + \sigma_I^2 + \sigma_n^2)$$

The double sum term in $E[W^2(n+1)]$, involves $E[F(m)F^*(q)]$ which is treated as follows:

$$E[F_k(m)F_k^*(q)] = E\left\{ D_k(m)X_k^*(m) D_k^*(q)X_k(q) \right.$$

$$\left. \prod_{p=m+1}^{n} \prod_{v=q+1}^{n} [1 - \mu |X_k(p)|^2][1 - \mu |X_k(v)|^2] \right\} \quad \text{(F-16)}$$

In the double sum, $q < m$, so that

$$\prod_{p=m+1}^{n} \prod_{v=q+1}^{n} (\cdot) = \prod_{p=m+1}^{n} \prod_{v=m+1}^{n} \prod_{v=q+1}^{m} (\cdot) \quad \text{(F-17)}$$

Thus, since both p and v range over indices that are greater than m and q,

$$E[F_k(m)F^*(q)] = E\left\{ \prod_{p=m+1}^{n} \prod_{v=m+1}^{n} [1 - \mu | X_k(p)|^2][1 - \mu | X_k(q)|^2] \right\}$$

$$\quad \text{(F-18)}$$

$$\cdot E\left\{ D_k(m)X_k^*(m)D_k^*(q)X_k(q) \prod_{v=q+1}^{m} [1 - \mu|X_k(v)|^2] \right\}$$

The first expectation was evaluated previously in equation (F-6). The second expectation, since q is always less than m, is

$$E\left\{D_k(m) X_k^*(m) D_k^*(q) X_k(q) \prod_{v=q+1}^{m} [1-\mu|X_k(v)|^2]\right\} = E[D_k^*(q)X_k(q)]$$

$$\cdot E\left\{D_k(m)X_k^*(m) [1-\mu|X_k(m)|^2]\right\} \prod_{v=q+1}^{m-1} E[1-\mu|X_k(v)|^2] \qquad (F-19)$$

We have already evaluated $E[D_k(q)X_k^*(q)]$ which gives $E[D_k^*(q)X_k(q)]$, and

$$E[1-\mu|X_k(v)|^2] = 1 - \mu P_T$$

Further

$$E[D_k(m)X_k^*(m)[1-\mu|X_k(m)|^2]] = E[D_k(m)X_k^*(m)]$$

$$- \mu E[D_k(m)X_k^*(m)X_k(m)X_k^*(m)] \qquad (F-20)$$

But, using the gaussian assumption

$$E[D_k(m)X_k^*(m)X_k(m)X_k^*(m)] \approx 2E[D_k(m)X_k^*(m)]E[|X_k(m)|^2]$$

$$+ E[D_k(m)X_k(m)]E[X_k^*(m)X_k^*(m)] \qquad (F-21)$$

Just as above,

$$E[X_k^*(m)X_k^*(m)] = \begin{cases} M(\sigma_s^2 + \sigma_s^2 + \sigma_n^2) \\ 0, \text{ otherwise} \end{cases}$$

and

$$E[D_k(m)X_k(m)] = S(m,\Delta) e^{-j\frac{2\pi}{M}\Delta k} + S(m,\gamma) e^{-j\frac{2\pi}{M}\gamma k} = A_3$$

so for $k \neq 0, M/2$

$$E[D_k(m)X_k^*(m)X_k(m)X_k^*(m)] = 2E[D_k(m)X_k^*(m)]E[\,|X_k(m)|^2] \qquad (F-22)$$

Therefore,

$$E[F_k(m)F_k^*(q)] = \begin{cases} [1-2\mu P_T + \mu^2 P_T^2]^{n-m} A_2^*(A_1 - 2\mu A_2 P_T)[1-\mu P_T]^{m-q-1}, k\neq 0, M/2 \\[2mm] [1-2\mu P_T + 3\mu^2 P_T^2]^{n-m} A_2^*[A_2 - 2\mu A_2 P_T + \mu A_3 P_T] \\[2mm] [1-\mu P_T]^{m-q-1}, k=0, M/2 \end{cases}$$

where

$$A_2 = (M-\Delta)\,\sigma_s^2\, e^{-j\frac{2\pi}{M}\Delta k} + (M-\gamma)\,\sigma_I^2\, e^{-j\frac{2\pi}{M}\gamma k} \qquad (F-23)$$

The double summation is then

$$\mu^2 \sum_{m=0}^{n} \sum_{q=0}^{m-1} E[F_k(m)F_k^*(q)] = |A_2|^2 [1-2\mu P_T] \sum_{m=0}^{n} \left[1 - 2\mu P_T + 2\mu^2 P_T^2\right]^{n-m}$$

$$\sum_{q=0}^{m-1} [1-\mu P_T]^{m-q-1}$$

$$= \begin{cases} \dfrac{|A_2|^2 [1-2\mu P_T]}{P_T^2} \left\{ \dfrac{1-(1-2\mu P_T + 2\mu^2 P_T^2)^{n+1}}{2-2\mu P_T} - \dfrac{[1-\mu P_T]^{n+1} - [1-2\mu P_T + 2\mu^2 P_T^2]^{n+1}}{1-2\mu P_T} \right\}, k\neq 0, M/2 \\[4mm] \dfrac{[\,|A_2|^2 - 2\mu\,|A_2|^2 P_T - \mu A_2^* A_3 P_T]}{P_T^2} \left\{ \dfrac{1 - (1-2\mu P_T + 3\mu^2 P_T^2)^{n+1}}{2-2\mu P_T} - \right. \\[4mm] \left. \dfrac{[1-\mu P_T]^{n+1} - [1-2\mu P_T + 3\mu^2 P_T^2]^{n+1}}{1-2\mu P_T} \right\} \; k=0, M/2 \end{cases}$$

Combining this with (F-15) to obtain the mean squared weight gives

F-10

$$E|W_k(n)|^2 = \frac{\mu A_1}{P_T(2-2\mu P_T)} \left[1-(1-2\mu P_T + 2\mu^2 P_T^2)^n\right]$$

$$+ \frac{2|A_2|^2 (1-2\mu P_T)}{P_T^2} \left\{ \frac{1-(1-2\mu P_T+2\mu^2 P_T^2)^n}{2-2\mu P_T} - \frac{(1-\mu P_T)^n-(1-2\mu P_T+2\mu^2 P_T^2)^n}{1-2\mu P_T} \right\} \quad k \neq 0, M/2$$

$$(F-24)$$

Taking the limit as $n \to \infty$ yields the steady state mean square weight,

$$E|W_k(\infty)|^2 = \begin{cases} \dfrac{\mu A_1}{P_T(2-2\mu P_T)} + \dfrac{2|A_2|^2 (1-2\mu P_T)}{P_T^2 (2-2\mu P_T)}, & k \neq 0, M/2 \\[3mm] \dfrac{\mu A_1}{P_T(2-3\mu P_T)} + \dfrac{2\left[|A_2|^2-2\mu|A_2|^2 P_T - \mu A_2^* A_3 P_T\right]}{P_T^2(2-3\mu P_T)}, & k=0, M/2 \end{cases}$$

$$(F-25)$$

Again, from reference [1], Appendix III, the mean weight is given by

$$E[W_k(n+1)] = \mu \sum_{n=0}^{n} E[D_k(m)X_k^\bullet(m)] \prod_{q=m+1}^{n} E\{1-\mu|X_k(q)|^2\}$$

$$= \mu \sum_{m=0}^{n} A_2 \{1-\mu P_T\}^{n-m} = \frac{A_2}{P_T} \left(1-(1-\mu P_T)^{n+1}\right) \quad (F-26)$$

The steady state mean weight is then

$$E[W(\infty)] = \frac{A_2}{P_T}$$

and

$$|EW(\infty)|^2 = \frac{|A_2|^2}{P_T^2}$$

Also, note that

$$A_1 = P_T^2 + |A_2|^2 + |A_3|^2$$

where

$$A_3 = S(M,\Delta) \, e^{j \frac{2\pi}{M} \Delta k} \, \sigma_s^2 + S(M,\gamma) \, e^{j \frac{2\pi}{M} \gamma k} \, \sigma_I^2$$

Then the steady state weight variance is

$$Var[W(\infty)] = \frac{\mu(P_T^2 + |A_2|^2 + |A_3|^2)}{P_T(2-2\mu P_T)} + \frac{2|A_2|^2(1-2\mu P_T)}{P_T^2(2-2\mu P_T)} - \frac{|A_2|^2}{P_T^2}$$

$$= \begin{cases} \dfrac{\mu(P_T^2 - |A_2|^2 + |A_3|^2)}{P_T(2-2\mu P_T)} \\[4mm] \dfrac{\mu(P_T^2 - 2A^*A_3 + |A_3|^2)}{P_T(2-2\mu P_T)} \, , \quad k=0,M/2 \end{cases} \qquad (F-27)$$

Suppose there is no interference, $\sigma_I^2=0$, and $\Delta=0$. Then

$$P_T^2 = M^2 (\sigma_s^2 + \sigma_n^2)^2$$

$$|A_2|^2 = M^2 \sigma_s^4 \qquad\qquad |A_3|^2 = 0 \quad k\neq 0$$

so

$$Var[W(\infty)] = \frac{\mu(P_T^2 - M^2\sigma_s^4)}{P_T(2-2\mu P_T)} = \frac{\mu M \sigma_n^2 [M\sigma_n^2 + 2M\sigma_s^2]}{M(\sigma_s^2 + \sigma_n^2)(2-2\mu M(\sigma_s^2 + \sigma_n^2))}$$

This agrees with the result for the case of $\sigma_I^2 = 0$ and $\Delta = 0$ derived in Reference [1]. Appendix III.

We are interested in the performance of the time domain adaptive tracker, for which windowing effects do not occur. Then in this case,

$$A_2 = M\sigma_s^2 \, e^{-j\frac{2\pi}{M}\Delta k} + M\sigma_I^2 \, e^{-j\frac{2\pi}{M}\gamma k}$$

$$A_3 = 0 \quad \text{if} \quad k \neq 0$$

Therefore,

$$E[W_k(\infty)] = \frac{\sigma_s^2}{\sigma_s^2 + \sigma_I^2 + \sigma_n^2} \, e^{-j\frac{2\pi}{M}\Delta k} + \frac{\sigma_I^2}{\sigma_s^2 + \sigma_I^2 + \sigma_n^2} \, e^{-j\frac{2\pi}{M}\gamma k} \quad \text{(F-28)}$$

and

$$\text{Var}[W_k(\infty)] = \frac{\mu M \sigma_n^2 [M\sigma_n^2 + 2M(\sigma_s^2 + \sigma_I^2)]}{M(\sigma_s^2 + \sigma_I^2 + \sigma_n^2)(2 - 2\mu M(\sigma_s^2 + \sigma_I^2 + \sigma_n^2))} \quad \text{(F-29)}$$

This is the same form as the variance without the interference but with the signal power replaced by the sum of the signal and interference powers.

Determination of Bias and Bearing Estimate Variance for Broadband Tracker with Broadband Interference

As in reference [1], it is assumed that the mean bearing estimate occurs at the peak of the mean weight function, $E[h(\tau)]$, or equivalently, at the zero crossing of the derivative, $E[\partial h(\tau)/d\tau]$, corresponding to this peak. Suppose we assume that the input signals and noise are flat for $|\omega| \epsilon [\omega_L \omega_u)$ and zero outside that range. Then using expression (F-28), the mean transfer function of the continuous adaptive filter can be seen to be

$$H(\omega) = \frac{1}{\sigma_s^2 + \sigma_I^2 + \sigma_n^2} \left[\sigma_s^2 e^{-j\omega\frac{d}{c}\sin\theta_s} + \sigma_I^2 e^{-j\omega\frac{d}{c}\sin\theta_I} \right] \tag{F-30}$$

The derivative of the mean weight function in the time domain is then

$$E\frac{\partial h(\tau)}{\partial \tau} = \frac{1}{2\pi} \int_{-\infty}^{\infty} j\omega H(\omega) e^{j\omega\tau} d\omega$$

$$= \frac{1}{\pi\left(\sigma_s^2 + \sigma_I^2 + \sigma_n^2\right)} \left\{ \sigma_s^2 \left[\sin(\omega_u(\tau-\tau_s)) - \sin(\omega_L(\tau-\tau_s))\right.\right.$$

$$- (\tau-\tau_s)(\omega_u \cos(\omega_u(\tau-\tau_s)) - \omega_L \cos(\omega_L(\tau-\tau_s)))]$$

$$+ \sigma_I^2 \left[\sin(\omega_u(\tau-\tau_I)) - \sin(\omega_L(\tau-\tau_I))\right.$$

$$\left.\left. - (\tau-\tau_I)(\omega_u \cos(\omega_u(\tau-\tau_I)) - \omega_L \cos(\omega_L(\tau-\tau_I)))\right] \right\} \tag{F-31}$$

We are interested in finding the location of the zero crossing of this function corresponding to the maximum of the weight function. Although this cannot

F-14

be determined explicitly, it can be found numerically on the computer. For convenience, we will consider the lowpass case, where $\omega_L = 0$, and

$$E \frac{\partial h(\tau)}{\partial \tau} = \frac{1}{\pi\left(\sigma_s^2 + \sigma_I^2 + \sigma_n^2\right)} \left\{ \sigma_s^2 [\sin(\omega_u(\tau - \tau_s)) - (\tau - \tau_s)\omega_u \sin(\omega_u(\tau - \tau_s))] \right.$$

$$\left. + \sigma_I^2 [\sin(\omega_u(\tau - \tau_s)) - (\tau - \tau_I) \omega_u \sin(\omega_u(\tau - \tau_I))] \right\} \qquad (F-32)$$

where

$$\tau_s = \frac{d}{c} \sin \theta_s \quad \text{and} \quad \tau_I = \frac{d}{c} \sin \theta_I$$

To compute the variance of the estimate from (F-1), we also need

$$\frac{\partial}{\partial \tau} E\left[\frac{\partial h(\tau)}{\partial \tau}\right] = \frac{1}{\pi\left(\sigma_s^2 + \sigma_I^2 + \sigma_n^2\right)} \left\{ \frac{\sigma_s^2}{(\tau - \tau_s)^3} \left[\cos(\omega_u(\tau - \tau_s)) - 1 \right.\right.$$

$$\left. + (\omega_u^2(\tau - \tau_s)^2 - 2) \sin(\omega_u(\tau - \tau_s)) \right]$$

$$+ \frac{\sigma_I^2}{(\tau - \tau_I)^3} \left[\cos(\omega_u(\tau - \tau_I)) - 1 + (\omega_u^2(\tau - \tau_I)^2 - 2) \right.$$

$$\left.\left. \cdot \sin(\omega_u(\tau - \tau_s)) \right] \right\} \qquad (F-33)$$

Finally, we need

$$\text{Var}\left[\frac{\partial h(\tau)}{\partial \tau}\right] = E\left[\left(\frac{\partial h(\tau)}{\partial \tau}\right)^2\right] - E^2\left[\frac{\partial h(\tau)}{\partial \tau}\right] = E\left[\left(\frac{\partial h(\tau)}{\partial \tau}\right)^2\right] \qquad (F-34)$$

F-15

since we will choose τ such that

$$E\left[\frac{\partial h(\tau)}{\partial \tau}\right] = 0$$

Using the mean and variance of the frequency domain weight vector above as in reference [1], we get

$$\text{Var}\left[\frac{\partial h(\tau)}{\partial \tau}\right] = \frac{1}{(2\pi)^2} \int_{-\infty}^{+\infty}\int_{-\infty}^{+\infty} K_1 \omega_1 \omega_2 \, e^{j\nu(\omega_1 - \omega_2)} (2\pi) \, \delta(\omega_1 - \omega_2) \, d\omega_1 d\omega_2$$

$$+ \frac{1}{(2\pi)^2} \int_{-\infty}^{\infty}\int_{-\infty}^{\infty} K_2 \omega_1 \omega_2 \, e^{j\nu(\omega_1 - \omega_2)} \, d\omega_1 d\omega_2$$

with

$$K_1 = \frac{\mu\sigma_n^2 \left[2\left(\sigma_s^2 + \sigma_I^2\right) + \sigma_n^2\right]}{\left(\sigma_s^2 + \sigma_I^2 + \sigma_n^2\right)\left[2 - 2\mu\left(\sigma_s^2 + \sigma_I^2 + \sigma_n^2\right)\right]}$$

and

$$K_2 = \frac{1}{\left(\sigma_s^2 + \sigma_I^2 + \sigma_n^2\right)} \left[\sigma_s^2 \, e^{-j\omega\tau}{}_s + \sigma_I^2 \, e^{j\omega\tau}{}_I\right] \tag{F-35}$$

With some algebra, it can be shown that the second integral in (F-35) is zero, and the result is

$$\text{Var}\left[\frac{\partial h(\tau)}{\partial \tau}\right] = \frac{2}{(2\pi)^2} \frac{(2\pi)\mu\sigma_n^2 \left[2(\sigma_s^2 + \sigma_I^2) + \sigma_n^2\right]}{(\sigma_s^2 + \sigma_I^2 + \sigma_n^2)\left[2 - 2\mu(\sigma_s^2 + \sigma_I^2 + \sigma_n^2)\right]} \left[\frac{\omega_u^3}{3}\right] \qquad (F-36)$$

Then as a function of τ_p, we can write (F-1) as

$$\text{Var}^{1/2}(\theta) = \frac{1}{1/2\,\tau_p} \frac{\left[\dfrac{\mu\sigma_3^2\left[2(\sigma_s^2 + \sigma_I^2) + \sigma_n^2\right]}{(\sigma_s^2 + \sigma_I^2 + \sigma_n^2)(2 - 2\mu(\sigma_s^2 + \sigma_I^2 + \sigma_n^2))}\right]^{1/2} \left[\dfrac{\omega_u^3 - \omega_L^3}{3}\right]^{1/2}}{\left[\begin{array}{l} \dfrac{1}{(\sigma_s^2 + \sigma_I^2 + \sigma_n^2)}\left\{\sigma_s^2\left[\cos(\omega_u(\tau_p - \tau_s)) - \cos(\omega_L(\tau_p - \tau_s))\right. \right. \\[2ex] \left. + ((\omega_u(\tau_p - \tau_s))^2 - 2)\sin(\omega_u(\tau_p - \tau_s)) \right. \\[2ex] \left. - ((\omega_L(\tau_p - \tau_s))^2 - 2)\sin(\omega_L(\tau_p - \tau_s))\right] \\[2ex] + \sigma_I^2\left[\cos(\omega_u(\tau_p - \tau_s)) - \cos(\omega_L(\tau_p - \tau_I))\right. \\[2ex] \left. + ((\omega_u(\tau_p - \tau_I))^2 - 2)\sin(\omega_u(\tau_p - \tau_I)) \right. \\[2ex] \left. \left. - ((\omega_L(\tau_p - \tau_I))^2 - 2)\sin(\omega_L(\tau_p - \tau_I))\right]\right\} \end{array}\right]}$$

$$(F-37)$$

Note this expression is actually valid only for values of τ_p such that

$$E\left[\frac{\partial h(\tau)}{\partial \tau}\right]\Bigg|_{\tau=\tau_p} = 0$$

The actual variance is obtained by substituting the value of τ_p from the numerical maximization of (F-31) in this expression.

Bearing Estimation with a Discrete Adaptive Tracker in the Presence of an Interference

The analysis in this section has followed the same course as that of Appendix IV of [1], using a continuous adaptive filter. As pointed out in Appendix V of that reference, however, in practice the adaptive filter is discrete in time and of finite length, and the peak of the impulse response must be found by interpolating between discrete sample points. This interpolation increases the variance of the bearing estimate with respect to that of the continuous case. The interpolation was of the type in which an interpolated impulse response was computed as

$$h_I(t) = \sum_{m=0}^{M-1} h(mTs)\, f(t - mTs) \tag{F-38}$$

where $h(mTs)$ are the discrete filter weights and $f(t)$ is a interpolation function, such as

$$f(t) = \frac{\sin 2\,Bt}{2\,Bt}$$

The algorithm then determines the peak of $h_I(t)$ as the estimate of time delay between half array phase centers.

Following the method of [6], the variance in the determination of the peak in $h_I(t)$ is

$$
\text{Var}^{1/2}[\hat{t}_z] = \frac{\text{Var}^{1/2}\left[\dfrac{\partial h_I(\tau)}{\partial \tau}\right]}{\dfrac{\partial E\left[\dfrac{\partial h_I(\tau)}{\partial \tau}\right]}{\partial \tau}}\Bigg|_{\tau = t_z}
$$

(F-39)

where t_z is the actual location of the zero crossing.

In the first part of this appendix, the statistics of the frequency domain weights of the adaptive tracker were developed. If we let $H(k)$ denote the weight in the kth frequency bin the time domain weights can be written as

$$
h(mT_s) = \frac{1}{M} \sum_{k=0}^{M-1} H(k)\, e^{j\frac{2\pi}{M}mk}
$$

(F-40)

and the interpolated impulse response ban be written are

$$
h_I(t) = \sum_{m=0}^{M-1} h(mT_s)\, f(t-mT_s)
$$

$$
= \frac{1}{M} \sum_{m=0}^{M-1} \sum_{k=0}^{M-1} H(k)\, f(t-mT_s)\, e^{j\frac{2\pi}{M}mk}
$$

(F-41)

F-19

Now, assume that the inputs to the adaptive filter are bandlimited to some bandwidth, B_S, so that

$$H(k) = 0 \text{ for } k > (J-1) = \lfloor B_S T_S \rfloor \frac{M}{2} \qquad (F-42)$$

where $\lfloor X \rfloor$ is the largest integer less than or equal to X. Further, in order for $h(mT_S)$ to be real, we require

$$H(k) = H*(M-k) \qquad (F-43)$$

Using (F-41), it can readily be verified that

$$\text{Var}^{1/2} [h'_I(t)] = \frac{1}{M^2} \sum_{k=0}^{M-1} \text{Var} [H(k)] \sum_{m_1=0}^{M-1} \sum_{m_2=0}^{M-1} f'(t-m_1 T_s)$$

$$\cdot f'(t-m_2 T_s) e^{j\frac{2\pi}{m}(m_1-m_2)k} \qquad (F-44)$$

and

$$\frac{\partial E[h'_I(t)]}{\partial t} = \frac{1}{M} \sum_{k=0}^{M-1} E[H(k)] \sum_{m=0}^{M-1} f''(t-mT_2) e^{j\frac{2\pi}{M}mk} \qquad (F-45)$$

We want (F-28) and (F-29) to satisfy (F-42) and (F-43), so

$$
E[H(k)] = \begin{cases}
\dfrac{1}{\sigma_s^2 + \sigma_I^2 + \sigma_n^2}\left[\sigma_s^2\, e^{-j\frac{2\pi}{M}\Delta k} + \sigma_I^2\, e^{-j\frac{2\pi}{M}\gamma k}\right] & , 0 \le k \le J-1 \\[3ex]
0 & , J-1 < k < M-J \\[3ex]
\dfrac{1}{\sigma_s^2 + \sigma_I^2 + \sigma_n^2}\left[\sigma_3^2\, e^{-j\frac{2\pi}{M}(M-\Delta)k} + \sigma_I^2\, e^{-j\frac{2\pi}{M}(M-\gamma)ky}\right. & , M-J \le k \le M-1
\end{cases}
$$

$$(F-46)$$

and

$$
\text{Var}\,[H(k)] = \begin{cases}
\dfrac{\mu M\sigma_n^2\,[M\sigma_n^2 + 2M\,(\sigma_s^2 + \sigma_I^2)]}{M(\sigma_s^2 + \sigma_I^2 + \sigma_n^2)(2 - 2\mu M(\sigma_s^2 + \sigma_I^2 + \sigma_n^2))} & \begin{matrix}0 \le k \le J-1 \\ \text{or} \\ M-J \le k \le M-1\end{matrix} \\[5ex]
0 & J-1 < k < M-J
\end{cases}
$$

$$(F-47)$$

F-21

Then, substituting in (F-44) and (F-45) gives

$$\text{Var}\,[h_I'(t)] = \frac{1}{M^2}\left[\frac{\mu M \sigma_n^2\,\{M\sigma_n^2 + 2M\,(\sigma_s^2 + \sigma_I^2)\}}{M(\sigma_s^2 + \sigma_I^2 + \sigma_n^2)(2 - 2\mu M(\sigma_s^2 + \sigma_I^2 + \sigma_n^2))}\right]$$

$$\cdot \left\{ \sum_{m_1=0}^{M-1} \sum_{m_2=0}^{M-1} f'(t_z - m_1 T s)\, f'(t_z - m_2 T s)\, \frac{\sin\left[\frac{\pi J}{M}(m_1 - m_2)\right]}{\sin\left[\frac{\pi}{M}(m_1 - m_2)\right]}\right.$$

$$\left. \cdot \cos\left[\left(\frac{J-1}{M}\right)\pi(m_1 - m_2)\right]\right\} \tag{F-48}$$

and

$$\frac{2E[h_I'(t)]}{2\,t} = \frac{1}{M}\sum_{m=0}^{M-1} f''(t - mT s)\left\{\frac{\sin\left[\frac{\pi J}{M}(\Delta - m)\right]}{\sin\left[\frac{\pi}{M}(\Delta - m)\right]}\cos\left[\frac{J-1}{M}\pi(\Delta - m)\right]\left[\frac{\sigma_s^2}{\sigma_s^2 + \sigma_n^2 + \sigma_I^2}\right]\right.$$

$$\left. + \frac{\sin\left[\frac{\pi J}{M}(\gamma - m)\right]}{\sin\left[\frac{\pi}{M}(\gamma - m)\right]}\cos\left[\frac{J-1}{M}\pi(\gamma - m)\right]\left[\frac{\sigma_I^2}{\sigma_s^2 + \sigma_n^2 + \sigma_I^2}\right]\right\} \tag{F-49}$$

Then the variance of the estimate, given t_z, is found by substituting (F-48) and (F-49) in (F-39). Given any interpolation function, f(t), and a value for t_z, the variance of the delay estimate can be evaluated numerically on the computer. The value of t_z, the location of the peak can be found numerically from (F-41).

It must be noted here that this result applies only when the variance of $h_I(t)$ falls in the linear portion of $h'_I(t)$ near the peak of $E[h_I(t)]$. This is equivalent to saying that the largest of the discrete weights must be in the vicinity of the true peak. This will be true when the mean of the largest weight is large in comparison to the variance of the weights. For a particular input signal to noise ratio, this can be assured by selecting the feedback coefficient, μ, sufficiently small.

APPENDIX G

Appendix G

Tracking of Moving Broadband Targets

Introduction

In [1], the variance of stationary bearing estimates, using the adaptive filter bearing tracker, was compared to the Cramer-Rao lower bound on the variance of any unbiased static estimator. The comparison showed about a 0.5 dB loss for the adaptive tracker. As a further comparison, the adaptive tracker was compared to the split beam correlator bearing tracker. In [6] it was shown that the ratio of the variance of the split beam correlator tracker to the Cramer-Rao lower bound is given by [6 - Eq (33)].

$$\frac{D^2(\theta)}{D^2(\hat{\theta})} = \frac{4}{3}\left[1 - \frac{1}{M^2}\right]$$

where M = total number of hydrophones. When M = 2, as when comparing to the adaptive tracker, the split beam correlator achieves the lower bound. Hence, on the basis of static estimation, for broadband signals, an adaptive tracker and a non-adaptive split beam correlator tracker are comparable. This Appendix addresses operation as a dynamic device (i.e., tracking changing bearing). It is therefore necessary to investigate the dynamic tracking capabilities of the two devices and make a comparison of each in a tracking mode. In this case the CR bound is no longer applicable.

The variance of the estimates of the relative time delay between the two half arrays is computed for both trackers under a number of simplifying assumptions. The mean weights of the adaptive filter are determined using an exponential correlation function for the input signal correlation for a

linearly changing delay. The variance of the weights with signal present is approximated by the noise alone variance. These two expressions are used to compute the variance of the delay estimate in the absence of bias errors. The location of the peak of the weights is then analytically determined and shown to lag the true delay, introducing a bias into the estimate.

For purposes of comparison, the performance of a first order discrete time split beam bearing deviation indicator tracker is investigated. The variance of this tracker is determined as a function of the statistics of the correlator. The bias error is determined for the same linearly changing delay as for the adaptive filter.

The two devices are then compared on the basis of the variance of their estimates for the same bias error. In this way, each device is designed to achieve the same dynamic performance with some resultant fluctuating errors. An expression is then derived for the ratio of the two fluctuation error variances.

Adaptive Filter Bearing Tracker Model

In [1], Appendix VI, an expression is derived for the mean weights of the adaptive tracker, for small signal-to-noise ratios when the input signal is a broadband correlated process with linearly time-varying delay, buried in uncorrelated noise.

$$E\left[W_j(n)\right] = \mu\sigma_s^2 \sum_{k=0}^{n-1} (1-\mu\sigma_n^2)^{n-k-1} \rho_0 \left|ck-j\right|\delta \tag{G-1}$$

where

μ =   adaptation parameter

σ_s^2, σ_n^2 =   signal and noise powers respectively

$\rho = e^{-b}$ =   exponential correlation function of signal

c =   linear rate of change of delay between two phase centers of the split array

It is shown in Addendum G I, at the end of this Appendix, that, for

$$(1 - \mu\sigma_n^2)/\rho^{c\delta} < 1$$

$$E\left[W_j(n)\right] = \frac{\mu\sigma_s^2 \rho^{(j-c\ell)\delta} (1 - \mu\sigma_n^2)^{n-\ell-1}}{1 - (1 - \mu\sigma_n^2) \rho^{c\delta}} + \mu\sigma_s^2 \rho^{c\delta} [n-1-j/c]$$

$$\bullet \left[\frac{1 - \left\{(1 - \mu\sigma_n^2) \rho^{-c\delta}\right\}^{n-\ell-1}}{1 - (1 - \mu\sigma_n^2) \rho^{-c\delta}}\right] \qquad j \leq c\,(n-1)$$

$$= \frac{\mu\sigma_s^2 \rho^{\delta[j-c(n-1)]}}{1 - (1 - \mu\sigma_n^2) \rho^{c\delta}} \qquad j \geq c\,(n-1)$$

$$\text{(G-2)}$$

where

ℓ = integer such that

$$\ell \leq \frac{1}{c} < \ell + 1$$

G-3

Assuming $|j - c\ell|\delta \ll 1$

$$\lim_{n \to \infty} E\left[W_j(n)\right] = \mu\sigma_s^2\left[\frac{(1-\mu\sigma_n^2)^{n-\ell-1}}{1 - (1-\mu\sigma_n^2)\rho^{c\delta}} + \frac{\rho^{c\delta(n-\ell-1)} - (1-\mu\sigma_n^2)^{n-\ell-1}}{1 - (1-\mu\sigma_n^2)\rho^{-c\delta}}\right]$$

$$j \le c\,(n-1)$$

$$= \frac{\mu\sigma_s^2}{1 - (1-\mu\sigma_n^2)\rho^{c\delta}}\,\rho^{-c\delta[n-\ell-1]}$$

$$j \ge c\,(n-1)$$

$$\text{(G-3)}$$

In Addendum GI, at the end of this Appendix, it is shown that the lag in the
peak of the weights in Eq (G-3) in comparison to the true delay, is given by

$$\text{Tap Lag} = xc = \left[\frac{c}{bc\delta + \ell n\,(1-\mu\sigma_n^2)}\right]$$

$$\text{(G-4)}$$

$$\cdot \ell n \cdot \left\{\frac{bc\delta\,[1 - (1-\mu\sigma_n^2)\rho^{c\delta}]}{-\ell n\,(1-\mu\sigma_n^2)\,[(1-\mu\sigma_n^2)\,(\rho^{-c\delta} - \rho^{c\delta})]}\right\}$$

Since $\mu\tau_n^2 \ll 1$ and $bc\delta \ll 1$, the tap lag is accurately approximated by

$$xc = \frac{1}{bc\delta - \mu\tau_n^2}\text{hrs} \qquad \frac{bc\delta}{2\mu\tau_n^2} + \frac{1}{2}$$

If, in addition, $\mu0_n^2 \gg bc\delta$, then

$$xc \approx \frac{0.69\,c}{\mu\sigma_n^2 - bc\delta}$$

$$\text{(G-5)}$$

Eqs (G-4) and (G-5) have been shown in good agreement with the lag displayed by numerical evaluation of Eq (GI-4).

It is shown in Addendum GII that, for $(1 - \mu\sigma_n^2) \ge \rho^{c\delta}$, one

$$\lim_{j \to \infty} E\left[W_j(n)\right] = \mu\sigma_s^2 (1 - \mu\sigma_n^2)^{n-\ell-1} \left[\frac{\rho^{(j-c\ell)\delta}}{1 - (1 - \mu\sigma_n^2)\rho^{c\delta}} + \frac{\rho^{-(j-c\ell)\delta}}{(1 - \mu\sigma_n^2)\rho^{-c\delta}-1} \right.$$

$$\left. \left\{ 1 - \left(\frac{\rho^{c\delta}}{1 - \mu\sigma_n^2} \right)^{n-\ell-1} \right\} \right]$$

$$(G-6)$$

Again, using the condition that $j - c\ell \approx 0$, so that

$$\lim_{j \to \infty} E\left[W_j(n)\right] \approx \mu\sigma_j^2 (1 - \mu\sigma_n^2)^{n-\ell-1} \left[\frac{1}{1 - (1 - \mu\sigma_n^2)\rho^{c\delta}} \right.$$

$$\left. + \frac{1 - \left(\dfrac{\rho^{c\delta}}{1 - \mu\sigma_n^2} \right)^{n-\ell-1}}{(1 - \mu\sigma_n^2)\rho^{-c\delta}-1} \right]$$

$$(G-7)$$

Eq (G-7) does not peak at the unbiased value of delay, $j = c(n-1)$, but also displays a delay in the location of the peak. Precise expressions for the delay will not be investigated for this case.

Split Beam Tracker Model

Figure G-1 shows a simplified version of a time domain split beam tracker for two half-array inputs. The mean and variance of y, the correlator output, are evaluated as follows:

The correlator output $y(t)$ is the product of the derivative of the process $x_1(t-\tau(t))$ and a delayed version of the process $x_2(t)$.

$$y(t) = x_1'(t - \tau(t)) \, x_2 (t - \hat{\tau}(t))$$

Since

$$x_1(t) = s(t) + n_1(t)$$

and

$$x_2(t) = s(t) + n_2(t)$$

where

s, n_1, and n_2 are independent zero mean gaussian random processes, it is straightforward to show that the mean of $y(t)$ is given by

$$E [y(t)] = - \sigma_s^2 \rho' (\tau(t) - \hat{\tau}(t)) \tag{G-8}$$

where

$\rho(\tau)$ = normalized autocorrelation function of the signal or the noise processes

$\tau(t)$ = time value of the moving delay parameter

$\hat{\tau}(t)$ = estimated value of the delay

σ_s^2, σ_n^2 = signal, noise power.
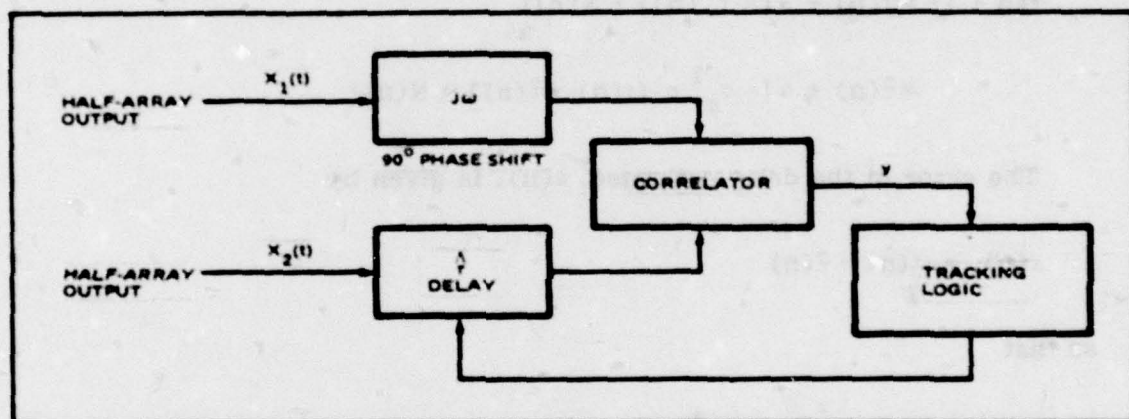
G-6

Figure G-1. Split-Beam Bearing Tracker

The first order tracking logic updates $\hat{\tau}(t)$ linearly with the value of $y(t)$. On the average when $\hat{\tau}(t) = \tau(t)$, then $\rho'(\tau(t) - \hat{\tau}(t)) = 0$ and no changes are made to the delay estimate. Thus

$$\hat{\tau}(n + 1) = \hat{\tau}(n) + \alpha\, y(n)$$

The process $y(n)$ can be represented as the mean value, $E[y(n)]$, given in (G-8) plus a zero mean fluctuating term, $N(n)$, so that

$$\hat{\tau}(n + 1) = \hat{\tau}(n) + \alpha[E(y(n)) + N(n)]$$

$$= \hat{\tau}(n) + \alpha[-\sigma_s^2 \rho'(\tau(n) - \hat{\tau}(n)) + N(n)]$$

The error in the delay estimates, $\epsilon(n)$, is given by

$$\epsilon(n) = \tau(n) - \hat{\tau}(n)$$

so that

$$\hat{\tau}(n + 1) = \hat{\tau}(n) + \alpha[-\sigma_s^2 \rho'(\epsilon(n)) + N(n)]$$

Expanding $\rho'(\epsilon(n))$ about the tracking solution, i.e., $\epsilon(n) = 0$, and using only the first term in the resulting Taylor series,

$$-\sigma_s^2 \rho'(\epsilon(n)) \approx -\sigma_s^2 \epsilon(n)\, \rho''(o)$$

and

$$\hat{\tau}(n + 1) = \hat{\tau}(n) + \alpha[-\sigma_s^2 \epsilon(n)\, \rho''(o) + N(n)]$$

This suggests the linearized mathematical model for the split beam correlator tracker shown in Figure G-2. The tracking logic is modelled as an integrator and a gain.
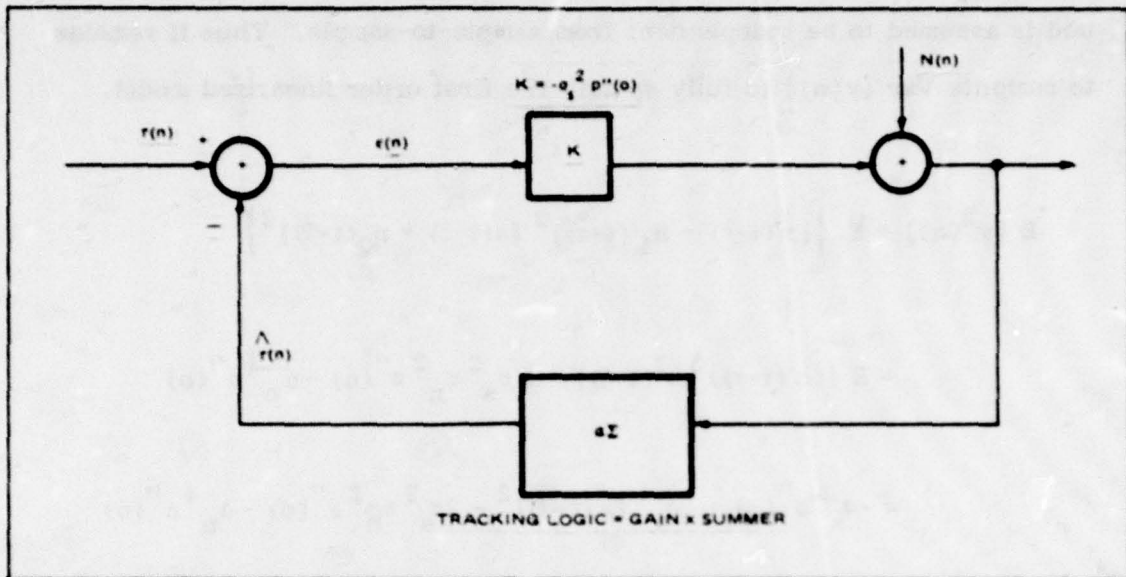
G-8

Figure G-2. Split-Beam Tracker — Linearized Mathematical Model

The power of the noise process $N(n)$ is given by the variance of $y(n)$ and is assumed to be independent from sample-to-sample. Thus it remains to compute Var $[y(n)]$ to fully specify the first order linearized model.

$$E[y^2(n)] = E\left\{[s'(t-\tau) + n_1'(t-\tau)]^2 [s(t-\hat{\tau}) + n_2(t-\hat{\tau})]^2\right\}$$

$$= E[(s'(t-\tau))^2 s^2(t-\hat{\tau})] - 2\sigma_s^2 \sigma_n^2 \rho''(o) - \sigma_n^4 \rho''(o)$$

$$= -\sigma_s^4 \rho''(o) + 2\sigma_s^4 [\rho'(\tau-\hat{\tau})]^2 - 2\sigma_s^2 \sigma_n^2 \rho''(o) - \sigma_n^4 \rho''(o)$$

The variance of $y(n)$ is found by subtracting the square of (G-8).

$$\text{Var}[y(n)] = -(\sigma_s^2 + \sigma_n^2)^2 \rho''(o) + \sigma_s^2 [\rho'(\tau-\hat{\tau})]^2$$

For small errors, i.e. when tracking, the second term is small and

$$\text{Var}[y(n)] = \text{Var}[N(n)] \approx -(\sigma_s^2 + \sigma_n^2)^2 \rho''(o) \qquad (G-9)$$

Since the system in Figure G-2 is linear, it is straightforward to compute the errors due to noise and the errors due to the dynamics of $\tau(n)$.

The z-transfer function from $\tau(n)$ to $\epsilon(n)$ is given by

$$H(z) = \frac{\epsilon(z)}{\tau(z)} = \frac{1 - z^{-1}}{1 + (\alpha K - 1) Z^{-1}} \qquad (G-10)$$

The z-transfer function from $N(n)$ to $\epsilon(n)$ is given by

$$G(z) = \frac{\alpha z^{-1}}{1 + (\alpha K - 1) z^{-1}} \qquad (G-11)$$

Thus, the fluctuation error variance is given by [3]

$$E\left[\epsilon^2(n)\right] = \alpha^2 \, \text{Var } N(n) \oint G(z) \, G(z^{-1}) \, z^{-1} \, dz$$

$$= \frac{\alpha^2 \, \text{Var } N(n)}{\alpha K \, [2 - \alpha K]} \qquad (G-12)$$

where Eq (G-12) has been obtained by the calculus of residues.

Dynamical Response to Ramp Inputs

In order to make a meaningful comparison to the adaptive filter bearing tracker, it is necessary to select the same inputs to both devices. The adaptive filter has been studied for a linearly varying time delay. Hence, $\tau(nt) = cnT$ where T = sample time, and the z-transform of the input is

$$\tau(z) = cT\left(\frac{z^{-1}}{1 - z^{-1}}\right)^2 \qquad (G-13)$$

and

$$\epsilon(z) = \tau(z)H(z) = \frac{cT}{[z - (1 - \alpha K)] \, [z - 1]} \qquad (G-14)$$

G-11

Inverse z-transforming yields

$$\epsilon(n) = \frac{cT}{\alpha K} [1 - (1 - \alpha K)^n] \qquad (G-15)$$

In steady-state,

$$\lim_{n \to \infty} \epsilon(n) = \frac{cT}{\alpha K} \qquad (G-16)$$

Note that, for the split beam tracking logic, $T = \delta$.

Comparison of Adaptive Filter and Split-Beam Bearing Trackers

In the previous two sections, the statistics of the two devices, relevant to making a performance comparison have been computed. Consider, first the performance of the adaptive filter using the approach of [6],

$$\text{Var}^{\frac{1}{2}} \tau = \frac{\text{Var}^{\frac{1}{2}} \left[\frac{\partial h(\tau)}{\partial t} \right]}{\frac{\partial}{\partial \tau} E \left[\frac{\partial h(\tau)}{\partial \tau} \right]} \qquad (G-17)$$

That is, the errors in the response of the weights can be mapped into the errors in one's ability to extract the peak of the weights. Since the results of the section before last were derived from expressions for the mean weights when $\sigma_s^2 \ll \sigma_n^2$, it is not unreasonable to set

$$\text{Var} \frac{\partial h(t)}{\partial t} = \frac{\mu \sigma_n^2}{2} \left[\frac{1 - \rho^\delta}{\delta} \right]^2 \qquad (G-18)$$

G-12

(i.e., the weight variance with no signal present multiplied by the mean slope of the weights squared). It might be noted that the equation at the bottom of page IV-3 of [1] is in agreement with Eq (G-18) for small b. That is, from [1]

$$\text{Var}\left[\frac{\partial h(t)}{\partial t}\right] = \frac{1}{\pi} \frac{\mu P_N (2 P_S + P_N)}{(P_S + P_N) [2 - 2\mu(P_S + P_N)]} \left[\frac{\omega_U^3 - \omega_L^3}{3}\right]$$

For $P_S \ll P_N$

$$= \frac{1}{2\pi} \frac{\mu P_N}{2(1 - \mu P_N)} \left[\int_{\omega_L}^{\omega_U} \omega^2 \omega + \int_{-\omega_u}^{-\omega_L} \omega^2 \omega\right]$$

$$= \frac{\mu P_N}{2(1 - \mu P_N)} \rho''(o)$$

If the flat spectrum used in [1] is replaced by $\rho(\tau) = e^{-b\tau}$, then $\rho''(o) = b^2$ and

$$\text{Var}\left[\frac{\partial h}{\partial \tau}\right] \approx \frac{\mu P_N}{2} b^2$$

Noting that

$$\lim_{b\delta \to o} \left[\frac{1 - \rho^\delta}{\rho}\right]^2 = b^2,$$ the equivalence to Eq (G-18) is demonstrated.

It is now assumed that the denominator of Eq (G-17) is given by the slope of the mean weights in the neighborhood of the peak (assuming the value of the slope for the lag given by Eq (G-4) does not differ significantly from the value of the slope at the true value of delay). It is also assumed that the shape of the envelope of the weights is well approximated by a decay of the form ρ^δ.

Then

$$E\left[\frac{\partial h(\tau)}{\partial d\tau}\right] = \frac{\mu\sigma_s^2}{1 - (1 - \mu\sigma_n^2)\rho^{c\delta}} \frac{1 - \rho^\delta}{\delta}$$

$$\frac{\partial}{\partial\tau} E\left[\frac{\partial h(\tau)}{\partial\tau}\right] = \frac{\mu\sigma_s^2}{1 - (1 - \mu\sigma_n^2)\rho^{c\delta}} \frac{\frac{1 - \rho^\delta}{\delta} - \frac{\rho^\delta - \rho^{2\delta}}{\delta}}{\delta}$$

$$= \frac{\mu\sigma_s^2}{1 - (1 - \mu\sigma_n^2)\rho^{c\delta}} \frac{[1 - \rho^\delta]^2}{\delta^2}$$

(G-19)

Using Eqs (G-18) and (G-19) in Eq (G-17) yields

$$\text{Var}^{\frac{1}{2}}\hat{\tau} = \frac{\sigma_n^2}{\sigma_s^2} \sqrt{\mu\sigma_n^2} \left[\rho^{c\delta} + \frac{1 - \rho^{c\delta}}{\mu\sigma_n^2}\right] \frac{1}{\sqrt{2}} \frac{\delta}{1 - \rho^\delta}$$

(G-20)

Note, as a check, that when $c \to 0$ and $\rho = e^{-b}$

$$\mathrm{Var}^{\frac{1}{2}}\, \hat{\tau} = \frac{\sigma_n^2}{\sigma_s^2} \sqrt{\frac{\mu \sigma_n^2}{2} \frac{1}{b}} \quad \text{which agrees with [1].}$$

Note also that Eq (G-20) has the correct behavior with

$$\left(\frac{\sigma_s^2}{\sigma_n^2} \right), \mu \sigma_n^2 \text{ (if c is small), and } \rho.$$

If c is sufficiently large, then decreasing $\mu \sigma_n^2$ degrades the performance because the weight adjustments cannot effectively keep up with the input. That is, there is lag (Eq (G-4)) in the location of the peak value of the mean weights and the amplitude of the mean weights also decreases (Eq G-19). Ignoring the lag, the variance of the estimate of the peak increases due to the amplitude effect.

The bearing tracker performance can be computed directly from Eq (G-12) since Var $\epsilon(n)$ is Var $\hat{\tau}(n)$. Thus, using Eqs (G-9) and (G-12) and Figure G-II,

$$\mathrm{Var}\, \hat{\tau}(n) = \frac{\alpha K}{[2 - \alpha K]} \left(\frac{\sigma_s^2 + \sigma_n^2}{\sigma_s^2} \right)^2 \frac{1}{[-\rho''(o)]} \qquad \text{(G-21)}$$

Equating the dynamical errors of the two systems as given by Eq (G-5) (multiplied by δ to yield time delay) and Eq (G-16) (with $T = \delta$) yields

$$\alpha K = \frac{\mu\sigma_n^2 - bc\delta}{0.69} \tag{G-22}$$

By using Eq (G-22) in Eq (G-21), assuming $bc\delta \ll \mu\sigma_n^2$ and using Eq (G-20), the ratio of standard deviations is given by

$$\frac{\text{Var}^{\frac{1}{2}}\hat{\tau}\Big|_{\text{adaptive filter}}}{\text{Var}^{\frac{1}{2}}\hat{\tau}\Big|_{\text{bearing tracker}}} = \sqrt{0.69}\left[\rho^{c\delta} + \frac{1-\rho^{c\delta}}{\mu\sigma_n^2}\right] \tag{G-23}$$

which can be further approximated as

$$\approx \sqrt{0.69}\left[1 + \frac{bc\delta}{\mu\sigma_n^2}\right] \tag{G-24}$$

Conclusions

The Adaptive Filter Bearing Tracker and the Split Beam Bearing Tracker are compared on the basis of tracking error variance for the same dynamical bias error when tracking the linearly time-varying delay of a broadband signal. In steady-state, both trackers display bias errors that are proportional to the rate of change of delay and inversely proportional to the loop gains. Expressions are presented for variances of each device which display the tradeoffs between signal-to-noise ratio, signal bandwidth and

linear rate of change of delay. The relative performance of the two devices is shown to be essentially independent of input signal-to-noise ratio and to depend primarily on the ratio of the product of the tap time delay, δ, the signal bandwidth, b, and the rate of change of delay, c, divided by the adaptive filter algorithm gain, $\mu \sigma_n^{\ 2}$. When $bc\delta << \mu \sigma_n^{\ 2} << 1$, the adaptive filter variance is 0.69 times as large as that of the split beam tracker.

ADDENDUM GI:

EVALUATION OF EQUATION (G-1) FOR $(1 - \mu\sigma_n^2) < \rho^{c\delta}$

Beginning with Eq. (G-1) and splitting the sum in two parts

$$E\left[W_j(n)\right] = \mu\sigma_s^2 \sum_{k=0}^{k\leq j/c} (1 - \mu\sigma_n^2)^{n-k-1} \rho^{(j-ck)\delta}$$

$$+ \mu\sigma_s^2 \sum_{k>\frac{j}{c}}^{n-1} (1 - \mu\sigma_n^2)^{n-k-1} \rho^{(ck-j)\delta}$$

$$= \mu\sigma_s^2 \rho^{j\delta} \rho^{-c\delta(n-1)} \sum_{k=0}^{k<j/c} \left[(1 - \mu\sigma_n^2) \rho^{c\delta}\right]^{n-k-1}$$

$$+ \mu\sigma_s^2 \rho^{c\delta(n-1)} \sum_{k>j/c}^{n-1} \left[\frac{1 - \mu\sigma_n^2}{\rho^{c\delta}}\right]^{n-k-1} \tag{GI-1}$$

The first summation represents a convergent power series since $1 - \mu\sigma_n^2 < 1$ and $\rho^{c\delta} < 1$. The second summation will converge if

$$\frac{1 - \mu\sigma_n^2}{\rho^{c\delta}} < 1 \ .$$

Now let

$$\ell = I\left[\frac{j}{c}\right] = \text{integer such that } \frac{j}{c} \geq \ell \text{ but } \frac{j}{c} < \ell + 1$$

Then, in the first summation

$$\sum_{k=0}^{\ell} \left[(1 - \mu\sigma_n^2) \, \rho^{c\delta} \right]^{n-k-1} = \left[(1 - \mu\sigma_n^2) \, \rho^{c\delta} \right]^{n-\ell-1}$$

$$\left[\frac{1 - \left\{ (1 - \mu\sigma_n^2) \, \rho^{c\delta} \right\}^{\ell+1}}{1 - (1 - \mu\sigma_n^2) \, \rho^{c\delta}} \right] \qquad \text{(GI-2)}$$

In the second summation,

$$\sum_{k=\ell+1}^{n-1} \left[\frac{1 - \mu\sigma_n^2}{\rho^{c\delta}} \right]^{n-k-1} = \frac{1 - \left(\dfrac{1 - \mu\sigma_n^2}{\rho^{c\delta}} \right)^{n-\ell-1}}{1 - (1 - \mu\sigma_n^2) \, \rho^{-c\delta}} \qquad \text{(GI-3)}$$

Using Eqs. (GI-2) and (GI-3) in (GI-1) yields

$$E\left[w_j(n) \right] = \mu\sigma_s^2 \, \rho^{(j-c\ell)\delta} (1 - \mu\sigma_n^2)^{n-\ell-1}$$

$$\cdot \left[\frac{1 - \left\{ (1 - \mu\sigma_n^2) \, \rho^{c\delta} \right\}^{\ell+1}}{1 - (1 - \mu\sigma_n^2) \, \rho^{c\delta}} \right]$$

$$+ \mu\sigma_s^2 \, \rho^{c\delta(n-1)} \, \rho^{-j\delta} \left[\frac{1 - \left\{ (1 - \mu\sigma_n^2) \, \rho^{-c\delta} \right\}^{n-\ell-1}}{1 - (1 - \mu\sigma_n^2) \, \rho^{-c\delta}} \right] \text{(GI-4)}$$

For large ℓ, the second term in the first set of brackets is negligible in comparison to one. This approximation yields the expression in Eq. (G2) for $j \le c(n-1)$.

For $j \ge c(n-1)$, Eq. (G-1) reduces to a single summation

$$E\left[w_j(n)\right] = \mu\sigma_s^2 \sum_{k=0}^{n-1} (1 - \mu\sigma_n^2)^{n-k-1} \rho(j-ck)$$

$$= \mu\sigma_s^2 \rho^{j\delta} \rho^{-c\delta(n+1)} \sum_{k=0}^{n-1} \left[(1 - \mu\sigma_n^2)\rho^{c\delta}\right]^{n-k-1}$$

$$= \mu\sigma_s^2 \rho^{\delta[j-c(n-1)]} \frac{1 - \left[(1 - \mu\sigma_n^2)\rho^{c\delta}\right]^n}{1 - (1 - \mu\sigma_n^2)\rho^{c\delta}} \tag{GI-5}$$

Hence

$$\lim_{n\to\infty} \left\langle w_j(n)\right\rangle = \frac{\mu\sigma_s^2 \rho^{\delta[j-c(n-1)]}}{1 - (1 - \mu\sigma_n^2)\rho^{c\delta}} \tag{GI-6}$$

As a check, note that at $j = c(n-1)$, Eq. (G3) is self consistent.

The approximate location of the peak weight in (GI-4) and (GI-6) can be determined by using the approximation $j \approx c\ell$ and assuming that $n-\ell-1$ can be approximated by a continuous variable.

Then, assuming the peak occurs for $j = c(n-1)$, Eq. (GI-4) simplifies to

$$E\left[w_j(n)\right] \approx \mu \sigma_s^2 \left[\frac{(1-\mu\sigma_n^2)^{n-\ell-1}}{1 - (1-\mu\sigma_n^2)\rho^{c\delta}} + \frac{\rho^{c\delta(n-1-\ell)} - (1-\mu\sigma_n^2)^{n-\ell-1}}{1 - (1-\mu\sigma_n^2)\rho^{-\delta c}}\right] \quad \text{(GI-7)}$$

$$= \mu \sigma_s^2 \left[\frac{e^{-\alpha x}}{A} + \frac{e^{-\beta x} - e^{-\alpha x}}{B}\right] \quad \text{(GI-8)}$$

where

$$x = (n-1-\ell)$$

$$e^{-\alpha} = (1-\mu\sigma_n^2)$$

$$e^{-\beta} = \rho^{c\delta} = e^{-bc\delta}$$

$$A = 1 - (1-\mu\sigma_n^2)$$

$$B = 1 - (1-\mu\sigma_n^2)\rho^{-c\delta} \quad \text{(GI-9)}$$

Differentiating Eq. (GI-8) on x and setting the result to zero to find the maximum, yields

$$x = \frac{1}{\beta - \alpha} \ell n \frac{\beta A}{\alpha (A-B)} \quad \text{(GI-10)}$$

Using Eq. (GI-9) in Eq. (GI-10) yields

$$x = \left[bc\delta + \ln (1 - \mu\sigma_n^2) \right]^{-1}$$

$$\cdot \ln \left\{ \frac{bc\delta \left[1 - (1 - \mu\sigma_n^2) \rho^{c\delta} \right]}{-\ln (1 - \mu\sigma_n^2) \left[(1 - \mu\sigma_n^2) (\rho^{-c\delta} - \rho^{c\delta}) \right]} \right\} \qquad \text{(GI-11)}$$

Since

$$\ell = n-1-x = j/c,$$

$$j = c(n-1) - xc, \qquad \text{(GI-12)}$$

the lag in number of taps is xc (recall the location of the correct delay at time n is c(n-1)).

ADDENDUM GII:

EVALUATION OF EQ. (G1) FOR $(1 - \mu\sigma_n^2) \geq \rho^{c\delta}$

Consider first the case of $j \leq c(n-1)$.

$$
E\left[w_j(n)\right] = \mu\sigma_s^2 \, \rho^{j\delta} \, \rho^{-c\delta(n-1)} \sum_{k=0}^{k \leq j/c} \left[(1-\mu\sigma_n^2)\rho^{c\delta}\right]^{n-k-1}
$$

$$
+ \mu\sigma_s^2 \sum_{k \geq j/c}^{n-1} (1-\mu\sigma_n^2)^{n-k-1} \, \rho^{(ck-j)\delta} \qquad\qquad (GII-1)
$$

The first term sums in the same manner as Eq. (GI-2). However, because of the condition $(1- \mu\sigma_n^2) > \rho^{c\delta}$, the second term sums differently than in Appendix GI.

$$
\sum_{k=\ell+1}^{n-1} (1-\mu\sigma_n^2)^{n-k-1} \, \rho^{(ck-j)\delta} = \rho^{-j\delta}(1-\mu\sigma_n^2)^{n-1} \sum_{k=\ell+1}^{n-1} \left[\frac{\rho^{c\delta}}{1-\mu\sigma_n^2}\right]^k
$$

$$
= \rho^{-j\delta}(1-\mu\sigma_n^2)^{n-1} \left[\frac{\rho^{c\delta}}{1-\mu\sigma_n^2}\right]^{\ell+1}
$$

$$
\cdot \sum_{k=0}^{n-\ell-2} \left[\frac{\rho^{c\delta}}{1-\mu\sigma_n^2}\right]^k
$$

G-23

$$= \rho^{-j\delta} (1 - \mu\sigma_n^2)^{n-1} \left[\frac{\left(\dfrac{\rho^{c\delta}}{1-\mu\sigma_n^2}\right)^{\ell+1} - \left(\dfrac{\rho^{c\delta}}{1-\mu\sigma_n^2}\right)^n}{1 - \dfrac{\rho^{c\delta}}{1-\mu\sigma_n^2}} \right] \tag{GII-2}$$

Hence for $(1 - \mu\sigma_n^2) > \rho^{c\delta}$

$$E\left[w_j(n)\right] = \mu\sigma_s^2 \rho^{(j-c\ell)\delta} (1 - \mu\sigma_n^2)^{n-\ell-1} \left[\frac{1 - \left\{(1-\mu\sigma_n^2)\rho^{c\delta}\right\}^{\ell+1}}{1 - (1-\mu\sigma_n^2)\rho^{c\delta}} \right]$$

$$+ \mu\sigma_s^2 \rho^{-j\delta} (1-\mu\sigma_n^2)^{n-1} \left[\frac{\left(\dfrac{\rho^{c\delta}}{1-\mu\sigma_n^2}\right)^{\ell+1} - \left(\dfrac{\rho^{c\delta}}{1-\mu\sigma_n^2}\right)^n}{1 - \dfrac{\rho^{c\delta}}{1-\mu\sigma_n^2}} \right] \tag{GII-3}$$

In steady-state as $n \to \infty$, Eq. (GII-2) reduces to Eq. (G6).

UNCLASSIFIED

SECURITY CLASSIFICATION OF THIS PAGE (When Data Entered)

REPORT DOCUMENTATION PAGE		READ INSTRUCTIONS BEFORE COMPLETING FORM
1. REPORT NUMBER	2. GOVT ACCESSION NO.	3. RECIPIENT'S CATALOG NUMBER
4. TITLE (and Subtitle) Final Report on Phase 2 of the Adaptive Tracking System Study		5. TYPE OF REPORT & PERIOD COVERED Research Report - October 1978 to October 1979
		6. PERFORMING ORG. REPORT NUMBER FR79-11-1123
7. AUTHOR(s) P. L. Feintuch, F. A. Reed, N. J. Bershad, C. M. Flynn		8. CONTRACT OR GRANT NUMBER(s) N00024-77-C-6251
9. PERFORMING ORGANIZATION NAME AND ADDRESS Hughes Aircraft Company P.O. Box 3310 Fullerton, CA 92634		10. PROGRAM ELEMENT, PROJECT, TASK AREA & WORK UNIT NUMBERS 806H160572
11. CONTROLLING OFFICE NAME AND ADDRESS Naval Sea Systems Command, Code 6312 Department of the Navy Washington, D.C. 20364		12. REPORT DATE October 1979
		13. NUMBER OF PAGES
14. MONITORING AGENCY NAME & ADDRESS(if different from Controlling Office)		15. SECURITY CLASS. (of this report) Unclassified
		15a. DECLASSIFICATION/DOWNGRADING SCHEDULE
16. DISTRIBUTION STATEMENT (of this Report) Distribution of this document is unlimited.		
17. DISTRIBUTION STATEMENT (of the abstract entered in Block 20, if different from Report) Adaptive Filters, Adaptive Bearing Trackers, Bearing Accuracy, Broadband Bearing Trackers, LMS Adaptive Filters, Linearly Varying Bearing Narrowband Bearing Trackers, Split Beam Trackers		
18. SUPPLEMENTARY NOTES		
19. KEY WORDS (Continue on reverse side if necessary and identify by block number)		

20. ABSTRACT (Continue on reverse side if necessary and identify by block number)

A specific split beam adaptive trackers using the LMS adaptive filter is investigated. The adaptive tracker does not require a priori information on input statistics, and can track using narrowband and broadband energy simultaneously.

The narrowband tracker is shown to perform within 0.5dB of the Carmer-Rao lower bound for narrowband targets. The bias and standard deviation are determined for a target with broadband and narrowband components, and

DD FORM 1473 EDITION OF 1 NOV 65 IS OBSOLETE

SECURITY CLASSIFICATION OF THIS PAGE (When Data Entered)

DD Form 1473: Report Documentation Page (Continued)

Block 20: Abstract (Continued)

with plane wave interference present. When tracking a narrowband input the bias effects due to interference dominate in areas in flucations in most cases. It is shown that the adaptive tracker is less sensitive to changes in input spectra relative to those assumed a priori than conventional split beam trackers, and the performance of the adaptive tracker for targets with linerly changing bearing is analyzed and compared to a conventional split beam tracker.

Commander
Naval Sea Systems Command
Department of the Navy
Washington, D.C. 20362
Attn: D.E. Porter, 63R

Commander
Naval Sea Systems Command
Department of the Navy
Washington, D.C. 20362
Attn: 660F

Commander
Naval Sea Systems Command
Department of the Navy
Washington, D.C. 20362
Attn: 660C

Commander
Naval Sea Systems Command
Department of the Navy
Washington, D.C. 20362
Attn: 661C

Commander
Naval Sea Systems Command
Department of the Navy
Washington, D.C. 20362
Attn: 660E

Commander
Naval Sea Systems Command
Department of the Navy
Washington, D.C. 20362
Attn: 06H12

Commander
Naval Sea Systems Command
Department of the Navy
Washington, D.C. 02362
Attn: Library 09G3

Defense Documentation Center
Defense Services Administration
Cameron Station, Building 5
5010 Duke Street
Alexandria, Virginia 22314

Director
Naval Research Laboratory
Department of the Navy
Washington, D.C. 20375

Chief of Naval Research
800 N. Quincy Street
Arlington, VA 22217
Attn: Code 466

Commander
Naval Ocean Systems Center
San Diego, CA 92152
Attn: Library

Officer in Charge
New London Laboratory
Naval Underwater Systems Center
New London, Connecticut 06320

David Taylor Naval Ship Research &
Development Center
Bethesda, MD 20034

Commander
Naval Surface Weapons Center
White Oak
Silver Spring, MD 20910

Commanding Officer
Naval Coastal Systems Center
Panama City, Florida 32407

Officer in Charge
New London Laboratory
Naval Underwater Systems Center
New London, CT 06320
Attn: Library

Commanding Officer
Naval Air Development Center
Johnsville
Warminster, Pennsylvania

Office of the Director of Defense
Research and Engineering
Room 3C128, The Pentagon
Washington, D.C. 20301